Multi-scale modeling of water resources in a tropical inland valley and a tropical floodplain catchment in East Africa

Dissertation

zur

Erlangung des Doktorgrades (Dr.rer.nat.)

der

Mathematisch-Naturwissenschaftlichen Fakultät

der

Rheinischen Friedrich-Wilhelms-Universität Bonn

vorgelegt von

Geofrey Gabiri

aus

Pallisa, Uganda

Bonn, August 2018

Angefertigt mit Genehmigung der Mathematisch-Naturwissenschaftlichen Fakultät der Rheinischen Friedrich-Wilhelms-Universität Bonn.

1. Gutachter : Prof. Dr. Bernd Diekkrüger

2. Gutachterin : Prof. Dr. Barbara Reichert

Tag der mündlichen Prüfung: 7th Febraury 2019

Erscheinungsjahr: 2019

Dedication

To my family who helped me in all ways, giving me ample time to concentrate and work throughout this PhD study. My wife Malson Natuhwera, I am soothed by your faith, love and encouragement. My children, Emmanuella Konso Humura and Ethan Sanghai Gabiri, I am grateful to take the future with you. My parents Mr. and Mrs. Sanghai Gabiri (RIP), life would have been meaningless without you but your arms, prayers, mentoring and sacrifices protected and guided me a lot. To my brothers Dr. Robert Tuke and Laban Miyo and sisters Leah Sabano and Sylvia Sagati, I am truly grateful for your support. Uncle Stephen Mukama and Aunt Alice Sagati thank you for your untiring sacrifice, encouragement and support you have rendered to me even after our parents waved goodbye to this world.

Acknowledgements

Finally, the day has come! The Glory and honor goes back to you Lord for the blessings and protection during this PhD course. I want to thank the German Federal Ministry of Education and Research (BMBF) and German Federal Ministry for Economic Cooperation and Development for funding this work under the auspice of GloBE: wetlands in East Africa project (FKZ: 031A250A-H): Reconciling future food production with environmental protection. We are equally grateful to the German Aerospace service (DLR) for providing TanDEM-X data under the project DEM_HYDR1039.

I am very much privileged to have worked with my supervisor Prof. Dr. Bernd Diekkrüger whose untiring support, guidance, comments, suggestions, commitment to listen to my questions which were sometimes unclear, the great humility and seemingly unlimited belief in me shaped this work. I learned a lot from him throughout our various discussions about hydrological science and modeling and human values and also our regular down to earth discussions on how to compile this PhD work together. My indebtedness can't be fully expressed in words but I say thanks a lot for ably guiding me through this study.

I am grateful to my tutor Dr. Constanze Leemhuis for her unwavering support, comments and keeping me on truck throughout the study. Your scientific rigor, suggestions and leads were instrumental to this work, especially in selecting the hydrological model and the land use management scenarios to be applied in the inland valley wetland. Thanks a lot for expertly guiding me through this study and consoling my frustrations whenever we hit a rock. I can't forget thanking your wonderful husband Patrick and lovely children Anton and Mina who tirelessly allowed you to travel to East Africa to guide me in the field work specifically, instrumentation and data collection and while in Bonn, I always felt welcomed at your home. I am indebted to Mr. Kristian Näschen for your suggestions and trainings which were invaluable especially in the Soil and Water Assessment Tool (SWAT) modeling. Also, your guidance and support outside academics while in Bonn will always be remembered in my life. You are a brother to me.

I convey my sincere thanks and gratitude to all my current and former colleagues and friends of the Hydrology Research Group at the University of Bonn for the great time we spent together, particularly Dr. Yira Yacouba for proof reading this work, Mr. Thomas Poméon, Dr. Alexandre-Eudes Danvi (we shared a lot about SWATgrid model), Dr. Felix Op de Hipt, Dr. Simone Giertz

for your support in the soil lab, Gero Steup, Dr. A. Y. Bossa, Dr. T. Cornelissen, Mouhamed Idrissou, Claudia Schepp, Inken Rabbel, Johannes Rosleff Sörensen, Piotr Przysucha, Martin Ziegler, and Emmanuel Nkudimana. Your wonderful contributions and support in all kinds were much appreciated. We did not only share about academics but we shared a lot of things including thoughts and purpose of life, football/soccer and politics. You were all amazing. Thank you for your clear thoughts and you will forever live in my memories.

I wish to express my sincere gratitude to the GloBE wetlands team for your support. Special thanks to Prof. Dr. Mathias Becker coordinator of the project; Dr. Micheal Ugen Adrigo, Uganda country coordinator; and Prof. Misana, Tanzania country coordinator, for creating an enabling environment to conduct my field work. Many thanks to all the current and former PhD students under GloBE wetlands project who shared the challenging tasks of a PhD as well as support during field work. In a special way, I thank Dr. Sonja Burghof for her contribution and support during the hydrological instrumentation and data collection, your enthusiasm and work rate is amazing! Mr. Julius Kwesiga for his support and supervision of the field assistants amidst his PhD tasks in Tanzania. I can't forget to thank my GloBE office mates at the University of Bonn for their wonderful support and encourage, particularly, Prof. Dr. Mathias Langensiepen, Dr. Miguel Alvarez, Kai Behn, Eike Kiene, Kristina Grotelüschen, Gereon Heller and Susanne Hermes. Last but not least, I am truly grateful to my field assistants Sama John, Francis Kimaro and Robert Mutebi for your tireless endeavors data in collection under all circumstances.

I am grateful to Moses Tenywa, Professor at the college of Agriculture and Environmental Sciences, Makerere University, Yazidhi Bamutaze, Associate Professor and Head at the department of Geography, Geo-informatics and Climate sciences, Makerere University and Joy Obando, professor at the Department of Geography Kenyatta University for recommending me to apply for this PhD study under the GloBE wetlands project. You remain my inspiration and friends. To Professor Moses Tenywa, your piety to me and zealous interest in all my academic works is a living testimony of freed love. There are special mentors and other friends that I must acknowledge due to their importance in my works however, it is not practical to list all of those that have contributed. I wish to thank all of you.

Abstract

This study investigated the dynamics of hydrological processes at the wetland-catchment scale through field scale based analysis, point scale modeling using Hydrus-1D model along a floodplain transect in Tanzania and wetland-catchment modeling with SWAT model in an inland valley in Uganda. The impact of different land use management options and the projected climate change on the water resources of the inland valley were also evaluated using a hydrological response unit (HRU)-based (ArcSWAT2012) and a grid-based setup (SWATgrid) of the SWAT model. The inland valley is located in Namulonge, central Uganda, and it is one of the headwater catchments of Lake Kyoga basin. The inland valley catchment covers an area of 31 km^2 with a wetland area of 4.5 km^2. The floodplain is located in Kilombero district, Southern Tanzania and the catchment area is 40,240 km^2 and the study area in a wetland is 96 km^2. Both sites reflect the prevailing diversity of wetland attributes and uses.

Monitoring of hydro-meteorological data for both sites was conducted for two hydrological consecutive years of 2015 and 2016. The cross–section of the wetland transect was subdivided into three major hydrological positions defined as riparian zone, middle, and fringe. Hydrological instrumentation and data collection for soil moisture, soil properties, depth to shallow groundwater was conducted along these hydrological positions for both wetland systems. In addition, there was data mining from other sources.

Following the field based analysis at a wetland scale in the inland valley, the spatial and temporal variability in soil moisture increased significantly ($p<0.05$) towards the riparian zone, however, no significant difference was observed between middle and riparian zone. The distribution of soil hydrological regimes, saturated, near and non- saturated regimes does not correlate with the hydrological positions. Precipitation strongly controlled the temporal variability while microscale topography, soil properties, distance from the stream, anthropogenic factors, and land use controlled the spatial variability of soil water availability in the inland valley

In the Kilombero floodplain, Hydrus-1D model was successfully calibrated (R^2 = 0.54–0.92, RMSE = 0.02–0.11 cm^3/cm^3) using measured soil moisture content. Satisfying statistical measures (R^2 = 0.36–0.89, RMSE = 0.03–0.13 cm^3/cm^3) were obtained when calibrations for one plot were validated with measured soil moisture for another plot within the same hydrological zone, indicating the transferability of the calibrated Hydrus-1D. The hydrological regimes correlated with

the hydrological positions in the floodplain. Soil moisture dynamics is controlled by overbank flow, precipitation, and groundwater control at the riparian and middle zone, while it is controlled by rainfall and lateral flow from mountains at the fringe during the long rainy seasons. In the dry and short rainy seasons, rainfall, soil properties, and atmospheric demands control soil moisture dynamics at the riparian and middle zone.

For the wetland-catchment scale hydrological modeling in the inland valley, good model performance was achieved from the calibration and validation of daily discharge (R^2 and NSE > 0.7) for both model setups (ArcSWAT2012 and SWATgrid). The annual water balance indicates that 849.5 mm representing 65% of precipitation is lost via evapotranspiration. Surface runoff (77.9 mm) and lateral flow (86.5 mm) are the highest contributors to stream flow. Four land use management options were developed in addition to the current land use system, with different water resources conservation levels (*Conservation, Slope conservation, Protection of the headwater catchment, and Exploitation*). There is a strong relationship between the first three management options with decreasing surface runoff, annual discharge and water yield while the fourth option will increase annual discharge and total water yield.

The future climate change in the inland valley was analyzed using climate scenarios RCP4.5 and 8.5 of six GCM-RCM models from the CORDEX-Africa project. Compared to the reference period of 1976-2005, a general increase in temperature of +0.9 ^{0}C to +1.9 ^{0}C over the period of 2021-2050 is projected by the model ensemble. A mixed change signal in annual precipitation (-30 to 43.9%) is projected among the six climatic models. However, on average, the models show an increase in annual precipitation of +7.4% and +21.8% under RCP4.5 and 8.5, respectively.

The application of the climate model ensembles in SWAT showed future discharge change similar to the projected precipitation change. The six climate models showed uncertainty in the annual discharge change ranging from -44 to 149% although on average, the climate models project an increase of +16% and +29% under RCP4.5 and 8.5, respectively. Wet and dry seasons are expected to get wetter and drier, respectively in the future. Compared to land use management options, climate change will have a dominant impact on the water resources in inland valleys. Adoption of C*onservation*, *Slope conservation and protection of the headwater catchment* options will significantly reduce the impacts of climate change on the total water yield and surface runoff and increase evapotranspiration and water availability in the inland valley.

Zusammenfassung

Im Rahmen der vorliegenden Untersuchung wurde die Dynamik hydrologischer Prozesse zweier Feuchtgebiete untersucht. Dabei wurden Feldmessungen auf Punktebene, Punktmodellierungen mit dem Modell Hydrus-1D entlang eines Überflutungsebenen-Transektes sowie Modellierungen auf Einzugsgebietsebene eines Talgrund-Feuchtgebietes mit dem Modell SWAT (Soil and Water Assessement Tool) durchgeführt. Die Auswirkungen verschiedener Landnutzungsarten auf die Wasserressourcen eines Talgrund-Feuchtgebietes in Uganda wurden mit Hilfe des klassischen SWAT Modells unter Nutzung hydrologischer Bezugseinheiten (HRU-Ansatz, ArcSWAT2012) und vergleichsweise mit einem rasterbasierten Aufbau (SWATgrid) des SWAT-Modells unter Berücksichtigung des Klimawandels bewertet. Das untersuchte Einzugsgebiet liegt bei Namulonge, nördlich von Kampala, und ist eines der Quellgebiete des Kyoga-Sees. Das Einzugsgebiet umfasst eine Fläche von 31 km², wovon das Feuchtgebiet eine Fläche von 4,52 km² einnimmt. Das zweite Untersuchungsgebiet dieser Arbeit ist eine Überflutungsebene, welche sich im Kilombero Distrikt im Süden Tansanias befindet. Das Einzugsgebiet ist 40,240 km² groß, wovon das Feuchtgebiet eine Fläche von 96 km² bedeckt. Beide Feuchtgebiete sind durch eine Vielfalt von hydrologischen Charakteristika und durch unterschiedliche Nutzungsformen geprägt.

Das Monitoring der hydrometeorologischen Daten für beide Standorte wurde für zwei aufeinander folgende hydrologische Jahre (2015 und 2016) durchgeführt. Dazu wurden in den untersuchten Einzugsgebieten mehrere Transekte angelegt, innerhalb derer drei hydrologisch definierte Positionen untersucht wurden. Als hydrologische Positionen wurden die Uferzone, der Talrand und eine dazwischen liegende Position (Mittelposition) definiert. In beiden Feuchtgebietssystemen wurden an diesen hydrologischen Positionen hydrologische Messungen von Bodenfeuchte, Bodenbeschaffenheit und Grundwasserflurabstand durchgeführt. Darüber hinaus wurden Daten aus anderen Quellen ausgewertet.

Die Auswertung der Feldmessungen auf Feuchtgebietsebene des Talgrund-Feuchtgebietes ergibt, dass die räumliche und zeitliche Variabilität der Bodenfeuchte zur Uferzone hin signifikant steigt ($p<0,05$), jedoch wurde kein signifikanter Unterschied zwischen Mittelposition und Uferzone beobachtet. Die Verteilung der bodenhydrologischen Regime (gesättigt, nahezu gesättigt und ungesättigt) korreliert nicht mit den hydrologischen Positionen. Die zeitliche Variabilität der bodenhydrologischen Regime hängt stark von der Niederschlagsverteilung ab, wohingegen die

Topographie auf Mikroskala, Bodenbeschaffenheit, Entfernung vom Gewässer, anthropogene Faktoren und Landnutzung die räumliche Variabilität der Bodenwasserverfügbarkeit im Talgrund-Feuchtgebiet kontrollieren.

In der Kilombero-Überflutungsebene wurde das Hydrus-1D-Modell mit Hilfe gemessener Daten der Bodenfeuchte erfolgreich kalibriert (R^2 = 0,54-0,92, RMSE = 0,02-0,11). Kalibrierte Modellergebnisse eines Punktes wurden mit gemessenen Bodenfeuchtedaten eines anderen Punktes innerhalb derselben hydrologischen Position validiert und ergaben zufriedenstellende statistische Maße (R^2 = 0,36-0,89, RMSE = 0,03-0,13). Dies lässt auf eine Übertragbarkeit der Ergebnisse des kalibrierten Hydrus-1D-Modells zur Vorhersage der Bodenfeuchte anderer Punkte mit ähnlichen hydrologischen Bedingungen schließen. Die Bodenwasserspeicherkapazität nimmt zur Uferzone hin zu und erreicht dort 262,8 mm/Jahr. Die bodenhydrologischen Regime korrelieren mit den hydrologischen Positionen in der Überflutungsebene. Überflutungen, Niederschläge und Grundwasser steuern die Bodenfeuchtedynamik in der Ufer- und Mittelposition, während am Talrand Niederschläge und laterale Zuflüsse von den umliegenden Gebirgszügen die Bodenfeuchte während der langen Regenzeiten steuern. In der Trockenzeit und während der kurzen Regenzeit steuern Niederschlag, Bodenbeschaffenheit und atmosphärische Bedingungen die Bodenfeuchtedynamik in der Ufer- und Mittelposition.

Für die hydrologische Modellierung der Feuchtgebiete im Talgrund-Feuchtgebiet wurde durch die Kalibrierung und Validierung der täglichen Abflüsse (R^2 und NSE > 0,7) für beide Modellaufbauten (ArcSWAT2012 und SWATgrid) eine gute Modellleistung erreicht. Bei Betrachtung des Wasserhaushaltes im Jahresverlauf wird deutlich, dass 849,5 mm durch Evapotranspiration verloren gehen. Dies entspricht 65 % des Gesamtniederschlags. Der Oberflächenabfluss (77,9 mm) und Zwischenabfluss (86,5 mm) tragen am meisten zum Gesamtabfluss bei. Zusätzlich zum derzeitigen Landnutzungssystem wurden vier Landnutzungsmanagement-Optionen entwickelt, die durch unterschiedliche Schutzniveaus der Wasserressourcen gekennzeichnet sind (*vollständiger Naturschutz*, *Schutz der Hangsysteme*, *Schutz des Quellgebietes* und *vollständige anthropogene Nutzung*). Die ersten drei Bewirtschaftungsoptionen gehen mit abnehmendem Oberflächenabfluss und abnehmendem jährlichem Gesamtabfluss einher, wohingegen bei der vierten Option höhere jährliche Abflüsse zu verzeichnen sind.

Der zukünftige Klimawandel im Talgrund-Feuchtgebiet wurde mit den Klimaszenarien RCP4.5 und 8.5 von sechs GCM-RCM-Modellen aus dem CORDEX-Afrika-Projekt analysiert. Im Vergleich zum Referenzzeitraum 1976-2005 prognostiziert das Modell-Ensemble einen allgemeinen Temperaturanstieg von +0,9°C bis +1,9°C über den Zeitraum 2021-2050. Die sechs Klimamodelle prognostizieren variierende Änderungen der jährlichen Niederschläge (-30 bis 43,9 %). Im Durchschnitt zeigen die Modelle jedoch einen Anstieg der jährlichen Niederschläge um +7,4 % (RCP4.5) bzw. +21,8 % (RCP8.5).

Unter Anwendung der Klimamodell-Ensembles ermittelt SWAT eine zukünftige Abflussänderung, die der prognostizierten Niederschlagsänderung ähnelt. Die sechs Klimamodelle zeigen hinsichtlich der jährlichen Abflussänderungen hohe Unsicherheiten und prognostizieren Änderungen zwischen -44 % bis +149 %. Im Durchschnitt prognostizieren die Klimamodelle einen Anstieg von +16% (RCP4.5) bzw. +29% (RCP8.5). In der Regenzeit wird im Talgrund-Feuchtgebiet eine Zunahme des Abflusses erwartet, wohingegen in den Trockenzeiten abnehmende Abflüsse berechnet wurden. Im Vergleich zu Landnutzungsänderungen übt der Klimawandel einen dominanten Einfluss auf die Wasserressourcenverfügbarkeit im Talgrund-Feuchtgebiet aus. Durch die Implementierung der untersuchten Landnutzungsmangement-Optionen *vollständiger Naturschutz, Schutz der Hangsysteme* oder *Schutz der Quellgebiete* werden die Auswirkungen des Klimawandels auf den Gesamtabfluss und den Oberflächenabfluss deutlich reduziert. Des Weiteren können durch Umsetzung dieser Landnutzungsoptionen Evapotranspiration und Wasserverfübarkeit im Talgrund-Feuchtgebiet gesteigert werden.

Table of Contents

List of Figures

List of Tables

Abbreviations

ADC	Digital Acoustic Current meter
BD	Bulk Density
BMBF	German Federal Ministry of Education and Research
CEC	Cation Exchange Capacity
CORDEX	Coordinated Regional Climate Downscaling Experiment
DEM	Digital Elevation Model
dgwl	Depth to ground water level
DJF	December January February season
EC	Electrical Conductivity
ESCO	Soil Evaporation compensation
ET	Actual Evapotranspiration
FAO	Food and Agricultural Organization
FDC	Flow Duration Curve
FDR	Frequency-Domain-Reflectometry
FLA	Functional Landscape Approach
GCM	General Circulation Models
G_i	Capillary rise/ groundwater discharge;
GNSS	Global Navigation Satellite Systems
G_o	Groundwater recharge;
GWQ	Groundwater flow
HH2	Hand held moisture meter
HRU	Hydrological Response Unit
JJA	June July August season
K_{sat}	Saturated hydraulic conductivity

LAI	Leaf Area Index
LATQ	Lateral flow,
LULC	Land use and Land cover
MAM	March April May season
NaCRRI	National Crops Resources Research Institute
PET	Potential Evapotranspiration
RCM	Regional Climate Model
RCP	Representative Concentration Pathways
SAGCOT	Southern Agricultural Growth Corridor
SCS	Soil Conservation Service
SOC	Soil Organic Carbon
SON	September October November season
SRTM	Shuttle Radar Topography Mission
SUFI-2	Sequential Uncertainty Fitting
SURQ	Surface runoff,
SWAT	Soil and Water Assessment Tool
SWAT-CUP	Calibration and Uncertainty program
TanDEM-X	TerraSAR-X digital elevation model
TOPAZ	TOPographic PArametriZation tool
WMO	World Meteorological Organization
WYLD	Water yield
ΔS	Change in soil water storage
95PPU	95% prediction uncertainty

1. General introduction

1.1. Problem statement

Water is a key resource for sustaining all form of life, agricultural production and promoting economic development (Nsubuga et al., 2014). However, water is becoming a scarce resource and it has gained increasing attention, particularly in Sub-Saharan Africa (SSA) (Gowing, 2003). According to the united nations world water development report (2018), the increasing population and the economic growth are highlighted as the major pressures on the ecosystems providing water and other water related services. Agricultural expansion, urbanization, climate change pose numerous threats to water availability on water related ecosystem services. Wetlands are characterized with sufficient soil water availability for agricultural production and other water related services throughout the year (von der Heyden and New, 2003; Dixon and Wood, 2003).

Wetlands are commonly defined as areas of marsh, fen, peat land or water, whether natural or artificial, permanent or temporary, with water that is static or flowing, fresh, brackish or salt, including areas of marine water the depth of which at low tides does not exceed six meters (Ramsar Convention Secretariat, 2010). According to Mitsch and Gosselink (2015), wetlands are characterized by two geomorphological prerequisites which include sufficient water (hydrologic condition) and the topographic situation that permits the retention of water at or close to the surface. In SSA, wetlands are estimated to cover about 4.7% of the total land area (Rebelo et al., 2009). In Uganda, the wetland coverage is about 11% of the country's total land surface (Uganda wetlands atlas, 2016) while in Tanzania, wetlands cover an area of 7% of the country's total land surface (NEMC/WWF/IUCN, 1990).

In contrast to large wetlands such as marshes, and those around the Lake Victoria basin or Nile basin, small wetlands in East Africa have received little international research attention (Sakané et al., 2011).These wetlands mainly consist of lakes and alluvial floodplains along rivers (Harper and Mavuti, 1996) and inland valleys (von der Heyden, 2004), whose size rarely exceed 500 ha (Dixon, 2002). Small wetlands make up more than 80% of East Africa's total wetland area (Mwita et al., 2013). Furthermore, small wetlands are seen to have the potential to become the future food baskets of the East African region (Dixon and Wood, 2003). In fact, floodplain wetlands are in the focus of agricultural development projects due to their water availability, large size and high abundance in the region. For example, the Southern Agricultural Growth Corridor in Tanzania (SAGCOT),

which includes the Kilombero valley wetland, covers approximately one-third of Tanzania's mainland and is designed to improve agricultural productivity, food security and livelihoods in Tanzania (Paul and Steinbrecher, 2013).

Floodplain wetlands of the alluvial lowlands originate from rivers with high discharge variations inundating adjacent to low lying areas during high flows as a result of over bank flooding (Roggeri, 1995) (Fig. 1.1a). Seasonal rains cause flooding on the impermeable soils found on flat terrains while semi-permanently flooded back swamps may occur on the elevated levees and low-lying fluvial features. On the other hand, inland valleys are highly diverse and complex systems of variable ecosystems and are defined as the upper reaches of river systems, comprising valley bottom which may be regularly flooded, the hydromorphic fringe and the contiguous upland slopes and crests, relative to a hydrological network (Andriesse and Fresco, 1991; Windmeijer and Andriesse, 1993; Rodenburg et al., 2014) (Fig.1.1b). They are also called the headwater lowlands (Roggeri, 1995) and originate where runoff, subterranean flows and groundwater meet.

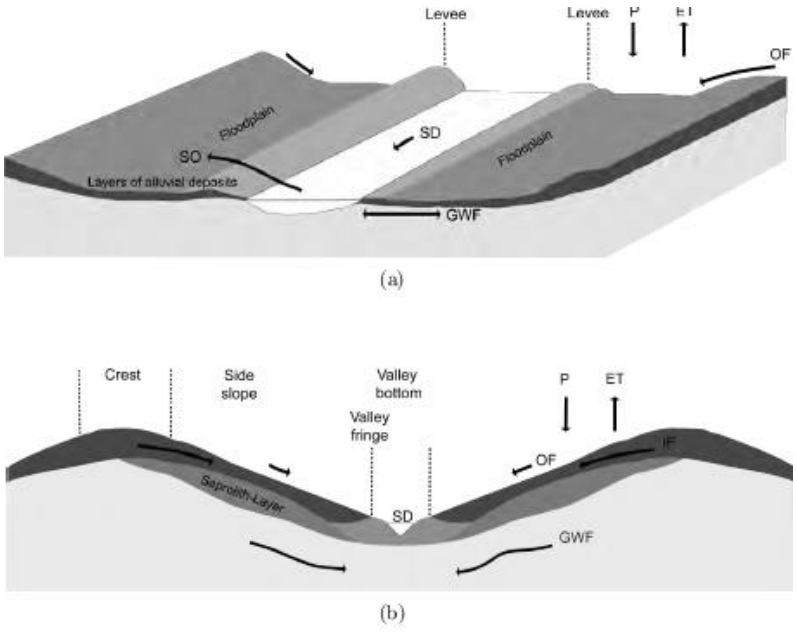

Fig. 1.1. Hydrological processes of two typical wetland types in East Africa. ET, Evapotranspiration; P, Precipitation; OF, Overland flow; GWF, Groundwater flow; SD, Stream discharge; SO, Spill-over; (a) Floodplain wetland; (b), Inland valley. Adopted from (Windmeijer and Andriesse (1993).

Wetlands fulfill a wide range of ecosystem services and functions which strongly vary with the type of wetland (MEA, 2005; Rebelo et al., 2010). To mention, the provisioning services (e.g. food

production, water, fibre, fuel and genetic materials), regulating services (e.g. climate and water regulation, water purification, erosion and natural hazard regulation, retention of sediments and habitat for pollinators), cultural (e.g. spiritual, recreational, and educational) and supporting functions (soil formation, nutrient cycling) ecosystem services.

While the cultivation of wetlands is considered to make a key contribution to food security, the conversion of pristine wetlands into production and settlement sites may jeopardize their ecosystem services, particularly the hydrological functioning (McCartney et al., 2011). Wetlands converted into agricultural and settlement sites have dramatically increased during recent decades in East Africa (Dixon and Wood, 2003; Sakané et al., 2011). For example, in Uganda, an increase of about 36.1% of the total wetland area under agriculture since 1994 is reported (Uganda wetlands atlas, 2016). According to MEA (2005) and Rebelo et al. (2010), the changes are attributed to factors such as urbanization, weak enforcement of wetland protection laws, soil nutrient depletion on the arable lands, the increasing demand for agricultural land to feed a rapidly growing population in the region (e.g. the population growth rate of 3.2% and 3.1% per annum is reported in Uganda and Tanzania, respectively (UBOS, 2017; National Bureau of Statistics, 2018), and the projected climate change, particularly the increased spatio-temporal variability of precipitation (Wood and van Halsema, 2008; Niang et al., 2014).

The conversion of wetlands into settlement and agricultural sites involves the clearing or frequent burning of the natural vegetation to create space for cultivation of subsistence food crops such as rainfed rice (*Oryza sativa. L*) or taro (*Colocasia esculenta*) during the wet season, or of maize along the wetland fringe (Böhme et al., 2016). Further, uncontrolled partial soil drainage is carried out at the fringes and riparian zones of the valley bottom which permit for upland crops' cultivation, mainly maize, sweet potatoes and beans in the rural areas and tomatoes and cabbage in the peri-urban areas (Kyarisiima et al., 2008). These changes in the land use management coupled with climate variability are likely to alter the spatio-temporal variability of the hydrological regimes and water resources such as water fluxes, water availability and hence the upstream-downstream interactions at the wetland-catchment scale.

Considering the current rate of wetland conversion and their diverse ecosystem services that wetlands fulfill, there is a need to provide scientific guidelines for future food production and water resources management. Such planning and management of the wetland water resources requires a

better understanding of their hydrological functioning and landforms at the different spatial scales (Chuma et al., 2012). Several examples of hydrological wetland research at different scales in East Africa exist. For instance, Näschen et al. (2018) quantitatively analyzed the water balance to understand the impact of land use changes and demographic growth on the water resources at the wetland-catchment scale for the Kilombero floodplain in Tanzania. Also, Burghof et al. (2017) developed a hydrogeological conceptual model at the wetland scale to understand the groundwater/surface water interaction in the Kilombero floodplain, Tanzania. Furthermore, the impacts of land use changes on the hydrological flow regimes for the Usangu wetland and the Great Ruaha River in Tanzania were studied by Kashaigili et al. (2007). In addition, Böhme et al. (2016) investigated the relationship between soil water availability, land use and morphology of an inland valley wetland in Kenya.

In the context of agricultural production, water resources, specifically water availability in wetland soils, is the most important hydrological attribute controlling nutrient dynamics (Danvi et al., 2018; Worou et al., 2012). Thus the management practices implemented at the wetland-catchment scale influence its availability and the hydrological regimes (Dixon and Wood, 2003; Wood and van Halsema, 2008; Böhme et al., 2016). In addition, climate change has an effect on the water resources of the wetland and its catchment (Lacombe et al., 2017; Danvi et al., 2018). Therefore, quantitative analysis of the impact of the ongoing changing climate and land use management on the hydrological functioning of these wetlands and their catchments at such a small scale require increased research attention in the face of wetland conversion into sites of agricultural production, given that their morphological settings are different from one wetland to another. However, to quantitatively analyse the land use management and climate change on the system's hydrological processes, simulation models that effectively represent these processes are required, more so in data scare regions like East Africa.

1.2. Research questions

The following research questions were formulated from the above problem statement;

(i) **What are the different hydrological regimes and the spatial and temporal dynamics of soil water availability in the inland valley wetland and how accurate and reliable are the freely available digital elevation models with different resolutions in determining these hydrological regimes?**

The first research question addresses the issue of soil hydrological regimes and soil water dynamics at a wetland scale for an inland valley. Soil water availability in wetlands is the most important hydrological attribute, determining their agricultural production potential. Agricultural disturbances and the wetland's micro-topographic variability influence the spatial and temporal variation of soil water and the hydrological regimes, thus the complexity of the hydrological behaviours in the inland valley wetlands. Consequently, there are limitations of common assumptions regarding relationship between hydrological and topographical regimes.

Microscale topography influences the wetland's hydrological processes e.g. hydrological regimes and varies from one wetland to another. Therefore, to understand the spatial distribution of hydrological processes at a broader scale, information on microscale topography is required. This arises the question on how good and reliable are the different globally available digital elevation models (DEMs) being used in modeling the hydrological processes, more so in financially constricted and data scarce regions. This knowledge can guide in simulating the wetland's hydrological regimes, water and solute fluxes and also guide in understanding their capacities for sustainable agriculture.

(ii) **What is the impact of different land use management options on the water resources of an inland valley?**

The investigated inland valley is one of the headwater catchments in the Lake Kyoga basin experiencing a high rate of land use management dynamics under changing climate. Yet there is limited literature available showing a clear trend on the impact of land use management approaches on the water resources at the wetland-catchment scale, more so at smaller scales which are intensively utilized for agriculture and little research attention is paid to them.

(iii) **How does possible future climate change impact the water resources of the inland valley**?

The vulnerability and resilience of wetland water resources to climate change, particularly variability in precipitation needs to be given attention since these ecosystems are seen as potential areas for food production due to the declining productivity of arable upland slope areas.

(iv) What are the spatial variabilities in soil water availability in a tropical floodplain and what factors influence them?

Analyzing the spatial distribution of soil moisture is critical for ecohydrological processes and for sustainable water management studies in wetlands. The characterization of soil water dynamics and its influencing factors in agriculturally used wetlands pose a challenge in data-scarce regions such as East Africa. High resolution and good-quality time series soil moisture data are rarely available and gaps are frequent due to measurement constraints and device malfunctioning.

To address these research questions, the following objectives are formulated.

1.3. Objectives of the study

The overall objective of this study is to acquire a better understanding of the impacts of land use management and climate change on the small-scale hydrological processes and water availability in the agriculturally used wetlands of East Africa. Further, this study aims to contribute to the sustainable development goals (SDG) 2 on wetlands and food security, and SDG 6 on wetlands and sustainable water management by improving wetlands productivity through sustainable wetland-catchment agriculture and water resources management in East Africa. However, to achieve the sustainable wise use of wetlands, a thorough understanding of the interaction of these wetland systems and their contributing catchments in terms of the hydrological behaviors and responses under the ongoing land use management and climate changes needs to be analyzed. Specifically, the objectives of the study are to:

(i) determine the hydrological regimes in an agriculturally used tropical inland valley wetland in central Uganda using soil moisture, groundwater, and digital elevation data,
(ii) assess the impact of land use management on the water resources in an inland valley,
(iii) assess the hydrological response to climate change in an inland valley by the mid- 21st century, and
(iv) improve the understanding of the soil water dynamics along a wetland transect in the Kilombero floodplain, Tanzania.

1.4. Project framework

This study was conducted within the framework of GloBE: wetlands in East Africa project (FKZ: 031A250A-H): Reconciling future food production with environmental protection. The project was funded by the German Federal Ministry of Education and Research and the German Federal Ministry for Economic Cooperation and Development. The objectives of the GloBE wetlands project were (1) to understand the wetland system, (2) to optimize wetland use considering wetland-catchment interaction, (3) to integrate data and assess scenarios at the wetland –sub-regional scale, and lastly, (4) to extrapolate the results and formulate recommendations at wetland –national scale. Based on the findings, science-based guidelines, tools and policy advice to facilitate the transformation of wetland areas into the breadbasket of East Africa, while protecting the environment and human health are developed. The thesis mainly addressed study objectives (1) and (3) from the hydrological point of view.

1.5. Structure of thesis

The thesis consists of nine chapters starting with this general introduction. Chapter 2 presents a general description of the study areas, whereas the instrumentation and data monitoring procedures applied are presented in Chapter 3. Chapter 4 addresses the modelling approaches used in the study at the different spatial scales notably (i) wetland-catchment scale interactions in a Ugandan inland valley: Soil and Water Assessment Tool (SWAT), and (ii) plot scale along the floodplain transect in Tanzania: Hydrus-1D model. In order to present the study in a systematic way, the research topics of Chapters 5 to 8 follow an order of study area scale, namely, wetland scale, wetland-catchment scale, and plot scale along a floodplain-wetland transect. Specifically, determining hydrological regimes in an agriculturally used tropical inland valley wetland in central Uganda using soil moisture, groundwater, and digital elevation data is presented in Chapter 5. In Chapter 6, model results of the impact of land use management on water resources in a tropical inland valley catchment in central Uganda are presented. Chapter 7 focuses on the hydrological response to climate and land use management change in an inland valley for the middle 21st century using an ensemble of CORDEX climate scenarios. In Chapter 8, the application of Hydrus-1D to simulate soil water dynamics in a tropical floodplain transect at plot scale is described. Lastly, chapter 9 presents the general conclusions and the perspectives derived from the study.

2. Study area

2.1. Introduction

The present study focuses on two riverine wetlands: an inland valley wetland of Namulonge in Uganda and a floodplain wetland of Kilombero in Ifakara, Tanzania. Both sites are considered representative reflecting the prevailing land use management and other features for the region according to the typology work described by Beuel et al. (2016). The two selected research areas are situated in the subtropical region of East Africa (Fig. 2.1). The Namulonge research area is situated in central Uganda, north of Kampala capital city. It is a small inland valley bottom wetland undergoing permanent land use changes and degradation like other wetlands in the region. This study covers the whole wetland and its contributing catchment to assess the hydrological behaviour of the ecosystem under changing land use and climate. The study area in Ifakara is a wetland transect located in the Kilombero district, Morogoro region, south central Tanzania. Ifakara is at the edge of the Kilombero valley, north eastern direction, a vast lowland floodplain wetland drained by the Kilombero River. As the wetland covers a main area of about 8000 km² from which 96 km^2 are investigated in this study and has a catchment of around 40000 km^2 (Näschen et al., 2018), the research area represents a small part of the wetland – catchment continuum to understand the hydrological processes dynamics. The following sections present more detailed description of the respective research areas.

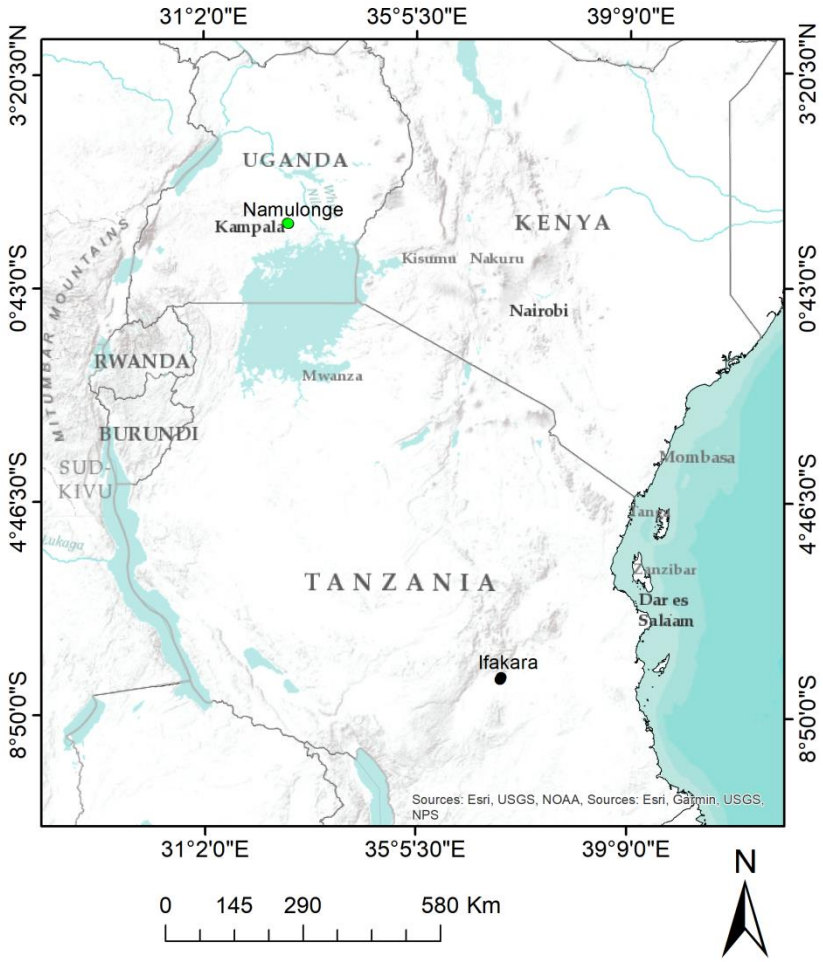

Fig. 2.1. Location of the two study areas (Namulonge, Uganda and Ifakara, Tanzania).

2.2. Namulonge study area

2.2.1. Location

The Namulonge inland valley is situated in a headwater catchment of the Lake Kyoga basin, Wakiso district, and lies between latitude 0˚ 30`– 0˚ 34´N and longitude 32˚ 34`– 32˚ 40´E. It is found 30 km north of the capital city Kampala in the central region of Uganda (Fig. 2.2). The catchment area of the inland valley comprises approximately 31.1 km^2 with about 4.5 km^2 of wetland area extending in north-east direction over a distance of 8.7 km to the outlet from the upper catchment.

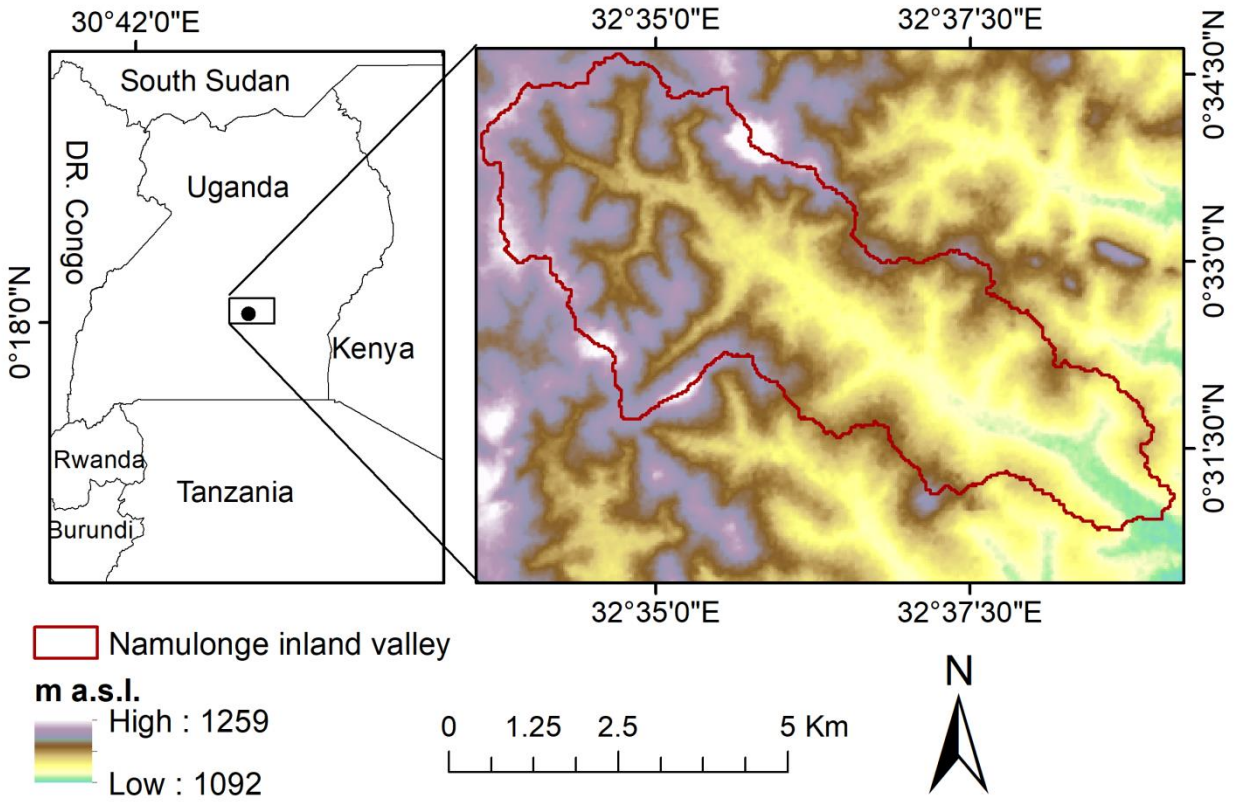

Fig. 2.2. Location of the study area in Uganda.

2.2.2. Climate

The climate is tropical wet and dry with a mean annual precipitation of 1200 mm. The annual precipitation is distributed in a bi-modal structure. The first rainy season, which is also the longest, occurs between March and May (MAM). The second and shorter rainy season occurs between September and November (SON). It is also noticed that the transitions between the rainy and dry seasons are not well marked and precipitation occurs through the year (Fig. 2.3). The average annual temperature is 22°C (Nsubuga, 2000). The area experiences the highest temperatures in February and the lowest in July. The difference in precipitation between the driest and wettest months is 115 mm and temperature varies by 1.7°C throughout the year (Fig. 2.3).

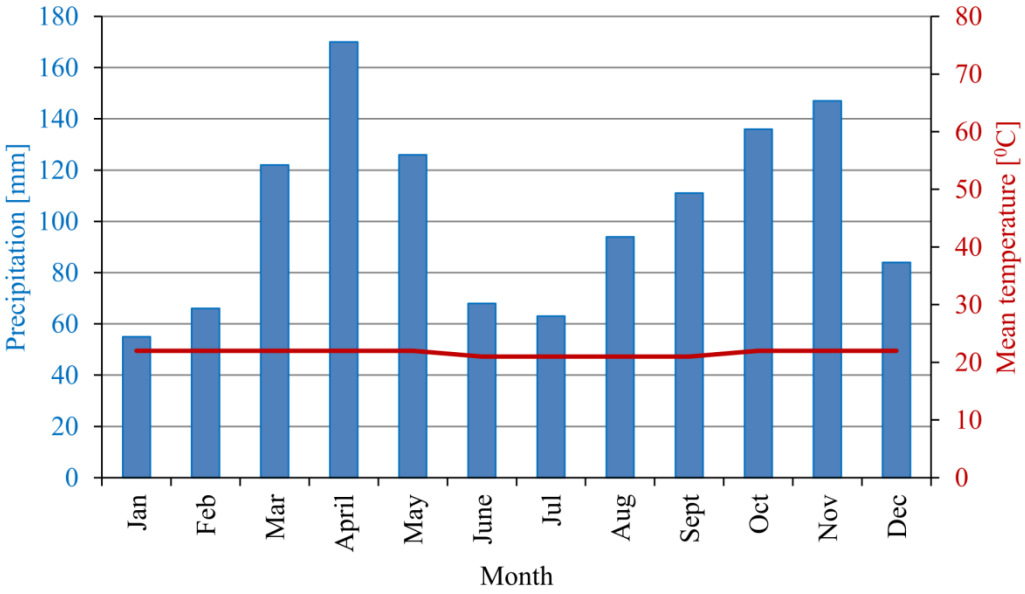

Fig. 2.3. Precipitation and temperature conditions of the Namulonge inland valley (modified after climate-data.org).

2.2.3. Hydrology

The main stream (locally called Nasirye) of the Namulonge inland valley wetland drains into Lake Kyoga through its tributary the Lwajali River (Fig.2.4). Lake Kyoga forms the second largest drainage sub basin in Uganda (Nsubuga, 2014). The Lake Kyoga basin consists of a vast network of diverse wetlands with abundant surface and groundwater resources. However, the wetland resources are continuously degraded by anthropogenic activities particularly by intensive agricultural activities (Ministry of Water and Environment, 2010). Due to its agricultural use, the main stream of the inland valley has been modified. At some positions along the channel the water is diverted to the small agricultural farmer plots in the valley for irrigation; especially during the dry season since the stream flow is perennial. Consequently, there is variable stream width (1 to 3 m) and depth (1 to 2 m) from the inlet (northwest) to the outlet (southeast), where it drains into the Lwajali River and only partly follows the local scale topography. This results in variable discharge volumes along the stream.

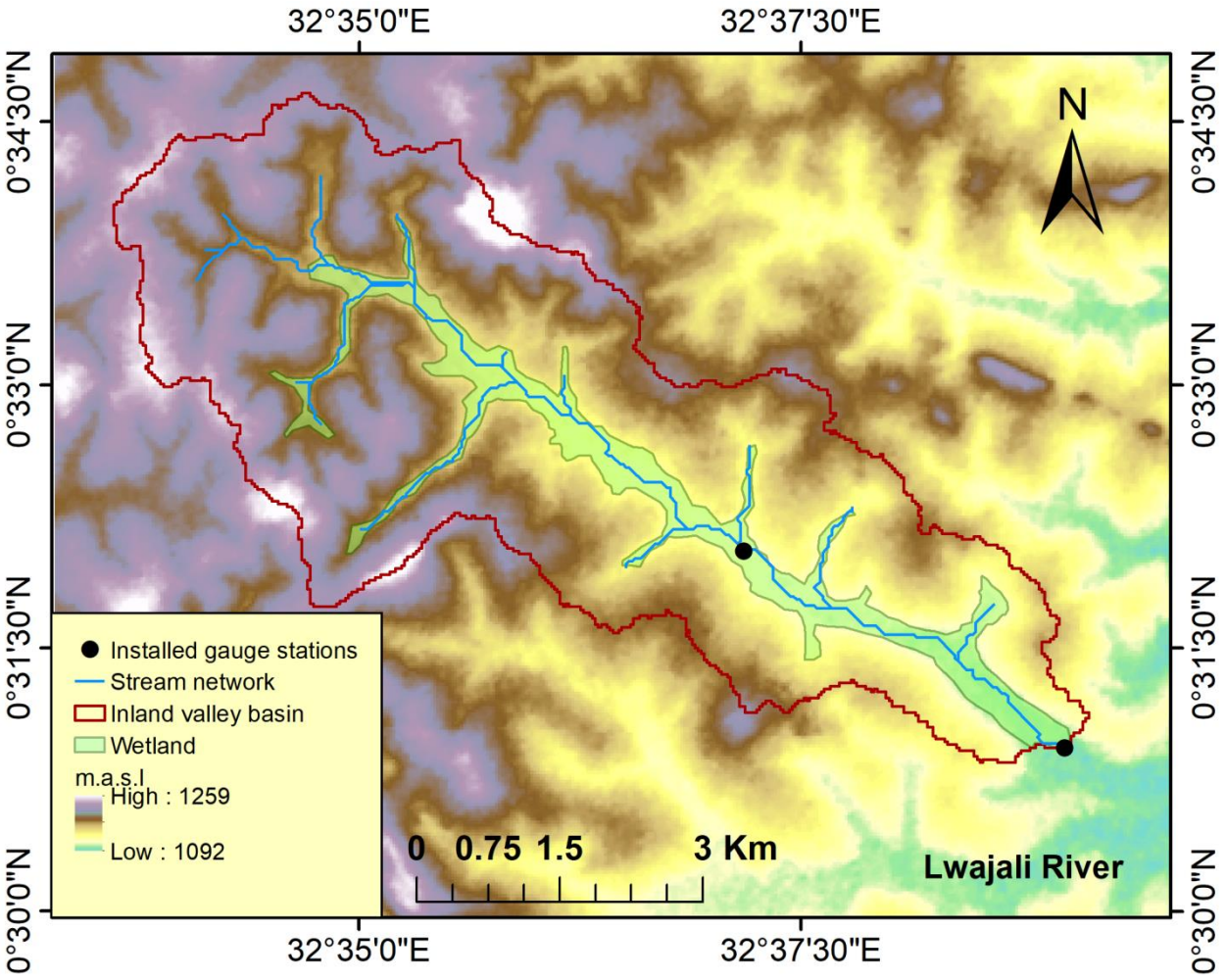

Fig. 2.4. Stream network of the Namulonge inland valley catchment.

2.2.4. Geology, geomorphology and soils

The inland valley catchment of Namulonge is situated at the boundary between the basement complex and the Buganda-Toro system (Burghof, 2017). The basement complex is comprised of orthogneisses and the Kampala granitoids, consisting heterogeneous granitoids and banded gneisses of mainly plutonic origin (Westerhof et al. 2014).The Buganda-Toro system is represented by the Buganda Group, with Victoria and Nile formations. The Victoria formation is characterized by orthoquartzites and conglomerates existing as small patches distributed in the catchment, and the Nile formation is represented by slates, shales, phyllites and porphyroblastic phyllites (Burghof, 2017). The valley of the catchment is filled with quaternary sediments described as alluvium swamp and lacustrine deposits (GTK consortium, 2012). The topography of the region is described by an undulating landscape, with gently, wavy slopes alternate with wetlands in the shallow valley

bottoms (Myamoto et al. 2012). The elevation decreases from west to east, with values ranging between 1090 metres above sea level (m.a.s.l.) and 1250 m.a.s.l. The major soil types of the inland valley catchment are Nitisols found on the slopes and Gleysols which mainly occur in the valley bottom and the wetland fringes. According to Jones et al.(2013), the Nitisols are undifferentiated at the slopes and hilltops, showing a deep red color with a well-developed nut-shaped structure, suitable for cultivation of a wide range of crops. Yost and Eswaran (1990) explains that Nitisols along the slopes are formed from quartzite, gneiss and laterite while in the valley they are mainly formed from alluvium.

2.2.5. Land use and vegetation

Namulonge is comprised of intensive smallholder agricultural practices and is also a research site of the National Crop Resources Research Institute (NaCRRI), whose mandate is to develop improved varieties and farming technologies for the people of Uganda (Nsubuga, 2000). Agriculture is mainly practiced by residents who are current or past employees of the research institute. The Namulonge inland valley is thus characterised by intensive smallholder subsistence agriculture with a mosaic of land use types and management practices. Native vegetation, mainly papyrus (*Cyperus papyrus* L.), exists at the lower valley section albeit increasingly converted to agricultural land for food crops which include rice (*Oryza sativa* L.), taro (*Colocasi*a e*sculenta (L.) Schott*) cultivated under saturated or near saturated conditions, and upland crops like maize (*Zea mays* L.), beans (*Phaseolus vulgaris* L.), sweet potatoes (*Ipomoea batatas* L.), and vegetables. Upland crops are cultivated in the wetland on artificially raised ridges with shallow drainage channels created around the plots to drain excess water since upland crops are susceptible to water logging. During the dry spell, drainage channels are used for irrigating plots after diverting stream water. This practice encourages continuous cultivation throughout the year. Some plots are abandoned as fallow in the valley after a long period of cultivation. The native vegetation of the inland valley is papyrus (*Cyperus papyrus L*) and tropical rainforests but has been significantly reduced by human activities. Intensive subsistence agriculture with a mosaic of land use types and management has increased in the inland valley catchment (Gabiri et al. 2018).

2.3. Kilombero floodplain

2.3.1. Location

The Kilombero catchment is part of the Rufiji basin, the largest basin in Tanzania. Administratively, the catchment is situated in the Kilombero and the Ulanga districts, Morogoro region, Southern Tanzania at around 8°S and 36°E. The catchment has elevations ranging from 250 to 2500 m a.s.l. (Fig. 2.5). The Kilombero catchment covers an area of 40,000 km^2 including the broad floodplain of the main Kilombero river with a spatial extent of about 8000 km^2 (Mombo et al., 2011) including the study area of about 96 km^2 (Fig. 2.5).

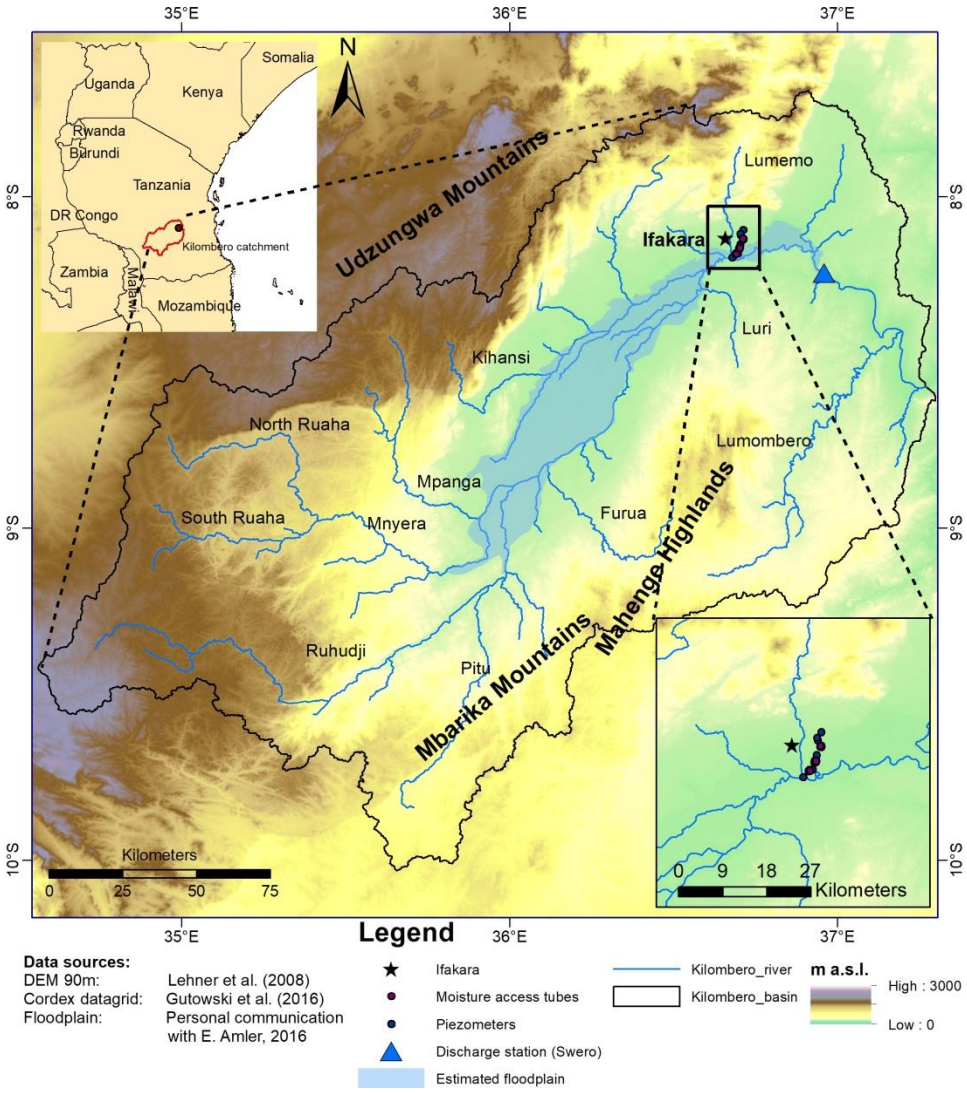

Fig. 2.5. Location of the Kilombero floodplain and the investigated area (Näschen et al., 2018).

2.3.2. Climate

The climate is sub-humid tropical with annual precipitation ranging from 1200 to 1400 mm possessing high interannual variability (Näschen et al. 2018). A high spatial variability exists between mountainous areas and the valley bottom. In fact, the total annual precipitation is 2100 mm in the mountains and 1100mm in the valley bottom (Jätzold and Baum,1968).The mean annual temperature is 25°C (Koutsouris et al., 2016) (Fig.2.6). The precipitation is distributed in a bi-modal structure. The long rainy season is from March to May (Snyder, 2005), which corresponds to the movement of the Intertropical Convergence Zone (ITCZ) (Näschen et al. 2018). The short rainy season spans from October to December (Mombo et al., 2011), (Fig.2.6). However, there is intermittent season (January and February) in which precipitation might be higher than in November and December. The flood peaks from both the precipitation and overbank flow from the Kilombero River are experienced mainly during the long rainy season although they can also happen as early as January.

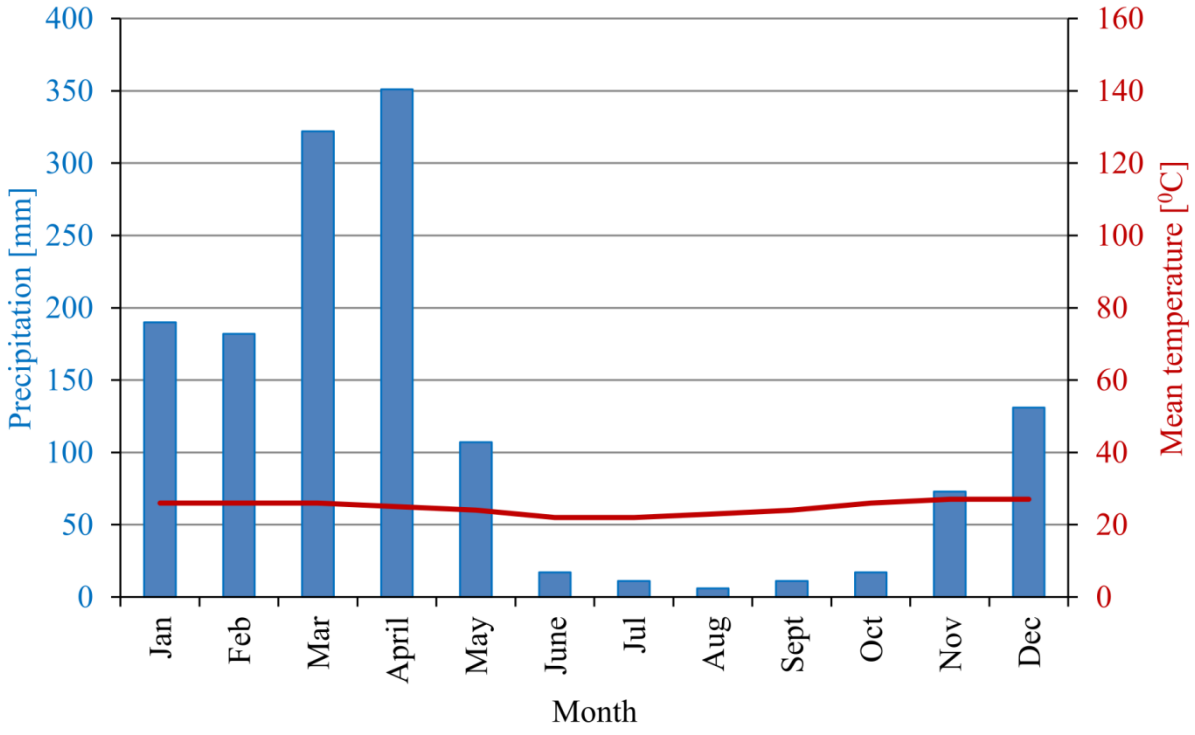

Fig. 2.6. Precipitation and temperature conditions of the Kilombero valley (modified after climate-data.org).

2.3.3. Geology, geomorphology and soils

The geological substrate in the floodplain includes mainly a sedimentary basin, forming a seasonal alluvial floodplain dominated by Fluvisols soils (Beck, 1964). However, according to Bonarius (1975), sediments constitute alluvial fans, river deposits, and colluvial materials. The alluvial fans mark the transition between the floodplain and the fringes, with high infiltration rates and high soil moisture variability (Bonarius, 1975). The soils tend to crack upon drying and experience ponding once the soil is swollen and cracks are closed. According to Näschen et al. (2018), the catchment is predominantly characterized by Fluvisols in the valley bottom and Acrisols and Nitisols in the upland realms. Lixisols are found mainly in the western upland soils, whereas Cambisols dominate the lower eastern part of the catchment (Näschen et al. 2018) (Fig. 2.7).

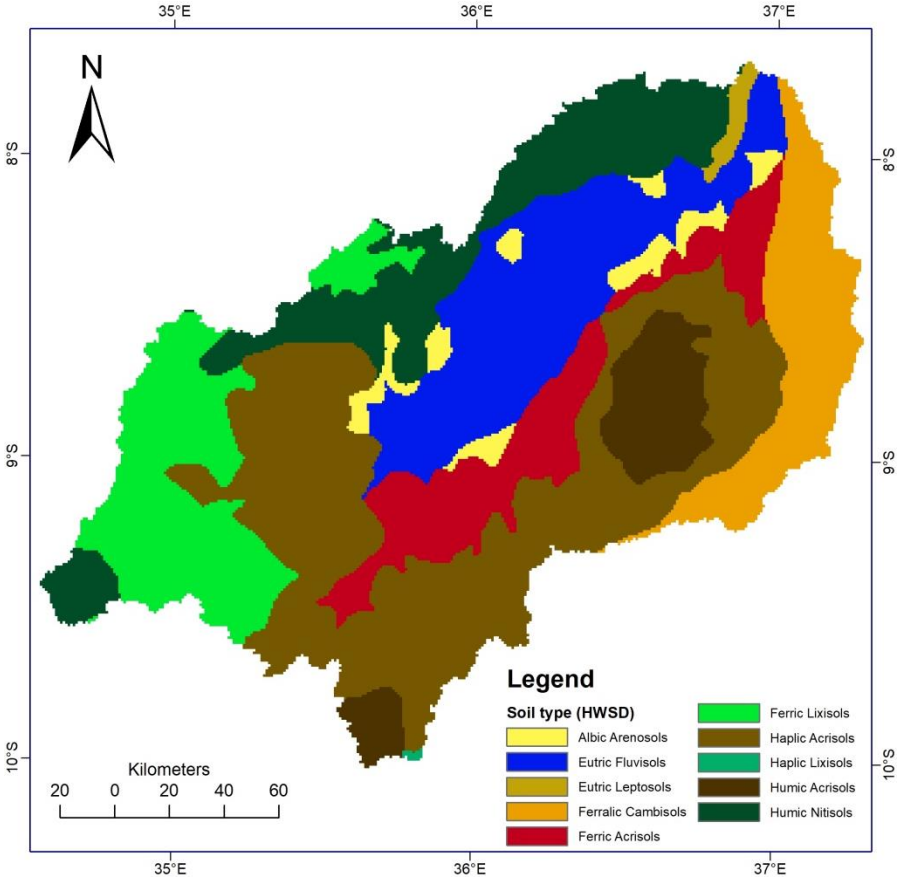

Fig. 2.7. Major soil groups in the Kilombero catchment according to the Harmonized World Soil Database (modified after Näschen et al. 2018).

2.3.4. Hydrology

The Ruhudji River is the main tributary of Kilombero River, flowing through steep and narrow valleys in the southwestern catchment to the valley bottom. Ruhudji River is joined by the Pitu and Mnyera Rivers from the south and west, respectively, and at this point, the Kilombero River begins its course according to FAO (1960). The valley is seasonally flooded with a water table fluctuation of about 6 meters (Yawson et al., 2005) and drained by the Kilombero River, which forms a typical braided river system due to the decreasing elevation gradient (Jätzold and Baum, 1968).

Kilombero River is an important tributary catchment of the Rufiji River Basin, contributing 62% of the total annual average basin water flow (Mwalyosi, 2000). A number of perennial and seasonal streams drain into the Kilombero River from the Udzungwa Mountains in the north-west and the Mahenge Mbarika escarpment in the south-east with elevation ranging from 250 to 2500 m a.s.l. (Mombo et al. 2011; Leemhuis et al. 2017). The Lumemo River is one of the major tributaries draining into the studied wetland transect from north to south. Overall, the Kilombero valley is dependent on mountainous water resources and year-round groundwater contribution (Näschen et al. 2018). Within the study area, groundwater flow is from north to south towards the Kilombero River throughout the year (Bonarius, 1975). Therefore, groundwater is the major source of drinking water for the communities within the catchment, with several small functional hand pumping wells observed (Burghof et al., 2017). With an average discharge rate of 520 m^3/s from the Swero station of Kilombero River, the overall runoff in the catchment is very high (FAO, 1960), and characterized by a distinct rainy and dry season (Yawson et al., 2005). Näschen et al. (2018) explains that lateral flow and surface runoff only occur in the rainy season, with peaks in March and April while base flow peaks are markedly observed in April and May, resulting into high total discharge in April. Evapotranspiration and potential evapotranspiration differ by 150 mm/month in September and October, signifying water deficit in the dry season (Näschen et al. 2018).

2.3.5. Land use and vegetation

The floodplain in the Kilombero catchment was declared a Ramsar site because of its rich and unique ecosystem (rsis.ramsar.org). The floodplain is characterized by diverse land uses, land use intensity gradients, and interactions between large- and small-scale crop farmers, landless herders and urban populations. Also, it is predominantly characterised by the Miombo woodlands which consist of mainly Brachystegia species and grasses such as reed (*Phragmites mauritianus*), guinea

grass (*Panicum maximum*), and elephant grass (*Penisetum purpureum*) (Nindi et al., 2014). Agriculture is the main economic activity in the valley. Agricultural production is practiced at both subsistence and commercial scale. Lowland rainfed rice is the dominating food and cash crop cultivated in the valley, however, other crops such as maize and peas are grown especially during the short rainy season.

However, the wetland poses a range of agro-industrial activities and has also been earmarked for future investments in agricultural development to enhance food security in the region through the "southern agricultural growth corridor" (SAGCOT) (Paul and Steinbrecher, 2013). In this framework, water will be withdrawn from the Kilombero River for irrigation agriculture (Ministry of Water URT, 2012).

Besides a range of agro-industrial uses (mainly sugar cane), cropland in the valley is dominated by rainfed rice (during the long rainy season). Several irrigation schemes allow for year-round irrigated rice production. In fact, the floodplain supplies about 9% of all rice produced in Tanzania (Camberlin, and Philippon, 2002).

3. Instrumentation and monitoring data

3.1. Introduction

Inland valleys and floodplains in East Africa are rarely hydrologically instrumented though they are often used for intensive agricultural practices towards achieving food security. Because of their complexities interms of their hydrology and geomorphological characteristics, they are rarely instrumented and assessed for hydrological monitoring yet they perform a vast of ecosystems services to the human welfare and environment. Therefore, good assessment of these ecosystems' properties is needed for sustainable wetland management. In this study, the hydrological processes were studied in space and time applying field scale based analysis, point scale modelling using the Hydrus-1D model for the floodplain and wetland-catchment modelling with the Soil and Water Assessment Tool (SWAT) in the inland valley. Monitoring of hydrological and meteorological data for both sites was conducted for two hydrological consecutive years of 2015 and 2016. The following sections document the models input data, field experimental designs and instrumentation and the data collected for the different studied wetlands.

3.2. Materials and methods

3.2.1. Study design and instrumentation at wetland scale

Namulonge inland valley

The longitudinal extent of the valley was subdivided into upper (T1), middle (T2, T3) and lower (T4) transects (Fig. 3.1). Distance between transects was 1.3 km for T1 and T2, 1.5 km for T2 and T3, and 0.9 km for T3 and T4. The cross–section of the valley (toposequence) was subdivided into four hydrological positions defined as riparian zone (poorly drained), valley bottom (moderately drained), fringe (seasonally wet), and valley slope (well drained) for each defined transect. Hydrological instrumentation and data collection was conducted along these transects and the four hydrological positions.

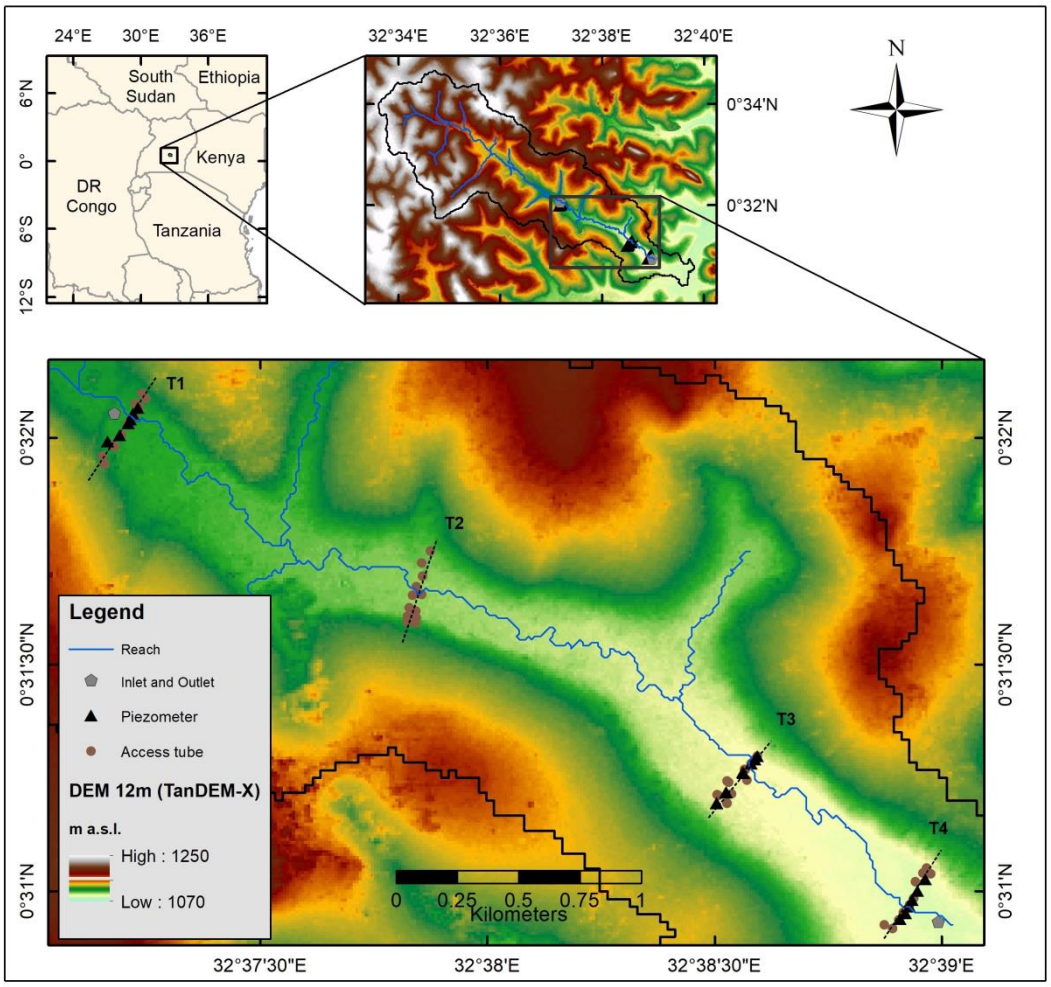

Fig. 3.1. Overview of wetland transects and instrumentation along the Inland valley. The map and reach or stream are derived from the TanDEM-X-12m digital elevation model (DEM).

Kilombero Floodplain

The valley was subdivided into three hydrological zones (riparian, middle, and fringe, see Fig. 3.2a) based on the origin of flooding water, its extent, and duration. A total of 462 Landsat 7 Enhanced Thematic Mapper Plus (ETM+) and 8 Operational Land Imager (OLI) surface reflectance images across 6 tiles from the years 2013 to 2015 with a cloud coverage < 80% were processed (Daniel et al., 2017). Their multi-temporal statistical values were classified in a Random Forest approach to delineate riverine flooded areas and generate inundation extents for seasonally flooded zones during the long rainy season (Fig. 3.2a). The non-flooded zone was defined as fringe, characterized by precipitation and groundwater table induced flooding (Burghof et al., 2017). The middle zone is partially flooded whereas the riparian zone is nearly completely flooded during the

long rainy season. Further spatial differentiation of the hydrological zones included the application of the TerraSAR-X digital elevation model with a resolution of 12 m (TanDEM-X-12 m) to derive the absolute height and the distance from river (Daniel et al., 2017). The lower parts of transect is flooded longer with higher water depth, thus the riparian zone was close to the river with lower absolute height altitude (Fig. 3.2a).

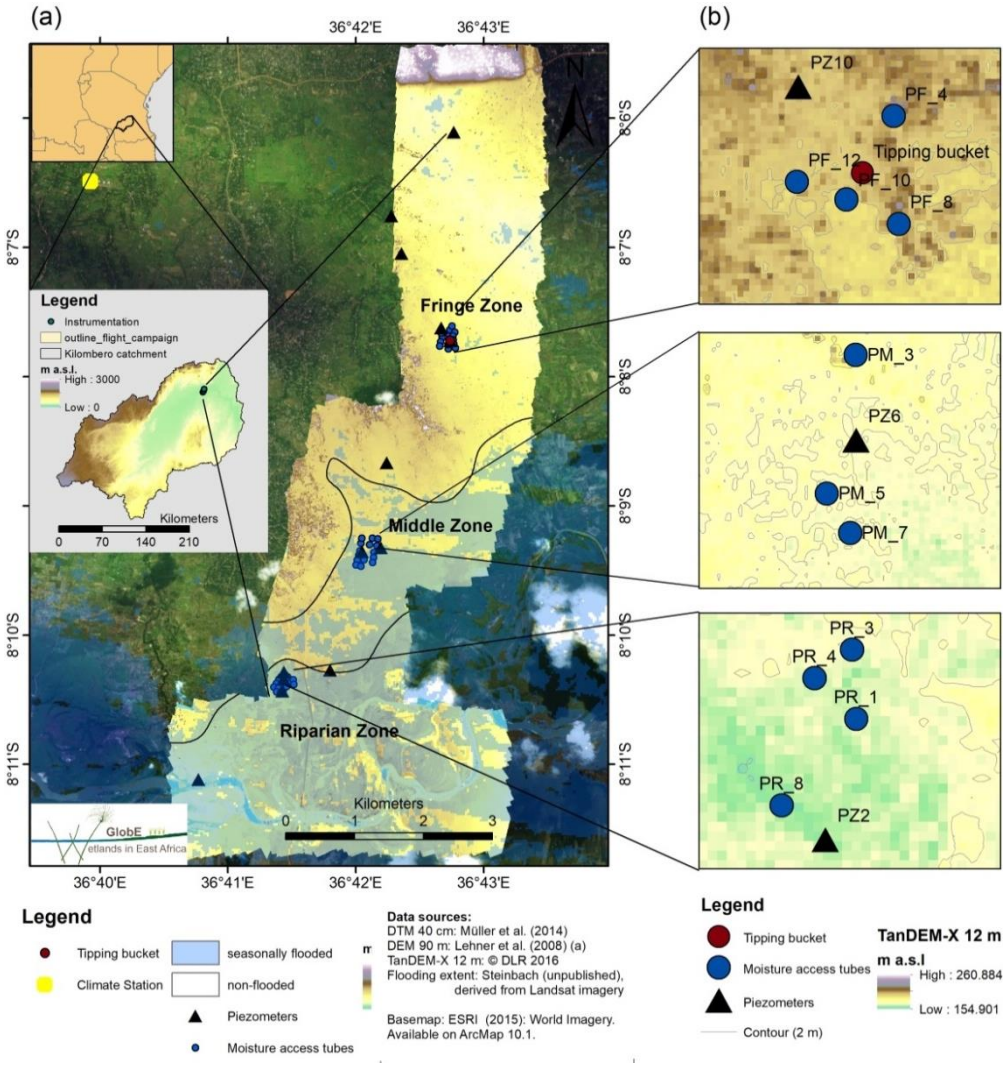

Fig. 3.2. An overall overview of hydrological zones and instrumentation in the Kilombero floodplain, Tanzania.

3.2.2. Climate data and climate scenarios

To conduct a field scale based analysis on the hydrological behaviour and hydrological regimes of the inland valley wetland as presented in Chapter 5 and the point scale modeling using Hydrus-1D in the floodplain, rainfall data was measured using a tipping bucket rain gauge with a 0.2 mm resolution (Stevens Water Monitoring Systems Inc., 2007). The rain gauge was installed at the fringe position of the inland valley wetland (Transect 3, Fig. 3.1) and the floodplain (Fig. 3.2b). The location of the tipping bucket was selected following recommendations after the World Meteorological Organisation (WMO). Moreover, to set up the Hydrus-1D model in the Kilombero floodplain, daily temperature, relative humidity, solar radiation and wind speed climate data were acquired from an automatic climate station situated close to the study area (Fig. 3.2a).
Furthermore, climate data including precipitation, temperature, relative humidity, wind speed and solar radiation were obtained from the National Crops Resources Research Institute (NaCRRI) automatic weather station database for the different periods in the Namulonge inland valley; i) 2015 to 2016 for the calibration and validation of the SWAT model, ii) 1976 to 2005 climate data from NaCRRI weather station for use as ground historical climate data in the analysis of climate change.

To assess the impact of climate change on the water resources in the inland valley as presented in Chapter 7, simulated climate data for an ensemble of six global-regional climate models (GCMs-RCMs) from Coordinated Regional Climate Downscaling Experiment (CORDEX - Africa) project (www.cordex.org) was downscaled by the Meteorology Institute, Köln University, Germany (http://www.geomet.uni-koeln.de/). The six models were selected by region i.e. Northern area (3-4° N, 28- 40° E) and southern area (10-3° S, 28- 40° E) and by per season (long and short rains). The selection was based on comparing simulations for the period 1986 to 2005 with modelled data for the period 2040 to 2059. The selected six models represent a wide spectrum of precipitation signals, with increasing, decreasing, and constant precipitation patterns when comparing the periods from 1986-2005 with 2040 - 2059. Two “Representative concentration pathways”–RCP (RCP 4.5 and RCP 8.5) were considered.

3.2.3. Hydrological data collection

Discharge data in Namulonge inland valley

To measure discharge at the outlet of the inland valley of Namulonge, the suitability of the location was warranted following the WMO (2008) guidelines, which include among others the straightness course of the stream, a free vegetation channel and readily accessible for ease in installation and monitoring. After the selection of the discharge measurement site at the catchment outlet (Fig. 3.1), measurement device (YSI 6- series sonde, Ecotech), (Fig. 3.3) was installed to continuously record the water pressure every 15 minutes interval. In addition, a stuff gauge was installed at the same position of the sonde (Fig. 3.3) as a backup, in case the probe experienced a breakdown. Several instantaneous discharge measurements at different periods were conducted using a digital acoustic current meter (ADC, OTT Hydromet GmbH) to establish the relationship between stage and discharge following the recommendations after Fenton and Keller (2001).

Fig. 3.3. Installation of the discharge gauge in the inland valley in Namulonge.

Shallow ground water data

Shallow groundwater monitoring was conducted at the wetland scale for all the study areas in order to understand its spatial and temporal variability at the different hydrological positions. Additionally, depth to shallow groundwater data was used for the Hydrus-1D modelling in the Kilombero floodplain (Chapter 8). Depth to shallow groundwater was measured hourly by pressure data loggers of Ecotech installed in 10-cm-diameter piezometers (Fig. 3.4) for both study sites (Fig. 3.1 and Fig. 3.2).

Fig. 3.4. Piezometer installation, (a), inland valley in Uganda, (b), floodplain in Tanzania.

In the inland valley wetland, 10-cm-diameter piezometer pipes were installed at each hydrological position except at the lower slope (Fig. 3.5), due to depth limitation of the hand drilling equipment (with drilling maximum depth of 5.5 m) used during piezometer installation. In this case, we could not equip the lower slope with piezometers due to its high depth to groundwater of larger than 5.5 meters. A total of 20 piezometers screened at different depths (1.5 to 2.99 m depth) due to variable aquifer depth were installed along three transects in the inland valley wetland (Fig. 3.5).

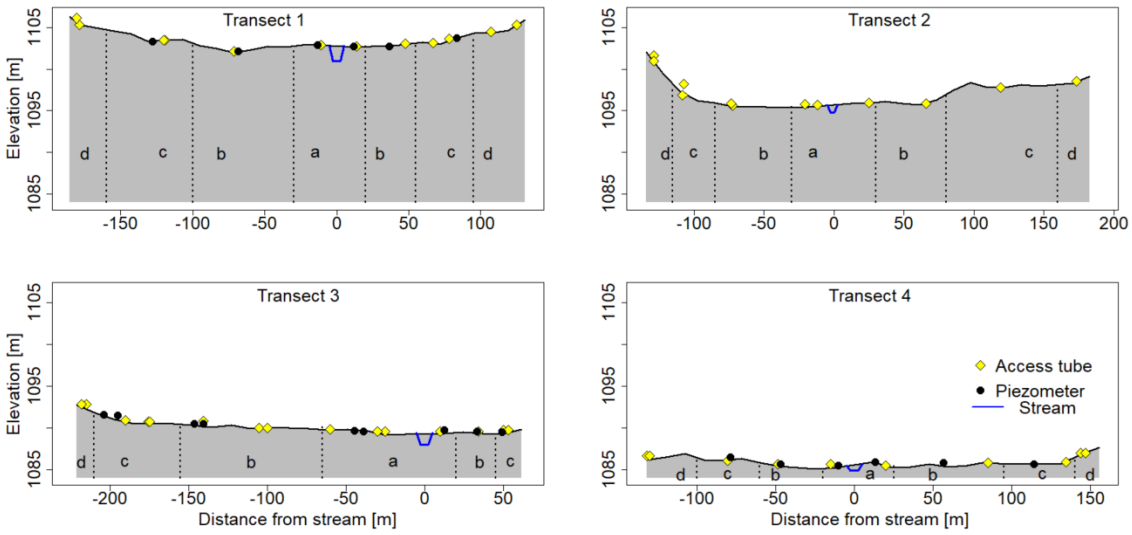

Fig. 3.5. Detailed instrumentation of piezometers and soil moisture access tubes at the inland valley wetland of Namulonge.

In the Kilombero floodplain wetland, a total of 12 piezometers screened at different depths (3.7 to 7.4 m depth) due to variable aquifer depth were installed along the three defined hydrological zones in the floodplain (Fig. 3.2a). For the modelling purposes using Hydrus-1D model, representative

piezometers with consistent depth to groundwater data were used at each hydrological zone, one piezometer was selected to facilitate hydrological modelling (Fig. 3.2b).

Soil moisture data

Measurements of soil moisture content were conducted along the defined hydrological positions for both study areas at the wetland scale. Soil moisture content measurement was performed using the principle of Frequency-Domain-Reflectometry (FDR) profile probe type PR2 (Delta-T Devices Ltd., 2006). FDR profile probe type PR2 measures profile soil moisture up to a depth of 40 cm or 100 cm when inserted into an access tube that has been installed in the soil. The profile probe type PR2 consists of a sealed polycarbonate rod, ~25mm diameter, with electronic sensors arranged at fixed intervals along its length, and has a measurement accuracy of ±0.06 m^3m^{-3}, 0 to 40^0C under generalised soil calibration in normal soils (Delta-T Devices Ltd., 2006). The probe creates a 100 MHz signal which is transmitted as an electromagnetic field extending about 100 mm into the soil. FDR is based on a unique relation between volumetric water content and dielectric constant of mineral soils. In this study, site specific calibrations were not conducted since calibration of FDR sensors to tropical wetland soil conditions have been established by Böhme et al. (2013) who approved their applicability with an error of 0.07 m^3m^{-3}. Therefore, the measured moisture results from the probes are reliable for the tropical wetland conditions.

The access tubes were installed along each defined hydrological positions for both study sites (Fig.4.1 and Fig. 4.2), according to the procedures described in the augering manual for PR2 by Delta-T Devices Ltd., (2005). Soil moisture readings were manually recorded at depths of 10, 20, 30, and 40 cm every two days with a hand held (HH2) moisture meter connected to a profile probe sensor (Delta-T Devices Ltd., 2013) (Fig. 3.6).

Fig. 3.6. Soil moisture measurement. (a), installation of soil moisture PR2 access tube; (b) reading soil moisture content using HH2 meter connected to PR2 sensor.

For the inland valley wetland of Namulonge, the installed access tubes covered the major land uses which included fallow, upland crops and taro (*Colocasia esculenta*) (Table 3.3). Fallow are uncultivated areas due to either weed infestation or excess moisture. Upland crops are cultivated along the well- drained sections or on raised ridges. The upland crops constitute the largest part of the inland valley and include subsistence crops mainly maize, (*Zea mays*), sweet potatoes (*Impomea batatus*), beans (*Phaseolus vulgaris*) and vegetables. Taro cultivation occurs under flooded conditions and involves labour-intensive land preparations which include clearing of the natural wetland vegetation. In total, 47 PR2 access tubes were installed in variable numbers at each hydrological position located at each transect (Fig. 3.5 and Table 3.1) in the inland valley wetland.

Table 3.1 Number of soil moisture sensors installed along and across the inland valley.

Longitudinal section	**major land use/crop type**	**Cross-section**			
		Riparian zone	Valley bottom	Fringe	Valley slope
Upper (T1)	Upland crops	2	1	3	4
	Fallow	-	1	1	-
	Taro	-	-	-	-
Mid (T2 and T3)	Upland crops	4	4	5	3
	Fallow	-	2	1	3
	Taro	2	1	-	-
Lower (T4)	Upland crops	-	2	2	3
	Fallow	-	-	-	1
	Taro	2	-	-	-

In the Kilombero floodplain wetland, the installed access tubes were mainly in the cultivated rice plots integrated with a maize crop since these are the major crops grown in the wetland. A total of 52 soil moisture access tubes were installed along the three defined hydrological zones (Fig. 3.2a). Because of flooding during the rainy seasons, most of the plots with access tubes were submerged with water thus we could not measure soil moisture content from these plots. Therefore, for modelling purposes, we used soil moisture data from at least 4 soil moisture access tubes (Fig. 3.2b) which had some significant amount of data albeit there were some data gaps (see Chapter 8 for detailed explanation of the results).

For both study sites, supplementary automatic soil water stations with soil Hydra Probe SDI-12 sensors connected to a data logger (Stevens Water Monitoring Systems Inc., 2007) were installed at the fringe position (transect T3 for the inland valley) (Fig. 3.7a). The Hydra Probe sensors have a length of 12.4 cm, with a diameter of 4.2 cm and a soil moisture measurement accuracy of ±0.03 m^3 m^{-3} (Stevens Water Monitoring Systems Inc., 2007). The Hydra Probe SDI-12 sensors use the principle of time domain reflectrometry which measures the time of travel of the electromagnetic waves. Hydra Probe sensors recorded soil moisture content at 10, 20, 30, and 40 cm depth every 15 minutes. The valley bottom and riparian zone at Transect, T3 of the inland valley wetland were equipped with Decagon's 5TE soil water content sensors (Decagon Devices Inc., 2016) connected to EM50 digital data loggers (Decagon Devices Inc., 2016) (Fig. 3.7b), to monitor soil moisture content under maize (*Zea may*) crop at 10 cm and 30 cm depths every one hour. At each depth, four 5TE sensors were installed. The 5TE sensor uses an oscillator running 70 MHz to measure the dielectric permittivity of the soil to determine the water content and has a measurement accuracy of ±0.03 m^3/m^3 (Decagon Devices Inc., 2016).

Also, the middle and riparian zone of the Kilombero floodplain wetland were equipped with Decagon's 5TE soil water content sensors to monitor soil moisture content at 10 cm and 30 cm depth every one hour. At each depth, four 5TE sensors were installed. Measurements from the Hydra Probe sensors and 5TE sensors were aggregated to daily resolution prior to analysis.

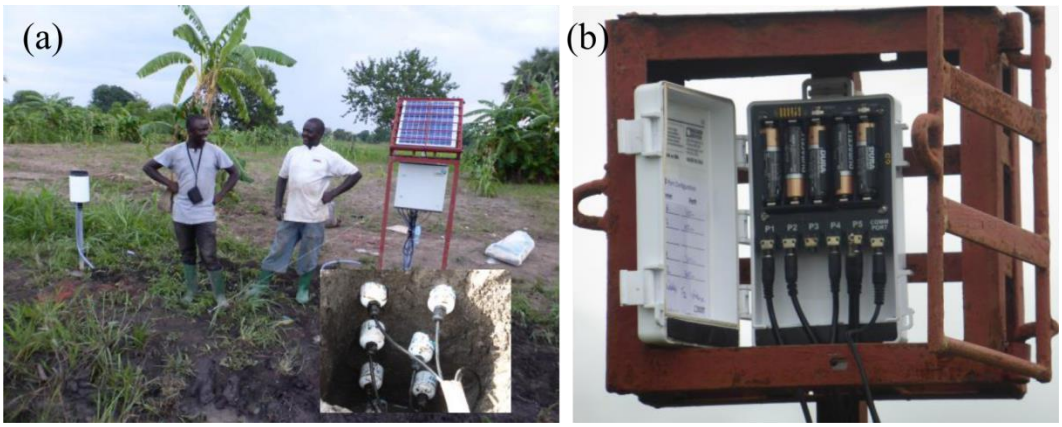

Fig. 3.7. Installed automatic soil water station. (a), data logger connected with soil Hydra Probe SDI-12 sensors and a tipping bucket; (b), EM50 digital data logger connected with 5TE soil moisture sensors.

Soil data at plot-wetland scale

To assess the variability of soil hydro properties within the Namulonge inland valley and Kilombero floodplain wetlands under the different land use and hydrological positions as presented in Chapter 5 and chapter 8, respectively, composite soil samples were collected using a soil hand auger of 50 mm diameter for soil texture and Soil Organic Carbon (SOC) determination. Undisturbed soil samples (100 cm^3) were analysed for bulk density (BD) using the core method by driving core sampler into the soil at a desired depth. All soil samples were collected at 15 - 25 cm distance from the access tubes to minimize soil disturbances within the electromagnetic sensor field. Soils were sampled at 0-10, 10-20, 20-30, and 30-40 cm depth below the surface. Soil particle size distribution was determined using a laser method (Horiba, 2010) while SOC was analysed using the modified Blackley Walkley wet method (Okalebo et al., 2002). Three undisturbed soil samples (250 cm^3) for each sampled soil depth were taken at each site for saturated hydraulic conductivity (K_{sat}) measurements using the constant head method with a laboratory permeameter (Eijkelkamp, 2013). As explained before, these soil properties analysed for the Kilombero floodplain wetland were used to derive hydraulic parameters for setting up the Hydrus-1D model and calibration.

3.2.4. Spatial assessment at wetland - catchment scale

Digital soil mapping in the Namulonge inland valley

The response of a catchment to a rainfall event is partly dependent on the nature and properties of the underlying soils (Shrestha et al., 2008).The SWAT model requires a soil map with soil property data such as the texture, physical properties, available moisture content, hydraulic conductivity, and organic carbon content for the different layers of each soil type. Therefore, a soil map was derived based on the FAO guidelines for soil mapping to assess the spatial distribution of predominant soil types and their properties in the inland valley catchment (FAO, 2006). The approach involved the usage of a topographic map at a scale of 1:20,000 (with a 2 m contour interval), including aerial image (Google images) to delineate major land form units, detailed soil profile description and soil sampling, extrapolation and delineation of soil boundaries, soil physical and chemical properties' laboratory analysis and map production. A reconnaissance study was conducted to establish the various soil units by the transect walk method (Gobin et al., 2000). Additionally, observations of soil properties were made through at excavation and road cuts as well as using the soil auguring and visual surface soil characteristics such as signs of erosion/deposition, status of the vegetation (species composition and cover), micro-topography, aspect, presence of fauna (e.g. ants, termites, moles) as suggested by Deckers et al. (2002). Soil boundaries were assessed and established by auger method down to approximately 120 cm depth and the readily observable soil properties such as soil color, texture, soil depth, stoniness, drainage, parent rock were recorded. Major soil types were identified, mapped using a handheld global positioning system (GPS), and described in detail (FAO, 2006). The analyzed soil parameters included particle-size distribution, bulk density (BD), pH, electrical conductivity (EC), soil organic carbon (SOC), exchangeable bases, and cation exchange capacity (CEC). The physical and chemical soil properties were analyzed in soil laboratories at the Makerere University, Kampala. The interpolation of soil boundaries between adjacent pits, auger points or observations points were made through analysis of topographic and vegetation boundaries as indicated on the satellite images. Field classification and delineation of soil boundaries were based on key intrinsic soil properties such as drainage type, subsoil texture, surface texture, parent material, depth to pedological features, diagnostic horizons, diagnostic properties, and diagnostic material (WRB,

2014). Based on laboratory data, field classification of the soil profile pits were updated and the soil map completed.

Land use map and land use scenarios

At the beginning of this study, detailed spatial information on the distribution of land use and land cover data at the scale of the inland valley in Uganda was missing, thus a land use and land cover (LULC) map with its related attributes had to be developed. The LULC map for the inland valley was developed from Sentinel-2 images of 2016 with 10 m spatial resolution (Drusch et al., 2012). To enhance the accuracy of land use classification, training data were systematically collected for each land use class using the handheld Global Positioning System (GPS). A total of 450 observation points were sampled during the months of November 2015 and February 2016. Based on the training data, a random forest classifier with 1000 trees method was used to classify the LULC types in the inland valley.

Four hypothetical land use management options/scenarios were developed and explored in addition to the reference land use map of 2015 applied for calibration and validation. The development of the land use management options was in accordance with the ongoing trends of land use change and with management efforts within the study area and across the East African region for the inland valleys. See chapter 6 for detailed description and explanation of these land use scenarios.

3.2.5 Digital elevation model (DEM) data

A high-resolution 5 m DEM was derived at the transect level in the inland valley wetland using global navigation satellite systems technology in real-time kinematic mode by applying a differential Global Positioning System with measurement capabilities within 1–4 cm accuracy (Chang et al., 2004). In addition, the freely available DEM products from the Shuttle Radar Topography Mission (SRTM) with 30 m resolution (NASA, 2014) and TerraSAR-X digital elevation model with a resolution of 12 m (TanDEM-X-12 m, © DLR 2016) were acquired for both study areas. For the inland valley at a wetland scale, evaluation of the different DEM resolutions in mapping the soil hydrological regimes were explored (see chapter 5 for details).

At the Kilombero floodplain wetland, The TanDEM-X-12 m was used to derive the absolute height and the distance from the river in order to delineate the different hydrological zones of the wetland (See section 4.2.2 for the detailed explanation).

3.3. Results and discussion

Results and discussions of the spatial and temporal dynamics of soil moisture, depth to shallow groundwater, soil properties are presented in detail in chapters 5 and 6 for the inland valley and Kilombero floodplain at wetland and plot scale, respectively.

3.3.1. Climate data

Precipitation data for both study areas was recorded at 15 minutes intervals. The data later on was aggregated into daily time step for field scale-based analysis in the inland valley wetland to assess the response of soil moisture and shallow groundwater to precipitation as explained in more detail in Chapter 5 and for the Hydrus-1D modeling to assess the spatial dynamics of soil water in the Kilombero floodplain as presented in more detail in Chapter 8.

Daily climate data was downscaled from the GCM-RCM models from the CORDEX- Africa project. The data concealed two periods: i) the historical period of 1976 to 2005, used as reference period in the climate change impact assessment; and ii) the projected period of 2021 to 2050. The representative concentration pathways used in this study included RCP4.5 and RCP8.5. See Chapter 8 for more detail on the impact of these climate scenarios on the water resources in the inland valley.

3.3.2. Discharge data

The yearly stage – discharge rating curves of the gauging station at the outlet of the inland valley, derived from measured event discharge and its corresponding stream water level after applying power-law equation, are given in Fig. 3.8. Results indicate a high correlation (>0.85) for rating curves, although, there is observed differences in the amount of discharge and hence changes in the stage-discharge relation rating curve for each year. This is partly explained by change in the channel conditions to modification of the channel by the farmers for crop irrigation (stream water is often blocked and diverted into small agricultural plots during the dry season or low rains). Other reasons to changes in the rating curve could be channel sediment deposits and measurement errors. It is worthwhile noting that regular over bank flows occurred during high rainfall (Fig.3.9) due to the narrow width and low depth of the main channel, therefore peak flows could not be captured adequately especially during the night when heavy rains poured. Henceforth, the exact peak flows are underestimated as shown in detail by the SWAT model in Chapter 6.

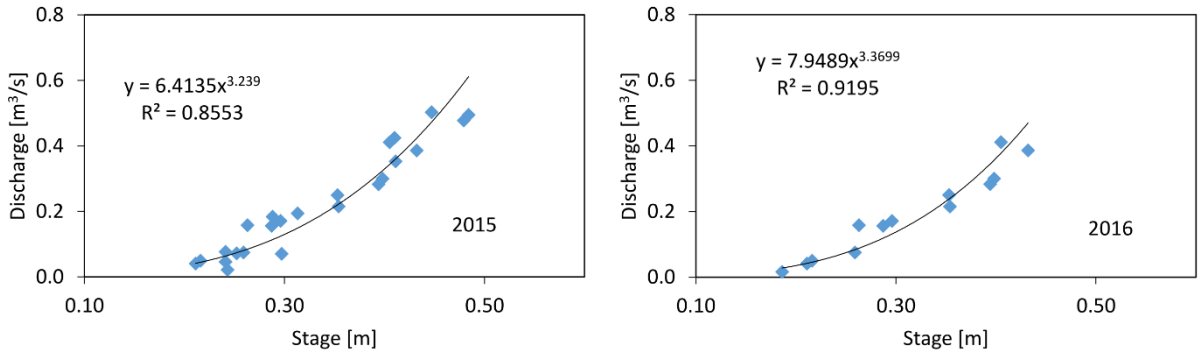

Fig. 3.8. Rating curves derived at the inland valley outlet for the calibration year 2015 and validation year 2016.

Fig. 3.9. Overbank flow in the main channel after a heavy rainfall pours.

3.3.3. Land use data in the inland valley

Fig. 3.10 depicts the land use and land cover types defined in the inland valley. A total of six LULC types were defined for the purposes of SWAT modelling. The predominant land use/cover types include agriculture (AGRL) with coverage of 64.8% of the total catchment area, mixed forest (FRST, tropical rainforest, 11.8%), and planted evergreen forests like eucalyptus (FRSE, 11.7% of the total catchment area) (Table 3.2). The spatial pattern of land use is very spotty and shows agricultural use as well as pasture (PAST) next to one another because the inland valley is mainly cultivated by smallholder farmers. Agriculture in the inland valley includes mainly annual crops like upland crops for example sweet potatoes (*Ipomoea batatas L*), beans (*Phaseolus vulgaris L*), maize (*Zea Mays L)*, vegetables and flood tolerant crops such as paddy rice (*Oryza sativa L*), Taro which are cultivated at the valley bottoms of the catchment. Upland crops are mainly cultivated at

the uplands and at relatively moist plots in the inland valley wetland especially at the fringe and ridged plots of the valley.

Table 3.2 Area of land use and land cover types (LULC) in the inland valley of Namulonge.

LULC type	Area [%] in the catchment
Agriculture (AGRL)	64.8
Forest ever green (FRSE)	11.7
Forest mixed (FRST)	11.8
Pasture (PAST)	8.5
Urban, low density (URLD)	2.0
Water (WATR)	1.2

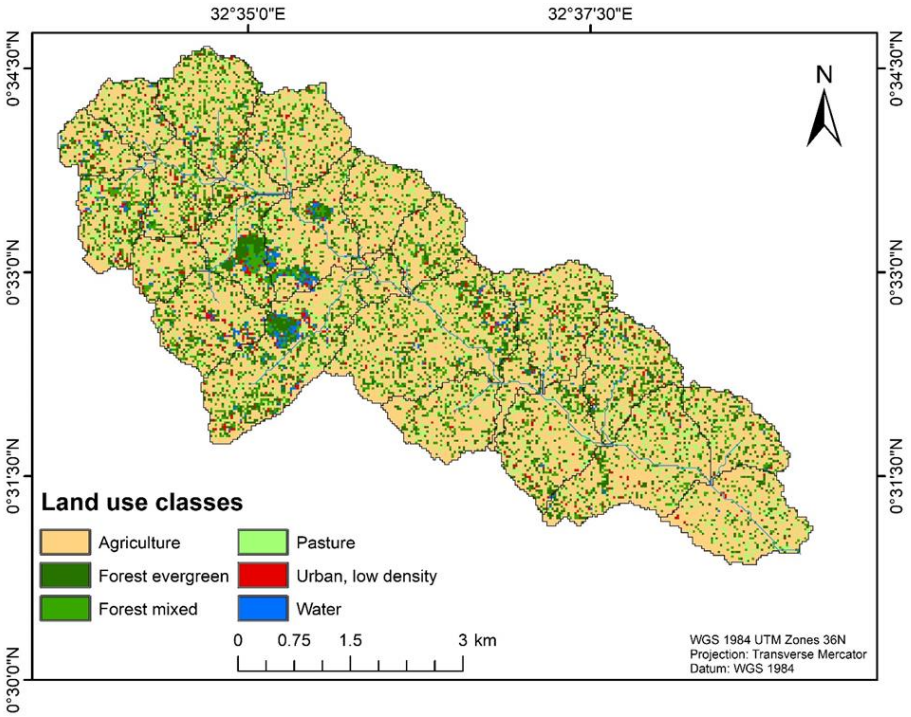

Fig. 3.10. Spatial distribution of land use and land cover types in the inland valley.

3.3.4. Soil distribution in the Namulonge inland valley

The soil types in the inland valley are presented in Fig. 3.11. The inland valley is characterized by six soil types with prefix qualifiers added to the name of reference soil group. The soil types were classified as Rhodic Nitisols, Rhodic Nitisols (colluvic), Umbric Gleysols, Gleyic Fluvisols and Gleyic Arenosols according to WRB (2014). Rhodic Nitisols are the predominant soil types (about 62.2% coverage in the catchment) in the inland valley found at the upper slope position (summit) followed by the Rhodic Nitisols (Colluvic), (about 23.4% coverage in the catchment) which occur

at the lower slopes of the catchment (Fig.4.12). Umbric Gleysols are the third most important soil type in the catchment (about 10.3%) and the predominant in the valley bottom and fringes of the wetland. The Gleyic Fluvisols (4.0% coverage in the catchment) are mainly observed at the tributaries of the main stream.

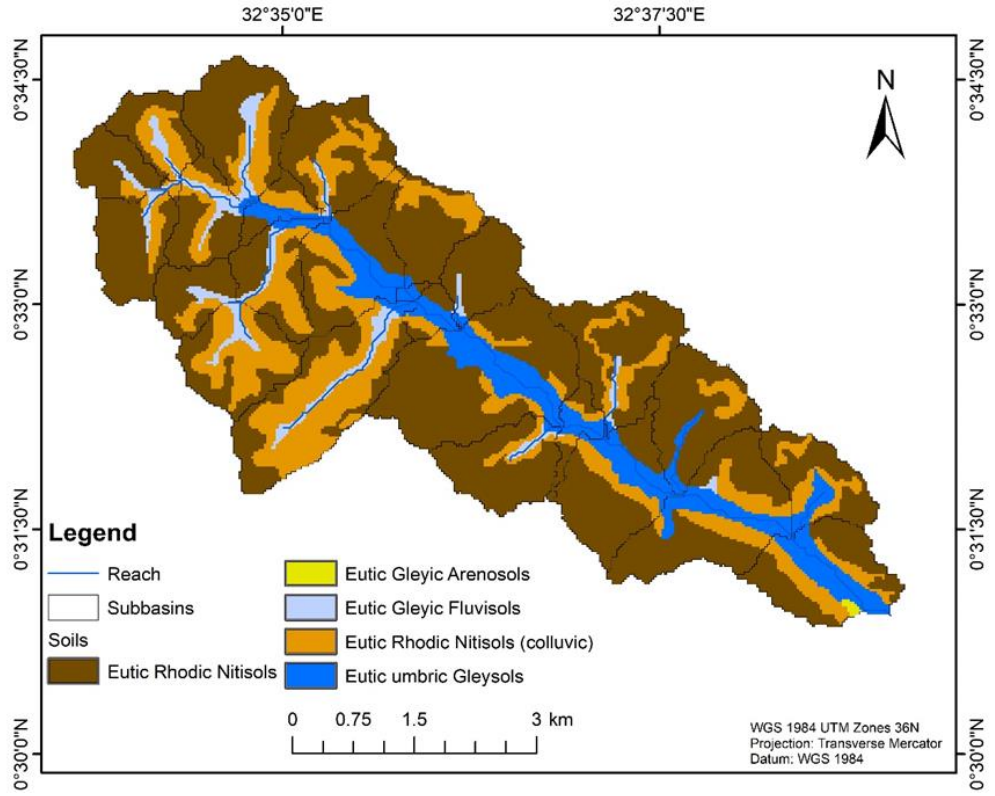

Fig. 3.11. Soil types in the inland valley of Namulonge.

More specifically, Nitisols are characterized by deep, well drained soils (WRB, 2014). As shown in Fig. 3.13, Rhodic Nitisols show increasing saturated hydraulic conductivity (K_{sat}) with depth due to the reduced percentage clay content. The soil texture is loam for layer 1 and silt loam for the subsoil soil (layer 2). The Rhodic Nitisols (Colluvic) have almost similar properties with the Rhodic Nitisols except that the later show Colluvic materials (stone line) at the second layer/horizon of the profile (Fig. 3.12). Soil texture is sandy loam for all the horizons/layers in the described profile (Fig. 3.13). Gleysols denote soil characterized by a gleyic color pattern in a 25% or more of the soil volume (WRB, 2014), also see Fig. 3.12. The mean soil properties in the profile of these soils are presented in Fig. 3.13. The soil texture is sandy clay loam at layer 1 and 2 and clay loam for layer 3. Soil organic carbon content decreases with depth. Measured saturated hydraulic conductivity is highest at the layer 2 due to lower percentage of clay content. Fluvisols

show weak horizon differentiation but with distinct topsoil horizon, with soils are characterized by high percentage of sand with low clay content (Fig. 3.13). Their soil texture is sandy loam for layer 1 and 4, loamy fine sand for layer 2 and fine sand for layer 3. Measured saturated hydraulic conductivity showed an increasing trend with soil depth due to the increasing trend of percentage sand content with depth. Soil organic carbon decreases with increase in depth while bulk density increases with increase in soil depth.

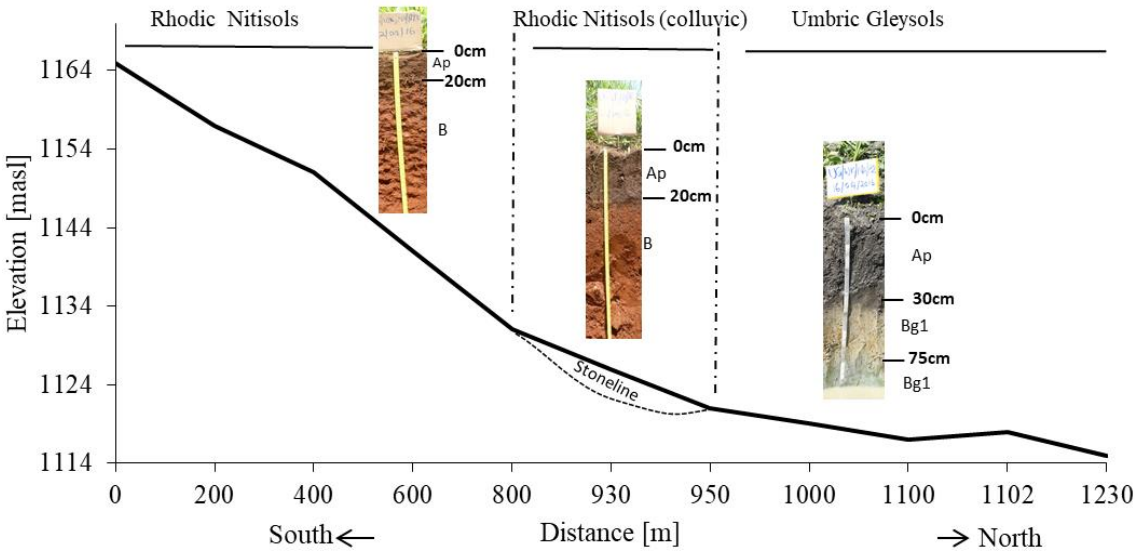

Fig. 3.12. Distribution of major soil types following a catena in the inland valley of Namulonge.

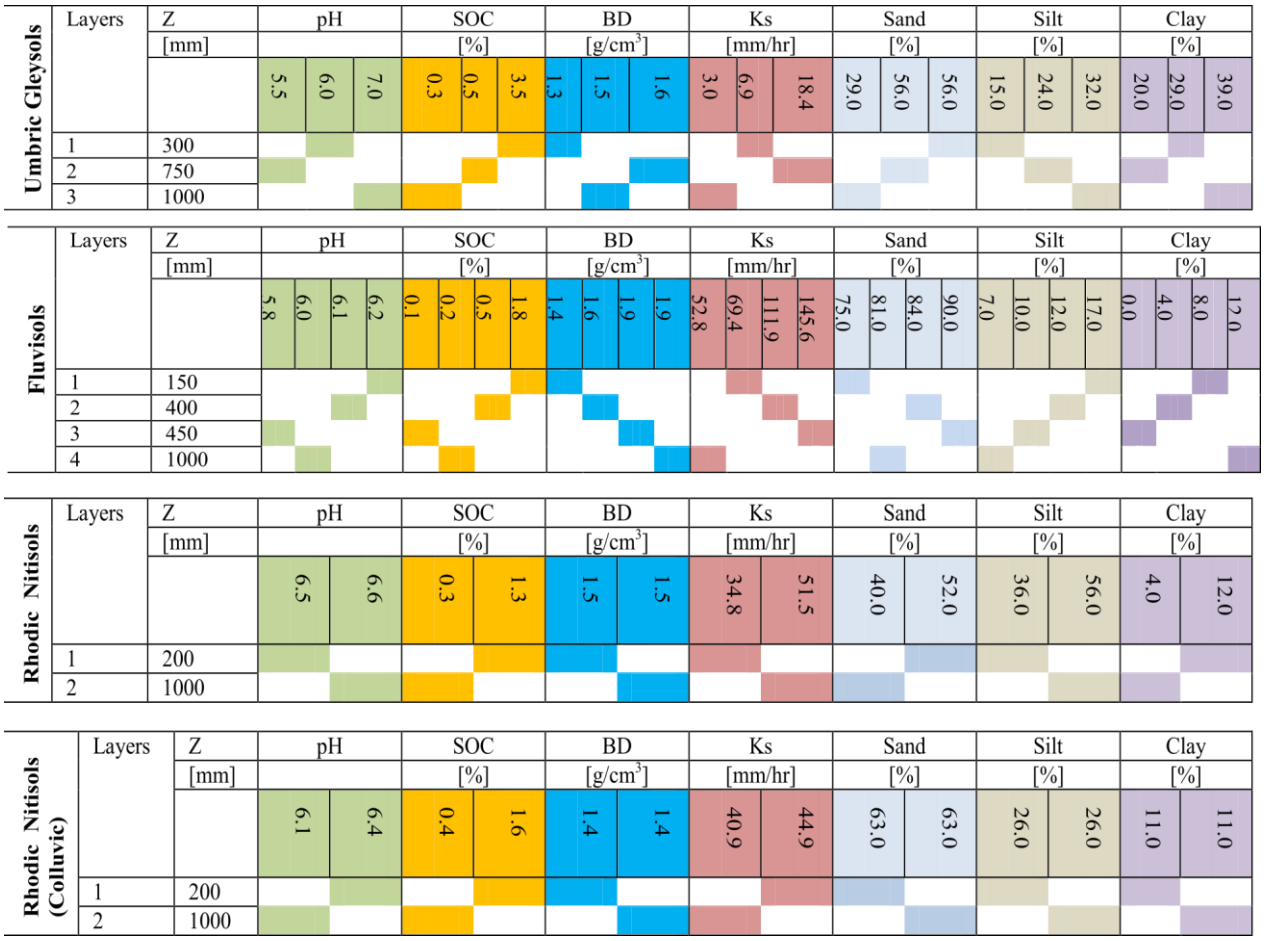

Fig. 3.13. Mean soil properties from the profiles of the major soil types. Z, depth of the soil layer in the soil profile, SOC, soil organic carbon content, BD, bulk density, Ks, saturated hydraulic conductivity.

3.4. Conclusion

The study design, instrumentation and data collection procedure explained in this chapter enabled to achieve relevant and sufficient data for field-based analysis at the wetland scale (chapter 5), wetland-catchment scale modeling to evaluate the impact of land use (chapter 6) and climate (chapter 7) change on the inland valley water resources, and plot scale modeling in the Kilombero floodplain (chapter 8). The data collected acts as a primary data base which was unavailable at the start of the study especially for the inland valley of Namulonge for future studies. Furthermore, the created database contributes to alleviating the high data scarcity in the region, more so for the wetlands ecosystems experiencing land use changes.

4. Modeling approach

4.1. Introduction

The study involved hydrological modelling at different scales, the wetland-catchment scale in the inland valley of Namulonge and the plot scale in the Kilombero floodplain wetland. At the wetland-catchment scale, the soil and water assessment tool (SWAT model) (Neitsch et al., 2009; Arnold et al., 2012) was applied to understand the hydrological behaviour of the inland valley of the Namulonge catchment under changing climate and land use. In addition, the Windows-based one-dimensional soil water dynamic model Hydrus-1D model v4.09 software package (Šimůnek et al., 2013) was applied to the simulate soil water dynamics at the plot scale along a valley transect of the Kilombero floodplain wetland. The following subsections give details of the models' descriptions.

4.2. Namulonge inland valley

4.2.1. SWAT model description

The implementation of land use catchment management strategies requires detailed understanding and evaluation of the hydrological processes at the catchment scale. Hydrological modelling has become one of the most powerful tools for catchment management. The Soil and Water Assessment Tool (SWAT) has been globally applied and extensively tested for hydrologic modelling at different spatial scales to investigate the land use management strategies on catchment hydrologic response under changing land use and climate. In the framework of this study, the SWAT model was used to assess the inland valley catchment hydrological processes and its response to the changing land use and climate.

The SWAT model (Neitsch et al., 2009; Arnold et al., 2012) is a physically based, process-oriented, computationally efficient, spatially semi-distributed and time - continuous catchment model. The model is designed to simulate and predict the impacts of land management practices on water quantity and quality in complex catchments with varying soils, land use and management conditions over long periods of time. In SWAT, the catchment is partitioned into a number of sub-catchments using topographic information. Sub-catchments in turn, are subdivided into hydrological response units (HRUs) which consist of a combination of unique soils, land cover and

slope classes (Arnold et al., 2013). All the hydrological processes are simulated on a daily or sub daily time step and driven by climate data. The hydrological cycle is partitioned into land and routing phases (Fig. 4.1). The land phase controls the amount of water, sediment, nutrient and pesticides moving into the main channel of each sub-catchment. The land phase involves processes like climate, hydrology (canopy storage, infiltration, evapotranspiration, surface runoff, lateral flow, and groundwater flow), erosion, plant growth and management operations. The routing phase involves the movement of water, through the channel network to the catchment outlet (Neitsch et al., 2009).

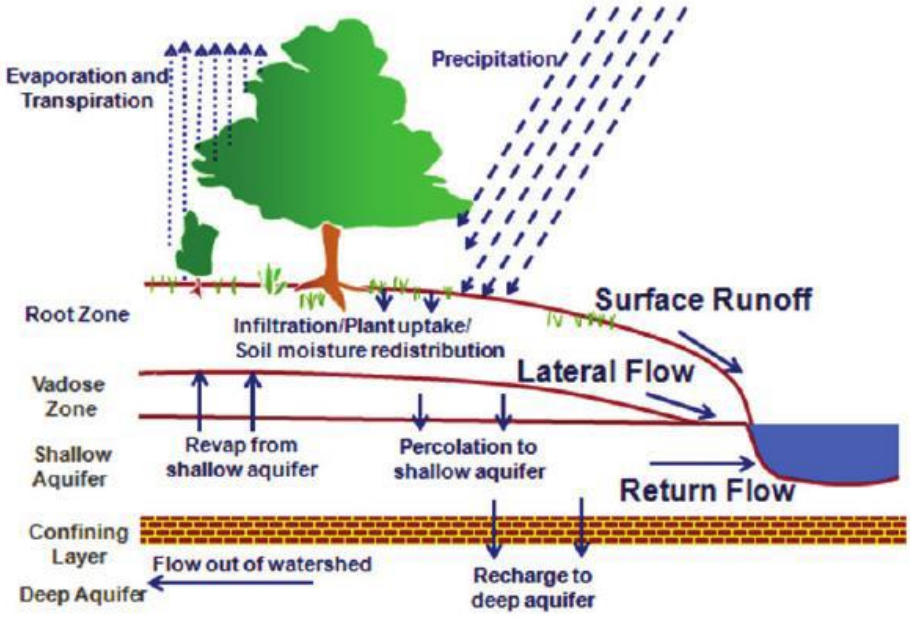

Fig. 4.1. SWAT schematic representation of hydrological cycle. Adopted from Neitsch et al. (2009).

In SWAT, five storages are considered to calculate the water balance: the canopy storage, the soil profile (with up to 10 layers), snow, a shallow aquifer and a deep aquifer. The water balance is expressed as:

$$SW_t = SW_0 + \sum_{t=1}^{t}\left(R_i - Q_i - ET_{a,i} - W_{seep,i} - Q_{gw,i}\right) \quad \text{(Eq. 4.1)}$$

Where SW_t is the final soil water content [mm], SW_0 is the initial soil water content on day i [mm], t is the time [days], R_i is the net precipitation on day i [mm], Q_i is the amount of surface runoff on day i [mm], $ET_{a,i}$ is the amount of evapotranspiration on day i [mm], $W_{seep,i}$ is the amount of water

entering the vadose zone from the soil profile on day i [mm], and $Q_{gw,i}$ is the amount of return flow on day i [mm] (Neitsch et al., 2009).

Surface runoff

Surface runoff is simulated separately for each HRU and routed to drive the total runoff for the catchment. There are two approaches incorporated in SWAT to calculate surfaces runoff, the Soil Conservation Service (SCS) curve number method (SCS, 1972) and the Green and Ampt infiltration method. In this study, the SCS curve number method was used during the simulation. The SCS curve number is a function of the soil's permeability, land use and antecedent soil moisture conditions as shown in the equation (Eq.4.2 to Eq.4.4).

$$Q = \frac{(R_{day} - 0.2S)^2}{(R_{day} + 0.8S)} \quad \text{for } R > 0.2S \qquad \text{(Eq. 4.2)}$$

$$Q = 0 \quad \text{for } R \leq 0.2S \qquad \text{(Eq. 4.3)}$$

$$S = 25.4\left(\frac{1000}{CN} - 10\right) \qquad \text{(Eq. 4.4)}$$

Where Q is the daily surface runoff [mm], R is the daily rainfall [mm], and S is a retention parameter (Neitsch et al., 2009).

Potential and actual evapotranspiration

Evapotranspiration is a collective term for all processes by which water at the earth's surface is changed to water vapor. It involves evaporation of water intercepted by the plant canopy, transpiration, sublimation and evaporation from rivers, lakes and bare soil. Potential soil water evaporation is estimated as a function of potential evapotranspiration and leaf area index. Potential evapotranspiration (PET) is estimated by SWAT model using three different methods incorporated in SWAT, the Penman-Monteith method (Monteith, 1965; Allen et al. 1989), the Priestley-Taylor method (Priestley and Taylor, 1972) and the Hargreaves method (Hargreaves et al., 1985) cited in Neitsch et al. (2009). In the framework of this study, the Penman-Monteith method (Eq.4.5) was adopted, which requires meteorological data such as solar radiation, air temperature, relative humidity and wind speed as inputs. Additionally, the method combines components that account

for energy needed to sustain evaporation, the strength of the mechanism required to remove the water vapor and aerodynamic and surface resistance terms. According to (Neitsch et al., 2009), the Penman-Monteith method is expressed as:

$$\lambda E = \frac{\Delta \,.\, (H_{net} - G) + \rho_{air} * c_p * \left[e_z^0 - e_z\right]/r_a}{\Delta + \gamma * \left(1 + \frac{r_c}{r_a}\right)}$$

(Eq. 4.5)

Where λE is the latent heat flux density [MJ m^{-2} d^{-1}], E is the depth rate evaporation [mm d^{-1}], Δ is the slope of the saturation vapor pressure-temperature curve [kPa $°C^{-1}$], H_{net} is the net radiation [MJ m^{-2} d^{-1}], G is the heat flux density to the ground [MJ m^{-2} d^{-1}], ρ_{air} is the air density [kg m^{-3}], c_p is the specific heat at constant pressure [MJ kg^{-1} $°C^{-1}$], e_z^0 is the saturation vapor pressure of air at height z [kPa], e_z is the actual water vapor pressure of air at height z [kPa], γ is the psychrometric constant [kPa $°C^{-1}$], r_c is the plant canopy resistance [s m^{-1}], and r_a is the diffusion resistance of the air layer (aerodynamic resistance) [sm^{-1}].

Actual soil water evaporation is estimated by using exponential functions of soil depth and water content. SWAT first evaporates any rainfall intercepted by the plant canopy and then calculates the maximum amount of transpiration and the maximum soil water evaporation using a modified approach of Ritchie (1972) cited in Neitsch et al. (2009). The depth distribution used to determine the maximum amount of water allowed to be evaporated is as follows:

$$E_{soil,z} = E_s^{"} . \frac{Z}{Z + exp(2.374 - 0.00713\,.\,Z)}$$

(Eq. 4.6)

Where $E_{soil,z}$ the evaporative demand at depth z [mm] is, $E_s^{"}$ is the maximum soil water evaporation on a given day [mm], and Z is the depth below the surface.

The coefficients in the equation were adopted such that 50% of the evaporative demand is extracted from the top 10 mm of soil and 95% of the evaporative demand from the top 100 mm of soil. SWAT does not allow a different soil layer to compensate for the inability of another layer to meet its evaporative demand leading to a reduction in actual evapotranspiration for the HRU. A soil evaporation compensation (ESCO) has been incorporated in the model to allow the user modify the depth distribution used to distribute the soil evaporative demand.

Percolation

SWAT calculates percolation for each soil layer in the profile. Percolation occurs when the water content exceeds the field capacity water content for that layer and if the layer below is not saturated. The storage routing methodology is used by SWAT to estimate the amount of water that moves from one layer to the underlying one based on the following equation:

$$\mathrm{SW}_{perc,ly} = \mathrm{SW}_{ly,excess} \cdot \left(1 - \exp\left[\frac{-\Delta t}{TT_{perc}}\right]\right) \quad \text{(Eq. 4.7)}$$

Where $SW_{perc,ly}$ is the amount of water percolating to the underlying soil layer on a given day [mm], $SW_{ly,excess}$ is the drainable volume of water in the soil layer on a given day [mm], Δt is the length of the time step [hrs], and TT_{perc} is the travel time for percolation [hrs] (Neitsch et al., 2009).

The water that percolates out of the lowest layer enters the vadose zone, which is the unsaturated zone between the bottom of the soil profile and the top of the aquifer.

Lateral flow

Lateral flow occurs when the percolated water encounters the impermeable layer in the profile. The water then ponds above the impermeable layer forming a saturated zone of water, sometimes referred to as perched water table, which is the source of water for lateral subsurface flow. SWAT incorporates a kinematic storage model for subsurface flow developed and summarized by Sloan et al. (1983) and Sloan and Moore (1984), respectively cited in Arnold et al. (1998). The kinematic storage model simulates subsurface flows in a two- dimensional cross-section along a flow path down a steep hill slope. The kinematic wave approximation of the saturated subsurface or lateral flow assumes that the lines of flow in the saturated zone are parallel to the impermeable boundary and the hydraulic gradient equals the slope of the bedrock. Lateral flow is calculated based on the following equation:

$$\mathrm{Q}_{lat} = 0.024 \cdot \left(\frac{2.SW_{ly,excess} \cdot K_{sat} \cdot slp}{\emptyset_d \cdot L_{hill}}\right) \quad \text{(Eq. 4.8)}$$

Where Q_{lat} is the water discharged from the hillslope (mm H_2O/day), $SW_{ly,excess}$ is the drainable volume of water in the saturated zone of the hillslope per unit area [mm], K_{sat} is the saturated

hydraulic conductivity [mmh^{-1}], slp is the slope as the increase in elevation per unit distance, $\emptyset_d$ is the drainable porosity of the soil layer [mm/mm], L_{hill} is the hillslope length [mm], and 0.024 is a conversion factor from meters to millimeter and hours to days (Neitsch et al., 2009).

Groundwater flow

In SWAT model, two aquifers are simulated in each sub basin. The shallow aquifer defined as unconfined aquifer that contributes to the main channel or reach flow of the sub basin as base flow. Base flow enters the reach only if the amount of water stored in the shallow aquifer exceeds a certain threshold value specified by the user. The deep aquifer is a confined aquifer from which the user can decide whether the water at this zone goes outside the catchment or contributes partly to the river discharge (Arnold et al. 2013).

The water balance for the shallow aquifer is calculated from the following equation:

$$\mathrm{aq}_{sh,i} = aq_{sh,i-1} + \mathrm{W}_{rchrg,sh} - Q_{gw} - W_{revap} - W_{pump,sh}$$

(Eq. 4.9)

Where $\mathrm{aq}_{sh,i}$ the amount of water is stored in the shallow aquifer on day i [mm], $aq_{sh,i-1}$ is the amount of water stored in the shallow aquifer on day i-1 [mm], $\mathrm{W}_{rchrg,sh}$ is the amount of recharge entering the shallow aquifer on day i [mm], Q_{gw} is the groundwater flow, or base flow, into the main channel on day i [mm] , W_{revap} is the amount of water moving into the soil zone in response to water deficiencies on day i [mm] and $W_{pump,sh}$ is the amount of water removed from the shallow aquifer by pumping on day i [mm].

The water balance for the deep aquifer is expressed as:

$$\mathrm{aq}_{dp,i} = aq_{dp,i-1} + \mathrm{W}_{deep} - W_{pump,dp}$$

(Eq. 4.10)

Where $\mathrm{aq}_{dp,i}$ the amount of water is stored in the deep aquifer on day i [mm], $aq_{dp,i-1}$ is the amount of water stored in the deep aquifer on day i-1 [mm], W_{deep} is the amount of water percolating from the shallow aquifer into the deep aquifer on day i [mm], $W_{pump,dp}$ is the amount of water removed from the deep aquifer by pumping on day i [mm]. Water percolating into the deep aquifer is not accounted for in the future water balance calculations and can be considered to be lost from the system (Neitsch et al., 2009).

4.2.2. SWAT grid model description

In addition to the ArcSWAT 2012 interface (Arnold et al., 2013), SWATgrid, a user interface for SWAT with a gridded discretization scheme (Rathjens et al., 2014) was set up to explicitly consider exchange of water and matter between the simulation units which is missing in the HRU approach.

The grid-based version of SWAT (SWATgrid) in its current version is not a standalone application, therefore, requires a running HRU version (Rathjens and Oppelt, 2012). Results from ArcSWAT and the TOPographic PArametriZation tool (TOPAZ) (Garbrecht et al., 2000) are used to define flow paths from the input digital elevation model (DEM). Thus, calibrated and validated ArcSWAT files were used to run SWATgrid in this study (Fig. 4.2). In SWATgrid surface runoff, lateral and groundwater flow processes are individually computed in each grid cell before being routed to one of the eight adjacent cells (Pignotti et al., 2017). Unlike the constant flow separation ratio used in ArcSWAT (Arnold et al., 2010), the spatial distribution of flow separation in the SWATgrid is controlled by a drainage density factor (Rathjens et al., 2014).

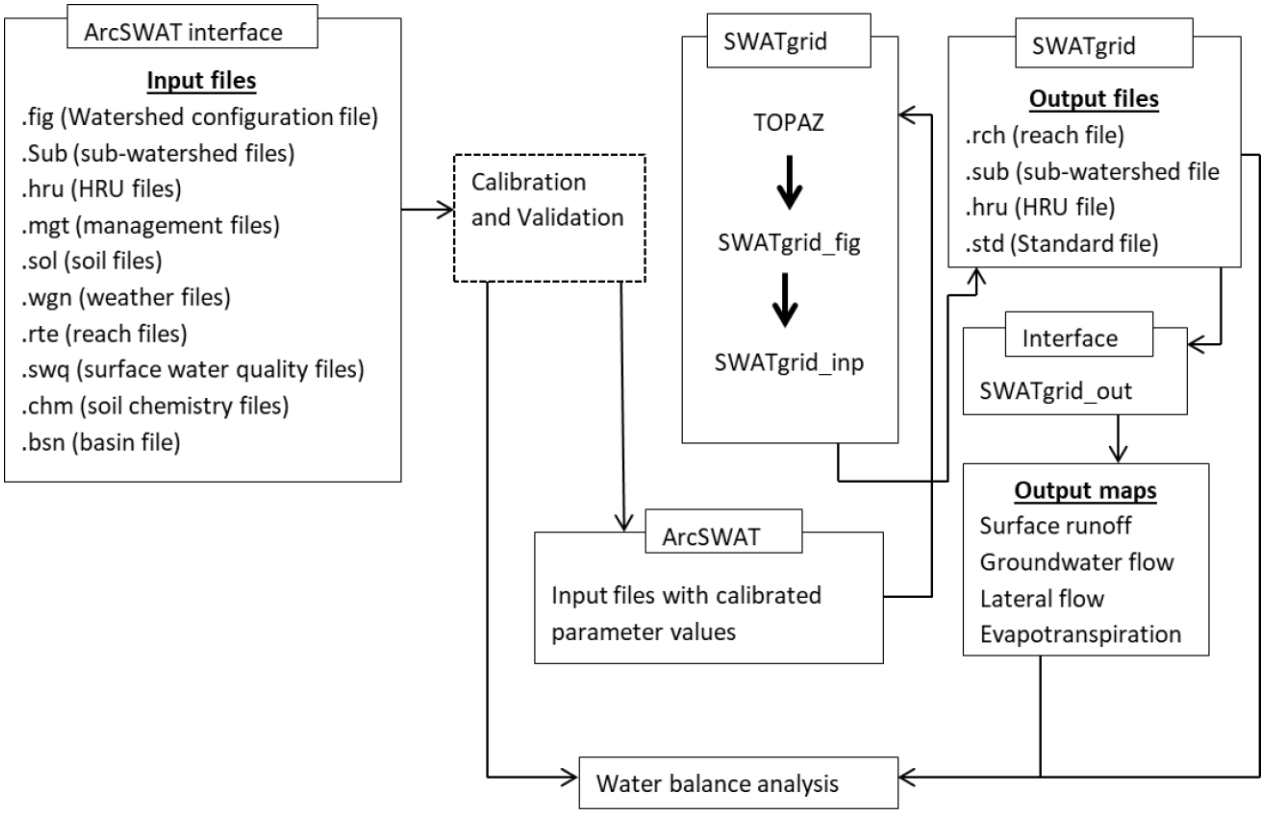

Fig. 4.2. SWATgrid modelling approach in this study.

4.2.3. Model input data

An array of input data was acquired to set up the SWAT model for the inland valley of Namulonge. Central Uganda. Input data included topography, land use. Soils, climate and stream discharge (Table 4.1). Shuttle Radar Topography Mission (SRTM) digital elevation model (DEM) with a resolution of 30 m downloaded from (U.S. Geological Survey - earthexplorer.usgs.gov) was applied to derive topographic information and generate stream networks and catchment configurations. At the beginning of the study, detailed spatial information on the distribution of land use and land cover, soil types, soil physical and chemical properties was missing. Thus, it was crucial to develop supporting maps to account for the different patterns and variations in soil and land use and land cover properties at the scale of the

inland valley.

Table 4.1 Spatial data used for the SWAT model.

Data set	Resolution/scale	Source	Data description and usage
Topography	30 m	SRTM	Digital Elevation Model (DEM)
Soil	1:20,000	Soil survey (Own ascertainment)	Soil physical properties
Land use	10 m	Own ascertainment	Land use classification based on Sentinel-2 image and field data
Climate	1 station	Namulonge automatic weather station	Daily weather data (1 Jan 2015 to 31 Dec 2016)
Discharge	15 minutes, 1 station	Own installation	Daily discharge data for model calibration and validation

4.2.4. Model setup

The basic initial model setup was carried out with the ArcSWAT interface. The initial setup included delineation of the catchment and sub-catchment areas using a 30 m DEM (Table 4.1), subdivision of sub-catchment into HRUs and generation of daily climate input files.

After the initial setup of ArcSWAT, calibration, validation, sensitivity, and uncertainty analysis of the model using a standalone program, SWAT-CUP (Calibration and Uncertainty program) was conducted with measured outlet discharge for the year 2015 (calibration) and 2016 (validation) in accordance with the availability of climate data and the daily discharge data, following the guidelines of Abbaspour et al. (2015). For calibration, sensitivity and uncertainty analysis, the optimization algorithm, SUFI-2 (Sequential Uncertainty Fitting) (Abbaspour, 2015) integrated in SWAT-CUP was adopted. SUFI-2 also quantifies the degree to which all uncertainties impact the model results. An uncertainty analysis is crucial to evaluate the strength of a calibrated model (Abbaspour, 2015). There are many uncertainties in a modelling exercise which include according to Beven (2012), (1) uncertainties in the model structure; (2) uncertainties in model parameter estimates; (3) uncertainties in the model drivers (initial and boundary conditions such as rainfall, soil and land use); (4) uncertainties that are overlooked by the modeler and not included in the model (can be unknown or known processes). Furthermore, Abbaspour (2015), underlines conceptual model uncertainties such as: (1) uncertainties due to simplification in the conceptual

model, (2) uncertainties due to processes that are included in the model, but their occurrence in the watershed is unknown.

In SUFI-2, uncertainty of parameters accounts for all sources of uncertainties stated above. Accumulation of uncertainties in the parameters results into uncertainties in the model output variables, which are expressed as 95% prediction uncertainty. 95% prediction uncertainty (95PPU) is calculated at the 2.5 and 97.5 percentiles of the cumulative distribution of an output variable attained through Latin Hypercube sampling, ignoring 5% of the very bad simulations due to bad parameter combination. The uncertainty band of 95PPU was used to account for the modelling uncertainty (Arnold et al., 2012). The degree and strength of uncertainties in the model output were measured by the P-factor and the R-factor, respectively (Abbaspour, 2015). The P-factor is the percentage of measured discharge enveloped by the 95PPU. The P-factor ranges between 0 and 1, in which 1 means 100% bracketing of the measured discharge by the model. The R-factor is the thickness of 95PPU envelop calculated by Eq 4.11. The R-factor divides the average distance between 2.5 and 97.5 percentiles with the standard deviation of the measured data (Arnold et al., 2012). The R-factor ranges from 0 to infinity, with values below 1, indicating a small uncertainty band (Arnold et al., 2012). A P-factor of one and R-factor of zero is a simulation that exactly corresponds to the measured discharge. The strength of calibration is judged by the degree of deviation of these numbers. A larger P-factor is achieved at the expense of a large R-factor.

$$\mathrm{R}-factor=\frac{1}{n\sigma_o}\sum_{n=1}^{n}(S_U-S_L) \qquad \text{(Eq.4.11)}$$

where n is the number of observations, σ_o is the standard deviation of the measured discharge, S_U and S_L are the 97.5th and 2.5th percentiles of the simulated 95PPU, respectively.

Comparatively, the SWATgrid version uses the calibrated ArcSWAT parameter set and no further calibration is carried out. Therefore, the calibrated parameter sets for ArcSWAT remained unchanged except for the discretization scheme, and the drainage density factor which was manually adjusted (Duku et al., 2015). In line with the resolution of the DEM used in ArcSWAT, SWATgrid discretized the catchment into 33,687 grid cells. Compared to ArcSWAT, the discretization scheme of SWATgrid provides better spatially detailed information for land use and

soil data. Also, a more accurate estimation of the water balance is expected at a catchment scale, due to the ability of SWATgrid to account for lateral fluxes between the grids (Rathjens et al., 2014). To ensure comparison of the two models, the SWATgrid was applied for the same time period as ArcSWAT. Because of the nearly 200 times more simulation units, the computation time for SWATgrid increased from 5 minutes to 27 hours using a 2.7 GHz computer.

4.3. Kilombero floodplain

4.3.1. Hydrus-1D description

Hydrus-1D is a software package for simulating one-dimensional variably saturated-unsaturated water flow, heat movement and solute transport (Šimůnek et al., 2013). The model simulates water flow by numerically solving Richard's equation (Eq. 4.12) with an assumption that the air phase has insignificant effect on the liquid flow and also water flow due to thermal gradients is neglected (Radcliffe and Šimůnek, 2010):

$$\frac{\partial \theta}{\partial t} = \frac{\partial}{\partial x}\left[K(h)\left(\frac{\partial h}{\partial x} + 1\right)\right] - S(h) \qquad \text{(Eq. 4.12)}$$

Where θ is the volumetric soil water content ($L^3.L^{-3}$), t is time (T), *x* is the vertical space coordinate (L), K is the hydraulic conductivity, *h* is the water pressure head (L), and S (h) is a water sink term accounting for plant root water uptake ($L^3.L^{-3}T^{-1}$).

The Hydrus-1D model integrates several boundary conditions and approaches for root water uptake of plants (Fig. 4.3) (Šimůnek et al., 2013). The user has options to select between different hydrological models which include single porosity and dual-porosity models. The single porosity model using the parameterization of the retention curve according to van Genuchten (van Genuchten, 1980) together with the model of Mualem (Mualem, 1976) cited in Šimůnek et al. (2009) was used in this study because it has the advantage that only the saturated conductivity is required and the unsaturated conditions are calculated within the program.

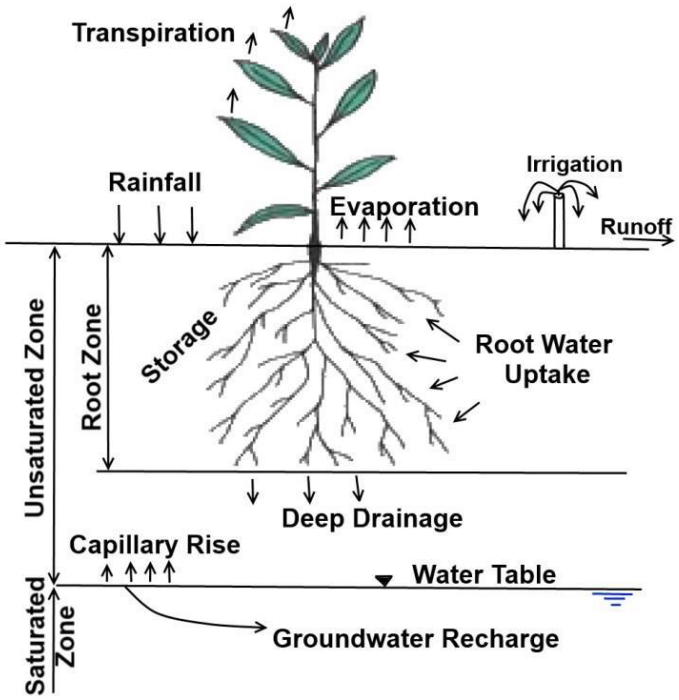

Fig. 4.3. Processes considered in the Hydrus-1D model (Šimůnek et al., 2009).

Root water uptake

The sink term S (h) in Eq. 4.13 is defined as volume of water derived from a unit volume of soil per unit time by plant roots. It accounts for actual root water uptake equivalent to actual transpiration, calculated by the model using Feddes equation (Soylu et al., 2011):

$$S(h) = \alpha(h) S_p \qquad \text{(Eq. 4.13)}$$

Where α (h) is the root water uptake stress response function prescribed dimensionless function of the soil water pressure head, h ($0 \leq \alpha \leq 1$). S_p is a potential root water uptake rate (L T^{-1}). From Fig. 4.4a root water uptake is assumed to be zero close to saturation (i.e. wetter than the "anaerobiosis point", h_1), and at dryer than the wilting point pressure head (h_4). Root water uptake optimum between pressure heads h_2 and h_3, while increases or decreases linearly with *h* when the pressure heads are between h_3 and wilting point (or between h_2). Potential root water uptake is equal to root water uptake rate during periods of no water stress (when $\alpha(h)$ =1).

The root water uptake can also be described by the S-shaped function proposed by van Genuchten (1987) cited in Šimůnek et al. (2009) as shown in Fig. 4.4b. When the potential water uptake is equally distributed over the root zone, S_p becomes

$$S_p = \frac{1}{L_R} T_p$$

(Eq. 4.14)

where T_p is the potential transpiration rate [LT^{-1}] and L_R the depth [L] of the root zone. The root depth can either be constant or variable during the simulation. For annual vegetation, a growth model is required to simulate the change in rooting depth over time. Hydrus assumes that the actual root depth is a product of the maximum rooting depth, L_m [L] and a root growth coefficient, fr [-] (Šimůnek and Suarez, 1993) cited in Šimůnek et al. (2009):

$$L_R(t) = L_m f_r\ (t)$$

(Eq. 4.15)

The classical Verhulst-Pearl logistic growth function is used for the root growth coefficient, fr(t)

$$f_t(t) = \frac{L_0}{L_0\ + (L_m - L_0)e^{-rt}}$$

(Eq. 4.16)

where L_0 is the initial value of the rooting depth at the beginning of the growing season [L], and r the growth rate [T^{-1}]. The growth rate is calculated either from the assumption that 50% of the rooting depth will be reached after 50% of the growing season has elapsed, or from given data.

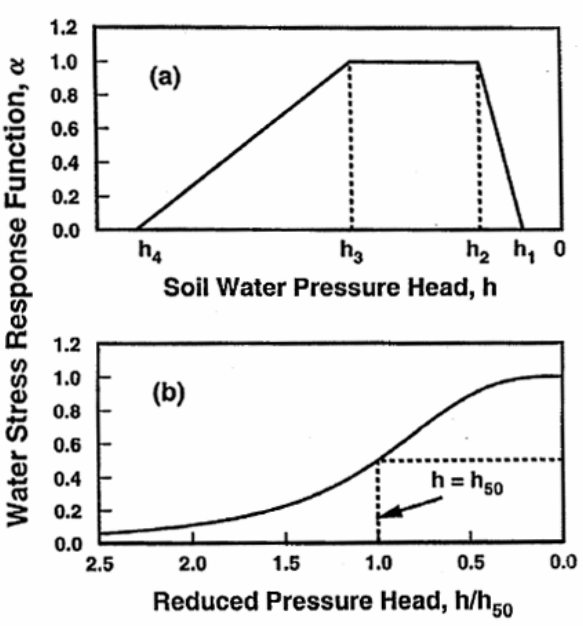

Fig. 4.4. Schematic illustration of the plant water stress response function, α(*h*), as developed by a) Feddes et al. (1978) and b) van Genuchten (1987) adopted from (Šimůnek et al., 2009).

The unsaturated soil hydraulic properties

The unsaturated soil hydraulic properties are represented by the parameterization given by (van Genuchten, 1980):

$$\theta(h) = \begin{cases} \theta_r + \dfrac{\theta_s - \theta_r}{\left[1 + |\alpha h|^n\right]^m} & h < 0 \\ \theta_s & h \geq 0 \end{cases} \qquad \text{(Eq. 4.17)}$$

$$K(h) = K_s S_e{}^l \left[\left(1 - S_e{}^{1/m}\right)^m\right]^2 \qquad \text{(Eq. 4.18)}$$

$$S_e = \frac{\theta - \theta_r}{\theta_s - \theta_r} \qquad \text{(Eq. 4.19)}$$

Where θ_r and θ_s are residual and saturated water contents ($L^3.L^{-3}$) respectively, K_s is the saturated hydraulic conductivity ($L.T^{-1}$), S_e is the effective saturation, α (L^{-1}), l and n represent empirical coefficients (the inverse air – entry point, pore connectivity and pore-size distribution parameter, respectively) affecting the shape of hydraulic functions, m = 1-1/n. The Hydrus- 1D model includes a Marquardt-Levenberg type parameter optimization algorithm for inverse estimation of the soil hydraulic parameters from the measured data.

Initial and boundary conditions

The Hydrus-1D model requires the knowledge of the initial and boundary conditions to simulate the soil water movement along the profile. The initial distribution of pressure head or water content is required within the flow domain. When the soil is wet, initial conditions can be assumed to be equal to water content at field capacity. The initial pressure head at field capacity is then calculated from the water content at field capacity using the van Genuchten (1980) retention curve.

The boundary conditions can be specified at the soil surface (top) or at the bottom of the soil profile according to the observed conditions and available data. At the bottom of the soil profile, different conditions can be selected which include free drainage, constant water content (water pressure) or variable water content (water pressure). At the soil surface, fluxes of precipitation and evapotranspiration are usually provided. Evapotranspiration is calculated using the integrated

FAO- Penman-Monteith method (Allen et al. 1998). Thus, meteorological data such as maximum and minimum temperature, relative humidity, wind speed and solar radiation are required.

The following main input parameters are required for the Hydrus-1D model to run. These include the upper and low boundary conditions, the water retention parameters for each soil layer, the initial condition of soil water content or pressure head for each soil layer, the saturated hydraulic conductivity and the horizontal distribution of the different soil layers. The major Hydrus-1D outputs are the modelled soil water content and pressure head values over a time period, the soil hydrological properties including the retention curve, all water fluxes over the simulated time, and the soil water balance.

4.3.2. Model input data

To conduct point scale soil water modeling in the floodplain, a range of data was required to set up Hydrus-1D model. These data included soil texture, soil organic carbon, soil hydraulic properties (derived from the pedo transfer functions), soil moisture, depth to shallow groundwater, climate, root depth, leaf area index (Table 4.2).

Table 4.2 Input data used for the Hydrus-1D model.

Data set	**Resolution/scale**	**Source**	Data description and usage
Soil hydraulic properties	point scale	Field measurements and pedotransfer functions	Saturated hydraulic conductivity, saturated water content, residual water content
Soil texture	point scale	Field and laboratory measurements	% clay, sand and silt content
Soil moisture	Daily/ point scale	Field measurement	Volumetric soil moisture content
Depth to shallow groundwater	Hourly/point scale	Field measurements	Pressure head
Leaf area index	Growth stages	Field measurements	
Climate	1 station	Namulonge automatic weather station	Daily weather data (1 Jan 2015 to 31 Dec 2016)

4.3.3. Model setup

To simulate the soil water dynamics along the transect of the Kilombero floodplain wetland, the initial conditions in the Hydrus-1D model were set to pressure heads in equilibrium with the measured depth to groundwater level which was taken as lower boundary condition. When the water table was above the soil surface, the pressure head was fixed to fully saturation to facilitate modelling. The upper boundary condition was specified as atmospheric boundary condition with a surface layer (to permit water build up due to flooding) using daily rainfall, potential evapotranspiration, and Leaf Area Index (LAI). Potential evapotranspiration (PET) was calculated by the FAO Penman-Monteith equation (Allen et al., 1998). The method uses meteorological data such as maximum and minimum temperature, relative humidity, wind speed and solar radiation. These data were obtained from the automatic climate station located within the Kilombero floodplain (Fig. 3.2a, Chapter 3). Actual evaporation and transpiration were directly computed by the model based on the given soil moisture conditions and root water uptake functions.

4.4. Model evaluation

Several methods have been proposed for quantifying the goodness of fit of observation data against model calculations however, none of them is free from limitations and are often ambiguous (Ritter and Muñoz-Carpena, 2013). If a single quantitative statistic is used it result into incorrect evaluation of the model. Instead, it is widely accepted that model evaluation should be approached in a multi-objective sense (Gupta et al., 1999).

In this study, model performance (SWAT and Hydrus-1D model) during calibration and validation was evaluated based on four quantitative statistics, specifically: (1) the coefficient of determination (R^2), (Eq.4.20); (2) the Nash-Sutcliffe efficiency (NSE) (Eq.4.21) (Nash and Sutcliffe, 1970); (3) the Kling-Gupta efficiency (KGE) (Eq.4.22) (Gupta et al., 2009) ; and the percent bias (PBIAS) (Eq.4.23) (Gupta et al., 1999), The coefficient of determination (R^2) was used to describe the proportion of variance explained by the model and ranges between 0 and 1.0, with high values indicating less error variance (Rathjens and Oppelt, 2012a). The NSE is a dimensionless model evaluation index, used to determine the relative magnitude of the residual variance between the simulated and measured data variance (Nash and Sutcliffe, 1970) and ranges from $-\infty$ to1.0. An NSE of 1.0 indicates a perfect fit between the simulated and observed data and it is very responsive to the peak flows (Moriasi et al., 2007). PBIAS was calculated to measure the average tendency of the simulated data to be larger or smaller than the measured values. The optimal value of PBIAS

is 0%, with positive and negative values indicating model underestimation and overestimation bias, respectively (Gupta et al., 1999). KGE is a dimensionless statistic which offers diagnostic insights into the model performance, it ranges from -∞ to 1.0, with 1.0 indicating a perfect fit between simulated and observed data (Kling et al. 2012). The model performance was considered to be satisfactory if NSE > 0.50, R^2 > 0.50, PBIAS ±25% (Moriasi et al., 2007).

$$R^2 = \frac{[\sum_{i=1}^{n}(O_i - \bar{O})(P_i - \bar{P})]^2}{\sum_{i=1}^{n}(O_i - \bar{O})^2 \sum_{i=1}^{n}(P_i - \bar{P})^2} \quad \text{(Eq. 4.20)}$$

$$NSE = 1 - \frac{\sum_{i=1}^{n}(O_i - P_i)^2}{\sum_{i=1}^{n}(O_i - \bar{O})^2} \quad \text{(Eq.4.21)}$$

$$KGE = 1 - \sqrt{(r-1)^2 + (\alpha - 1)^2 + (\beta - 1)^2} \quad \text{(Eq.4.22)}$$

$$PBIAS = 100 * \frac{\sum_{i=1}^{n}(O_i - P_i)}{\sum_{i=1}^{n} O_i} \quad \text{(Eq.4.23)}$$

where $O_i$and P_i are the measured and simulated data, respectively, $\bar{O}$ and $\bar{P}$ are the mean of measured and simulated data, n is the number of observations, $\alpha = \frac{\sigma_P}{\sigma_O}$, and $\beta = \frac{\mu_P}{\mu_O}$, and r, is the linear regression coefficient betweem simulated and measured data., σ_P and σ_O are the standard deviation of simulated and measured data, and μ_P and μ_O are means of simulated and measured data.

In addition to the above quantitative statistics for model evaluation, the root mean square error (RMSE) (Eq.4.24) was considered in the Hydrus-1D model. RMSE is an error index statistic which measures the difference between simulated and observed values.

$$RMSE = \sqrt{\frac{\sum_{i=1}^{n}(O_i - P_i)^2}{n}} \quad \text{(Eq.4.24)}$$

5. Determining hydrological regimes in an agriculturally used tropical inland valley wetland in central Uganda using soil moisture, groundwater, and digital elevation data[1]

Abstract

Inadequate knowledge exists on the distribution of soil moisture and shallow groundwater in intensively cultivated inland valley wetlands in tropical environments which are required for determining the hydrological regime. This study investigated the spatial and temporal variability of soil moisture along four hydrological positions segmented as riparian zone, valley bottom, fringe, and valley slope in an agriculturally used inland valley wetland in central Uganda. The determined hydrological regimes of the defined hydrological positions are based on soil moisture deficit calculated from the depth to the groundwater table. For that, the accuracy and reliability of satellite-derived surface models, SRTM-30 m and TanDEM-X-12m, for mapping microscale topography and hydrological regimes is evaluated against a 5m DEM derived from field measurements. Soil moisture and depth to groundwater table were measured using Frequency-Domain-Reflectometry sensors and piezometers installed along the hydrological positions, respectively. Results showed that spatial and temporal variability in soil moisture increased significantly ($p<0.05$) towards the riparian zone, however, no significant difference was observed between valley bottom and riparian zone. The distribution of soil hydrological regimes, saturated, near and non- saturated regimes does not correlate with the hydrological positions. This is due to high spatial and temporal variability in depth to groundwater and soil moisture content across the valley. Precipitation strongly controlled the temporal variability while microscale topography, soil properties, distance from the stream, anthropogenic factors, and land use controlled the spatial variability in the inland valley. TanDEM-X DEM reasonably mapped the microscale topography and thus soil hydrological regimes than SRTM DEM. The findings of the study contribute to improved understanding of the distribution of hydrological regimes in an inland valley wetland which is required for a better agricultural water management planning.

***Keywords**:* Soil hydrological regimes, soil moisture, groundwater, digital elevation data, inland valley wetlands.

[1]Published as: G. Gabiri, B. Diekkrüger, C. Leemhuis, S. Burghof, K. Näschen, I. Asiimwe, and Y. Bamutaze. 2018. Determining hydrological regimes in an agriculturally used tropical inland valley wetland in central Uganda using soil moisture, groundwater, and digital elevation data. *Hydrological Processes, 2018;32:349-362.*

5.1. Introduction

Wetlands offer a significant contribution to food security in East Africa (Kangalawe and Liwenga, 2005) and contribute to rural welfare (Turner et al., 2000; Schuyt, 2005; Horwitz and Finlayson, 2011). Wetlands modify hydrological processes and provide a number of ecosystem services (Rebelo et al., 2010; Junk and An, 2013). However, with declining quantity and quality of upland arable land (Maitima et al., 2009), wetlands are seen as potential areas for agricultural expansion, intensification, and food security (Dixon and Wood, 2003; Rodenburg et al., 2014). Prolonged periods of water availability and relatively fertile soils (von der Heyden and New, 2003), high annual population growth rate (Sakané et al., 2011), and the projected variations in precipitation (Collins et al., 2013; Adhikari et al., 2015) are the driving forces for using wetland for agricultural production, especially in tropical regions.

Small wetlands of less than 500 ha (Dixon, 2002) are seen to be the main potential agricultural areas. Small wetlands cover a proportion of 80% of the total wetland area in East Africa (Mwita et al., 2013) and are characterised by extensive small-scale subsistence agriculture (Wood and van Halsema, 2008; Mwita, 2012).The agricultural potential of small wetlands depends on the distribution of hydrological regimes which is controlled by the spatial and temporal dynamics of soil moisture content and depth to groundwater being highly heterogeneous in space and time (Gómez-Plaza et al., 2000; Mitsch and Gosselink, 2015). This is due to variability in soil properties, precipitation pattern, wetland's morphology, land use, and management (Robinson et al., 2008; Böhme et al., 2016).

In Uganda, wetlands vary from one region to another in terms of morphology. For example, in the southern and western region, they form an extensive low-gradient drainage system in steep V-shaped valley bottoms with a permanent wetland core and relatively narrow seasonal wetland edges. Broad floodplains are observed in the north while in the east and central region, inland valleys with a network of small, vegetated valley bottoms in a slightly undulating landscape (NEMA, 2008) exist which are seasonally flooded (Kaggwa et al., 2009). Inland valley wetlands are seasonally flooded wetlands comprising of a valley bottom and hydromorphic fringe (the area close to the valley bottom where the groundwater table is sufficiently shallow to be within the reach of crops) (Windmeijer and Adriesse, 1993; Rodenburg et al. 2014). Heterogeneity in morphological characteristics influences the wetland's soil moisture content and groundwater table in time and

space hence consequently, affecting soil hydrological regimes (SHR) at various scales in the valleys. The concept of soil hydrological regimes may help to assess the interactions between physical hydrology and biological processes (Poff et al., 1997). Because SHR show spatial and temporal scales of hydrological processes, they may contribute to evaluating changes in wetlands' water resources due to agricultural disturbances.

Although several studies have been conducted to understand soil moisture and depth to groundwater variability in the inland valleys of East Africa (Dixon, 2002; Böhme et al., 2013; Böhme et al., 2016) and wetland - agricultural interactions, (van Dam et al., 2007; Kyarisiima et al., 2008; Kaggwa et al., 2009; Kakuru et al., 2013), inadequate knowledge still exists on the spatial and temporal variations of soil moisture content and shallow groundwater in the intensively cultivated inland valley wetlands. Because for broader scale applications, information on microscale topography is required, the question arises on how good and reliable are the different globally available digital elevation models (DEMs) being used in hydrological process modelling. This knowledge is important for determining wetland's hydrological regimes and simulating water and solute fluxes, as well as understanding the capacities of wetlands for sustainable agriculture given the fact that these inland valleys are heterogeneous in their hydrology, climatic conditions, land use management, and morphology. Soil moisture and shallow groundwater availability are not only relevant in agricultural production and determining soil hydrological regimes, but also a key driver for mapping hotspots of likely wetland degradation (Leemhuis et al., 2016), and biodiversity (Robinson et al., 2008). Therefore, efforts targeting on understanding soil moisture and groundwater distribution and how they influence distribution of soil hydrological regimes is an essential step towards developing improved scientific knowledge on planning sustainable wetland agriculture and water management programs at the local scale. The main objectives of the study were:

i) to analyse the spatial and temporal variability of soil moisture content and depth to groundwater across four hydrological positions defined as valley slope, fringe, valley bottom, and the riparian zone,

ii) to test the hypothesis that soil hydrological regimes determined based on soil moisture deficit are correlated with the hydrological positions (riparian zone, valley bottom, and fringe) in the inland valley.

iii) to evaluate the accuracy and reliability of available digital elevation models i.e. Shuttle Radar Topography Mission (SRTM) with 30 m resolution (NASA, 2014) and TanDEM-X (Wessel et al., 2016) with 12 m resolution against a 5 m resolution DEM derived from local scale measurements in mapping ground surface elevation and microscale topography. Ground surface elevation and microscale topography influence depth to groundwater which determines soil hydrological regimes in the inland valley.

5.2. Materials and methods

The location of the inland valley wetland is presented in Fig. 2.2 in chapter 2. Detailed description of the procedure used for monitoring soil moisture content, shallow ground water and precipitation data is shown in chapter 3. Characterization of soil properties along the defined hydrological positions is also discussed in detail in chapter 3.

The overall study design took into consideration the prevailing land uses (fallow, upland crops and flood tolerant crops/taro) and the morphological characteristics of the inland valley. The aim was to record measurements at locations representing the variability of soil moisture and shallow groundwater to determine the existing soil hydrological regimes. The detailed study design and instrumentation is described in chapter 3.

5.2.1. Determining soil hydrological regimes along the defined hydrological positions

To determine soil hydrological regimes along the defined hydrological positions, we calculated soil moisture deficit in the soil profile assuming equilibrium in soil suction between depth to groundwater and soil surface. The equilibrium state assumes that soil moisture tension at a given depth depends on the distance to groundwater table (Beldring et al.,1999). The soil moisture deficit thresholds varied due to differences in soil texture and hence saturated water content along the defined positions. To calculate moisture deficit, we used the relationship between depth to groundwater and van Genuchten hydraulic parameters as described by van Genuchten (1980) equation as follows:

$$\Delta\theta = \int_{-d_s}^{0} \theta_s - \theta(h) \ \mathrm{dh} \qquad \text{(Eq 5.1)}$$

in which,

$$\theta(h) = \theta_r + (\theta_s - \theta_r)\,[1 + (\alpha.h)^n]^{-m} \qquad \text{(Eq 5.2)}$$

Where $\Delta\theta$ = soil moisture deficit [mm], h = soil suction, d_s = depth to groundwater; θ_s and θ_r are saturated and residual water content, respectively; α is the inverse of air entry pressure [1/mm], n and m (m = 1-1/n) are the dimensionless shape parameters of the retention curve.

Van Genuchten hydraulic parameters were derived from measured soil texture and bulk density using the Rawls and Brakensiek pedotransfer function (PTF) (Rawls and Brakensiek, 1985). Values of soil texture and bulk density used to derive soil hydraulic parameters were averages from the four soil sampled depths (0-10, 10-20, 20-30, and 30 -40 cm depth). Therefore, we calculated soil moisture deficit based on these derived soil hydraulic parameters in a 40 cm soil profile and variable depth to groundwater for this study. Variability in the hydraulic parameters at the different hydrological positions has implications on moisture deficits and hence the soil hydrological regimes in the valley.

Soil hydrological regimes were determined as saturated when depth to groundwater rises above surface thus moisture deficit is zero, near-saturated when the depth to groundwater table rises to 60 cm depth below surface and moisture deficit is 72 mm at riparian zone, 56 mm at the valley bottom and 50 mm at fringe positions due to differences in saturated soil water content, and finally as non-saturated when depth to groundwater is always lower than 60 cm depth below surface. Saturated soils are soils where all the pores are filled by water. Under these conditions, many crops will suffer except flood tolerant crops like taro and rice. Near saturation is when the soil is between field capacity and saturation points, and non-saturated soils occur when soil moisture is at or below field capacity. At near saturation and non-saturated conditions, most crops can thrive because the pores are filled both with air and water. In our calculation of moisture deficit, the negative values of depth to ground water (when the groundwater level was above surface) were converted to 0.0 mm indicating soil saturation. Furthermore, soil hydrological regimes were defined by calculating the percentage of time soil was saturated and the maximum consecutive days of saturation over one year.

5.2.2. Evaluation of different DEM resolutions in mapping soil hydrological regimes

The aim of the DEM analysis was to evaluate the accuracy and reliability of different DEM resolutions in mapping ground surface elevation and thus microscale topography. Derived ground surface elevation was used to calculate the depth to groundwater required to determine soil hydrological regimes in the inland valley. A high-resolution 5m DEM was derived covering transects T3 and T4 (Fig. 3.1, chapter 3) using global navigation satellite systems (GNSS)

technology in real-time kinematic mode using differential GPS with measurement capabilities within 1-4 cm accuracy (Chang et al., 2004). The 5m DEM was used as a reference DEM (Fig. 5.1a). A total of 959 points were sampled. We assessed the spatial height error of the freely available DEM products from the Shuttle Radar Topography Mission (SRTM) with 30 m resolution (Fig. 5.1b) and TanDEM-X with 12 m resolution (Fig. 5.1c) against the reference DEM. We clipped the SRTM and TanDEM-X to the extent of the 5 m DEM. The relative vertical error is < 10 m for SRTM (Farr et al., 2007) and <2 m for TanDEM-X- 12 m (Wessel, 2013).

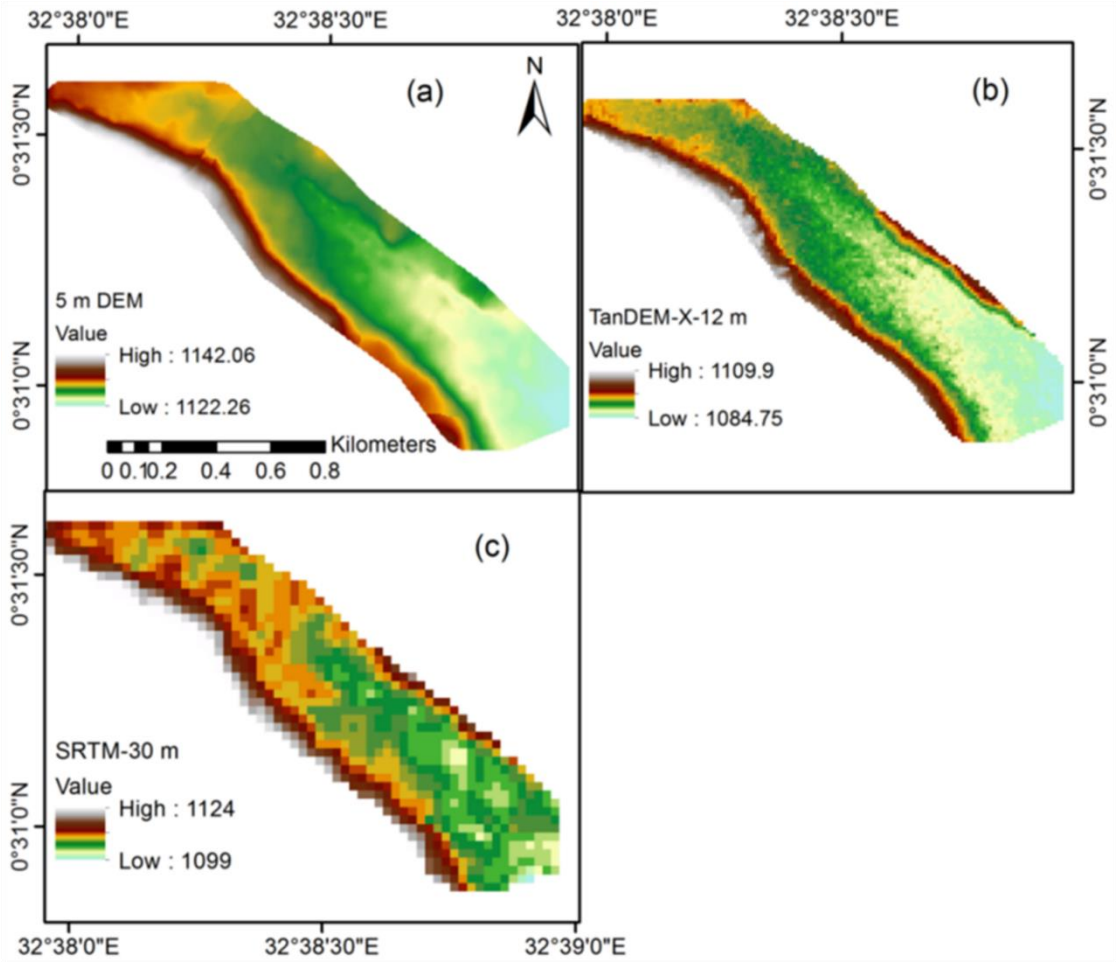

Fig. 5.1. Original digital elevation model (DEMs). (a) Derived 5 - m DEM; (b) clipped 12m TanDEM - X ©DLR, 2016; and (c) clipped 30 m Shuttle Radar Topography Mission. Source: NASA (2014).

For comparison of the different DEMs, the clipped SRTM and TanDEM-X were resampled to 5 m DEM by bilinear interpolation. For adapting mean heights of the DEMs, we subtracted mean elevation data from SRTM and TanDEM-X DEMs and afterwards added mean elevation of the

reference DEM. Stream networks were derived for each original DEM using flow accumulation method in Arc Map 10.2 to evaluate stream positional accuracy compared to the reference DEM. For the assessment of cross-sectional profiles, two approaches were considered, i) the transformed SRTM and TanDEM-X elevation data were sampled at 5 m interval along each transect; ii) the original SRTM and TanDEM-X elevation data points were also sampled at 5 m interval along similar transects. Elevation data from both DEMs were referenced with other data obtained from a known location using differential GPs. The reason for this approach was to assess the accuracy and reliability of these DEMs in mapping ground surface elevation and thus microscale topography at a wetland scale with and without the knowledge of vegetation cover. The accuracy of both DEMs was assessed based on the computation techniques described by Erasmi et al. (2014).

5.2.3. Data analysis

Variability of SOC, bulk density, soil texture, soil moisture content, depth to groundwater, and moisture deficit was analysed using standard descriptive statistics and analysis of variance tests. Daily standard deviations for soil moisture content and moisture deficit from all the measurement sites at each defined hydrological position were calculated. We calculated the percentage of time the soil was saturated and the maximum consecutive days of saturation to determine the soil hydrological regimes. We evaluated the accuracy of different DEMs for mapping microscale topography and hydrological regimes by computing standard deviation, relative and vertical accuracy errors. Relative and vertical accuracy of DEMs were expressed in terms of root mean square height errors. Cross-sectional profile graphs with depth to groundwater were plotted from the different DEMs.

5.3. Results

5.3.1. Variability in soil properties along the hydrological positions

Soil analysis indicated high variability in soil properties throughout the inland valley. The predominant soil texture in the wetland is loamy soil according to the USDA classification (United States Department of Agriculture, 2014). However, at the valley bottom, silt loam prevails (Table 5.1). Mean values between 1.32 ± 0.78 and 2.49 ± 1.70% were observed for SOC while bulk density ranged from 1.06 to 1.37 g/cm^3. Comparison of means showed significant differences among soil properties. For instance, a significant decrease of 47% for SOC ($p<0.001$), and 15% for silt

(*p<0.001*) were revealed from the riparian zone to the fringe position. Bulk density (*p<0.001*) and clay content (*p<0.001*) increased significantly towards the fringes at 25% and 13%, respectively. Mean values of SOC can be classified as moderate to high while bulk density as low to moderate according to Hazelton and Murphy, (2007). The SOC values observed are in line with those observed by Kamiri et al. (2013) in the degraded tropical wetlands of East Africa and lower than those observed by Böhme et al. (2013) in the tropical inland valley wetlands of East Africa. The observed SOC values were above the threshold of 1.74 % recommended for sustainable crop production in low-input tropical soils (Okalebo et al., 2002) at the riparian and valley bottom zones. Fringe and valley slope exhibited SOC values below the threshold and this is indicative of fertility degradation for agricultural production.

Table 5.1 Mean ± standard deviation of soil properties along the hydrological positions.

	n	Hydrological position				*p-value*
		Riparian zone	Valley bottom	Fringe	Valley slope	
BD (g cm^{-3})	76	1.06 ± 0.33^{a}	1.19 ± 0.36^{b}	1.33 ± 0.32^{c}	1.37 ± 0.17^{c}	< .001
SOC (%)	76	2.49 ± 1.7^{a}	2.10 ± 1.50^{b}	1.62 ± 1.30^{c}	1.32 ± 0.78^{c}	< .001
Clay (%)	62	16.27 ± 8.71^{a}	15.45 ± 4.91^{a}	18.32 ± 5.81^{b}	22.22 ± 1.31^{c}	< .001
Silt (%)	62	48.24 ± 15.53^{a}	51.55 ± 12.00^{b}	41.95 ± 9.29^{c}	32.45 ± 6.85^{d}	< .001
Sand (%)	62	35.49 ± 19.90^{a}	33.00 ± 11.94^{a}	39.73 ± 11.54^{b}	45.33 ± 7.90^{c}	< .001

Values followed by the same letters in a row are not significantly different at p < .05; n, sample size; BD, Bulk density; SOC, Soil Organic Carbon.

Table 5.2 shows the derived van Genuchten soil moisture retention curve parameters used to calculate soil moisture deficit for computing hydrological regimes at the defined hydrological positions. Results showed increasing and decreasing trends in saturated (θ_s) and residual (θ_r) water contents towards the riparian zone and valley slope, respectively (Table 5.2).

Table 5.2 van Genuchten parameters derived from the Brakensiek (1985) pedotransfer function based on measured soil texture and bulk density.

Hydrological positions	θ_s [cm^3/cm^3]	θ_r [cm^3/cm^3]	α [1/cm]	n
Riparian zone	0.58	0.067	0.061	1.33
Valley bottom	0.54	0.065	0.048	1.34
Fringe	0.50	0.074	0.048	1.33

Valley slope	0.49	0.087	0.059	1.31

5.3.2. Spatial variability in soil moisture content

Fig. 5.2 shows variation of measured soil moisture content at 10 cm depth interval. In general, mean soil moisture was significantly ($p<0.05$) highest in the riparian zone of the inland valley. Mean moisture (average moisture in the whole profile of 0- 40 cm depth) was 41.8 ± 8.50% at riparian zone, 40.3 ± 7.0% at valley bottom, 36.96 ± 5.50% at fringe and 29.92 ± 6.40% at valley slope positions. Comparisons of mean soil moisture content at 10 cm depth interval indicated significant differences across hydrological positions except at the valley bottom and riparian zone. Fringe exhibited remarkably high soil moisture (34.76%) at 0- 10 cm depth compared to other hydrological positions (Fig. 5.2).

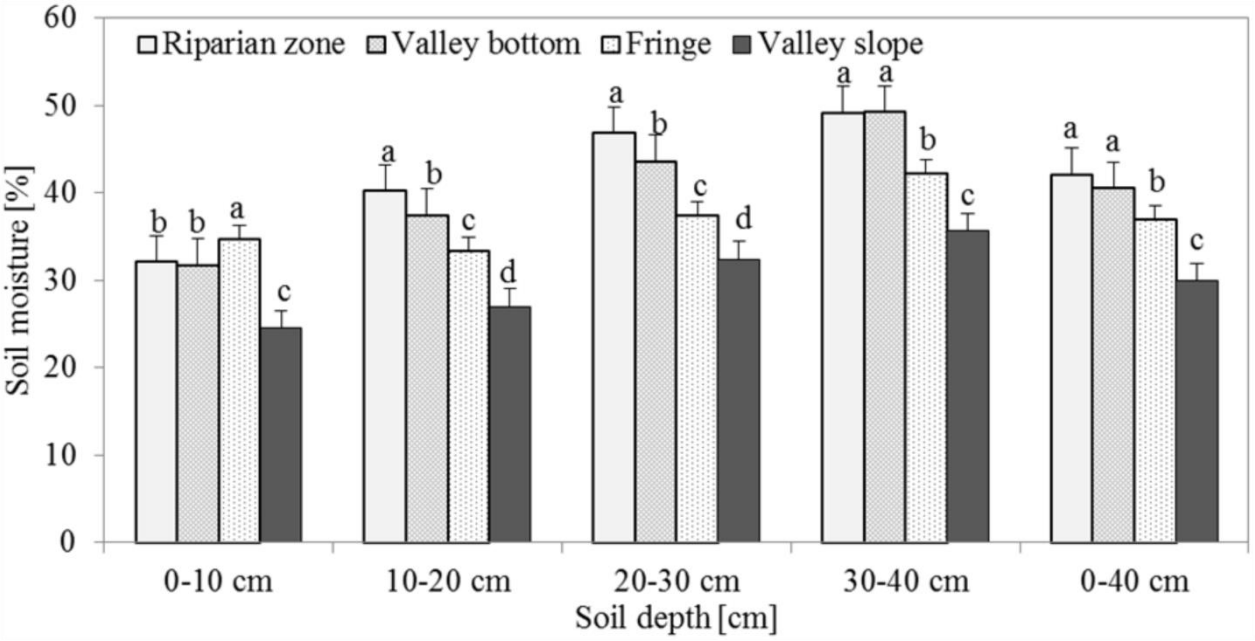

Fig. 5.2. Mean soil moisture content at 10 cm soil depth increment across the hydrological positions. Similar lowercase letters over the bars indicate no significant difference at p < .05 among hydrological positions.

Fig. 5.3 shows the impact of land use (taro, fallow and upland crops) on soil moisture content in the valley bottom. Mean soil moisture content (0- 40 cm) was higher in fallow (44.43 ± 13.30%) than in taro (41.43 ± 8.40%) and upland crops (33.13 ± 8.10%). Comparisons revealed significant differences ($p<0.05$) across land uses at 0-10 cm depth. No significant differences were revealed between fallow and taro land uses at 10-20 and 20-30 cm depth was observed. Mean soil moisture

variations are due to mechanistic and human modifications of the landscape to facilitate crop production which is typical practice in the inland valley.

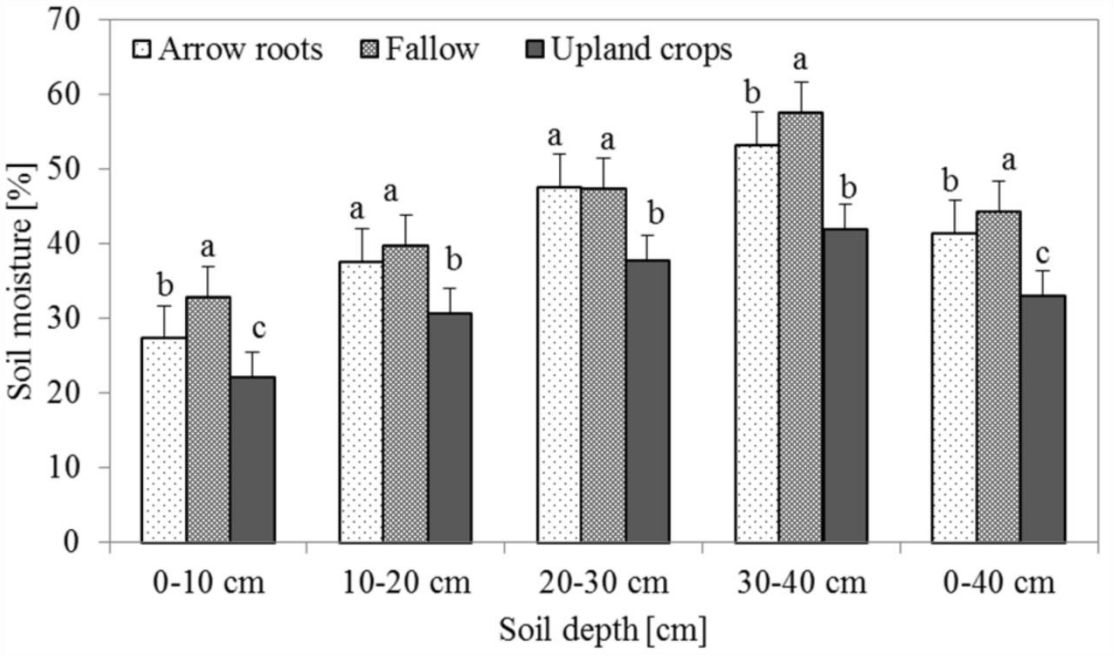

Fig. 5.3. Mean soil moisture content at 10 cm soil depth increment across the major agricultural land use types. Similar lower-case letters over the bars indicate no significant difference at $p < .05$ among hydrological positions.

5.3.3. Temporal variability in soil moisture at the riparian zone and fringe positions

A strong seasonal differentiation in soil moisture under maize (*Zea may*) crop for both the riparian and the fringe zone was observed as shown in Fig.5.4. This indicates that topography, rainfall and soil properties play a great role in controlling soil moisture dynamics. Rainfall events caused increase in soil moisture for both soil depths at the hydrological positions, albeit at different rates of change in soil moisture content. Temporal variations in soil moisture content were higher at the upper 10 cm depth and lower at 30 cm depth, with a lag effect in soil moisture decrease following the end of a rainfall event. Water retention and the time required for the wetting front to descend through the soil profile explain the temporal variations. This affects crop yields especially for shallow rooted crops like rice (Oryza sativa. L) as well as the distribution of soil hydrological regimes across the landscape. Generally, the riparian zone exhibited higher soil moisture content than the fringe position at all soil depths.

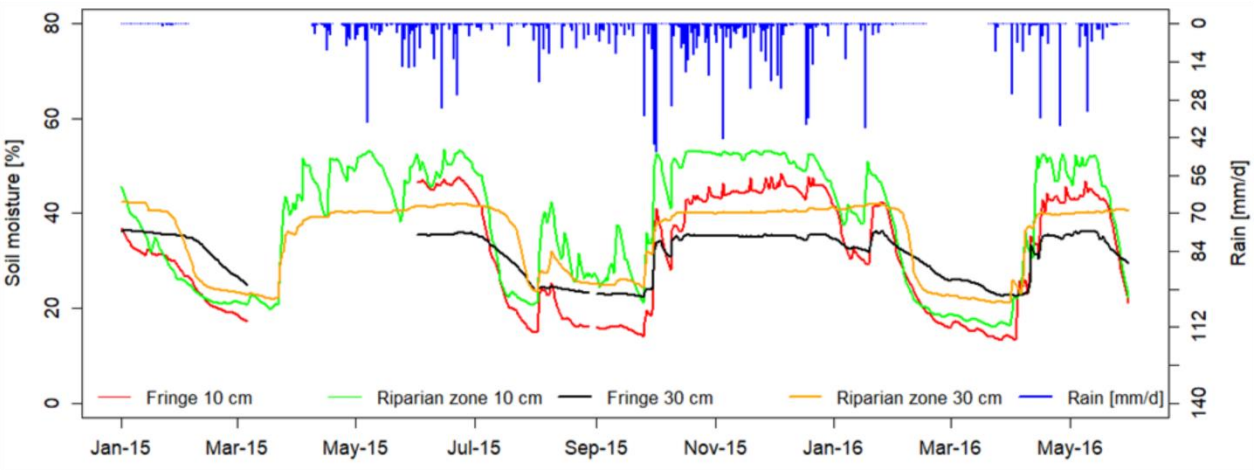

Fig. 5.4. Time series soil moisture for two contrasting hydrological positions under maize (Zea mays L.). Gaps in the soil moisture and precipitation indicate missing data due to sensor failure.

5.3.4. Hydrological regimes along the wetland transects

Results indicate that saturated, near- saturated, and non-saturated regimes exist at all the defined hydrological positions. Thus, we could not clearly delineate distinct soil hydrological regimes for each hydrological position due to high variations in depth to groundwater and hence soil moisture deficit (Fig. 5.5 and 5.6). For instance, in Fig. 5.7a, soil moisture deficit quartiles vary considerably across the observation sites along the different transects. During the rainy season, all the observation positions show saturated soil hydrological regimes with both varying percentage time and maximum consecutive days of saturation (Fig. 5.7b). In general, the results show that soil hydrological regimes are not correlated with hydrological positions and hence cannot be reliably predicted based on the hydrological positions in the inland valleys.

Along transect T3, riparian zone has the highest time of soil saturation (60%) and maximum consecutive days of saturation (70 days). This is followed by valley bottom (30%, 56 days) and the fringe (5%, 20 days). However, the trend is not consistent with other measurement positions for the respective transect. In general, the inland valley experiences saturation and near saturation regimes since most of the time, soil moisture deficit is 0 mm and < 72 mm, respectively throughout the year (Fig. 5.5 and 5.6) according to our indices described in the methodology.

Depth to groundwater ranged from 0.4 m above the surface (Fig. 5.5a) to 1.0 m below surface (Fig. 5.6a). Soil moisture deficit was in the range of 0.0 mm to 119.4 mm over the entire study period. Differences in temporal depth to groundwater and moisture deficit between rain and dry periods

were distinct. During the dry season, fringe of T4 showed the largest depth to groundwater and highest soil moisture deficit compared to other hydrological measurement positions. Overall, there is a high variability of depth to groundwater fluctuation hence soil moisture deficit within the inland valley making it difficult to delineate distinct soil hydrological regimes at each hydrological position.

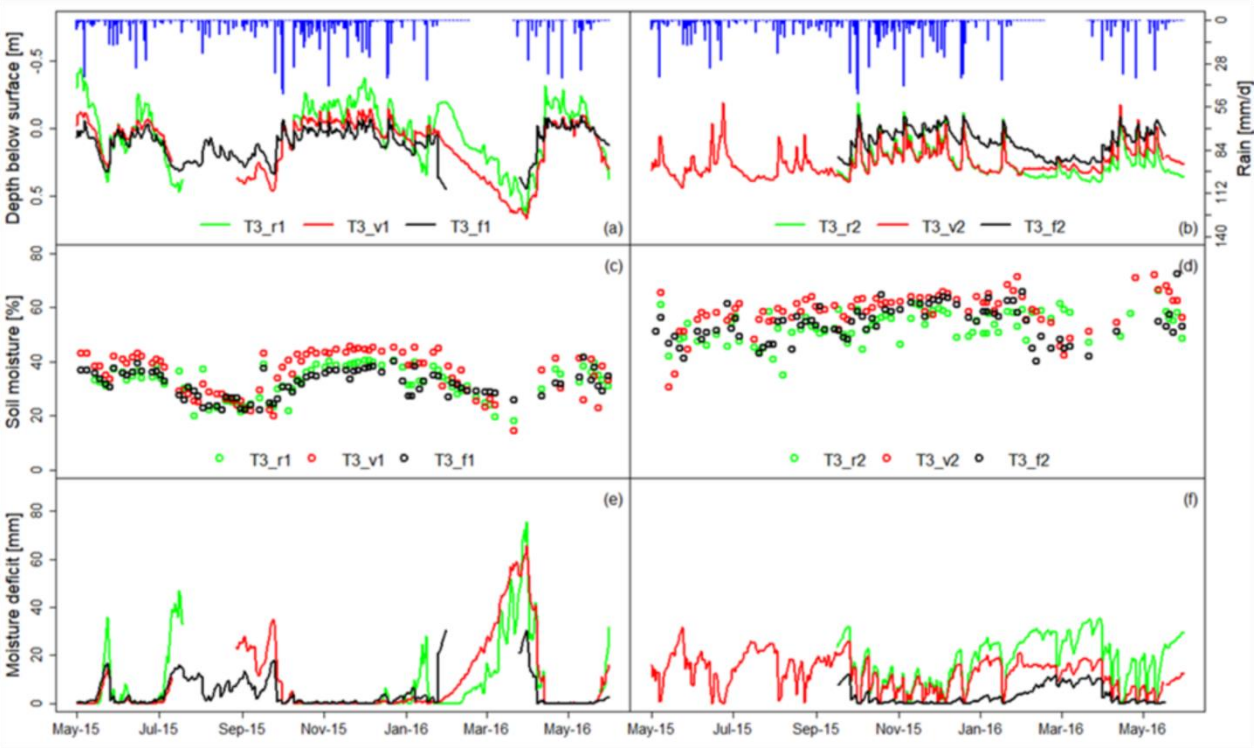

Fig. 5.5. Time series of shallow groundwater, soil moisture, and moisture deficit at different hydrological positions along transect T3. The letters r, v, and f denote the riparian zone, valley bottom, and fringe, respectively. The characters r1, v1, f1, r2, v2, and f2 denote measurement sites. Gaps in rainfall, depth to groundwater, and moisture deficit indicate missing data due to sensor failure.

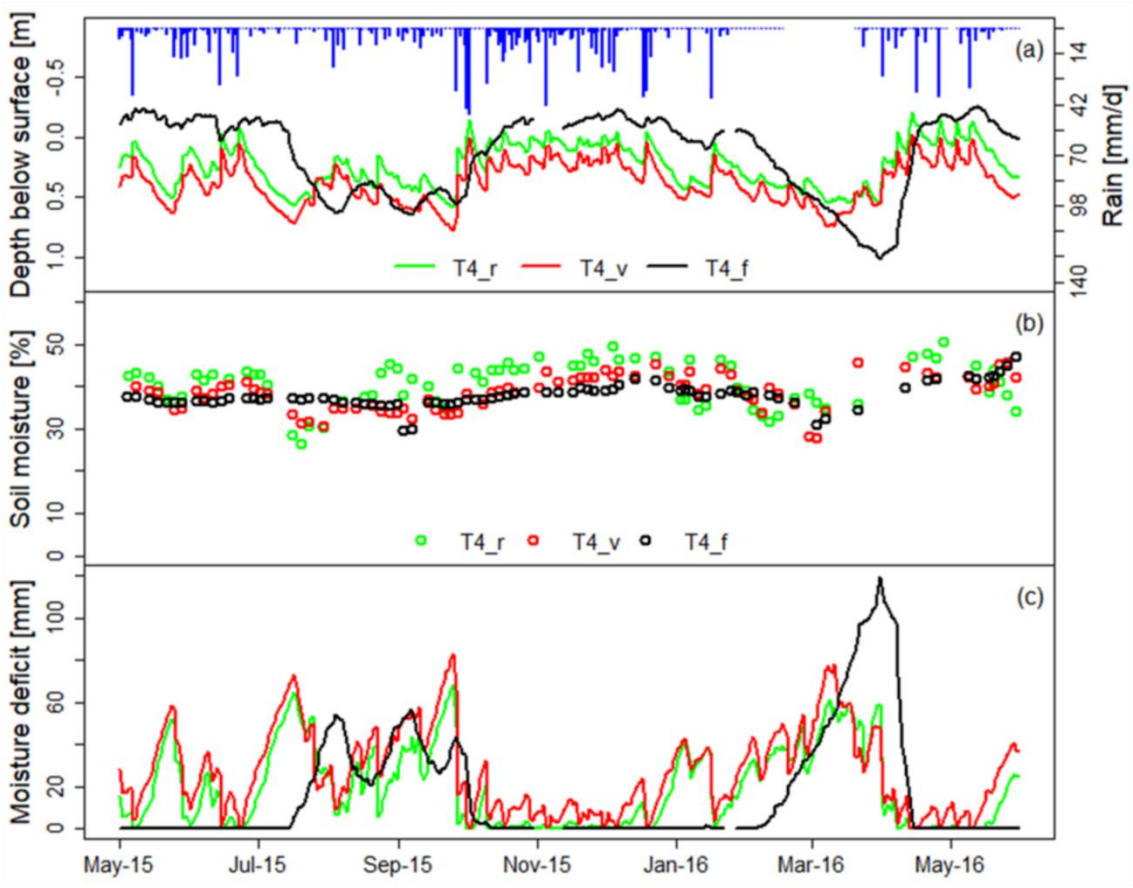

Fig. 5.6. Time series of depth to groundwater table, soil moisture, and moisture deficit at different hydrological positions for the lower transect T4. The letters r, v, and f denote the riparian zone, valley bottom, and fringe, respectively. The characters r1, v1, f1, r2, v2, and f2 denote measurement sites. Gaps in precipitation, depth to groundwater, and moisture deficit indicate missing data due to sensor failure.

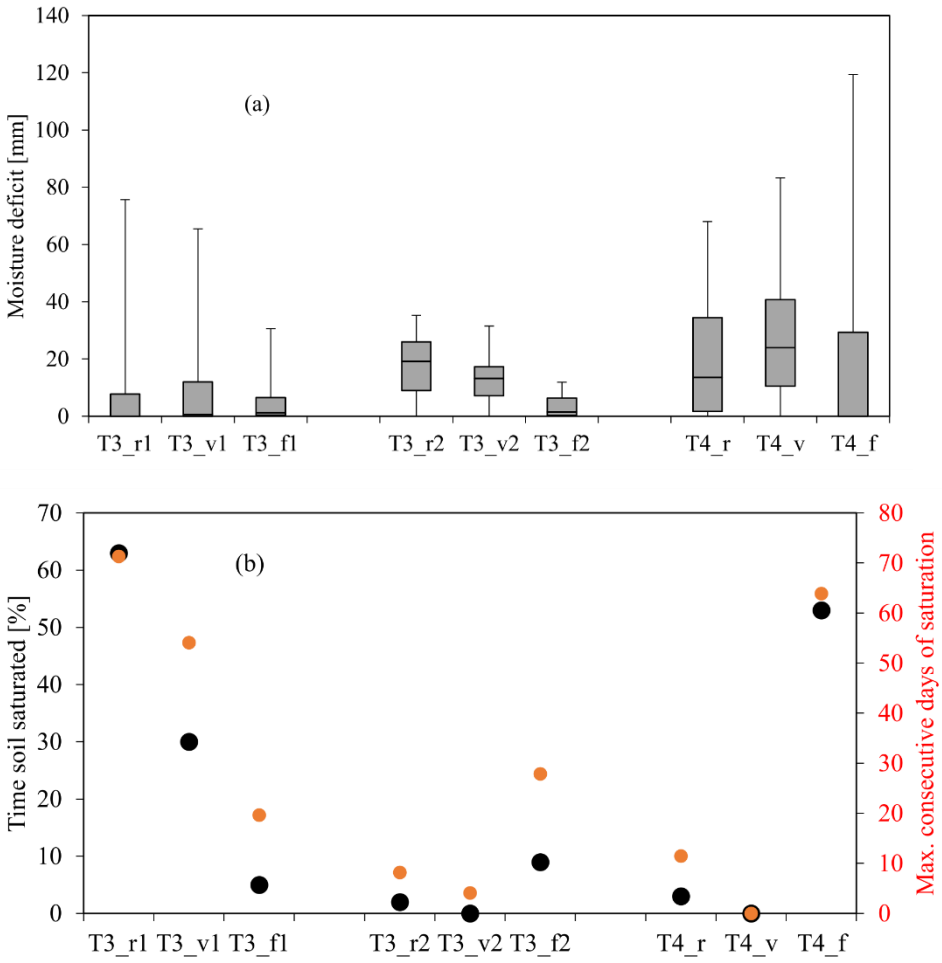

Fig. 5.7. Summary statistics: (a) distribution of mean soil moisture deficit (May 2015 to May 2016), (b) soil saturation extent during the rainy season (October 2015 to January 2016) across the hydrological positions of transects T3 and T4. The letters r, v, and f denote the riparian zone, valley bottom, and fringe, respectively. The characters r1, v1, f1, r2, v2, and f2 denote measurement sites.

5.3.5. Effect of DEM resolution in mapping micro-scale topography and soil hydrological regimes

Fig. 5.8 shows how TanDEM-X and SRTM mapped ground surface elevation, depth to groundwater and microscale topography in reference to the 5 m DEM along the cross-sectional profiles of the described transects T3 and T4 (Fig.4.1, chapter 4). The results are from the original elevation data points shifted to one reference point of the 5 m DEM. TanDEM-X reasonably provides a better estimate of ground surface elevation and microscale topography than SRTM. Therefore, a better estimation of ground surface elevation and microscale topography by TanDEM-

X provided a better estimation of depth to groundwater which defines the distribution of soil hydrological regimes than SRTM. However, TanDEM-X showed high small-scale variability in ground surface elevation in the cross-sectional profile for all transects (Fig.5.8).

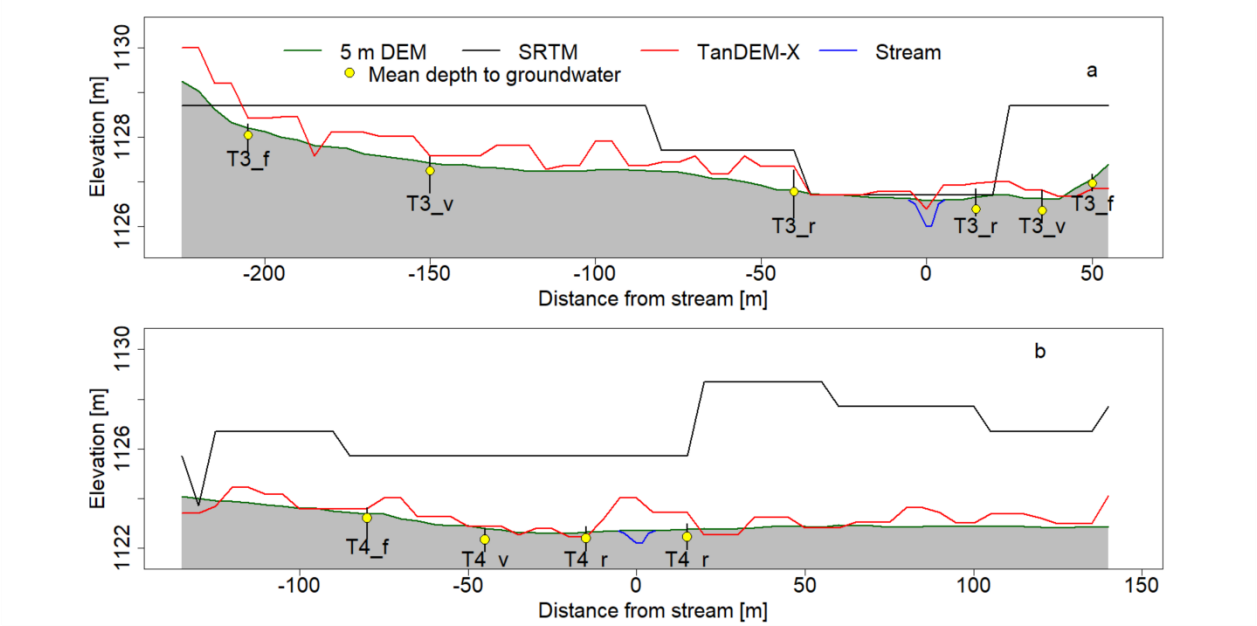

Fig. 5.8. Elevation profile derived from the three digital elevation models along transects. (a) Transect T3 and (b) transect T4. The letters r, v, and f denote the riparian zone, valley bottom, and fringe, respectively. Minimum and maximum depth to groundwater values are below and above the yellow circle, respectively.

With respect to 5 m DEM, TanDEM-X had a better relative and absolute vertical accuracy and standard deviation than SRTM. Comparing the two height error correction approaches, all the DEMs showed better results when resampled to the mean of the 5m DEM than when the elevation data points of the original resolutions were corrected to one reference point of the 5 m DEM (Table 5.3). This could be attributed to the total number of representative elevation data points sampled to derive the mean for each DEM, more sampled points increase accuracy and precision. However, the two approaches had relative vertical height errors within the predefined standard specifications of < 2 m for TanDEM-X-12 m (Wessel, 2013) and >10 m for SRTM-30m (Farr et al., 2007). Our findings are in line with a study conducted by (Purinton and Bookhagen, 2017) in Southern Central Andean plateau which revealed higher relative accuracy in TanDEM-X-12 m DEM than SRTM - 30 m DEM.

Table 5.3 Difference statistics of TanDEM-X and SRTM after correcting the elevation data (m) to the reference DEM at different spatial scales.

Data set	Description	Min	Max	Mean	SD	RV	AV
	Original DEM resolution elevation data shifted to one reference point						
TanDEM-X	Transect T3	-0.23	0.97	0.30	0.25	0.25	0.39
SRTM		-0.56	2.08	0.88	0.69	0.34	1.11
TanDEM-X	Transect T4	-0.67	1.32	0.27	0.41	0.36	0.49
SRTM		-0.29	5.95	3.73	1.3	0.68	3.95
	Resampled DEM elevation data corrected with spatial mean						
TanDEM-X	Transect T3	-1.72	0.24	-1.26	0.24	0.13	1.3
SRTM		-3.58	0.62	-2.67	0.64	0.16	2.7
TanDEM-X	Transect T4	-2.04	0.31	-1.35	0.31	0.24	1.38
SRTM		-2.40	3.03	0.001	1.22	0.27	1.2

SD; standard deviation, RV, relative vertical height error, AV, Absolute vertical height error

The elevation data maps derived after correction by a spatial mean, and the delineated stream networks from the three DEMs are shown in Fig. 5.9. TanDEM-X gives a smoother (although partly spotty) and more realistic representation of topographic data with regard to the reference 5 m DEM (Fig. 5.9a). SRTM has large errors with many local holes (Fig. 5.9b). TanDEM-X produced a more accurate stream layer close to the reference DEM and the existing mapped stream, albeit its dense drainage densities. The delineated stream network from SRTM compared to the reference DEM was completely different and partly discontinuous at some parts along the valley (Fig. 5.9c). This is partly due to the fact that the SRTM has a 30 m resolution. Therefore, using different DEM resolutions impacts on the derived stream network typology especially for smaller catchments and therefore, on the derived soil hydrological regimes. A localized error in elevation may direct a major surface water stream line in a wrong direction. Consequently, this affects surface water hydrology, and thus the distribution of the soil hydrological regimes in the inland valley wetlands.

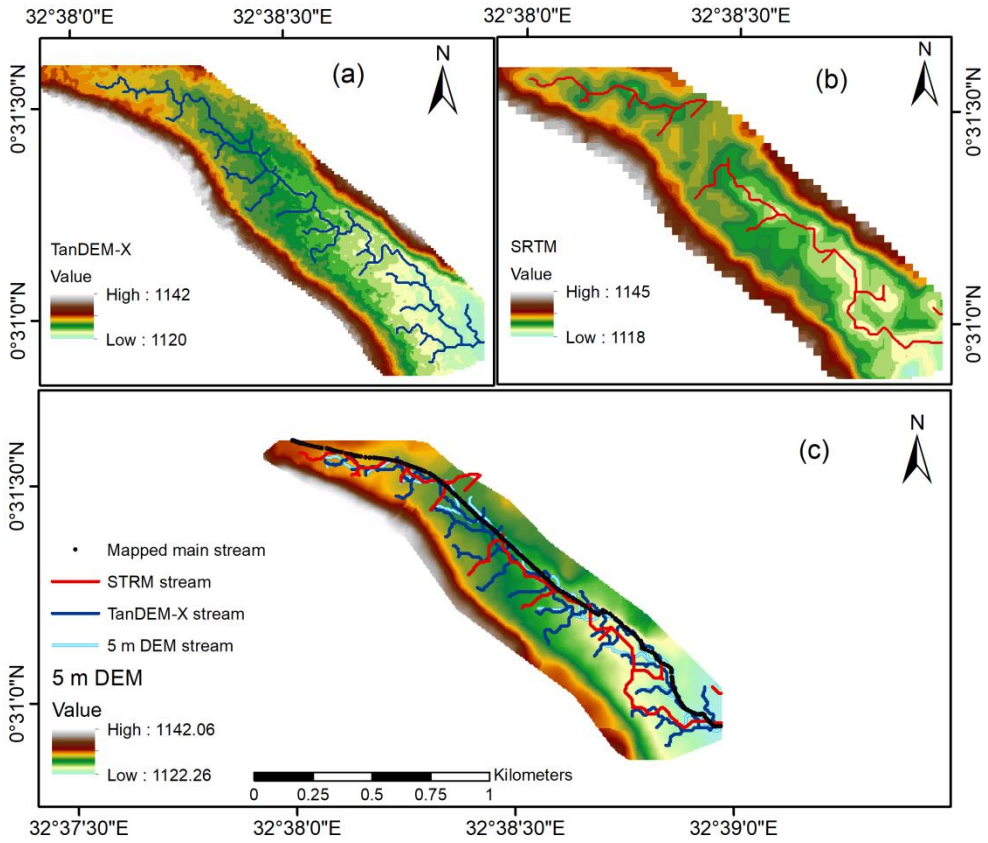

Fig. 5.9. Corrected digital elevation maps: (a) TanDEM-X-12m, (b) SRTM-30m, and (c) derived stream networks from the three digital elevation models (DEMs) against the mapped stream.

5.4. Discussion

5.4.1. Spatial and temporal variability in soil moisture

Soil moisture analysed from all the FDR sites in the inland valley increased significantly ($p<0.05$) towards the riparian zone at all soil sampled depths, however, no significant difference was observed between valley bottom and riparian zone at 0 - 10 cm, 30 - 40 cm, and 0 - 40 cm soil depths. The soil moisture trends show high agricultural potentials at the riparian and valley bottom zones. Therefore, there are high chances of increased cultivation, already visible at these zones, more so in the dry season. Adoption of soil and water conservation strategies is an opportunity to ensure sustainable agricultural production and environmental protection in these zones. The spatial variability in soil moisture content observed in the inland valley depends on topography, land use and management practices, and heterogeneity in soil properties. High silt, SOC and saturated water content observed towards the valley bottom are caused by deposition of both organic and inorganic

coarse material along the transport path. Temporal variability is controlled strongly by rainfall patterns and soil sampled depths. The mean and extremes of soil moisture are higher in wet than in dry periods. The soil sampled depths control variability during the dry period whereby deeper soil layers (30 cm depth) retain higher soil moisture content than upper layers (10 cm depth). Higher soil moisture content at the upper soil layers (10 cm) of the fringe can be explained by the influence of lateral flow from the slopes as observed by a patchy pattern of springs found in some parts of the fringe.

The low mean soil moisture content values observed from areas cultivated with upland crops can be explained by the uncontrolled traditional drainage and tillage practices occurring in the inland valley. Upland crops are normally cultivated on artificially raised plots surrounded by local shallow drainage channels to drain excess water during the rainy season in the valley. These channels are used for irrigation from stream water during the dry season. This is a common practice for most of the inland valley wetlands of the region (Kyarisiima et al., 2008). These practices lead to a reduction in soil moisture retention (Dixon and Wood, 2003; Snyder, 2005; Sławiński et al., 2012) and degradation of soil properties (Thomsen et al., 1999; Kamiri et al., 2013).The findings concerning the mean soil moisture content measured in upland crops concur with the study of Böhme et al. (2013) in the Tegu inland valley of Kenya which revealed lower moisture levels in upland crops compared to taro, which is always cultivated under saturated or near- saturated conditions. Saturated or near- saturated conditions in wetland soils entail anaerobic conditions in which soil organic carbon build ups (Mitsch and Gosselink, 2015) enriching wetland soils with nutrients (Reddy et al., 2010). Therefore, continuous cultivation of upland crops coupled with uncontrolled drainage has negative impacts on the soil properties, soil moisture and increases drawdown of shallow groundwater table (Dixon, 2002; Kamiri et al., 2014) in the valley. Consequently, this alters the inland valley's soil hydrological regimes (Wantzen et al., 2008) and thus, its hydrological cycle and ecosystem services (Sweeney et al., 2004).

5.4.2. Soil hydrological regimes along the hydrological positions

The determined soil hydrological regimes (saturated, near and non-saturated), do not correlate with the defined hydrological positions in the study area. This is due to the high spatial variability of depth to groundwater and hence moisture deficit within the valley. Spatial variability in depth to groundwater can be explained by the influence of microscale topography existing in the inland valley. This partly explains the non-significant differences in soil moisture content between the

riparian zone and valley bottom position. Micro-scale topography further influences flooding frequency, duration, and hence soil saturation (Beldring et al.,1999) through water storage in the soil matrix, macropore flow, and groundwater flow paths (Post and Jones, 2001).

Depth to groundwater and soil moisture variability depends also on the distance from the stream and human activities which are on-going in the valley. For example, during the dry season, the main stream network is blocked by farmers at several positions along the channel network, diverting water into the agricultural plots mainly at the riparian and valley bottom zones. Furthermore, the main channel was partly modified and shifted by farmers from its original flow path for irrigation and drainage. Consequently, this results in stream water level fluctuations at different parts of the main channel. These activities have significant impacts on soil moisture and groundwater table variability thus, soil hydrological regimes at the riparian and valley bottom zones. Our findings are similar to those reported by Böhme et al. (2016) in the Tegu inland valley of Kenya which indicated that drainage channels are usually blocked by farmers during the dry season thus redirecting water into plots and controlling the rise of water table while in wet seasons the channels are unblocked to allow water flow out of the inland valley. These varying soil hydrological regimes have significant implications for the inland valley hydrologic response to disturbance, agriculture, biogeochemical cycling, biodiversity, and climate change.

5.4.3. Accuracy and reliability of TanDEM-X and SRTM in mapping hydrological regimes

TanDEM-X outperforms SRTM in terms of level of detail, accuracy and consistency in mapping ground surface elevation and microscale topography. The ground surface elevation was used to compute depth to groundwater, and stream network which determine the distribution of soil hydrological regimes in the studied inland valley. The high inaccuracy in SRTM was expected because of its very course resolution hence missing topography details. However, all the DEMs showed different degrees in elevation errors with regard to the reference DEM, partly due to the fact that they are surface models hence affected by the land use data. The high dynamic and spotty elevation patterns depicted in TanDEM-X DEM could be explained by heterogeneity in vegetation cover, slope, and radar beam geometry. The penetration depth of the radar wave in vegetation is higher for SRTM with C-band than for TanDEM-X with X- band (Smith and Sandwell, 2003; Erasmi et al., 2014). Hence TanDEM-X is more sensitive to vegetation cover than SRTM. In

addition, TanDEM-X only represents heights of the canopy thus limited information for the underneath layer (Schreyer and Lakes, 2016). As can be seen from Fig.5.8b, a positive bias in elevation was observed at the stream at transect 4 due to the high canopy cover (Sugarcane) compared to relatively short canopy cover close to the stream position at transect 3 (Fig.5.8a). The discrepancies between these DEMs highlight the importance of selected space-born DEM and hence grid resolution for detailed hydrological studies at the wetland scale. Relatively small changes in wetlands' topography can impose large influence on channel flow and its travel time distribution when deriving hydrological behaviour. Therefore, the penetration depth of the radar waves and information on land use data should be taken into account especially at small scale investigations.

5.5. Conclusion

Our findings show that soil moisture content significantly increases towards the riparian zone. However, there is no significant difference in soil moisture content t between riparian zone and the valley bottom. Contrasting hydrological regimes, saturated, near-, and non-saturated, exist across the hydrological positions due to temporal and spatial variability in soil moisture content and depth to groundwater. Therefore, the hypothesis that soil hydrological regimes correlate with hydrological positions could not be supported for inland valley. Precipitation and soil sampling depth have a strong control on temporal variability while mosaic-like topographic variability, soil properties, distance from the stream, anthropogenic activities and land use practices control the spatial variability in soil moisture content and depth to groundwater. Therefore, defining catena-like transects across the inland valley may not be representative to describe the different soil hydrological regimes existing in the inland valley. These soil hydrological regimes are driven by a bunch of factors. DEM resolution has a significant impact on mapping ground surface elevation and microscale topography thus depth to groundwater which determines the different soil hydrological regimes in the inland valleys. TanDEM-X reasonably provides a better estimate of ground surface elevation and microscale topography, which influence depth to groundwater and thus soil hydrological regimes in the valley than SRTM. Therefore, since developing a high-resolution DEM might be time-consuming and expensive, the application of TanDEM-X-12 m data can be used as an option to predict soil hydrological regimes especially in data scarce regions like Sub-Saharan Africa. Therefore, TanDEM-X-12 m resolution can be used in modelling hydrological behaviours for the different inland valleys. However, knowledge of land use data prior to the DEM

analysis would improve the accuracy of the output of TanDEM-X. The findings of the study contribute to improved understanding of the existing and distribution of hydrological regimes and their controls in the inland valley wetlands of the region for better wetland agricultural water management planning at local levels.

6. Modeling the impact of land use management on water resources in a tropical inland valley catchment of central Uganda, East Africa[2]

Abstract

Due to rapid population growth, increasing demand for food, and urbanization effects in the East African region, inland valleys have been subjected to considerable changes of natural vegetation into agriculture and settlements. This study investigates the impact of land use changes on the hydrological processes in a tropical inland valley in Uganda. A hydrological response unit (HRU)-based (ArcSWAT2012) and a grid-based setup (SWATgrid) of the Soil Water Assessment Tool (SWAT) model are applied to the inland valley of Namulonge, central Uganda, which is representative for other inland valleys undergoing land use changes in the region. Good model performance was achieved from the calibration and validation of daily discharge with values of R^2 and NSE higher than 0.7 for both model setups. The annual water balance indicates that 849.5 mm representing 65% of precipitation is lost via evapotranspiration. Surface runoff (77.9 mm) and lateral flow (86.5 mm) are the highest contributors to stream flow in the inland land valley. Four land use management options are developed in addition to the current land use system, with different water resources conservation levels (*Conservation, Slope conservation, Protection of the headwater catchment, and Exploitation*). There is a strong relationship between the first three management options with decreasing surface runoff, annual discharge and water yield while the fourth option will increase annual discharge and total water yield. This suggests that if poor management and increasing exploitation of the inland valleys persist, the availability of water resources for human consumption and plant growth will decrease. This study contributes to improving the scientific knowledge on the impact of land use management change on hydrological processes in the wetland-catchment nexus to support sustainable water resources management in inland valleys of East Africa.

Key words: Wetland degradation, Soil and Water Assessment Tool, Wetland-Catchment interaction, Water balance.

[2]Published as: Geofrey Gabiri, Constanze Leemhuis, Bernd Diekkrüger, Kristian Näschen, Stefanie Steinbach, Frank Thonfeld. 2019. Modeling the impact of land use management on water resources in a tropical inland valley catchment of central Uganda, East Africa. *Science of the Total Environment 653 (2019) 1052-1066.*

6.1. Introduction

Wetlands are estimated to cover about 4.7% in Sub Saharan Africa (SSA) (Rebelo, 2010). These wetlands consist mainly of the alluvial floodplains and inland valleys in the region and cover an area of around 0.17 Mio. km^2 in East Africa (Stevenson and Frazier, 1999) from which in East Africa, 80% of the total wetland area is covered by inland wetland types (Leemhuis et al., 2016). Inland valleys are defined as flat, relatively shallow valleys, which are widespread in undulating landscapes. They are characterized by a valley bottom, hydromorphic fringe, their upstream position relative to a hydrological network and its seasonally water logged depression (Windmeijer and Andriesse, 1993; Rodenburg et al., 2014). Inland valleys offer a range of ecosystem services (MEA, 2005; Rebelo et al., 2010) for livelihood and wellbeing as well as important ecosystems in river basin management (Ramsar Convention, 1999).

In fact, in East Africa inland valleys are seen as potential niches for agricultural expansion (Dixon and Wood, 2003; Rodenburg et al., 2014) due to the declining quantity and quality of upland arable land (Maitima et al., 2009). Additionally, their nutrient rich soils and the prolonged water availability throughout the year induce potential interest for agricultural intensification to achieve food security (Von der Heyden and New, 2003; Dossou-Yovo et al., 2017). Besides provisioning services such as food and water, inland valleys provide a range of other regulating, cultural and supporting services (Rebelo et al., 2010).

Despite the value and importance of these inland valleys to the communities in SSA, they are becoming threatened due to land use and land cover change (LULCC) as a result of increasing socio-economic development and population pressure with a concomitant increase for food demands (Thornton et al., 2010; Sakané et al., 2011) as well as climate change, globalization effects and limited information on the consequences of land use changes (Turner et al. 2000; Schuyt 2005). Additionally, degradation of over-exploited upland fields for settlement and the need to earn cash income (Wood and van Halsema 2008) foster LULCC in the inland valleys. In Uganda, wetland degradation has been attributed to illegal settlement in urban areas and conversion to small scale farm lands in rural areas (Uganda Wetland Atlas, 2016). In fact, a decline of over 53.8% of wetlands in the lake Victoria basin and 14.7% in the lake Albert drainage basin has been documented (Uganda Wetland Atlas, 2016). The uncontrolled transformation of pristine inland valley wetlands to different land uses significantly changes their biophysical state, ultimately affecting the quantity

and quality of water resources (Dixon and Wood, 2003; Motsumi et al., 2012), This implies an impact on the hydrological functioning and response of the wetland and the surrounding catchment (Troy et al., 2007). The linkage between wetlands and their catchments from where water and sediments are derived and the influence of land use changes in the wetlands and catchments influence the temporal and spatial distribution of the hydrological processes (Wood et al., 2013).

Inland valleys are highly diverse and complex systems of variable ecosystems including upland areas, the hydromorphic fringe and the valley bottom, with its own typical hydrology of each individual valley (Andriesse and Fresco, 1991). They are regularly flooded during the rainy season and have noticeable impacts on catchment hydrology (Giertz et al., 2012). Considering the geomorphological setting of the inland valley wetland, surface and subsurface inflow may have a strong impact on its water balance besides precipitation (Leemhuis et al., 2016). Factors such as land use management within the wetland and its surrounding catchment and climate variability mainly influence the seasonal surface and subsurface inflow, thus water availability of the wetland. Wetlands can't be described and managed as isolated ecosystems but the surrounding catchment needs to be considered in a nested wetland-catchment approach to assess the spatial and temporal distribution of the hydrological processes within the catchment context (Von der Heyden and New, 2003). A better understanding of the wetland-catchment interaction and how land use change influences the hydrology of the wetland and catchment may help water resource managers in sustainable land use planning and water resources management (Dixon and Wood, 2003; Ramsar Convention Secretariat, 2010; Dossou-Yovo et al., 2017; Liu et al., 2017), to deal with issues such as flood mitigation, groundwater exploitation and biodiversity conservation in a more integrated and sustainable manner.

Sustainable water resources management depends on a thorough knowledge of the hydrological processes under changing land use at different spatial and temporal scales (Zalewski, 2002). Efforts to improve water resource management and land use in both wetlands and catchments in ways that recognise their functional inter-linkages have been carried out in the Sub Saharan Africa (SSA). The functional landscape approach (FLA) has been developed as a potential strategy to achieve sustainable wetland use and enhance ecosystem services for livelihood development in SSA (Wood et al., 2013). Accordingly, the FLA recognises that wetland sustainability is based on biophysical processes not only in the wetlands but also in their catchments i.e. maintaining a balance of ecosystem service use within the wetlands as well as improving land use management in the

catchment. This approach has been successfully applied and qualitatively evaluated in the country of Malawi, Africa (Wood et al., 2013). However, the quantitative analysis of the different land use management decisions implemented within this approach on the hydrological processes is not clearly documented. Yet quantitative analysis of the impact of land use management on the hydrological processes is vital in guiding decision making on land use planning and water resources at wetland – catchment scale.

Quantitative analysis of the impact of land use management on the water resources at different spatial and temporal scales, more so at the wetland - catchment level, requires hydrological modelling (Agarwal et al., 2002). Hydrological models have been used as supporting tools to improve the understanding and sensitivity of key processes due to land use changes (Lambin et al., 2000). Physically based semi-distributed hydrological models represent the underlying hydrologic and land surface processes in greater details (Beven, 2012). The Soil and Water Assessment Tool (SWAT) (Arnold et al., 2013) is one of these tools which has been successfully applied at the catchment scale to evaluate the impact of land use management on water resources in SSA (Mango et al., 2011; Memarian et al., 2014; Danvi et al., 2018; Naschen et al., 2018).

In East Africa, a significant number of studies have been conducted to improve the knowledge of LULCC impacts on water resources at local and regional scale (Githui et al., 2009; Kimwaga et al., 2012; Anaba et al., 2017; Guzha et al., 2018). Admittedly, limited number of studies (e.g. Böhme et al., 2016) have assessed the impact of LULCC on the water resources of inland valleys through hydrological modelling. Given the fact that the hydrological response of the individual inland valleys to the changing land use management is highly diverse, there is a need to invest in more research on understanding the impact of the changing land use management on these valuable and vulnerable ecosystems, this particularly obvious in East Africa where wetlands are undergoing drastic land use management changes. Therefore, the aim of the study is to improve the understanding of the feedback between land use management and hydrology in order to assist sustainable water resources management at a wetland - catchment scale. Specifically, the study has the following objectives i) to set up two hydrological models with different spatial discretization, i.e. the hydrological response unit (HRU)-based interface (ArcSWAT) and the grid-based interface (SWATgrid) suitable for land use management impact assessment at the wetland-catchment scale and ii) to analyse the impact of land use management practice on the stream discharge and water balance components of a tropical inland valley catchment.

6.2. Materials and methods

The location of the inland valley of Namulonge is described in Chapter 2. The model input data such as soil, land use, hydrological and climate data are shown in Chapter 3. The modeling approach (model setup, calibration and validation, model evaluation procedures) applied for this study is presented in Chapter 4.

6.2.1. Land use management options

The impact of land use management options on the water balance of the inland valley catchment was evaluated after validation of the SWAT model. Hypothetical land use management options were developed and explored in addition to the reference land use map of 2015 applied for calibration and validation. The land use management options were derived due to lack of a series of detailed land use maps at the scale of the study area for the past years, which would allow analysis of land use and land cover changes over time and how these changes have impacted on the inland valley's hydrology. The development of the land use management options was in accordance with the ongoing trends of land use change and with management efforts within the study area and across the East African region for the inland valleys. Therefore, we adopted the functional landscape approach (FLA) described by Dixon et al. (2012) in the development of these land use management options. The FLA recognizes the wetland –catchment linkage to achieve sustainable wetland use and water resource management (Wood et al., 2013). The land use management options included; 1. *Exploitation:* This option involved total conversion of the valley bottom of the wetland into agriculture, the wetland fringes to forest evergreen (FRSE) like eucalyptus trees and the catchment slopes into agriculture and residential areas (Fig. 6.1a). This option represents the ongoing land use change and management trend within the study area and the region. Exploitative land use has been reported as one of the major causes of inland valley catchment degradation in the region (Uganda wetland atlas, 2016). 2. *Conservation*: Complete conversion of the inland valley catchment into its natural state. The option involved total conversion of the wetland valley bottom into wetland non-forested (natural papyrus), a typical characteristic of the tropical wetlands in the region (Okeyo-Owuor and Raburu, 2016), wetland fringe into wetland forested and catchment slopes into tropical rainforest (mixed forest) (Fig. 6.1b). 3. *Slope conservation:* This option involved conversion of the valley bottom and lower slopes into agriculture, wetland fringes into wetland forested and the upper catchment slopes into tropical

rainforest (mixed forest) (Fig. 6.1c). 4. *Protection of the headwater catchment:* This option was adopted from the Rwanda Environmental Management Authority (REMA) wetland - catchment conservation approach (unpublished). It involved total protection of the headwater catchment with tropical forests (mixed forest; FRST) while at the lower catchment, the valley bottom was converted into agriculture, wetland fringes into forested wetlands and the catchment slopes into tropical rainforests (mixed forest; FRST) (Fig. 6.2). The land use proportions in the inland valley catchment after implementation of the hypothetical land use management options are shown in Table 6.1.

Table 6.1 Land use proportion (in %) according to land use management options.

Land use type	***Reference***	***Exploitation***	***Conservation***	***Slope conservation***	***Protection of the headwater catchment***
Agriculture (AGRL)	64.1	79.2	-	7.14	26.49
Forest evergreen (FRSE)	11.6	7.2	-	-	-
Mixed forest (FRST)	11.8	-	85.69	85.69	69.70
Wetland non-forested (WETN)	-	-	7.14	-	-
Wetland forested (WETF)	-	-	7.18	7.18	3.82
Built - up areas (URLD)	2.2	13.6	-	-	-
Water (WATR)	1.3	-	-	-	-
Pasture (PAST)	9.0	-	-	-	-

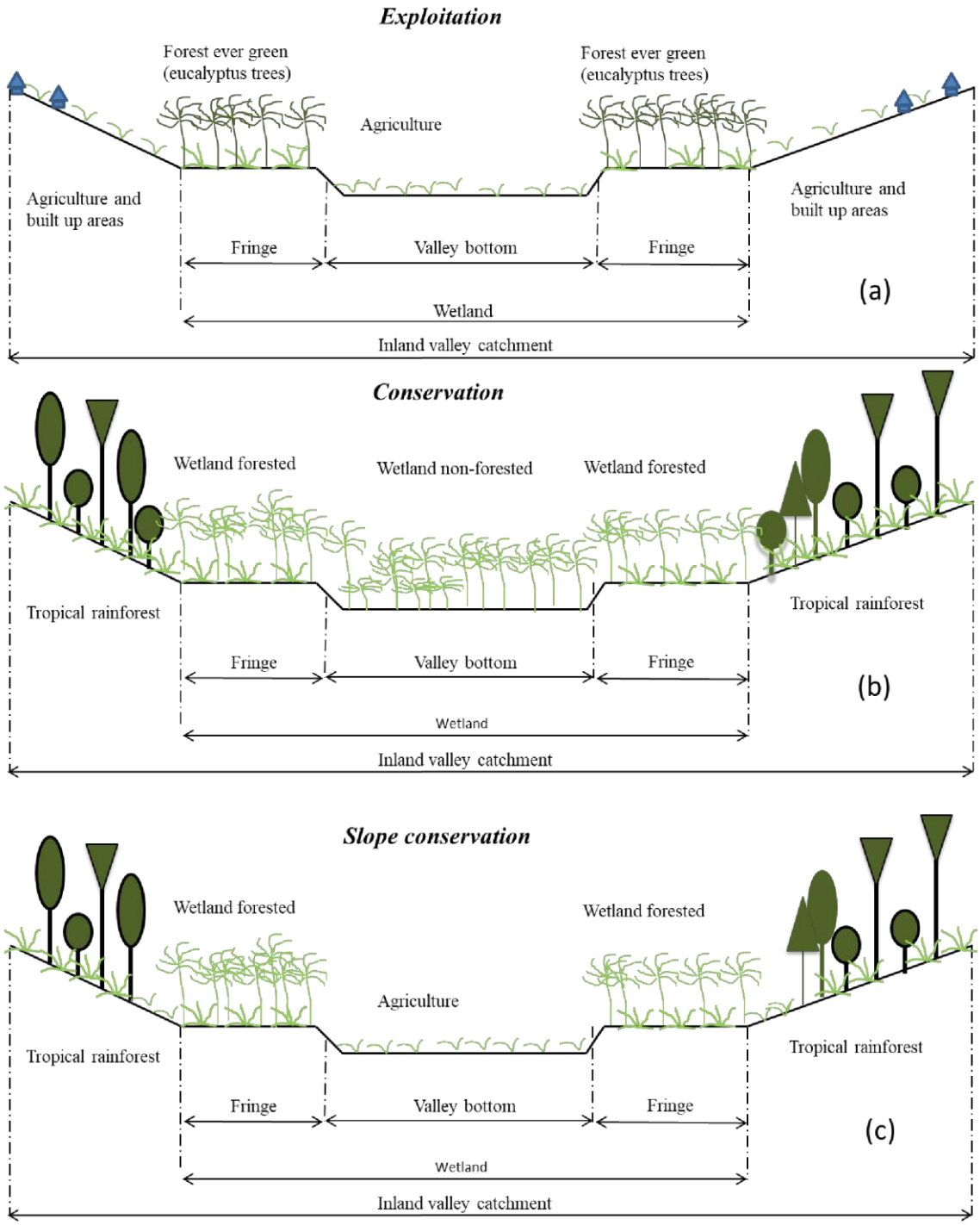

Fig. 6.1. Schematic illustration of land use management options in the inland valley catchment.

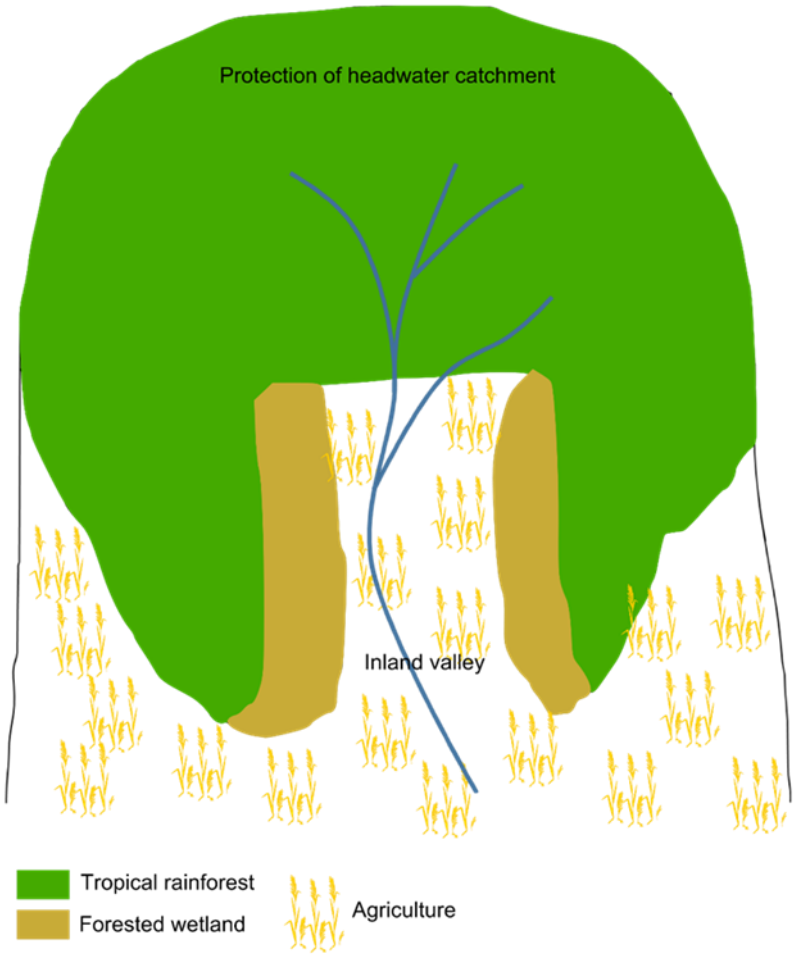

Fig. 6.2. Schematic illustration for *protection of the headwater catchment* option.

6.3. Results

6.3.1. Model performance comparisons

The comparisons between the simulated and observed discharge (Q) from the ArcSWAT and SWATgrid model setups for the year 2015 and 2016 at the catchment outlet are presented in Fig. 6.3. The figure shows good accordance between the simulated and observed discharge albeit some peaks are overestimated by both model setups. The misrepresentation of peak flows can be explained by measurement errors during high discharge events as overbank flow was often observed at the gauging station due to the size of the stream and the management practices along the stream which hindered the natural flow pattern of the stream. SWATgrid simulated higher peak flows than ArcSWAT setup, however, the simulated daily discharge derived from the two model setups matched well each other (R^2=0.95) (Fig. 6.4).

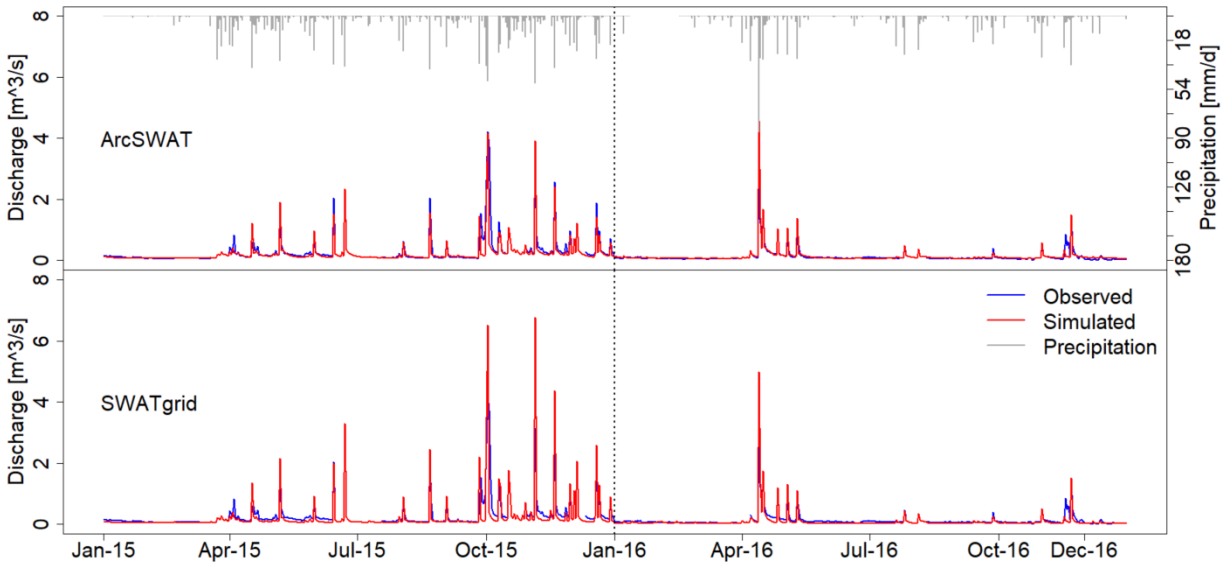

Fig. 6.3. Observed and simulated discharges for the calibration (2015) and validation (2016) periods at the catchment outlet from the two model setups (quality measures see Table 6.2).

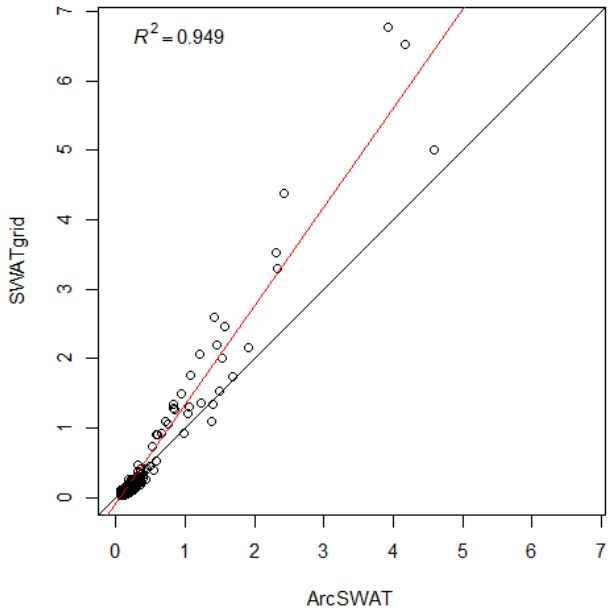

Fig. 6.4. Correlation between simulated discharge [m^3/s] from ArcSWAT and SWATgrid model setups.

Table 6.2 shows the model performance measures for the calibration and validation of ArcSWAT and SWATgrid. The performance of ArcSWAT is considered to be acceptable for the discharge calibration and validation at inland valley outlet. The statistical indicators (R^2, NSE, and KGE) were greater than 0.5. PBIAS indicator showed positive values indicating that the model

underestimated the discharge during calibration. However, an overestimation of discharge with a negative PBIAS was seen during validation. The goodness of fit and degree to which the calibrated model accounts for the parameter uncertainty in SUFI-2 algorithm is assessed by the p-factor and r-factor. The p-factor is the percentage of observed data falling into the 95% prediction uncertainty (95PPU) band. The r-factor is the thickness of the 95PPU envelop (Abbaspour, 2015). The p-factor values indicated that 84% of the observed discharge data was enveloped by the model. The r-factor reached an acceptable value of 0.27 during the calibration period. However, the model indicated some uncertainties in the simulation of low and peak discharge during the calibration period. Generally, the p-factor and r-factor reveals that the simulated discharge by ArcSWAT fit to the observed data.

For the SWATgrid model setup, the measures of model quality were satisfactorily achieved in the simulation of discharge, especially during the calibration period. In comparison with the ArcSWAT model, SWATgrid performed equally well in the prediction of discharge at the outlet during the study period. The R^2, NSE, KGE were above 0.50 while the PBIAS indicator showed that the model underestimated discharge.

Table 6.2 ArcSWAT and SWATgrid model performance indicators for discharge at the catchment outlet.

Model set up	**Calibration**						**Validation**					
	p-factor	r-factor	R^2	NSE	KGE	PBIAS [%]	p-factor	r-factor	R^2	NSE	KGE	PBIAS [%]
ArcSWAT	0.84	0.27	0.75	0.73	0.72	16.0	0.70	0.34	0.80	0.69	0.65	-8.1
SWATgrid	-	-	0.69	0.51	0.64	19.1	-	-	0.80	0.50	0.45	23.5

6.3.2. Comparison of annual water balance from ArcSWAT and SWATgrid models in the inland valley

A comparison of the mean annual water balance of the ArcSWAT and SWATgrid model setups is provided in Table 6.3, which shows the performances for the calibration period.

Table 6.3 Mean annual water balance components simulated by SWATgrid and ArcSWAT.

Water balance components	ArcSWAT	SWATgrid	Diff.
Precipitation [mma^{-1}]	1300.0	1300.0	0.0
Surface runoff [mma^{-1}]	77.9 (6.0%)	138.4 (10.6%)	60.5
Lateral flow [mma^{-1}]	86.5 (6.7%)	62.6 (4.8%)	-23.9
Groundwater flow [mma^{-1}]	72.1(5.5%)	58.5 (4.5%)	-13.6
Water yield [mma^{-1}] (284.8 mma^{-1} observed water yield)	236.5 (18.2%)	259.5 (20.0%)	23.0
Deep aquifer recharge [mma^{-1}]	172.6 (13.3%)	142.0 (10.9)	-30.6
Actual evapotranspiration [mma^{-1}]	849.5 (65.0%)	893.2 (69.0%)	43.7
Potential evapotranspiration [mma^{-1}]	1157.4	1170.5	13.1

Note: Percentage value in brackets is a component ratio to precipitation

Results of ArcSWAT and SWATgrid show that water from precipitation is predominantly lost to evapotranspiration in the inland valley catchment at ratios of 65.0% and 69.0%, respectively. The second predominant process through which water is lost in the inland valley catchment is the deep aquifer recharge. Deep aquifer recharge accounts for 13.3% and 10.9% of the total precipitation received in the inland valley catchment according to ArcSWAT and SWATgrid model setup, respectively. The surface runoff and evapotranspiration calculated by SWATgrid are 60.5 mm, and 43.7 mm, respectively more than that from ArcSWAT. However, ArcSWAT compensates this effect by higher amounts of lateral flow (23.9 mm), groundwater flow (13.6 mm), and deep aquifer recharge (30.6 mm). Total water yield simulated by SWATgrid was 23.0 mm higher than that calculated by ArcSWAT due to the higher surface runoff exhibited by SWATgrid compared to ArcSWAT. For both models, the total water yield simulated is lower than the observed one in the inland valley catchment. From both model setups, runoff contributes more to stream discharge than groundwater flow in the inland valley catchment. In detail, for ArcSWAT, 12.7% of the precipitation is converted to stream discharge (6.0% surface runoff and 6.7% lateral flow), and 5.5% of precipitation contributes to groundwater flow. Results from SWATgrid model indicate that 15.4% of the precipitation (10.6% surface runoff and 4.8% lateral flow) is converted to stream discharge while 4.5% of precipitation is transformed into groundwater flow (Table 6.3). Despite the differences in the magnitude of the simulated hydrological processes, the two model setups show similar trends of the dominant processes in the inland valley catchment.

6.3.3. Effect of Land use management on water quantity in the inland valley catchment

The comparison of the simulated annual water balance of the year 2015 with respect to the model setups and the applied land use management options gives a general overview about the impact of land cover change on the hydrological performance of the studied inland valley. Table 6.4 and 6.5 and Fig. 6.5 document the annual water balances for the two model setups after application of the land use management options.

For ArcSWAT, a decrease in the total annual discharge (surface runoff, lateral flow and groundwater flow) among the land use management options is simulated following the order *Conservation, Slope conservation, Protection of head water catchment,* and *Exploitation* (Table 6.4). More explicitly, *Conservation* land use led to a decrease of 68.7 mm in surface runoff, followed by *Slope conservation* with 67.1 mm, *Protection of headwater catchment* with 40.5 mm and *Exploitation* with 3.9 mm less surface runoff from the reference land use. The different land use management options caused an increase of annual actual evapotranspiration from the reference by 16.0%, (from *Conservation), 15.*0% (from *Slope conservation),* 8.0% (*Protection of headwater catchment*) and 1.0% (*Exploitation*). This means if conservation management is considered, more water is stored in the vegetation and lost through transpiration. Furthermore, land use management change led to a decrease in the total water yield of 44.0%, 42.0%, 27.0%, and 1.0% for the *Conservation*, *Slope conservation*, *Protection of headwater catchment* and *Exploitation* options, respectively (Fig. 6.5). Deep aquifer recharge showed a decreasing trend from the reference among the land use management options in the order *Conservation* < *Slope conservation* < *Protection of the headwater catchment* < *Exploitation.*

Table 6.4 Changes in water balance according to land use scenarios simulated using ArcSWAT. Deviations [mm] from the reference are shown in brackets.

Water balance components	***Reference***	***Exploitation***	***Protection of headwater catchment***	***Conservation***	***Slope conservation***
Precipitation [mma^{-1}]	1300.0	1300.0	1300.0	1300.0	1300.0
Surface runoff [mma^{-1}]	77.9	74(-3.9)	37.4 (-40.5)	9.2(-68.7)	10.8 (-67.1)
Lateral flow [mma^{-1}]	86.5	92.6 (6.1)	82.1(-4.4)	79.5(-7.0)	80.2 (-6.3)
Groundwater flow [mma^{-1}]	72.1	68.3(-3.8)	52.4 (-19.7)	44.0(-28.1)	46 (-26.1)
Water yield [mma^{-1}]	236.4	234.9 (-1.5)	171.9(-64.5)	132.7 (-103.7)	137(-99.4)
Deep aquifer recharge [mma^{-1}]	172.6	164.4(-8.2)	128.4(-44.2)	103.7 (-68.9)	108.4(-64.2)
Actual evapotranspiration [mma^{-1}]	849.5	856.5(7.0)	919.2(69.7)	986.6 (137.1)	975.1 (125.6)
Potential evapotranspiration [mma^{-1}]	1157.4	1157.4	1157.4	1157.4	1157.4

Table 6.5 Changes in water balance according to land use scenarios simulated using SWATgrid. Deviations [mm] from the reference are shown in brackets.

Water balance components	***Reference***	***Exploitation***	***Protection of headwater catchment***	***Conservation***	***Slope conservation***
Precipitation [mma^{-1}]	1300.0	1300.0	1300.0	1300.0	1300.0
Surface runoff [mma^{-1}]	138.4	169.6 (31.2)	50.8(-87.6)	5.9 (-132.5)	11.7 (-126.7)
Lateral flow [mma^{-1}]	62.6	53.9 (-8.7)	90.8(28.2)	102.8 (40.2)	102.8 (40.2)
Groundwater flow [mma^{-1}]	58.5	53.9 (-4.6)	77.1(18.6)	83.6 (25.1)	83.8 (25.3)
Water yield [mma^{-1}]	259.4	277.4 (18)	218.7(-40.7)	192.3 (-67.1)	198.3 (-61.1)
Deep aquifer recharge [mma^{-1}]	142.0	132.0 (-10)	142.3(0.3)	102.1 (-39.9)	103 (-39)
Actual evapotranspiration [mma^{-1}]	893.2	883.7 (-9.5)	927.3(34.1)	994.0 (100.8)	988.0 (94.8)
Potential evapotranspiration [mma^{-1}]	1170.5	1170.5	1170.5	1170.5	1170.5

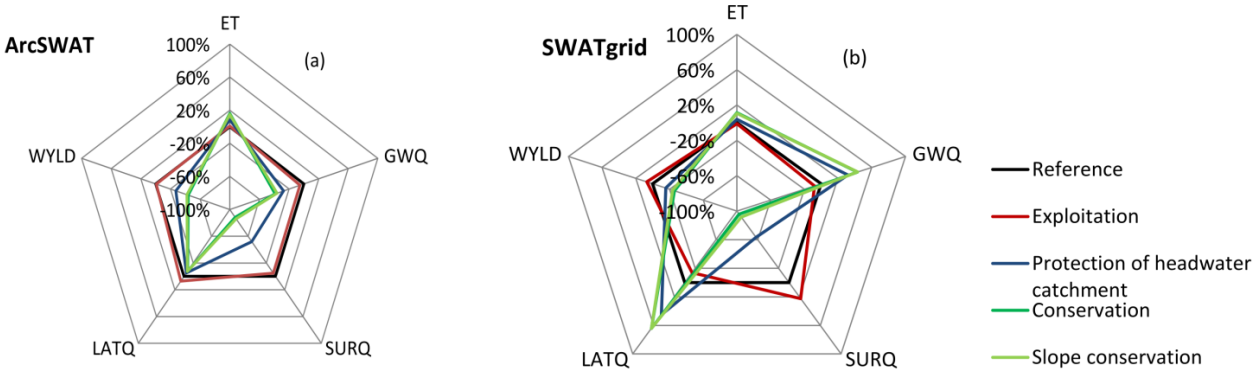

Fig. 6.5. Percentage change in water balance. ET; Actual evapotranspiration, WYLD; Water yield, LATQ; Lateral flow, SURQ; Surface runoff, GWQ; Groundwater flow.

With regard to the SWATgrid model setup, Table 6.5 shows a significant decrease in the total annual discharge (surface runoff, lateral flow and groundwater flow) among the land use options following the order *Conservation* < *Slope conservation* < *Protection of the headwater catchment* < *Exploitation*. Contrary to the ArcSWAT, *Exploitation* leads to a significant increase in surface runoff by 31.2 mm from the reference in the SWATgrid model. Moreover, a decrease in lateral flow (8.7 mm) and ground water flow (4.6 mm) from the *reference* due to *Exploitation* land use was noted while an increase for both components (lateral and groundwater flow) was observed in the *Conservation, Slope conservation* and *Protection of the headwater catchment* land uses. A decrease of 26.0%, 24.0%, and 16.0% in annual water yield was observed for *Conservation*, *Slope conservation* and *Protection of the headwater catchment* land uses, respectively while an increase of 7.0% was noted from the *Exploitation* land use (Fig. 6.5). Likewise, there was an increase in the actual evapotranspiration for the applied land use options except for the *Exploitation* land use (Table 6.5, Fig. 6.5). Actual evapotranspiration from *Conservation* land use increased by 100.8 mm more than that of the *Reference*, *Slope conservation* had 94.8 mm and *Protection of the headwater catchment* resulted into 34.1 mm more actual evapotranspiration. A decrease of 9.5 mm due to *Exploitation* land use was noted (Table 6.5). A decline in deep aquifer recharge was generally observed among the different land use management options. In summary, both model setups showed similar behaviour in the simulation of the water balance components although there were differences in the magnitude.

The main advantage of the SWATgrid setup relative to ArcSWAT is its explicit consideration of spatial patterns (Pignotti et al. 2017). Therefore, spatial patterns of runoff (lateral flow and surface runoff) were analysed for the SWATgrid. The spatial patterns of these fluxes show the impact of topography, landscape position, and land use and soil types on the model output.

Fig. 6.6 shows the spatial distribution of lateral flow (LATQ) in the inland valley. Lateral flow (LATQ) values are highest at the steep slopes, and almost no lateral flow occurs in the valley bottom which is an expected pattern. Topography, soil properties, and land use management are the main factors determining the amount of LATQ in the inland valley. Steep slopes allow lateral flow while in flat areas the water will percolate towards the shallow aquifer. LATQ increases between the land use management options in the order: *Conservation* > *Slope conservation* > *Protection of the headwater catchment*. This can be explained by the increased mixed forest proportions in the same order along the slopes which encourage infiltration.

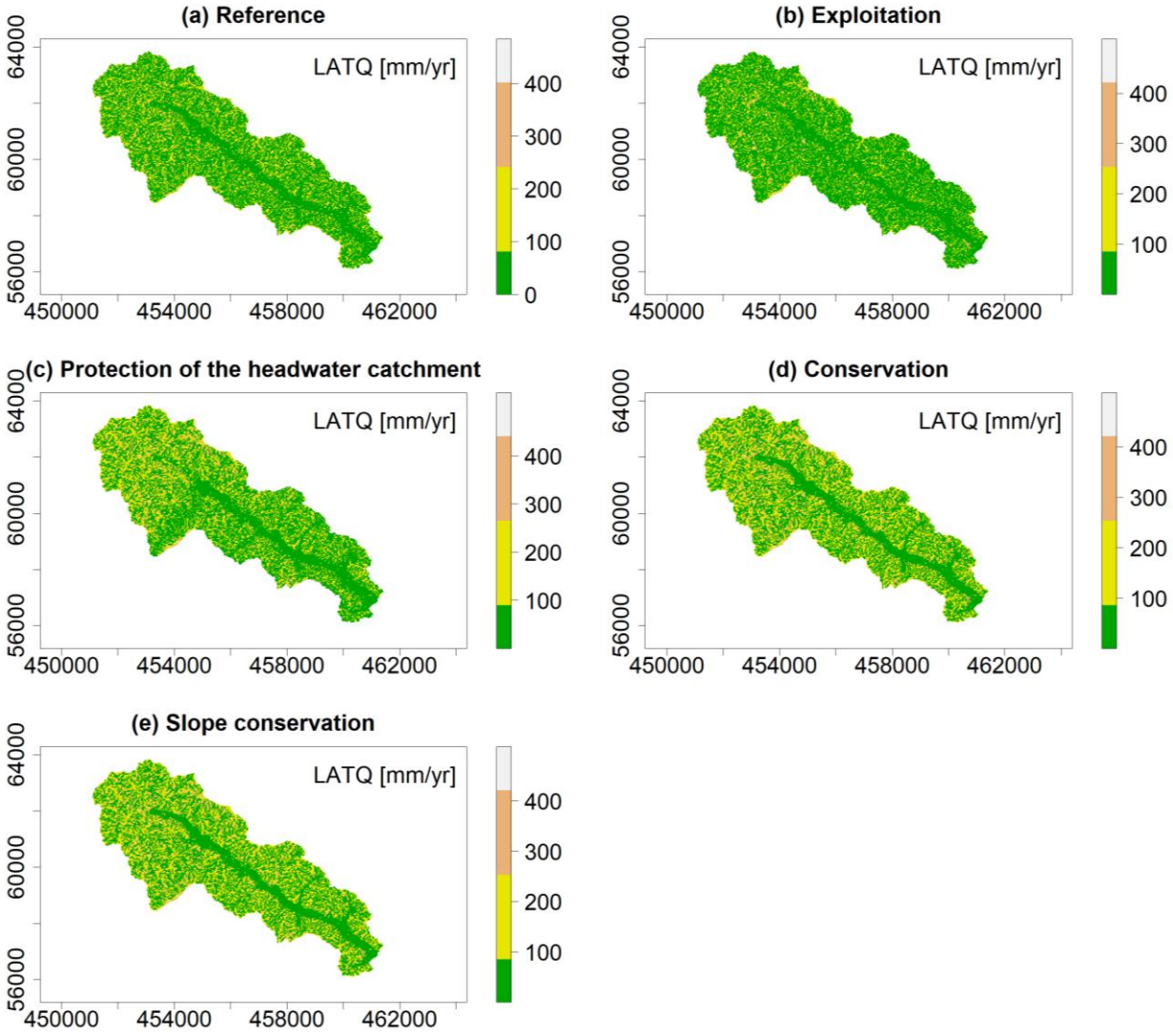

Fig. 6.6. Spatially explicit distribution of lateral flow (LATQ) for the different land use management options simulated by SWATgrid.

Fig. 6.7 presents the spatial distribution of surface runoff simulated by the SWATgrid. The model simulates higher runoff at the upslope than in the valley bottom and in the grid cells with Fluvisols for the *Reference* and *Exploitation* land uses. This can be explained by the increased percentage of agricultural land use and built-up areas together with the steep slopes which lower the infiltration rate inducing surface runoff. Contrary to the *Exploitation* land use option, the upslope grid cells under land use management options *Conservation*, *Slope conservation* and *Protection of the headwater catchment* exhibit lower surface runoff than the valley bottoms. The low surface runoff at the upslope can be attributed to the high percentage of mixed forest land use which increases the infiltration rate in the soil, resulting in increased subsurface flow. Increase in surface runoff among

the land uses occurs in the order *Exploitation* > *Protection of the headwater catchment* > *Slope conservation* > *Conservation*. Land use management options and slope play an important role in controlling surface runoff in the inland valley catchment. For example, *Protection of the headwater catchment* land use shows higher runoff at the wetland fringes than the valley bottom (under the agricultural land use) due to the slope effect while for the *slope conservation* land use management, the valley bottom exhibits higher runoff than the fringe mainly due to the agricultural land use implemented (Fig. 6.7).

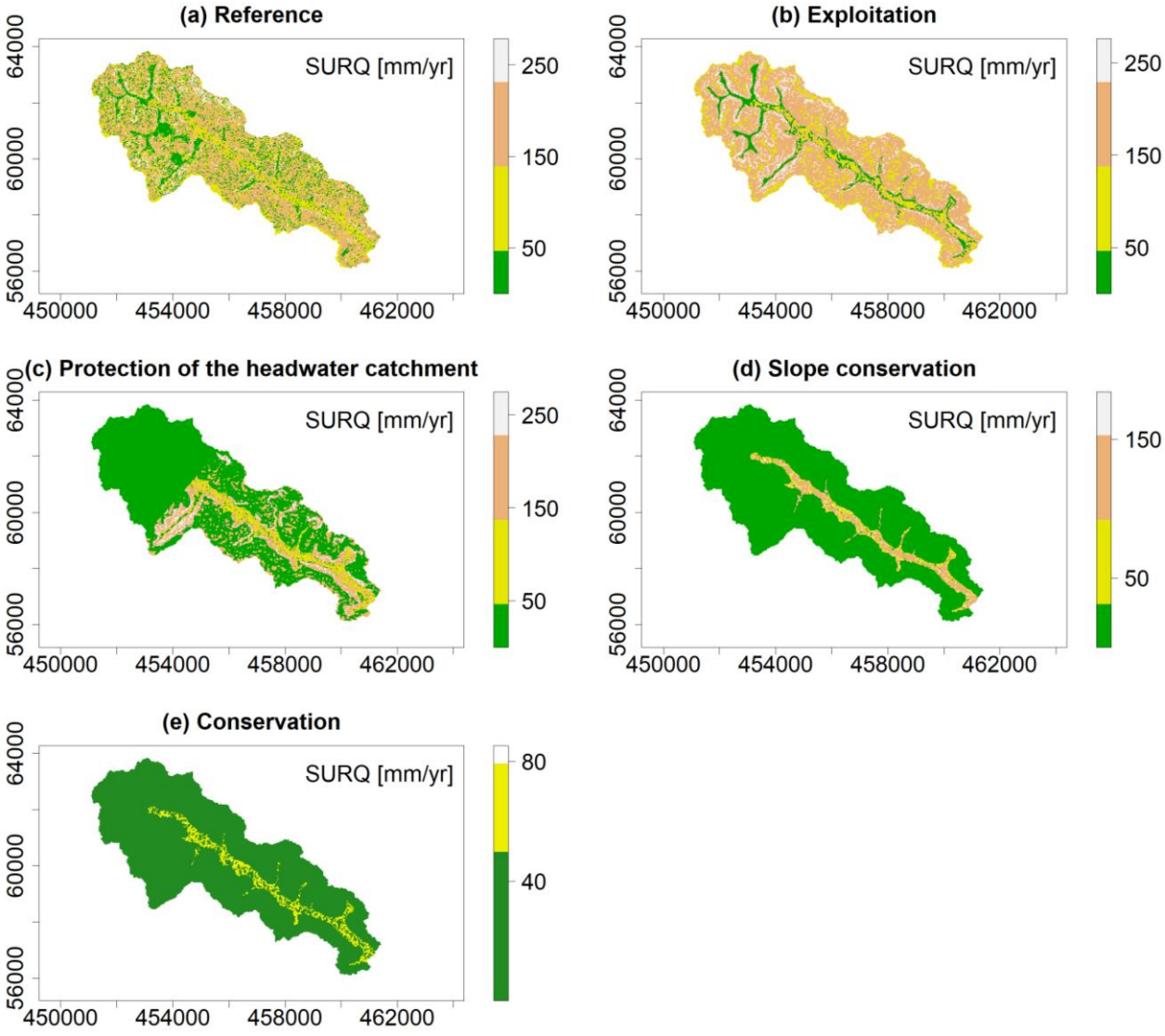

Fig. 6.7. Spatially explicit distribution of surface runoff (SURQ) for the different land use management options simulated by SWATgrid. Note the different scales for (d) and (e) which are required to illustrated differences within the single maps.

From the spatial analysis, the SWATgrid setup enabled us to identify the hydrologically sensitive areas (HSAs) to land use change at a finer spatial resolution. Thus, understanding and analysing the spatial distribution of the different hydrological processes on the HSAs is essential in maintaining stream flow regimes (Duku et al., 2015) and managing the water resources at a wetland-catchment scale.

As explained before, both model setups show similar behaviour in simulating daily discharge. Therefore, we used the ArcSWAT model setup to evaluate the impact of land use management options on the exceedance probability of annual discharge (with emphasis on the low and peak flows) for 30 years (1976-2005), using the historical downscaled climate data of the study area. We used climate data for 30 years to understand the long term impact of land use on the annual discharge in the inland valley since there was no sufficient and long term measured discharge and climate data for the study area. The historical climate data was downscaled from the Coordinated Regional Downscaling Experiment (CORDEX) Africa (Gutowski et al., 2016).

Fig. 6.8 depicts the results of the daily flow duration curve (FDC) from the different land use scenarios. All analysed scenarios indicate increasing high and low flows within the simulated period (1976-2005). However, the slope of the daily FDC is unchanged for the simulated period. There are no pronounced changes observed between the *Conservation* and the *Slope conservation* land use options although the flow duration curve for *Conservation* is lower than the *Slope conservation* FDC. Equally important, the *Exploitation* and *Reference* land use management show marginal differences for the high and low flows.

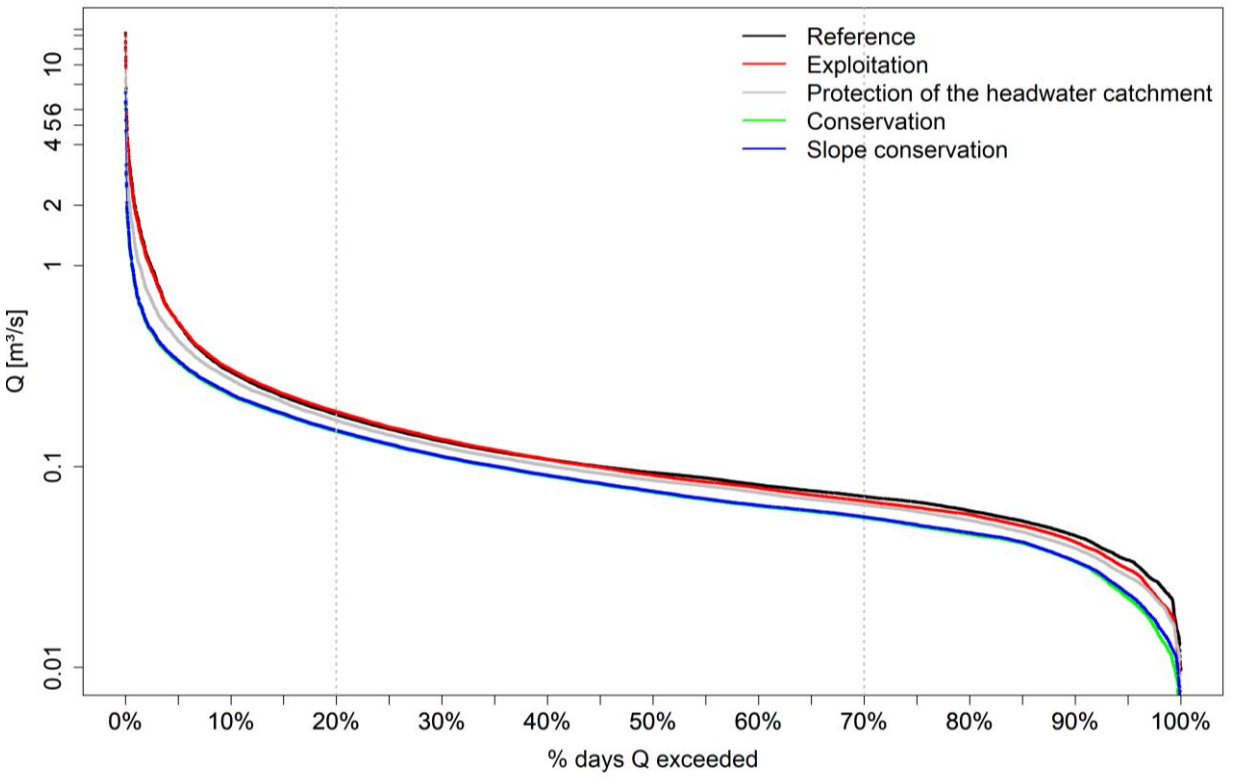

Fig. 6.8. Flow duration curves from ArcSWAT for the five land use management options. The y-axis is plotted on a log scale.

Furthermore, the FDC for the *Conservation* and *Slope conservation* land use options show significant decrease in high (10% exceedance) and increase in low (90% exceedance) flows compared to the *Exploitation* and *Reference* land use options. The *Protection of the headwater catchment* land use management option also shows a considerable decrease in high flows (5% exceedance) and increase in low flows (90% exceedance) compared to the *Reference* and *Exploitation* land use options. In general, implementation of the *Conservation* land use option as a management strategy for water resources in the inland valley strongly decreases high flows followed by the *Slope conservation* management option, and then the *Protection of the headwater catchment* management option. The results imply that the *Exploitatio*n land use option has a higher impact on the high flows than on the low flows. Therefore, feasible land use management strategies which enhance low flows like the protection of the headwater catchment and slope conservation can be appropriate for water resources management in the inland valleys.

In general, both model setups show that the *Exploitation* land use option has the largest impact on total discharge and the increase in surface runoff. Also, a reduction in discharge amounts and water

yields following the conservation land use scenarios is in the order: *Conservation > Slope conservation > Protection of the headwater catchment* for both model setups.

6.4. Discussion

6.4.1. Hydrological modelling calibration and validation

The two model setups showed good results in the simulation of the annual discharge during the calibration and validation periods. This shows that the applied methodology by calibrating ArcSWAT using common techniques (Arnold et al., 2012; Abbaspour et al., 2015; Moriasi et al., 2007) is appropriate for running a grid-based SWAT model. Similar observations were made by Danvi et al. (2017) for three inland valleys in Benin, West Africa. This reveals that the simulated discharge is insensitive to the different discretization schemes but differs in the importance of runoff components. Specifically, the discretization scheme applied in SWATgrid resulted in increased surface runoff, water yield and actual evapotranspiration in the inland valley. The increment was to some extent compensated by higher lateral flow, groundwater flow and total aquifer recharge simulated by ArcSWAT. The discrepancies have previously been observed and discussed by Rathjens and Oppelt (2012a). The authors attribute these discrepancies in the discharge components simulations to the higher degree of details concerning the hydrological characteristics like soil type, land use and slope resolved by the SWATgrid model (Rathjens and Oppelt, 2012b).

Additionally, the differences can also emanate from the different routing concepts applied in which lateral fluxes between the grid cells are accounted for in SWATgrid, unlike ArcSWAT, by which no interaction between HRUs occurs. Indeed, according to Arnold et al. (2010), a constant flow separation ratio is applied in ArcSWAT to partition the amount of flow into landscape and channel flows. On the contrary, in SWATgrid, a spatial distribution of flows and transport processes are taken into account by using the modified topographic index. This index is mainly adjusted by the drainage density and applied to identify areas of high probability of runoff occurrence within the catchment (Rathjens et al., 2014).

In the inland valley, actual evapotranspiration is the dominant water loss pathway, as over 60% of the precipitation received is lost which is also supported by Danvi et al. (2017). Furthermore, runoff (surface runoff and lateral flow) is the second most important process in the study area representing

about 13.0% (from ArcSWAT) and 16.0% (for SWATgrid) of the precipitation received. The high surface runoff experienced in the inland valley is a result of the land use, soil properties, and slope gradient observed in the study area. In the inland valley, agriculture (small scale agriculture with a mosaic of land uses) dominates with 64.1% area coverage. Steeper slopes prevail at the fringes and uplands of the valley. Expansions of agricultural land coupled with steeper slopes encourage overland flow due to the low infiltration rate (Burt et al., 2005; Gomi et al., 2008). As a result, surface runoff and therefore, flooding risk may increase due to the on-going high level of upland-wetland cultivation.

6.4.2. Impact of land use management on hydrological processes

From our study, the decrease in water yield and total discharge (surface runoff, lateral flow and groundwater flow) following the land use management options (*Conservation, Slope conservation* and *Protection of headwater catchment*) can be attributed to the reduction in the Hortanian surface runoff. A decrease in the peak flows and increase in low flows among land use options *Conservation, Slope conservation* and *Protection of the headwater catchment* compared to the *Exploitation* land use and the current land use system (*Reference*) are also related to a reduction in surface runoff. Low surface runoff is induced by the increase in vegetation/canopy cover as a result of increased mixed forest (FRST; 85.7%) and wetland forested (WETF; 7.2%) coverage for both *Conservation* and *Slope conservation* land use options, and 69.7%, FRST and 3.8%, WETF for the *Protection of headwater catchment* land use option along the slopes and fringes of the inland valley. The higher the spatial coverage of mixed and wetland forested the higher the reduction in surface runoff. The trend in stream discharge and total water yield of the different land use management options was as follows: *Exploitation* > *Protection of headwater catchment* > *Slope conservation* > *Conservation*. Similar findings were documented by Li et al. (2015) who related a decrease in surface runoff to the expansion of forest land while assessing the impact of land use change on the water resources in the middle and upper reaches of the Heihe River Basin in north western China. In addition, Nugroho et al. (2013) reported a decrease in surface runoff as a result of increased forest land cover which increased interception and soil infiltration of through fall. Furthermore, a review study by Guzha et al. (2018) on the impact of land use and land cover changes on surface runoff and annual discharge in East Africa reported that loss of forest/vegetation cover led to an increase in surface runoff and peak discharge.

The impacts of land use coverage on the groundwater and lateral flow for each individual model setup is very complex. Land use cover, for example agriculture, may have a negative or positive effect on lateral and base flow, based on the management practices (Price, 2011). On the one hand, according to Loch (2000), increase in land coverage strongly increase infiltration rates due to improved soil porosity as a result of root activity and reduction in surface runoff, as a result increasing groundwater and lateral flow. Dense land coverage has a high potential of groundwater recharge as it is characterized by a full or partial pervious surface.

The increase in total discharge observed from the current land use system (*Reference*) and the *Exploitation* land use options can be explained by the increase in the agricultural land use in the inland valley. Leemhuis et al. (2007) attribute the increase in total discharge to the expansion of agricultural land as a result of reduced vegetation height and canopy cover. As a result, interception losses decrease resulting in a higher net precipitation that reaches the surface and thus, higher risk of surface runoff. Several authors (Githui et al., 2009; Mango et al., 2011; Yira et al., 2016; Anaba et al., 2017; Danvi et al., 2018; Näschen et al., 2018) have reported the impact of changing land use cover on the hydrologic systems of catchments, which can diversely impact the water resources at different spatial and temporal scales. In summary, the increase in the vegetation coverage among the land use management options (*Conservation > Slope conservation > Protection of headwater catchment > Exploitation*) generally resulted in decreased total water yield simulated from the individual model setup, as a result of increased actual evapotranspiration.

6.4.3. Impacts of land use management on spatial distribution of total discharge

Simulated hydrological effects for land use scenarios are fundamental to decisions aiming to optimize landscape functions (Memarian et al., 2014). The increase in groundwater and lateral flow distribution along the slopes and wetland fringes after implementation of conservation land use scenarios was induced by the increased vegetation coverage land area (mixed forest and non-wetland forest land at the slopes and fringes, respectively) and soil types. As discussed before, increase in vegetation coverage increases water infiltration into the soils thus resulting in more subsurface flows in the catchment. On the other hand, exploitative practices (increase in agricultural land) will greatly reduce the groundwater resources and lateral flow along the catchment slopes and wetland fringes. The spatial distribution of surface runoff in the inland valley is controlled by topography, soil type and land use management options. Implementation of

conservation management scenarios will greatly reduce surface runoff along the slopes and the wetland fringes of the inland valley. Additionally, conservation measures which protect the surrounding catchments of the wetland, will improve the wetland's ecosystem services.

In summary, the current land use system (*Reference*) and the *Exploitation* land use options (expansion of wetland agriculture) show increased water yield, total discharge and higher peak flows resulting in a low potential for the regulating ecosystem services like reduction of flood peaks, climate regulation (carbon storage), and the recharge of aquifers in the wetland. On the other hand, *Conservation*, *Slope conservation* and *Protection of headwater catchment* land use options show a reduction in the total water yield, total discharge and peak flows in the inland valley by improving infiltration of precipitation and water storage. Consequently, the period for which water is available in the wetland will also increase. Another positive effect is that infiltration zones of natural vegetation at the wetland / upland interface can act as a buffer for sediment deposition and a biodiversity adaptation area (Wood and Dixon, 2008).

6.5. Conclusion

This study evaluated the impact of on-going land use and land use management practices on the water resources of an inland valley catchment located in Namulonge, central Uganda. To achieve this goal, an HRU-based interface (ArcSWAT2012) and a grid-based interface (SWATgrid) of the Soil and Water Assessment Tool (SWAT) model were applied to simulate the hydrological processes in the inland valley. Overall, a good representation of daily discharge dynamics was achieved by the two models with a realistic water balance. This is an important finding as both models have advantages and disadvantages. The HRU concept of ArcSWAT is computationally efficient but has no lateral exchange between the simulation units. Therefore, the spatial arrangement of the most important attributes soil, land use, topography is of minor importance which is acceptable for larger catchments. SWATgrid requires significant larger computing time but considers the spatial pattern in a landscape. In studies where this is of importance like in the catchment - wetland interaction study as discussed here, this provides the possibility to evaluate management options which ArcSWAT does not offer.

Both model setups indicated similar trends albeit difference in magnitude in the total discharge (surface runoff, lateral and groundwater flows) following the application of land use scenarios. A decrease in total discharge and annual water yield following land use management options in the

order *Conservation* < *Slope conservation* < *Protection of headwater catchment* < *Exploitation* was found. Moreover, an increase in the total discharge and annual water yield for exploitation land use option was observed. From the analysis of FDC, adoption of the conservation management land use options will reduce the peak flows in the inland valley. Contrary, as a result of agricultural expansion (exploitation and current land use), runoff generation and flooding risks may increase related to higher peak flows. Consequently, an increase in the sediment and nutrient flows downstream can also be expected. Therefore, we emphasize adoption of conservation land use management strategies (operational land scape approach) which recognise wetland - catchment interactions for sustainable water resources management in the inland valley. This is particularly important in East Africa, which is experiencing exorbitant pressure on the fragile water resource ecosystems like inland valley wetlands (once called "wastelands"), due to the changing climate and population growth.

Therefore, future efforts should focus on understanding the combined impact of climate and land use change on the water quantity and quality (sediments and nutrient flows) of these agriculturally used inland valleys in the region.

7. Hydrological response to climate and land use management change in a tropical inland valley in central Uganda, East Africa

Abstract

The potential hydrological responses to climate and land use management change in the inland valley of Namulonge, central Uganda are studied. Data from an ensemble of six RCM-GCM climate models and two greenhouse gas concentration scenarios, RCP4.5 and 8.5 were downscaled from the Coordinated Regional Climate Downscaling Experiment (CORDEX-Africa) project up to the middle of the 21st century. A statistical bias correction (empirical quantile mapping and linear regression) was applied on daily precipitation and temperature data, respectively with ground observations (1976-2005). The SWAT model was applied to assess the impact of climate and land use change on the hydrological response of the inland valley. Daily climate variables were used as model inputs for two periods; 1976-2005 (baseline) and 2021-2050. A general increase in temperature by 1.4 ^{0}C and 1.6 ^{0}C under RCP4.5 and 8.5 climate scenarios, respectively is expected in the future (2021-2050). A mixed change signal in precipitation is projected among the six climatic models. However, models ensemble mean project an increase in annual precipitation (7.4% and 21.8% under RCP4.5 and RCP8.5). The variability in precipitation change signal results in considerable uncertainty in the projected annual discharge and water balance. Therefore, a potential increase and decrease in future discharge and water balance has to be considered when planning for adaptation climate change strategies in the inland valleys. The rain and dry seasons are projected to get wetter and drier, respectively. Compared to land use management options, climate change will have a dominant impact on the water resources in the inland valley. Adoption of C*onservation, Slope conservation and protection of the headwater catchment* land use management approaches will significantly reduce the impacts of climate change on the total water yield and surface runoff and increase evapotranspiration and water availability in the inland valley. This suggests that if sustainable climate smart management practices are adopted in these inland valleys, the availability of water resources for human consumption and plant growth will increase. This study contributes to improving the scientific knowledge on the impact of climate and land use management change on hydrological processes in the catchment-wetland nexus to support sustainable water resources management in the inland valleys of East Africa.

Key words: Water resources, wetland-catchment nexus, SWAT model, Climate change

7.1. Introduction

The effects of climate change such as rising temperature and changes in the intensity and pattern of precipitation has become undeniably unequivocal in East Africa, impacting water resources, ecosystems, biodiversity, agricultural and food systems (Hartmann et al., 2013; Adhikari et al., 2015; Souverijns et al., 2016). In developing countries with high vulnerability (IPCC, 2014) such as East Africa, climate impacts are reverberating through the economy from threatening water availability to decreased agricultural production and thus impairing food security (Waithaka, et al., 2013) . The negative impacts associated with climate change are also compounded by many factors like, exacerbating poverty and high population density which is anticipated to increase demand for food and water in the future (Hepworth and Goulden, 2008; Wathaika et al., 2013). Future impacts on water resources are projected to worsen as temperature continue to rise and as precipitation becomes more variable (WWF, 2006). In fact, numerous Global (GCM) and Regional Climate Model (RCM) studies projected increase in temperature of 1.7 – 5.4°C and precipitation of 5 – 20% by the end of the 21st century in East Africa (Shongwe et al., 2011; Akurut et al., 2014; Adhikari et al., 2015; Ongoma et al., 2017), in a large part caused by human activities (IPCC, 2014; Souverijns et al., 2016) . However, the Intergovernmental Panel on Climate Change (IPCC) Fifth Assessment Report (AR5) reports large levels of uncertainty in the temporal and spatial variability of precipitation events over East Africa (Niang et al., 2014). Even though annual precipitation is positive, seasonal variations may have impacts on the water resources and crop production.

In addition to climate change, land use changes associated with rapid urbanization and uncoordinated intensive agricultural practices may cause severe impacts on aquatic systems by influencing water quantity (Danvi et al., 2018). Arguably, water resources have been compromised due to unpredictable and unreliable precipitation, causing seasonal shifts in the flow frequency and shortening growing seasons (Mango et al., 2011; Li and Jin, 2017; Guzha et al., 2018). Consequently, amplify water stress hence low agricultural productivity especially in regions of limited water resources. Similarly, precipitation variability is expected to significantly intensify the magnitude and frequency of flood and drought events that are both detrimental to water availability, other hydrological processes, and agricultural production (Thornton et al., 2014; Adhikari et al., 2015; Hawinkel et al., 2016) in the catchments of the rainfed agricultural systems of East Africa. Therefore, ensuring adaptive strategies on water quantity and seasonality is an important issue for policy makers and stakeholders in these regions.

Among the adaptive strategies to cope with climate change in East Africa, smallholder farmers have resorted to converting the pristine inland valleys to agricultural sites to increase local food production (Dixon and Wood, 2003; Rodenburg et al., 2014; Wood and Dixon, 2008). These inland valleys are seen to possess a huge potential for agricultural production due to their yearly available soil water and the inherent soil fertility (Von Der Heyden and New, 2003; Mitsch and Gosselink, 2015) which encourage continuous crop production. Also, the rapidly growing population has further increased the pressure on wetland food production due to the loss of arable land on the uplands (Sakané et al., 2011). Inland valleys are characterized by a valley bottom, hydromorphic fringe, their upstream position relative to a hydrological network and its seasonally water logged depression (Windmeijer and Andriesse, 1993; Rodenburg et al., 2014). Inland valleys provide a number of ecosystem services (MEA, 2005; Junk and An, 2013; Rebelo et al., 2010) noteworthy, their hydrological functioning and food provisioning services. Although wetland cultivation contributes significantly to food and livelihood security under changing climate in the short term, there are concerns over the sustainability of this utilization and maintenance of wetland benefits such as the hydrological functioning services in the long term (Dixon and Wood, 2003). Therefore, understanding more about the interacting impacts of climate change and land use management on the hydrological processes in these wetlands is a step forward to selecting the best management strategies in ensuring sustainable agricultural development and water resources management (Danvi et al., 2018).

Many studies have demonstrated the impact of climate and land use change on the hydrological processes in the catchments of East Africa and Uganda per se at larger spatial scales (Mileham et al., 2009; Kigobe and Griensven, 2010; Anaba et al., 2017; Vanderkelen et al., 2018), but their quantitative future impact on the hydrological processes in the inland valleys is much less known. Yet these studies are important to evaluate the possible vulnerability and resilience of these ecosystems to climate change, in particular the impacts of prolonged precipitation deficits. The study is therefore aimed to assess the potential impacts of climate change and land use management options on the water resources of the inland valley of Namulonge, central Uganda using Soil and Water Assessment Tool (SWAT). In particular, to analyze: (1) the future impact of climate change on the hydrological processes within the inland valley; (2) which land use management options may alleviate the negative effects of climate change on water quantity in the inland valley. The projected results seek to provide supporting scientific information for decision making on

sustainable planning for agricultural production and water resources management at local scale in the inland valleys under changing climate and land use.

7.2. Materials and methods

The location of the study area is presented in Chapter 2. The model inputs are shown in Chapter 3. SWAT model description, model set up and evaluation are given in detail in Chapter 4.

7.2.1. Future climate change scenarios

To assess the impact of future climate change on the water availability in the inland valley, we used scenarios RCP4.5 and 8.5 (Representative Concentration Pathways), from the IPCC AR5 (Fifth Intergovernmental Panel on Climate Change assessment report) (Carvalho-Santos et al., 2017) for the period 2021-2050. RCP 4.5 is a medium stabilization scenario where total radiative forcing is stabilized at 4.5Wm^{-2} post year 2100 (approximately 650 ppm CO_2-equivalent) with all countries undertaken emissions mitigation policies simultaneously and effectively (Thomson et al., 2011). RCP 8.5 is a rising scenario with total radiative forcing increasing at 8.5Wm^{-2} in 2100 (approximately 1370 ppm CO_2-equivalent) (Riahi et al., 2011).

An ensemble of six GCM – RCM datasets was explored in the study (Table 7.1). The GCM – RCM simulations were performed in the framework of the CORDEX-Africa project. The CORDEX-Africa project provides simulations with a spatial resolution of 0.44° by 0.44° (about 50 km by 50 km) and a daily output frequency (Nikulin et al., 2012). Compared to Global Climate Models (GCMs), RCMs have a high spatial resolution and are therefore able to represent regional and local scale forcings (Kim et al., 2014). Each dataset consists of historical runs and projected climate variables based on the RCP4.5 and 8.5 emission scenarios (Moss et al., 2010). The climate variables downscaled (precipitation, temperature, relative humidity, wind speed and solar radiation) range from 1976-2005 and from 2021-2050 for the RCPs and were used as hydrological model inputs at a daily basis for water balance simulation. The selected six models represent a wide spectrum of precipitation signals, with increasing, decreasing, and constant precipitation patterns when comparing the periods from 1976-2005 with 2021 - 2050.

Table 7.1 GCM-RCM datasets and the corresponding abbreviation used in the study.

Driving GCM	RCM	Institution	Abbreviation used in the study
CanESM2	CanRCM4_r2	Canadian Centre for Climate Modeling and Analysis (CCma)	CanESM – CanRCM
CanESM2	RCA4_v1	Rossby Centre, Swedish Meteorological and Hydrological Institute (SMHI)	CanESM – RCA
CNRM-CM5	CCLM4-8-17_v1	Climate Limited-area Modeling Community (CLMcom)	CNRM – CCLM
EC-EARTH	CCLM4-8-17_v1	Climate Limited-area Modeling Community (CLMcom)	EC-EARTH – CCLM
EC-EARTH	RCA4_v1	Rossby Centre, Swedish Meteorological and Hydrological Institute (SMHI)	EC-EARTH – RCA
MIROC5	RCA4_v1	Rossby Centre, Swedish Meteorological and Hydrological Institute (SMHI)	MIROC – RCA

7.2.2. Bias correction of precipitation and temperature data

Precipitation and temperature data from the weather station of National Crops Resources Research Institute (NaCRRI) for the period of 1976-2005 was considered for the bias-correction of future climate. All the other climate variables used are raw output from the six regional climate models (RCMs) selected within the CORDEX project because there was no observation to be used for bias correction. Modeled temperature values for the historical time frame were bias-corrected with the observed data of 1976-2005 FROM NaCRRI weather station, by using a linear regression on a monthly basis for the minimum and maximum temperatures. The precipitation data for the six GCMs-RCMs was bias corrected using the empirical quantile mapping (Gudmundsson et al., 2012). For each model, transfer functions were derived using observed and simulated temperature and precipitation for the period of 1976-2005; afterwards, the transfer functions were applied to the projected climate scenarios (period of 2021-2050). The bias correction for temperature and rainfall was conducted by the meteorology institute, Köln University, Germany (http://www.geomet.uni-koeln.de/). The difference between the projected and historical values was

determined by calculating the change signal (Δ) of climate and the hydrological variables (precipitation, temperature and discharge) (Yira et al., 2017):

$$\Delta\, Var = \frac{(Var_{Proj} - Var_{Ref}) \times 100}{Var_{Ref}} \qquad \text{(Eq 7.1)}$$

Where Δ Var is the change signal for the evaluated variable (e.g., precipitation); (e.g., discharge); Var_{Proj} is the projected value of the variable for a period of 2021–2050 under RCP4.5 and RCP8.5); and Var_{Ref} is the reference value of the variable for the period of 1971–2000.

7.2.3. Combined scenarios analysis

We investigated the combined impact of climate change and the different land use management on water availability in the inland valley. The GCM - RCM ensemble mean under RCP4.5 and RCP8.5 and the land use management (explained in detail in Chapter 3) scenarios were applied in the SWAT model as illustrated in Table 7.2.

Table 7.2 Scenario combination of climate and land use management.

Scenario combination	Description
RCP4.5/RCP8.5+LU1	Combined climate and *Exploitation* land use management (LU1) scenarios
RCP4.5/RCP8.5+LU2	Combined climate and *Protection of the headwater catchment* land use management (LU2) scenarios
RCP4.5/RCP8.5+LU3	Combined climate and *Conservation* land use management (LU3) scenarios
RCP4.5/RCP8.5+LU4	Combined climate and S*lope conservation* land use management (LU4) scenarios

7.3. Results

7.3.1. Future climate of Namulonge inland valley: Model and scenario variability

Fig. 7.1 illustrates the trend in annual and monthly observed and historical precipitation for the period of 1976 -2005 before and after bias correction. A mixed trend of over- and under estimation of both annual and monthly precipitation for the GCM - RCM ensemble is depicted when precipitation data are not bias corrected (UC) (Fig. 7.a and c). After bias correction (BC), there is an improvement in the GCM - RCM ensemble annual precipitation estimate in relation to the

ground observations. Moreover, a better agreement in intrannual precipitation as simulated by the GCM - RCM ensemble and the observed precipitation is noted (Fig.7.1d). The change in monthly precipitation among the six climate models and the observed before bias correction ranges from -50 to 292 mm/month and -1 to 6 mm/month after bias correction.

Fig. 7.2 shows mean monthly temperature for the GCM-RCM ensemble and the ground observation for the period 1976-2005. There is a large deviation of up to 2.2°C between the GCM-RCM ensemble and the ground observation data before bias correction (Fig. 7.2a). However, after bias correction, the deviation is reduced up to a maximum of 0.5°C (Fig. 7.2b). Therefore, bias correction improved and reduced the deviation between the ground observations and the RCM-GCM ensemble precipitation and temperature estimated in the inland valley.

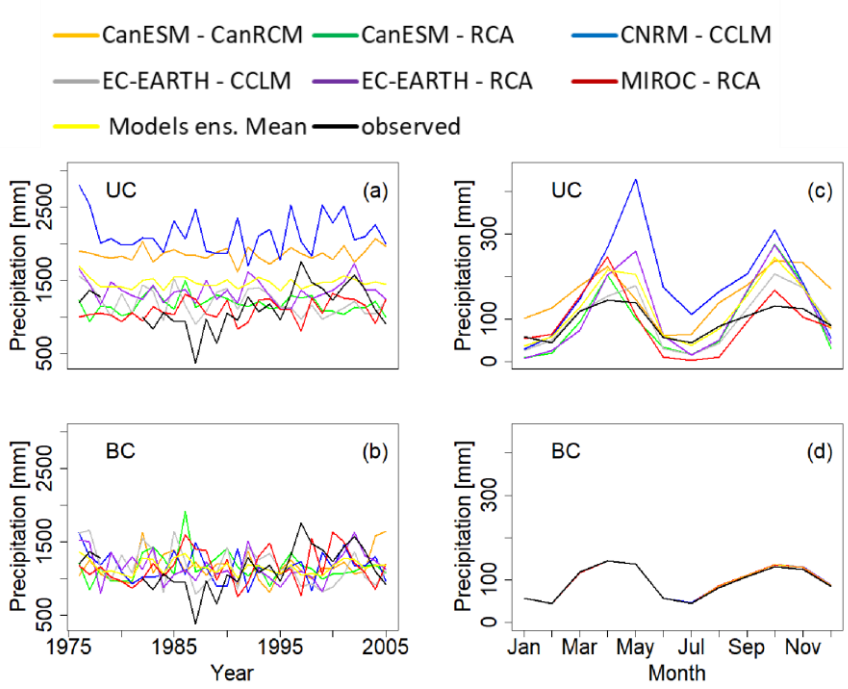

Fig. 7.1. Historical mean annual (a,b) and mean monthly (c,d) precipitation (1976-2005). UC refers to non-bias corrected, BC to bias corrected.

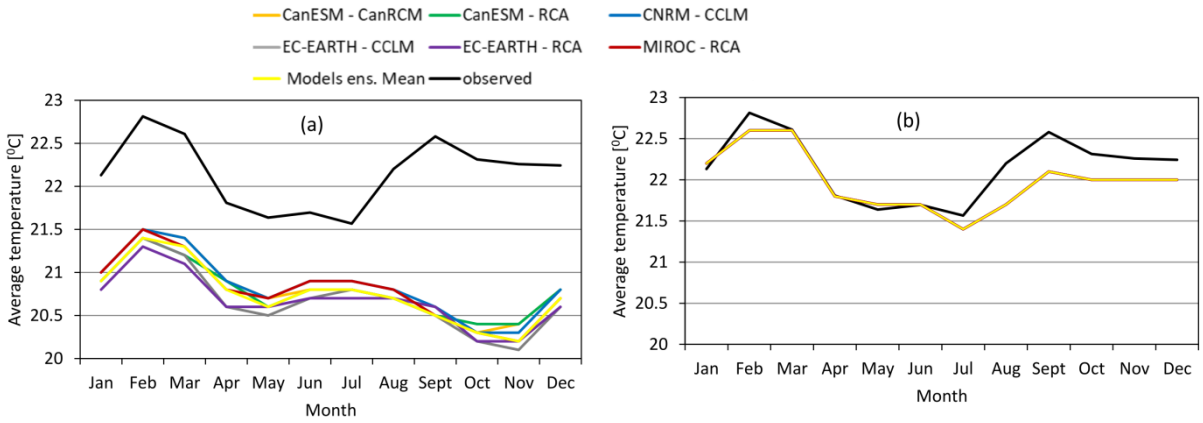

Fig.7.2. Mean monthly temperature for the period 1976-2005. (a) Not bias corrected, and (b) bias corrected.

Table 7.3 shows the projected change in the annual precipitation between the reference (1976–2005) and future (2021–2050) periods with non- bias corrected and bias corrected GCM-RCM based simulations. In the future, a general increase of annual precipitation is projected under the climate scenarios in the inland valley. Annual precipitation will increase up to 7.4% under RCP4.5 and 21.8% under RCP8.5 after bias-correction of precipitation. The bias-correction has a strong impact on the changes as the magnitude of projected precipitation increase ranges from 15.3% to 43.9% and the decrease is from 2.2% to 4.6% after bias correction.

The change in precipitation however, shows high uncertainty among the six selected climate models. The CanESM – CanRCM, CanESM – RCA, EC-EARTH – RCA and MIROC – RCA models project an increase in annual precipitation, whereas CNRM – CCLM and EC-EARTH – CCLM project a decrease (Table 7.3). Also, at a monthly scale, the RCM-GCM ensemble exhibits uncertain change in monthly precipitation between the reference (1976-2005) and future (2021-2050) period. Thus there is no clear trend in precipitation change within the year (Fig. 7.3).

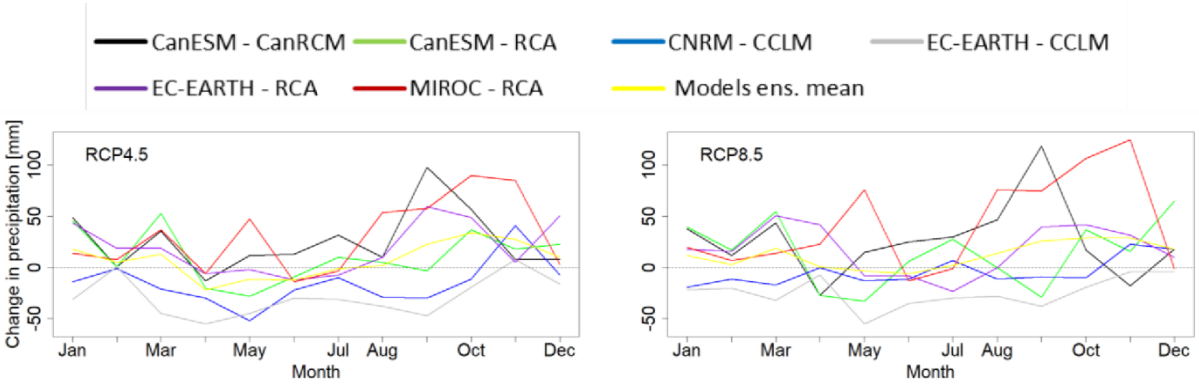

Fig. 7.3. Monthly change signal for precipitation under RCP4.5 and 8.5. Data is bias corrected.

In comparison to the reference conditions (1976-2005), the GCM-RCM ensemble mean show an increase in mean annual temperature of 1.4°C under the RCP4.5 and 1.6°C under RCP8.5 climate scenarios for period 2021-2050 (Table 7.4). At a monthly scale, mean temperature will generally increase in the dry season (JJA and DJF) and decrease during the wet season (MAM and SON) in the inland valley (Fig.7.4).

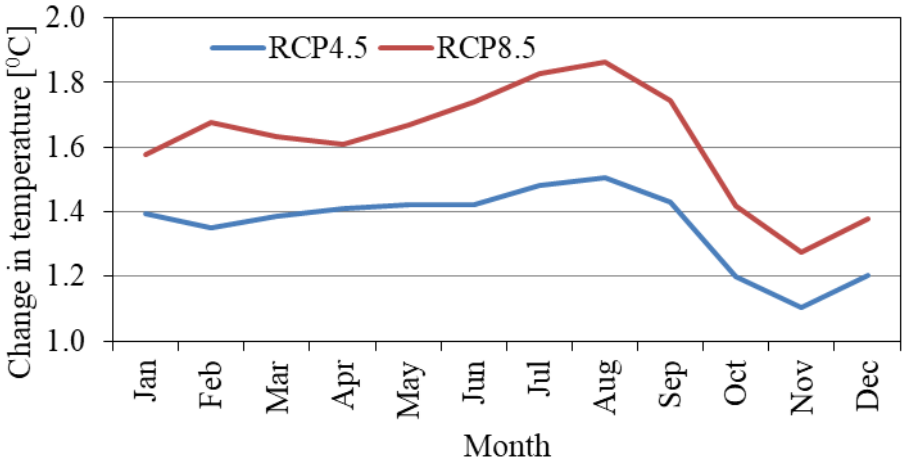

Fig. 7.4. Change in monthly mean temperature for the GCM-RCM ensemble (period 2021-2050). Temperature not bias corrected.

Table 7.3 Projected precipitation change between the reference (1976–2005) and future (2021–2050) periods with non- bias corrected and bias corrected GCM-RCM based simulations.

GCM-RCM models	Non bias corrected			Bias corrected		
	Historical precipitation (mm)	Precipitation change RCP4.5 (%)	Precipitation change RCP8.5 (%)	Historical precipitation (mm)	Precipitation change RCP4.5 (%)	Precipitation change RCP8.5 (%)
CanESM - CanRCM	1861	+8.8	+6.6	1160	+26.7	+27.5
CanESM - RCA	1179	+0.7	+1.8	1160	+11.4	+15.1
CNRM - CCLM	2141	-12.8	-3.2	1160	-16.0	-4.6
EC-EARTH - CCLM	1204	-21.8	-19.5	1159	-30.0	-25.5
EC-EARTH - RCA	1357	+4.3	+4.8	1161	+19.8	+18.3
MIROC - RCA	1098	+10.7	+15.3	1159	+32.4	+43.9
Models ens. mean	1473	-2.2	+0.8	1160	+7.4	+21.8

Table 7.4 Projected change in mean temperature between the reference (1976–2005) and future (2021–2050) periods. Data is non-bias corrected.

GCM-RCM models	Historical temperature	Temperature change, RCP4.5	Temperature change, RCP8.5
		^{0}C	
CanESM - CanRCM	20.8	+1.6	+1.9
CanESM - RCA	20.8	+1.7	+1.9
CNRM - CCLM	20.8	+1.0	+1.1
EC-EARTH - CCLM	20.7	+1.5	+1.7
EC-EARTH - RCA	20.7	+0.9	+1.5
MIROC - RCA	20.8	+1.5	+1.6
Models ens. mean	20.8	+1.4	+1.6

7.3.2. Impact of climate change scenarios on annual water balance

The impact of climate change scenarios (2021-2050) on the water availability of the inland valley is presented in Fig. 7.5. The changes in the annual water balance components reveal the effect of climate change on water availability within the inland valley from 2021 to 2050. A mixed trend in the changes is simulated which follows the patterns in the variability of projected precipitation for the individual climate models. For example, a potential increase in precipitation (CanESM - CanRCM, CanESM – RCA, EC-EARTH – RCA, MIROC – RCA models) will cause increase in the water balance components (groundwater flow, lateral flow, surface runoff, and deep aquifer recharge. Furthermore, a reduction in precipitation as projected by CNRM – CCLM and EC-EARTH – CCLM models under both climate scenarios will trigger a reduction in the aforementioned water balance components in the inland valley. Likewise, actual evapotranspiration is projected to increase as simulated by CanESM - CanRCM, CanESM – RCA, EC-EARTH – RCA, and MIROC – RCA models under RCP4.5 and RCP8.5 and the reverse is true for the CNRM – CCLM and EC-EARTH – CCLM models. There is a projected marginal increase in potential evapotranspiration (PET) which does not exceed 0.8% under RCP 4.5 and 0.5% under RCP8.5 for all the models.

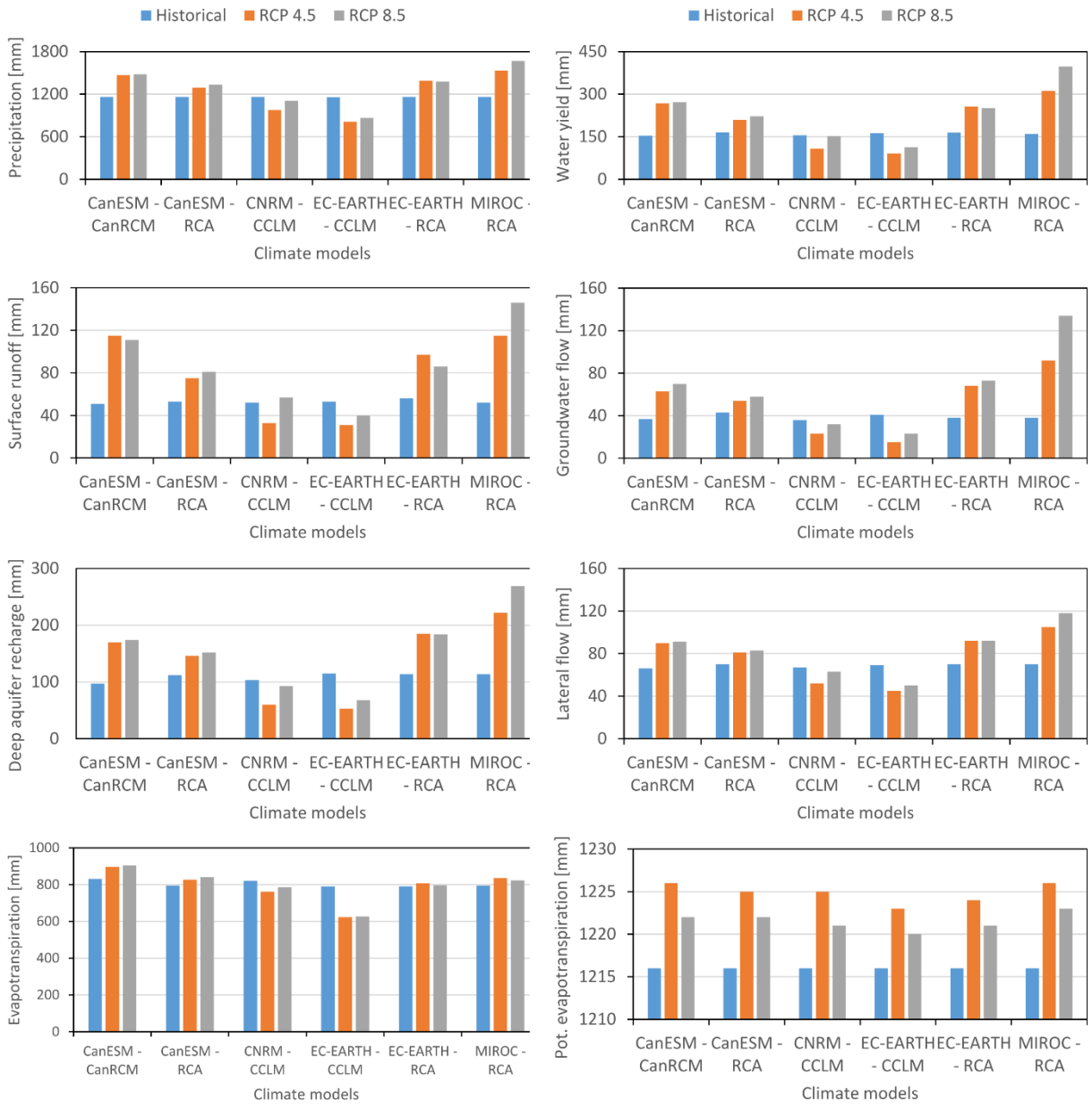

Fig.7.5. Annual water balance according to the GCM-RCM for the periods (1976-2005 and 2021-2050). Simulations from biased corrected precipitation and temperature.

7.3.3. Impact of climate change scenarios on discharge

The projected change in annual discharge for the period 2021 to 2050 for the two climate scenarios compared to the reference period (1976 to 2005) is presented in Table 7.5. Similar to precipitation, a mixed change in annual discharge pattern is projected by the GCM-RCM ensemble. Models (CanESM – RCA, CanESM – CanRCM, EC-EARTH – RCA, and MIROC – RCA) under RCP4.5 and RCP8.5 project high to very high (27-149%) increase in total discharge, although the increase is higher under RCP 8.5 than RCP 4.5. On the contrary, CNRM – CCLM and EC-EARTH – CCLM models from both climate scenarios simulate a reduction in annual discharge.

Table 7.5 Change in projected mean annual discharge by GCM-RCM ensemble for the period 2021-2050 compared to the reference period 1976-2005.

GCM-RCM models	Discharge of reference period [mm]	Change in discharge RCP4.5 [%]	Change in discharge RCP 8.5 [%]
CanESM - CanRCM	154	+74	+77
CanESM - RCA	166	+27	+34
CNRM - CCLM	155	-30	-1.9
EC-EARTH - CCLM	163	-44	-31
EC-EARTH - RCA	164	+57	+53
MIROC - RCA	160	+95	+149
Model ens.mean	101	+16	+29

Simulation performed with biased corrected precipitation and temperature

The monthly change in discharge projected by the six climate models (Fig.7.6) follows the projected change signal in the monthly precipitation. This indicates that precipitation is a key factor in determining discharge in the investigated inland valley. Noteworthy, a markedly high change in discharge is projected by CanESM – CanRCM and MIROC – RCA models in the short (SON) rainy season (Fig. 7.6).

Fig. 7.7 depicts the intrannual variability in mean monthly discharge projected by the GCM-RCM ensemble mean for climate scenarios, RCP4.5 and 8.5. The mean monthly discharge will be seasonally affected by the changes in precipitation. In fact, there is a distinct difference between the wet (MAM and SON) and dry (JJA and DJF) seasons in the year. More discharge is projected in the long (MAM) and short (SON) rainy seasons, although a large magnitude is noticed in the SON season. Also, low discharge is simulated in the dry season (January, February, June, July and December) by the climate change scenarios.

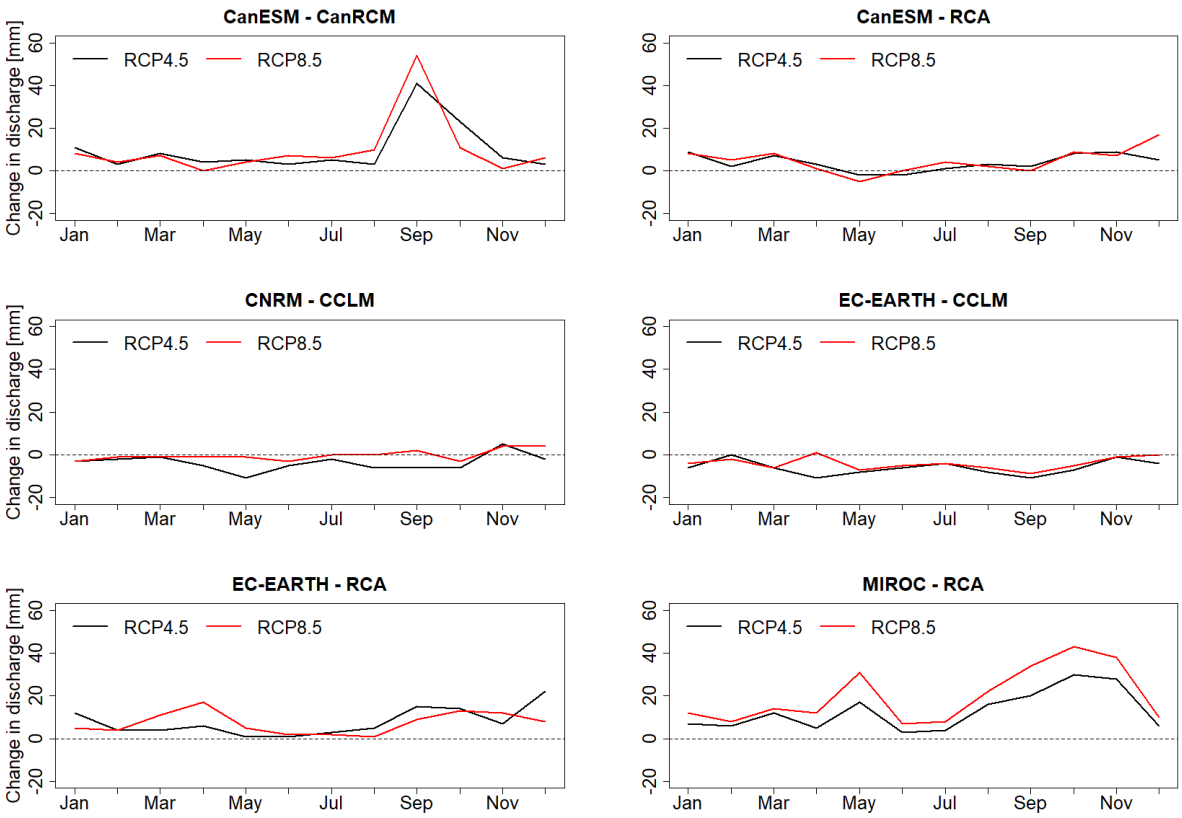

Fig. 7.6. Monthly discharge change between the reference period (1976-2005) and the future period (2021-2050) under emission scenarios RCP4.5 and RCP8.5. Bias corrected precipitation and temperature.

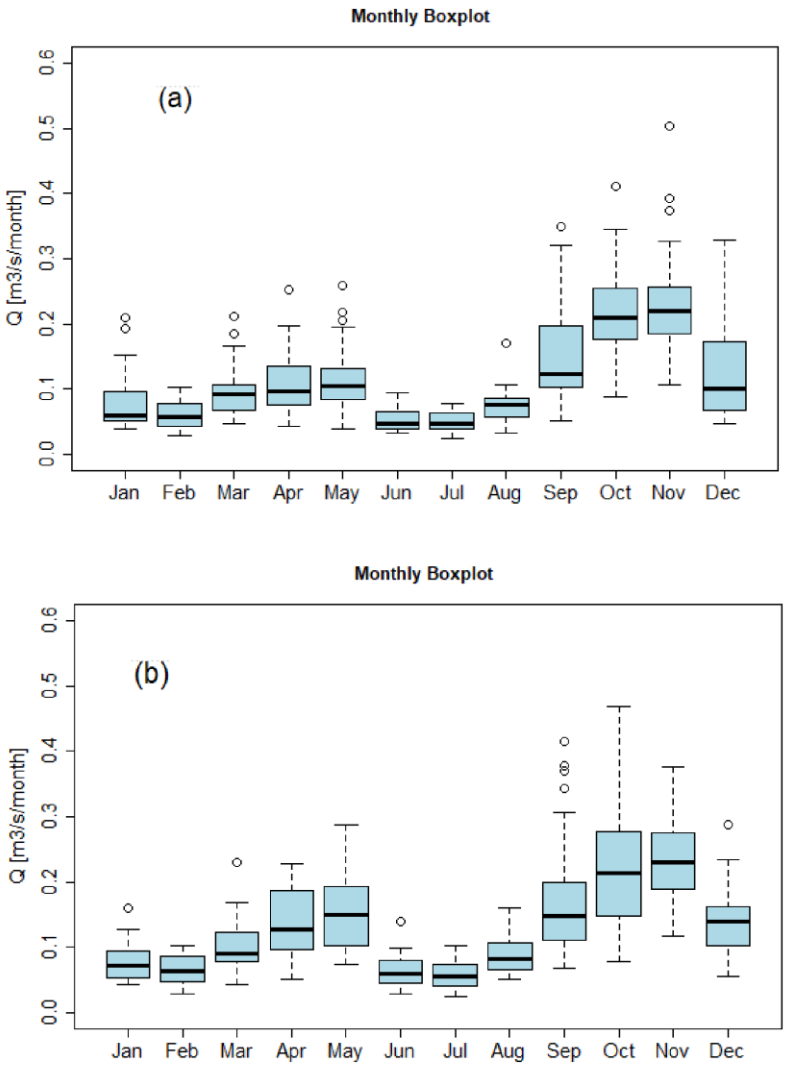

Fig. 7.7. Box plots for projected monthly average discharge under ensemble mean climate scenarios, (a), RCP4.5 and (b), RCP8.5.

The impact of climate change scenarios on the exceedance probability of annual discharge is illustrated in Fig. 7.8 using the flow duration curve (FDC). The FDC indicates likelihood of over- and under estimation of the low and high flow between the observed and historical discharge for the period 1976-2005. The overestimation of the high flows is about 12% while for the low flows is about 20% of the exceedance probabilities by the model.

The RCMs ensemble mean project a likelihood of more low and high flows compared to the historical and observed flows due to the high projected precipitation by the climate scenarios. However, the projected extreme peaks are rarer (~0-2%) from the observed discharge. In summary,

the observed, historical and projected low flows account for about 30-35% of the annual discharge while high/extreme peak flow account for 20-25% in the inland valley. Taking into account the variability of the modelling projections, RCP 4.8 forecasts more total discharge at the inland valley outlet for the period 2021–2050 than RCP4.5. One may infer from these results that the projected increase in groundwater flow, lateral flow and surface runoff as a result of increasing precipitation, will result into more low and high flows in the inland valley during the dry and wet seasons, respectively.

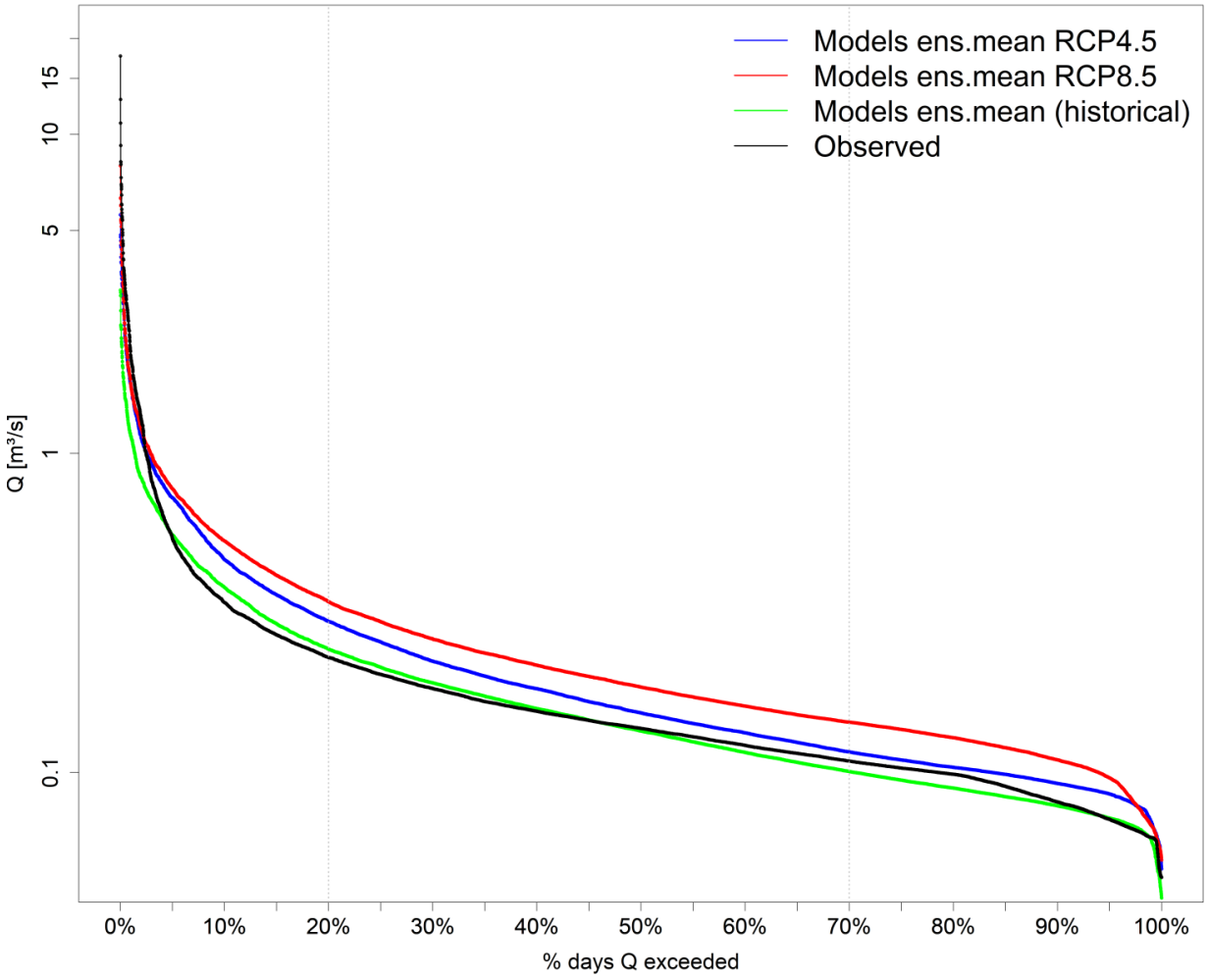

Fig. 7.8. Impact of climate change scenarios on the exceedance probability of discharge in the inland valley. The y-axis is plotted on a log scale. Discharge is simulated from bias corrected precipitation and temperature.

7.3.4. Impact of land use management scenarios on annual water balance

In addition to land use management simulations in chapter 6, the long term impact of land use management/conservation levels on water resources were evaluated using model ensemble mean climate data for the period of 1976-2005. Table 7.6 presents the annual water balance components according to the different land use management scenarios. The increase in the land use conservation levels (*Conservation* > *Slope conservation* > *Protection of the headwater catchment*) results in a decrease in the total water yield, groundwater flow, deep aquifer recharge and surface runoff. *Exploitation* land use management approach will cause an increase in the total water yield, lateral flow, and surface runoff and a decrease in groundwater flow and deep aquifer recharge is noticed. Conversely, actual evapotranspiration increases after applying the land use management scenarios.

Table 7.6 Annual water balance according to the land use management approaches.

Water balance components	*Reference*	*Exploitation*	*Protection of the headwater catchment*	*Conservation*	*Slope conservation*
Precipitation [mma^{-1}]	1161	1161	1161	1161	1161
Water yield [mma^{-1}]	101	105 (+4)	85 (-16)	76 (-25)	77 (-24)
Groundwater flow [mma^{-1}]	41	38 (-3)	27 (-14)	20 (-21)	20 (-21)
Surface runoff [mma^{-1}]	5	7 (+2)	2 (-3)	0.1 (-4.9)	0.3 (-4.7)
Lateral flow [mma^{-1}]	55	60 (+5)	56 (+1)	56 (+1)	56 (+1)
Deep aquifer recharge [mma^{-1}]	90	84 (-6)	62 (-28)	48 (-42)	49 (-41)
Evapotranspiration [mma^{-1}]	905	912 (+8)	968 (+63)	1000 (+95)	997 (+92)
Potential evapotranspiration [mma^{-1}]	1216	1216	1216	1216	1216

7.3.5. Combined effect of climate and land use management change on the annual water balance

The results of the combined impact of climate and land use management scenarios on the annual water balance are shown in Table 7.7 and Fig. 7.9. A marked increase in evapotranspiration and a decrease in surface runoff and water yield follows the order of increasing land use management conservation levels (*Conservation* > *Slope conservation* > *Protection of headwater catchment* > *Exploitation*) and climate scenarios (RCP8.5 >RCP4.5) is projected. Likewise, a combined effect of land use management and climate scenarios resulted in an increase in potential evapotranspiration. An increase in evapotranspiration of up to 13%; and in lateral flow of up to

38% is projected in the future (2021-2050). A decrease in surface runoff of up to 92%; groundwater flow of up to 24% is projected from *Conservation,* S*lope conservation* land use management under the two climate scenarios. *Protection of the headwater catchment* under the two climate scenarios shows no effect on the surface runoff and an increase in groundwater flow of up to 15% is projected. The combined effect of climate and *Exploitation* land use management scenarios markedly increases surface runoff by 140%, under RCP4.5 and 180% under RCP8.5. In addition, groundwater flow increase up to 17% under RCP8.5 and no effect is projected under RCP4.5. An increase in water yield of up to 36% and in deep aquifer recharge of up to 46% is projected under the two scenarios for the *Exploitation* and *Protection of the headwater catchment* and *Conservation* and *Slope conservation* (under RCP8.5 scenario) land use management approaches. A decrease in water yield and deep aquifer recharge of up to 10% is exhibited by the Conservation and *Slope conservation* land use management approaches under the RCP4.5 climate scenario.

Table 7.7 Annual water balance according to the combined climate and land use scenarios

	Land use (2015)	Exploitation land use		Protection of the headwater catchment land use		Conservation land use		Slope conservation land use	
	Reference (1976-2005)	RCP4.5	RCP8.5	RCP4.5	RCP8.5	RCP4.5	RCP8.5	RCP4.5	RCP8.5
Precipitation [mma^{-1}]	1161	1246 (85)	1305 (144)	1246 (85)	1305 144)	1246 (85)	1305 (144)	1246 (85)	1305 (144)
Water yield [mma^{-1}]	101	124 (23)	137 (36)	105 (4)	116 (15)	97 (-4)	111(10)	98 (-3)	112 (11)
Groundwater flow [mma^{-1}]	41	41(0)	47 (7)	35 (6)	40 (1)	31(-10)	38 (-3)	31(-10)	39 (-2)
Surface runoff [mma^{-1}]	5	12 (7)	14 (9)	5 (0)	5 (0)	0.4 (-4.6)	0.5 (-4.5)	0.7 (-4.3)	0.8 (-4.2)
Lateral flow [mma^{-1}]	55	70 (15)	76 (21)	65 (10)	71(6)	66 (11)	72 (17)	66 (11)	72 (17)
Deep aquifer recharge [mma^{-1}]	90	114 (24)	131(41)	94 (4)	109 (19)	81(-9)	97 (7)	82 (-8)	98 (8)
Evapotranspiration [mma^{-1}]	905	920 (15)	931(26)	975 (70)	993 (88)	1005 (100)	1023 (118)	1002 (97)	1020 (115)
Potential evapotranspiration [mma^{-1}]	1216	1225(9)	1221(5)	1225(9)	1221(5)	1225(9)	1221(5)	1225(9)	1221(5)

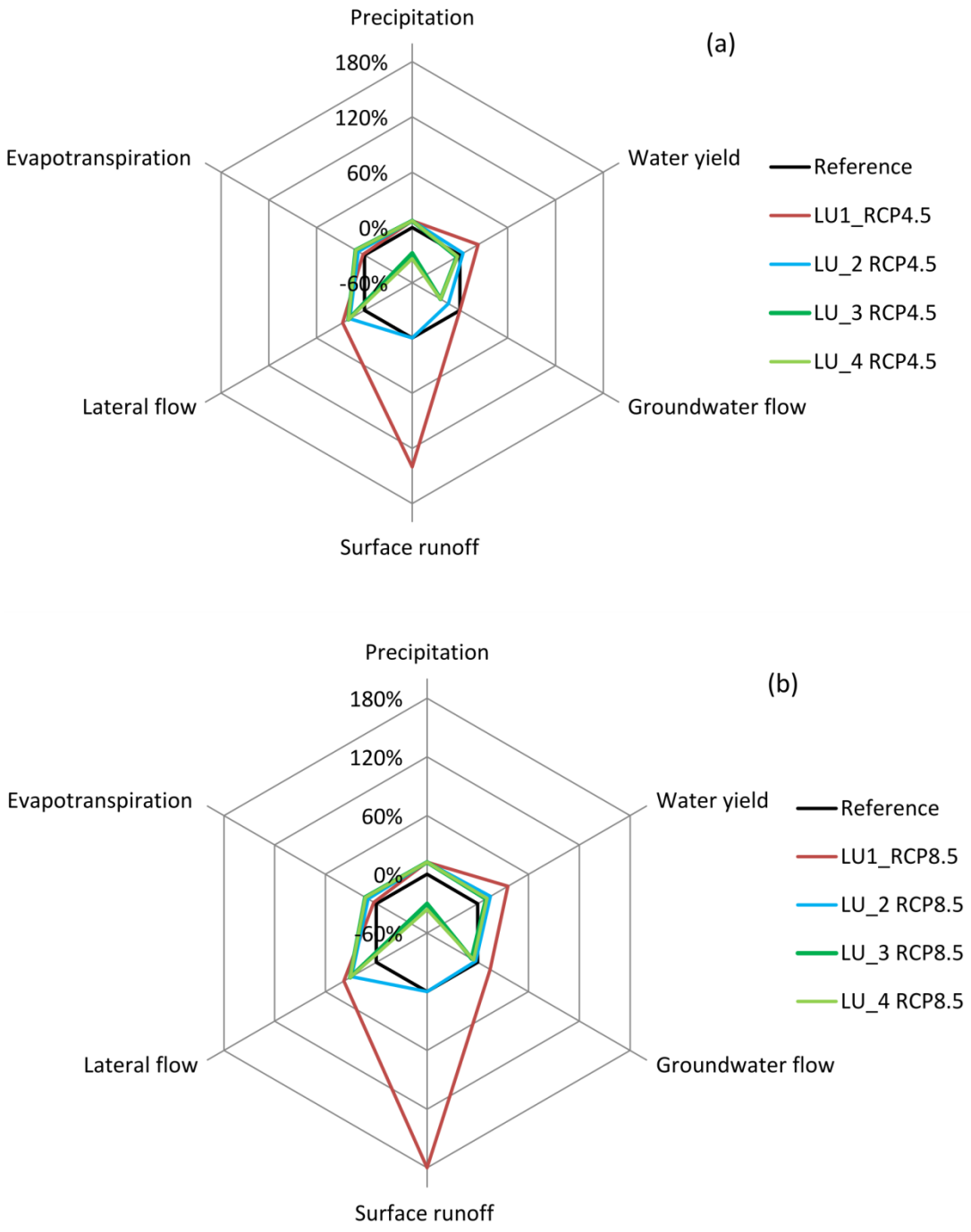

Fig. 7.9. Predicted changes in water balance according to the combined land use and climate scenarios. LU1, *Exploitation*; LU2, *Protection of headwater catchment*; LU3, *Conservation* approach; and LU4, *Slope conservation* land use management, Reference is the land use management for 2015 with historical climate data (1976-2005).

7.4. Discussion

7.4.1. Historical climate

The systematic bias and large deviation in the precipitation simulated by the RCM-GCM models compared to the ground observations is also reported by several authors (e.g.Shongwe et al., 2011; Souverijns et al., 2016; Vanderkelen et al., 2018) in the East African region. One of the reasons for the systematic bias and deviation could be the lower resolution of the models used to capture the data (Bruyère et al., 2013; Maraun, 2016). After bias correction, the amplitude of deviation significantly reduces for all the individual climate models. Hence reliable estimates of local scale precipitation from each climate model were clearly visible. Bias corrected data may serve as the basis for conducting future climate impact studies as well as assessment of the potential hydrological changes for real- world adaptation decisions and management strategies (Maraun, 2016). The ability of the models ensemble to simulate the mean seasonal precipitation and its cycle is also noticed by (Nikulin et al., 2012). The mean annual temperature change range of 0.9-1.9°C predicted by the individual climate models falls within the range of 0.9-3.3°C projected in Uganda (Zinyengere et al., 2016). On average, the predicted change in annual temperature of 1.4°C and 1.6°C under RCP4.5 and 8.5, respectively by the climate models concur with the range of 1.4 – 5.8°C projected by GCM and RCM models over East Africa (IPCC, 2014; Adhikari et al., 2015). This confirms the common acknowledgement of global warming reported in the region.

7.4.2. Projected change in precipitation and temperature

The projected uncertain change in annual precipitation between the reference (1976-2005) and future (2021-2050) period simulated by the RCM-GCM ensemble could be due to seasonal variations in precipitation, location of the study area and the internal model variability (Maraun, 2016; Carvalho-Santos et al., 2017). In fact, internal model variability for precipitation is recognized as an important source of uncertainty in climate projections (Northrop and Chandler, 2014). A similar situation was found in a sensitivity study of water resources to climate change in the Kyoga Basin, where changes in annual precipitation ranged from −6 to 65% (Kigobe and Griensven, 2010). Additionally, a study conducted in the Lake Victoria Basin by Vanderkelen et al.(2018) indicated changes in annual precipitation from -79 to 78% using CCLM4-8-17, RACMO22T, RCA4 and REMO2009 and HIRHAM5 models. The highest increase in monthly

precipitation is projected in the long (MAM) and short (SON) rain seasons (Souverijns et al., 2016) which also correspond to the two rainy seasons in the inland valley (Nsubuga, 2000).

7.4.3. Projected change in the water balance

The increase in the water balance components (total water yield , groundwater flow, lateral flow, and surface runoff) simulated by CanESM - CanRCM, CanESM – RCA, EC-EARTH – RCA, MIROC – RCA models as a result of projected high precipitation may have negative implications for flood risks in the inland valley thus reducing its water storage capacity under the current land use situation (Praskievicz and Chang, 2009). While the projected reduction in the aforementioned water balance components from CNRM – CCLM and EC-EARTH – CCLM models due to the low precipitation, may initiate a long term occurrence of limited water availability for agricultural production in the inland valley as well as affecting its hydrological functioning and other ecosystem services. The projected increase in actual evapotranspiration by CanESM - CanRCM, CanESM – RCA, EC-EARTH – RCA, and MIROC – RCA models under RCP4.5 and 8.5 is attributed to the unlimited soil water availability in the system as a result of high precipitation and the high energy from the rising temperature (Praskievicz and Chang, 2009). Likewise, the reduction in projected actual evapotranspiration by CNRM – CCLM and EC-EARTH – CCLM models could be as a result of the limited soil water availability from the low precipitation (Soylu et al., 2011). Lastly, the potential evapotranspiration doesn't exceed the input precipitation for all the climate models which simulate project higher precipitation, indicating that the system is energy limited rather than water limited.

7.4.4. Discharge change

The mixed change signal in the discharge projected by the GCM-RCM ensemble for the period 2021 to 2050 has been reported by several studies conducted in the East African region. For example a negative change in discharge (CNRM – CCLM and EC-EARTH – CCLM): Mango et al. (2011) reports a discharge decrease of 25% due to predominance of evapotranspiration in the water balance in the Mara River Bain, Kenya albeit being a macro-scale catchment. Other studies predict a positive change of discharge (CanESM – RCA, CanESM – CanRCM, EC-EARTH – RCA, and MIROC – RCA) as Githui et al. (2009) report a discharge increase of 6-115% after considering the results of the CCSR, CSIRO, ECHAM4 and GFDL models in the Nzoia River

catchment (meso-scale) in Western Kenya. The mixed trend in the annual discharge change could be attributed to the high uncertainties associated with the projected precipitation change in the inland valley. These uncertainties have also been reported by the IPCC, (2014) over East Africa.

The projected increase in monthly discharge in the rain (MAM and SON) seasons is consistent with the results obtained by Kigobe and Griensven, (2010) in the Mpologoma catchment situated in Lake Kyoga basin, Eastern Uganda. The more projected water in the inland valley during the rain seasons can bring benefits for crop production and other ecosystem functioning. On the other hand, it may bring risk of floods, especially if precipitation occurs in strong and short episodes. Nonetheless, attention should be paid to the future due to low discharge projected in the dry season (JJA and DJF) which may cause water shortages for agricultural production, problems in water quality and negative impacts on the aquatic biodiversity (Hughes et al., 2012) in the inland valley.

7.4.5. Combined impact of climate and land use management scenarios

Compared to the land use management scenarios, climate change will dominate in inducing the increase and decrease in the hydrological processes. Similar observations have been deduced by Danvi et al. (2018) in the simulation of the impact of climate and land use change on stream flow in the inland valleys of Benin. The patterns in change of the hydrological processes induced by the combined effect of climate and land use management change scenarios are consistent with the individual effect of land use management scenarios. However, the magnitude of change is larger under the combined climate and land use management change scenarios. For example, the higher increase in evapotranspiration is driven by the combined effect of rising temperatures, high projected precipitation and the increasing land use management conservation levels (Conservation> Slope conservation > Protection of the headwater catchment > Exploitation).

The increase in land use management conservation level: *Conservation > Slope conservation > Protection of the headwater catchment> Exploitation*, causes a decline in total water yield, surface runoff and increase in evapotranspiration under the changing climate. This is attributed to the increase in canopy coverage with increase in land use management conservation level. More canopy coverage reduces surface runoff through increased interception, evaporation and soil infiltration of through fall (Leemhuis et al., 2007; Nugroho et al., 2013). Therefore, adoption of management strategies that enhance water availability in the system will reduce the negative

impacts of climate change on the water resources in the inland valleys which are undergoing tremendous changes from their pristine state to cultivation and settlement sites.

7.5. Conclusion

In this study, the potential implications of climate and land use management change for water balance and total discharge in a tropical inland valley of Namulonge, central Uganda were simulated using the SWAT model. An ensemble of six RCM-GCM data from CORDEX-Africa project framework were forced to SWAT model as inputs to simulate the hydrological response to climate change by mid-21st century. Bias correction of the climate models improved estimates of local precipitation and temperature in relation to the ground observations in the inland valley. The applied bias correction method did not alter the precipitation change signal except the magnitude compared to the historical data.

In the future (2021-2050), a general increase in temperatures is expected in the inland valley, but the projected change in precipitation is more uncertain in the inland valley. The variability given by the different climate models and scenarios with respect to precipitation change signal will result in considerable uncertainty in the inland valley discharge and water balance by 2050. Since discharge and water balance in the inland valley is strongly controlled by precipitation, no clear trend in the future development of water resources can be concluded. Climate models predicting more precipitation show an increase in the discharge and water balance, whereas models predicting less precipitation indicate a decrease. This variability in the future discharge and water balance has to be taken into account when planning for climate change adaptation strategies for the inland valley in the region. Seasonal changes would be significant, with more discharge in the rain (MAM and SON) season and less in dry (JJA and DJF) season.

Compared to land use management approaches, climate change will have a dominant effect on the hydrological processes in the inland valley. However, adoption of functional landscape approach (FLA) described by Dixon et al. (2012) such as: C*onservation, Slope conservation and protection of the headwater catchment* land use management approaches, will reduce the impacts of climate change on the water balance components (e.g. total water yield and surface runoff.) and increase evapotranspiration and lateral flow in the inland valley. Therefore, increasing water availability and improving other ecosystem functions in these inland valleys undergoing changes from their pristine state in the East African region.

Future efforts should focus on understanding the combined impact of climate and land use change on the water quality (sediments and nutrient fluxes; nitrogen and phosphorus) and the degradation rate of these agriculturally used inland valleys in the region.

8. Modeling spatial soil water dynamics in a tropical floodplain, East Africa[3]

Abstract

The characterization of soil moisture dynamics and its influencing factors in agriculturally used wetlands pose a challenge in data-scarce regions such as East Africa. High resolution and good-quality time series soil moisture data are rarely available and gaps are frequent due to measurement constraints and device malfunctioning. Soil water models that integrate meteorological conditions and soil water storage may significantly overcome limitations due to data gaps at a point scale. This study evaluated if the Hydrus-1D model would adequately simulate soil water dynamics at different hydrological zones of a tropical floodplain in Tanzania, to determine controlling factors for wet and dry periods and to assess soil water availability. The zones of the Kilombero floodplain were segmented as riparian, middle, and fringe along a defined transect. The model was satisfactorily calibrated (R^2 = 0.54–0.92, RMSE = 0.02–0.11) on a plot scale using measured soil moisture content at soil depths of 10, 20, 30, and 40 cm. Satisfying statistical measures (R^2 = 0.36–0.89, RMSE = 0.03–0.13) were obtained when calibrations for one plot were validated with measured soil moisture for another plot within the same hydrological zone. Results show the transferability of the calibrated Hydrus-1D model to predict soil moisture for other plots with similar hydrological conditions. Soil water storage increased towards the riparian zone, at 262.8 mm/a while actual evapotranspiration was highest (1043.9 mm/a) at the fringe. Overbank flow, precipitation, and groundwater control soil moisture dynamics at the riparian and middle zone, while at the fringe zone, rainfall and lateral flow from mountains control soil moisture during the long rainy seasons. In the dry and short rainy seasons, rainfall, soil properties, and atmospheric demands control soil moisture dynamics at the riparian and middle zone. In addition to these factors, depths to groundwater level control soil moisture variability at the fringe zone. Our results support a better understanding of groundwater-soil water interaction, and provide references for wetland conservation and sustainable agricultural water management.

Keywords: Hydrological zones, depth to groundwater level, soil moisture content, Hydrus-1D, Kilombero floodplain, Tanzania.

[3] Published as: G. Gabiri, S. Burghof, B. Diekkrüger, C. Leemhuis, S. Steinbach, and K. Näschen. 2018. Modeling spatial soil water dynamics in a tropical floodplain, East Africa, *Water 10,191*.

8.1. Introduction

Analyzing the spatial and temporal distribution of soil moisture content is essential for understanding ecohydrological wetland processes and for the development of sustainable agricultural water management wetland studies (Blume et al., 2009; Venkatesh et al., 2011). Soil moisture content is an important variable in regulating and predicting a range of hydrological processes like flooding (Qiu et al., 2001), plant water availability (Schenk and Jackson, 2002; Mulebeke et al., 2013; Böhme et al., 2016), and soil water-groundwater interaction (Wu et al., 2014). Soil moisture content is equally crucial in the hydrological cycle for the estimation of the plot-catchment scale water balance (Sánchez et al., 2012). Therefore, a better spatial and temporal assessment of soil moisture content yields valuable insights into hydrological processes and supports weather forecasting as well as climate projections (Blume et al., 2009; Vereecken et al., 2008; Zehe et al., 2010).

Wetlands rely on water, whether derived from precipitation, surface, or sub-surface water, to fulfill their ecosystem functions such as nutrient retention, flood mitigation, and food provisioning through agricultural support (Mitsch and Gosselink,2015; McCartney et al., 2010). Indeed, knowledge of hydrology is indispensable for wetland conservation and agricultural production (Thompson and Polet, 2000; von der Heyden and New, 2003; Acreman and Miller, 2007). In East Africa, floodplain wetlands are increasingly being utilized for agricultural production development projects, as a key intervention to synergistically achieve food security in the region (Dixon and Wood, 2003). This is due to their relatively large size, high soil nutrient stocks, and prolonged periods of soil water availability (Wood and van Halsema, 2008; Reddy et al., 2010; Sakané et al., 2011). This is also evident for the floodplain wetland in the catchment of Kilombero River, the most important tributary of the Rufiji river basin, representing one of the largest basins of Tanzania. The catchment is, however, increasingly used for agricultural production, especially during periods of inundation in the long rainy season. According to References (Futoshi, 2007; Nindi et al., 2014), rain-fed rice production has recently increased in the Kilombero floodplain. In fact, the wetland supplies about 9% of all rice produced in Tanzania. It is noteworthy that the Kilombero river catchment is also targeted for agricultural expansion through the project Southern Agricultural Growth Corridor of Tanzania (SAGCOT) (Paul and Steinbrecher, 2013), a large-scale agricultural intensification project. In this context, assessment and an improved understanding of the amount and spatial dynamics of soil moisture is fundamental for crop growth, land use planning, and the

evaluation of the potential impacts of agricultural management interventions on the hydrology and other ecosystem services of the floodplain.

Spatial and temporal soil moisture dynamics in floodplain wetlands are influenced by a range of factors; thus, assessing these factors through field observations is difficult and time-consuming. Soil moisture exhibits tremendous spatial heterogeneity even over small catchments, resulting from the interplay of hydrological, biological, and meteorological processes (Rosenbaum et al., 2012). In order to better understand the spatial pattern of soil moisture for wetland conservation and land use planning, good-quality time series data is required. However, there is a paucity of reliable field-scale measured data, and the remotely sensed soil moisture data is too coarse in the spatial resolution and refers to 5-cm depth soil moisture (Mohanty et al., 2017). Often, data gaps for the available soil moisture time series exist due to measurement constraints, device malfunctioning, or site inaccessibility during flooding periods. Moreover, during dry conditions, soil cracking affects the measuring moisture sensors and, therefore, data quality (RoTimi et al., 2015). Statistical and data-driven methods are an option for filling in missing values in distributed soil moisture datasets. Alternatively, models that integrate meteorological conditions, soil water storage, land use, and depth to groundwater table (Singh and Singh, 1996) may significantly overcome data gaps at a point scale, which are inevitable under field conditions. Once these models are well calibrated and validated, assessment of the impacts of agricultural management on the ecosystem functioning of wetlands is feasible.

In this study, a widely used soil water model, Hydrus-1D (Šimůnek et al., 2013), which simulates one-dimensional water, heat, and solute transport in variably saturated and unsaturated media, was applied to simulate the spatial soil moisture dynamics in the Kilombero floodplain. Models such as MODular Hydrologic Modelling System (MODHMS) (Varut et al., 2011), European Hydrological System (MIKE SHE) (Graham et al., 2005), and Hydrus-2D and -3D (Šimůnek et al., 2012) can be adopted to simulate soil water dynamics. However, they are data demanding, require large computer resources, and are difficult to adapt to the investigated study area because of complex boundary conditions. Hydrus-1D, in comparison, is less data demanding and can easily be adopted at the local scale as well as at the East African regional scale, and has also been proven to be an effective tool for evaluating various water and solute fluxes in agricultural fields with different crops and various irrigation schemes (Kandelous et al., 2012; Siyal et al., 2012). Hydrus-1D has been successfully applied in numerous studies for predicting soil moisture content and movement under different conditions (Chen et al., 2014; Jing et al., 2014; Li et al., 2015; Xu et al.,

2016). In spite of these previous efforts, there is still limited research on the assessment of the spatial soil moisture dynamics at the different hydrological zones of a tropical wetland using Hydrus-1D, especially for data-scarce tropical regions such as East Africa. Most of these studies (Kandelous et al., 2012; Jing et al., 2014; Xu et al., 2016) have been conducted in temperate regions, yet tropical regions continue to face data scarcity and quality challenges, especially in the recently degrading wetland ecosystems. The similarity of this study to previous works is the type of data (soil moisture content, depth to groundwater level, soil physical properties, leaf area index, and climatic data) used for model calibration and simulation of soil water dynamic and vertical fluxes.

Many studies have described and explained the factors that influence soil water dynamics (Böhme et al., 2016; Böhme et al., 2013; Gabiri et al., 2018) and soil moisture retention (Dixon and Wood, 2003; Snyder, 2005; Sławiński et al., 2012) at the wetland-catchment scale in East Africa. However, these studies are tailored to inland valley wetlands, yet floodplain wetlands exhibit different hydrological behavior compared to the inland valley wetlands. Therefore, there is paucity of sufficient scientific information for proper floodplain wetland agricultural management planning in the region. This calls for more research on these floodplains to improve the scientific knowledge base for decision-making. The purpose of the study is to conduct a thorough study of the soil water dynamic based on field measurements so as to evaluate the agricultural usability of the different hydrological zones of the tropical floodplain wetland. This contributes to soil and land management as it provides the required scientific basis for decision-making and agricultural planning. Accordingly, the study has the following objectives (i) to test the applicability of the Hydrus-1D model for simulating spatial soil moisture content dynamics along different hydrological zones of the floodplain; (ii) to determine factors controlling soil moisture content dynamics at each hydrological zone during drying and wetting periods; and (iii) to assess soil water availability for each hydrological zone. In addition, a sensitivity analysis on selected water flux parameters, with varying depth to groundwater levels, was conducted for each hydrological zone. This was performed to understand how changes in groundwater levels, which may be caused by water extraction and catchment scale processes, will influence local water availability and water fluxes.

8.2. Materials and methods

The location of the Kilombero floodplain wetland and the study site is described in detail in Chapter 2. The study design, instrumentation, delineation of the hydrological zones of the floodplain wetland, hydrological data (soil moisture content, shallow groundwater, and soil parameters) and meteorological data collection procedures are fully described in Chapter 3. Description of the Hydrus- 1D model applied in this chapter to simulate soil water dynamics at the defined hydrological zones of the floodplain, and the criterion for model performance are presented in detail in Chapter 4.

8.2.1. Initial and boundary conditions

Time series for meteorological conditions used for the simulation period (2015 to 2017) are depicted in Fig. 8.1. Actual evaporation and transpiration were directly computed by the model based on the given soil moisture conditions and root water uptake functions.

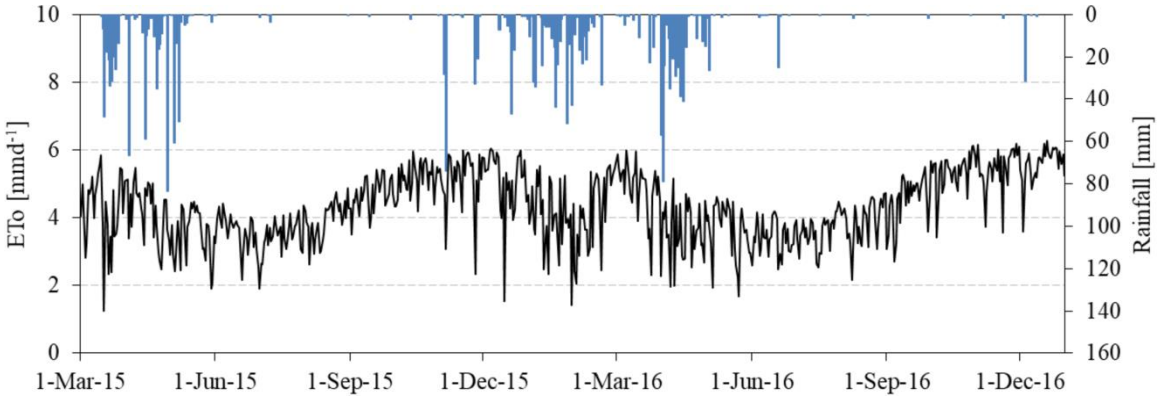

Fig. 8.1. Daily rainfall and ET_0 values used during the simulation period.

Leaf area index (LAI) values were measured at different growth stages of rainfed lowland rice using a LI-COR area meter, an indirect method. Direct methods like planimetrical approach and gravimetric procedure can be used but are time consuming and destructive (Danner et al., 2015). The LI-COR area meter is fast and uses a fisheye lens to project a nearly hemispheric image of the canopy and sky onto a ringed detector. This enables quick measurement of leaf area index and foliage orientation over a large area. In this study, LAI values were linearly interpolated between the measurement dates to obtain time series values.

8.2.2. Model calibration and validation

The model was calibrated for one year (March 2015 to March 2016), by comparing the simulated and field measured daily soil moisture content at the different soil depths (10, 20, 30, and 40 cm), and plots for each hydrological zone. Plots PR_1, PR_3, PR_4, and PR_8 for the riparian zone, PM_3, PM_5, and PM_7 for the middle zone, and PF_4, PF_8, PF_10, and PF_12 for fringe zone were used for calibration (Fig. 4.2b, chapter 3). The one-year period included the drying and wetting conditions, allowing us to fit the model at a wide range of soil moisture conditions in the floodplain. The soil material layer/horizon was defined in accordance with depth intervals used for monitoring soil moisture content in a profile of 200 cm. A profile of 200 cm was defined because the observed groundwater table is within this range.

Hydrus-1D was calibrated using site specific boundary conditions, and field measured soil moisture content. Van Genuchten hydraulic parameters which describe the soil retention and unsaturated hydraulic conductivity functions were optimized through inverse modeling with no hysteresis. In the Hydrus-1D model, inverse parameter estimation employs a relatively simple, gradient based, local optimization algorithm based on Marquardt-Levenberg method (Šimůnek et al., 2013). The aim of this method is to determine the best estimate of the hydraulic model parameters (Radcliffe and Šimůnek, 2010). Hydraulic parameters estimated via the Rosetta pedotransfer functions (Schaap et al., 2001) using measured soil particle size distribution (percentage clay, silt, and sand) and bulk density were used as initial estimates, in addition to the measured saturated hydraulic conductivity (Table 8.1). Alpha, n, and saturated water content parameters were fitted first since Hydrus–1D model could optimize only 15 parameters at a time. Residual water content and the l parameter were the last to be estimated. The values of K_{sat} were reviewed and re-adjusted accordingly.

Table 8.1 Measured soil physical properties at the three hydrological zones of the floodplain.

Hydrological zone	Soil depth	BD	K_{sat}	SOC	Clay	Silt	Sand	Texture class
	cm	(gcm^{-3})	(cmd^{-1})	%				
Riparian	10	1.03	114.50	1.88	35.02	56.18	8.80	Silty clay loam
	20	1.21	38.00	1.43	36.44	48.06	15.50	Silty clay loam
	30	1.27	17.13	0.83	34.27	37.87	27.86	Clay loam
	40	1.28	19.38	0.59	29.50	35.84	34.66	Clay loam
Middle	10	1.43	116.94	1.36	18.84	58.27	22.89	Silt loam
	20	1.33	120.57	1.56	21.58	61.92	16.50	Silt loam
	30	1.39	33.91	1.11	20.9	56.21	22.89	Silt loam
	40	1.38	27.62	0.91	29.4	56.17	14.43	Silty clay loam
Fringe	10	1.27	174.05	1.42	13.89	57.25	28.86	Silt loam
	20	1.36	180.93	1.39	14.20	59.07	26.73	Silt loam
	30	1.36	305.00	1.13	15.39	60.30	24.32	Silt loam
	40	1.39	101.01	0.99	15.86	58.37	25.77	Silt loam

BD; Bulk density, K_{sat}; Saturated hydraulic conductivity, SOC; Soil Organic Carbon

During the rice growing period, Feddes' parameters for the tropical climate were taken from (Singh et al., 2006): h_1= 100 cm, h_2= 55 cm, h_3= -160 cm, h_4= -250 cm, h_4 = -16000 cm and the root distribution with a maximum of 40 cm were specified according to (Slaton et al., 1990). After rice harvest (i.e. during the dry and the short rainy seasons, in which the sites were under fallow), we used the Feddes' parameters for grass implemented in Hydrus-1D.

The calibrated model from each plot was validated for one year, with measured soil moisture data for the neighboring plots at each hydrological zone. The aim of this approach was to test the transferability of the calibrated model to predict spatial soil moisture for sites with similar biophysical properties and climate conditions. At each hydrological zone, two calibrated plots were validated with measured moisture data of the neighboring plots. At the riparian zone, plot PR_1 and PR_4 were validated with measured soil moisture data from plot PR_3 (88 m distant) and PR_1 (75 m distant), respectively. At the middle zone, plot PM_3 and PM_7 were validated with measured soil moisture values from plot PM_7 (400 m distant) and plot PM_5 (102 m distant), respectively. At the fringe, plot PF_10 and PF_8 were validated with measured soil moisture data from plot PF_12 (109 m distant), and PF_4 (225 m distant), respectively (Fig. 4.2b, chapter 3).

8.2.3. Sensitivity analysis

A sensitivity analysis was performed to analyse the impact of changes in depth to groundwater level (dgwl) on root water uptake, evaporation, and change in soil water storage parameters. Evapotranspiration (transpiration and evaporation) is the major water loss in the wetlands (Xu et al., 2016; Bidlake, 2000), while soil water storage is the most important state variable for crop growth. Therefore, understanding the impact of changes in depth to groundwater level is essential to assess the water balance of the study area for sustainable agricultural and wetland management planning. Considering data for one year (July 2015 – June 2016) as reference, the mean dgwl was increased and decreased by 15, 30, 45, and 60%. To evaluate the sensitivity of each parameter, sensitivity index, SI for each percentage change in dgwl was calculated according to de Roo (1993) cited in (Giertz et al., 2006):

$$\mathrm{SI} = \frac{|P_i - P_m|}{P} \qquad \text{(Eq.8.1)}$$

With P_i = model output with a 15, 30, 45, and 60 % increase in the mean dgwl

P_m = model output with a related 15, 30, 45, and 60 % decrease in the mean dgwl

P = model output with base dgwl

A number of sensitivity analyses methods exist for example variance based methods, correlation and regression analysis methods, and Monte Carlo Methods (Pianosi et al., 2016). We used the sensitivity index method for this study because of its simplicity and because the sensitivity is clearly attributed to one model parameter.

8.3. Results

8.3.1. Simulation of spatial soil water dynamics at different scales

Hyrus-1D was set-up, calibrated, and validated at the riparian, middle, and fringe hydrological zones of the floodplain.

Calibration results

A comparison of model performances and quality of statistical measures are presented in Table 8.2 for the riparian zone. Time series soil moisture content was well captured by the model for the four calibrated individual plots. A good agreement between modeled and observed soil moisture content

as indicated by high R^2 (0.67–0.92), NSE (0.63–0.91), and low RMSE (0.03–0.06) was obtained (Table 8.2). The best fit of van Genuchten hydraulic parameters for each plot is shown in Table 8.3. The calibrated hydraulic parameters showed slight differences among the plots at soil depths of 10, 20, 30, and 40 cm. The final calibrated saturated hydraulic conductivity was higher than the measured values (Tables 8.1 and 8.3).

Table 8.2 Statistical measures of Hydrus-1D model performance for simulations of soil moisture content at the riparian zone after calibration.

Statistic measure	Soil depth			
	10 cm	20 cm	30 cm	40 cm
			Plot PR_4	
R^2	0.78	0.88	0.73	0.83
NSE	0.77	0.87	0.73	0.83
RMSE (cm^3cm^3)	0.06	0.03	0.05	0.03
			Plot PR_1	
R^2	0.90	0.81	0.82	0.70
NSE	0.89	0.80	0.82	0.70
RMSE (cm^3cm^3)	0.04	0.06	0.05	0.06
			Plot PR_8	
R^2	0.40	0.88	0.80	0.67
NSE	0.37	0.88	0.79	0.63
RMSE (cm^3cm^3)	0.14	0.05	0.05	0.04
			Plot PR_ 3	
R^2	0.85	0.89	0.92	0.76
NSE	0.79	0.81	0.91	0.74
RMSE (cm^3cm^3)	0.05	0.04	0.02	0.03

Table 8.3 Calibrated van Genuchten hydraulic parameters for the different plots at the riparian zone of the floodplain.

Soil depth (cm)	Plot	θ_r ($cm^3cm^{3)}$	θ_s ($cm^3cm^{3)}$	α (cm^{-1})	n	K_{sat} (cmd^{-1})	l
10	PR_4	0.08	0.43	0.05	2.00	78.87	0.50
	PR_1	0.06	0.38	0.03	2.500	738.5	0.68
	PR_8	0.08	0.43	0.03	2.98	300	0.50
	PR_3	0.04	0.39	0.13	1.83	609.15	0.45
20	PR_4	0.11	0.43	0.04	1.95	7.95	0.22
	PR_1	0.05	0.45	0.02	2.66	171.8	0.13
	PR_8	0.08	0.47	0.03	2.86	214	0.5
	PR_3	0.09	0.45	0.05	2.18	3.50	0.07
30	PR_4	0.1	0.47	0.04	1.66	209.8	0.12
	PR_1	0.1	0.49	0.02	2.40	323.6	0.7
	PR_8	0.08	0.51	0.02	2.11	6.53	0.5
	PR_3	0.12	0.47	0.05	1.78	12.08	0.01
40	PR_4	0.1	0.47	0.06	1.42	7.27	0.5
	PR_1	0.09	0.54	0.03	1.57	6.24	1.2
	PR_8	0.08	0.52	0.07	1.28	7.84	0.5
	PR_3	0.12	0.49	0.13	1.36	6.2	0.23

Soil moisture content dynamics for both the rainy and dry seasons were well reproduced by the model for all of the soil layers. Measured and modeled soil moisture content values increased with soil depth. Flooding from both river overbank flow and local rainfall occurred during the long rainy season (March to May) and in the months of January to February 2016, which experienced heavy rains, correlated to El Niño–Southern Oscillation (ENSO) (Hastenrath et al., 1993; Goddard and Graham, 1999) and the Indian Ocean zonal mode (IOZM) (Black et al., 2003).

At the riparian zone, the depth to groundwater level increased on average up to 1.6 m above the soil surface during the long rainy seasons; thus, the soils were fully saturated. During these periods, the model was able to reproduce soil moisture content trends and showed constant values (indicating soil saturation) until the floods receded (Fig. 8.2). During flood recession (when the depth to groundwater level increased below the surface i.e., after June 2015), both modeled and measured soil moisture content showed a similar decreasing trend. For the short rainy season, the depth to groundwater level continued to increase below the surface until it reached 150 cm. Interestingly, measured and modeled soil moisture content at the different soil

depths responded positively to rainfall events. Therefore, rainfall controlled soil moisture dynamics during this period (Fig. 8.2). In addition, soil moisture dynamics could be explained by the differences observed in calibrated hydraulic parameters along the soil depths. The calibrated soil hydraulic parameters showed slight differences among the plots by visual comparison (Table 8.3). Thus, within the hydrological zones, there were relatively similar soil moisture patterns among the plots. This was depicted in the measured and modeled soil moisture content for the individual plots in the riparian zone, which showed almost similar trends throughout the different seasons (Fig. 8.2).

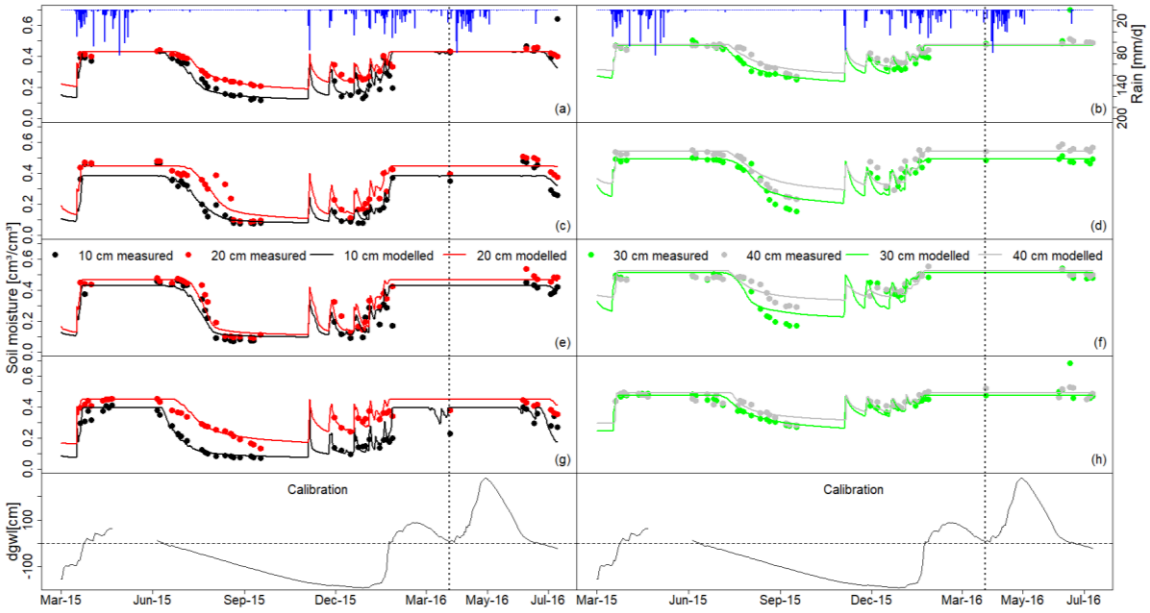

Fig. 8.2. Measured and modelled soil moisture content for calibration at the four plots in riparian zone. (a) and (b); plot PR_4, (c) and (d); plot PR_1, (e) and (f); plot PR_8, (g) and (h); plot PR_3; dgwl, measured depth to groundwater level.

Fig. 8.3 presents the time series measured depth to groundwater level and calibration results of soil moisture content at the middle hydrological zone of the floodplain. Results revealed that the modeled soil moisture content exhibited variation tendencies quite similar to the measured data at the different soil depths in all of the plots. Modeled and measured soil moisture content increased with increase in soil depth.

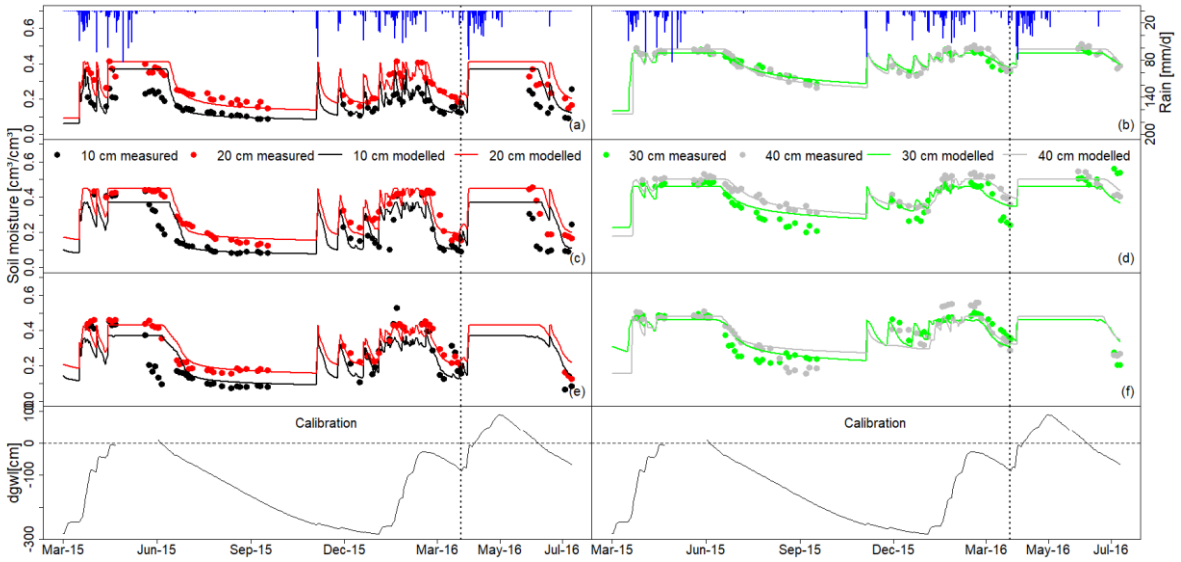

Fig. 8.3. Measured and modelled soil moisture content after calibration at the four plots for the middle zone. (a) and (b); plot PM_3, (c) and (d); plot PM_5, (e) and (f); plot PM_7, dgwl; measured depth to groundwater level.

Overall, there was a good agreement between modeled and measured soil moisture content after calibration (R^2 = 0.59–0.89, NSE = 0.51–0.88, and RMSE = 0.02–0.10 cm^3/cm^3) (Table 8.4). The best fit of the van Genuchten hydraulic parameters for individual plots are shown in Table 8.5. There was almost no difference observed between the calibrated hydraulic parameters among the plots, except for saturated hydraulic conductivity. Hence, small variations between the modeled and measured soil moisture content values were noted among the plots.

Table 8.4 Statistical measures of Hydrus-1D model performance for simulations of soil moisture content at the middle zone after calibration.

Statistic measure	Soil depth			
	10 cm	20 cm	30 cm	40 cm
			Plot PM_3	
R^2	0.76	0.82	0.82	0.88
NSE	<<0	0.71	0.82	0.88
RMSE (cm^3cm^3)	0.07	0.04	0.03	0.02
			Plot PM_5	
R^2	0.65	0.88	0.87	0.89
NSE	0.63	0.87	0.72	0.87
RMSE (cm^3cm^3)	0.09	0.04	0.05	0.03
			Plot PM_7	
R^2	0.59	0.84	0.74	0.88
NSE	0.51	0.85	0.77	0.71
RMSE (cm^3cm^3)	0.10	0.04	0.05	0.06

Table 8.5 Calibrated van Genuchten hydraulic parameters for the different plots at the middle zone of the floodplain.

Soil depth (cm)	Plot	θr ($cm^3cm^{3)}$	θs ($cm^3cm^{3)}$	α (cm^{-1})	n	K_{sat} (cmd^{-1})	l
10	PM_3	0.04	0.37	0.08	1.85	85.4	0.49
	PM_5	0.04	0.37	0.03	1.7	128	0.49
	PM_7	0.04	0.37	0.03	1.53	65.72	0.48
20	PM_3	0.06	0.41	0.07	1.91	21.45	0.41
	PM_5	0.06	0.45	0.06	1.46	100	0.41
	PM_7	0.06	0.43	0.04	1.38	150	0.42
30	PM_3	0.04	0.46	0.02	1.8	0.93	0.0002
	PM_5	0.04	0.46	0.04	1.35	0.55	0.0002
	PM_7	0.04	0.46	0.01	1.36	2.49	0.002
40	PM_3	0.03	0.48	0.04	1.72	3.04	3.36
	PM_5	0.03	0.50	0.03	1.54	2.34	3.36
	PM_7	0.03	0.48	0.14	1.35	5.08	3.32

The depth to groundwater level at the middle hydrological zone increased up to approximately 100 cm above the soil surface, causing full saturation of the soil layers during the long rainy season (March–June) (Fig. 8.3). In the dry and short rainy seasons, the depth to groundwater level gradually declined up to 300 cm below the surface. Moreover, the model was capable of simulating the seasonal soil moisture content variations. During the short rainy season, both

simulated and measured soil moisture content strongly responded to rainfall events in spite of the continued declining depth to groundwater level (Fig. 8.3). Therefore, rainfall and soil properties played an important role in controlling soil moisture dynamics during dry and short rainy seasons at the middle zone. Modeled soil moisture dynamics during this period were well captured, except for some plots in which the simulated soil moisture showed high amplitude from the measured soil moisture content. Overall, the simulations were in agreement with the measurements.

Fig.8.4 and Table 8.6 show the calibrated results of soil moisture and model performance, respectively at the fringe zone of the floodplain. The modeled soil moisture content depicted a trend relatively similar to the measured soil moisture over time at the 10-cm depth intervals among the plots. The R^2 among the calibrated plots varied from 0.54 to 0.87, RMSE ranged from 0.03 to 0.11 cm^3/cm^3, and NSE varied from <0 to 0.85 (Table 8.6). Although modeled values were satisfactory, the model somewhat over- and underestimated soil moisture content at all of the plots (Fig. 8.4).

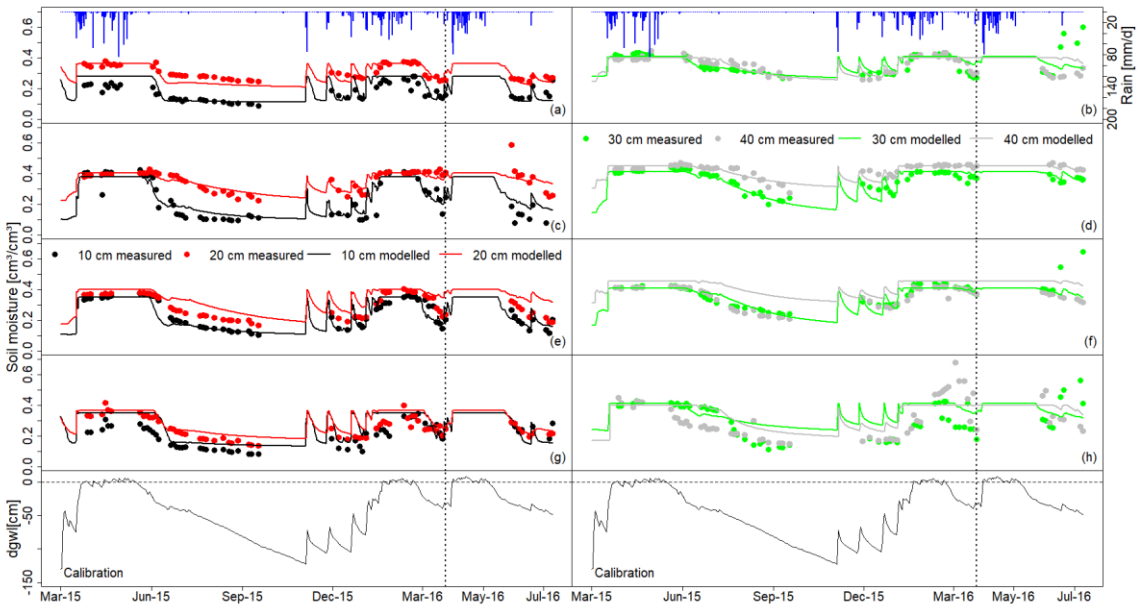

Fig. 8.4. Measured and modelled soil moisture content after calibration at the four plots for the fringe zone. (a) and (b); plot PF_12, (c) and (d); plot PF_10, (e) and (f); plot PF_4, (g) and (h); plot PF_8, dgwl; measured depth to groundwater level.

Table 8.6 Statistical measures of Hydrus-1D model performance for simulations of soil moisture content at the fringe zone after calibration.

Statistic measure	**Soil depth**			
	10 cm	20 cm	30 cm	40 cm
			Plot PF_8	
R^2	0.68	0.73	0.54	0.47
NSE	<<0	0.35	0.11	0.34
RMSE (cm^3cm^3)	0.08	0.06	0.10	0.11
			Plot PF_10	
R^2	0.87	0.85	0.85	0.74
NSE	0.85	0.82	0.85	0.73
RMSE (cm^3cm^3)	0.05	0.03	0.03	0.02
			Plot PF_4	
R^2	0.84	0.82	0.85	0.80
NSE	0.83	0.09	0.44	<<0
RMSE (cm^3cm^3)	0.04	0.08	0.06	0.08
			Plot PF_12	
R^2	0.82	0.73	0.67	0.58
NSE	0.33	0.47	0.67	0.58
RMSE (cm^3cm^3)	0.04	0.03	0.04	0.03

Likewise, the calibrated van Genuchten hydraulic parameters showed slight variations at 10-cm depth intervals within and across the individual plots. This could be due to the low heterogeneity in soil texture (clay, sand, and silt content) and bulk density within the fringe position. Saturated hydraulic conductivity greatly varied along the four soil depths within and across the plots (Table 8.7), which can be explained by the effect of soil macrospores, the cracking, and the occurrence of slickensides as a consequence of swell-and-shrink behavior, which were commonly encountered in clay-rich horizons during sampling.

Table 8.7 Calibrated van Genuchten hydraulic parameters from the different plots at the fringe zone of the floodplain.

Soil depth (cm)	Plot	θ_r ($cm^3cm^{3)}$	θ_s ($cm^3cm^{3)}$	α (cm^{-1})	n	K_{sat} (cmd^{-1})	l
10	PF_12	0.09	0.28	0.002	1.56	28.4	0.26
	PF_10	0.08	0.38	0.05	2.5	64.2	0.5
	PF_4	0.08	0.35	0.04	2.5	24.62	0.5
	PF_8	0.08	0.35	0.002	1.35	24.62	0.5
20	PF_12	0.03	0.36	0.002	1.16	1.76	0.5
	PF_10	0.03	0.4	0.02	1.7	48.6	0.5
	PF_4	0.03	0.4	0.02	2.2	1.1	0.5
	PF_8	0.03	0.37	0.006	1.27	1.1	0.5
30	PF_12	0.04	0.41	0.1	1.19	1.3	0.05
	PF_10	0.05	0.41	0.03	2.36	65.2	0.5
	PF_4	0.05	0.41	0.03	2.1	1.3	0.5
	PF_8	0.05	0.41	0.08	1.32	1.92	0.5
40	PF_12	0.15	0.4	0.08	1.53	10.8	0.07
	PF_10	0.09	0.45	0.05	1.36	12.54	0.5
	PF_4	0.09	0.46	0.05	1.34	18.46	0.5
	PF_8	0.09	0.4	0.1	1.64	6.13	0.5

Modeled and measured soil moisture time series showed a positive response to rainfall events, although high dynamics were observed during the wetting and drying periods (October to December 2016) for all of the soil depths across the plots. The monitored plots were flooded for a short time during the rainy season (March to June during the study) and in the short heavy rains (January to February 2016) (Fig. 8.4). The depth to groundwater level gradually increased up to approximately 50 cm above the soil surface, saturating the soil layers. Thereafter, the depth to groundwater level declined to approximately 120 cm below the surface during the dry season (July to September 2015). However, in comparison to the riparian and middle zones, the variations in the depth to groundwater level were lower at the fringe zone. Equally important, the model was able to capture the seasonal soil moisture variability at the different plots amidst the existing data gaps in the measured soil moisture content. Also, the discrepancies between the simulated and measured soil moisture time series at the fringe were not different from those observed at the riparian and middle zones across the calibrated plots. Unlike at the riparian and middle zones, the depth to groundwater level and soil moisture content exhibited a positive response to single rainfall events during the wetting and drying periods (October to December

2016) at the fringe zone. Thus, the depth to groundwater level, rainfall, and soil properties control the soil moisture dynamics at this zone.

Additionally, we tested the hypothesis that the model can simulate soil moisture dynamics averaged from individual plots, after aggregating the plot-specific calibrated hydraulic parameters within the hydrological zone. Therefore, the calibrated van Genuchten hydraulic parameters for each plot from the respective hydrological zones were averaged at each soil depth (Table 8.8).

Table 8.8 Averaged calibrated hydraulic parameters at each hydrological zone.

Hydrological zone	**Soil depth**	**θr (cm^3 $cm^{3)}$**	**θs (cm^3 $cm^{3)}$**	**α (cm^{-1})**	**n**	**K_{sat} (cm d^{-1})**	**l**
Riparian zone	10	0.07	0.41	0.06	2.33	431.63	0.53
	20	0.08	0.45	0.04	2.41	99.31	0.23
	30	0.10	0.49	0.03	1.99	138.00	0.33
	40	0.10	0.51	0.07	1.41	6.88	0.61
Middle	10	0.04	0.37	0.05	1.69	93.04	0.49
	20	0.06	0.43	0.06	1.58	90.48	0.41
	30	0.04	0.46	0.02	1.50	1.32	0.0009
	40	0.03	0.49	0.07	1.54	3.49	3.35
Fringe	10	0.08	0.34	0.02	1.98	35.46	0.44
	20	0.03	0.38	0.01	1.58	13.14	0.5
	30	0.05	0.41	0.06	1.74	17.43	0.39
	40	0.11	0.43	0.07	1.47	11.98	0.39

Hydrus-1D model was set up with these averaged hydraulic parameters to simulate soil moisture content for each hydrological zone. The simulations were evaluated by comparing the modelled soil moisture content with the averaged measured soil moisture content at 10 cm depth increment. Fig. 8.5 shows typical results.

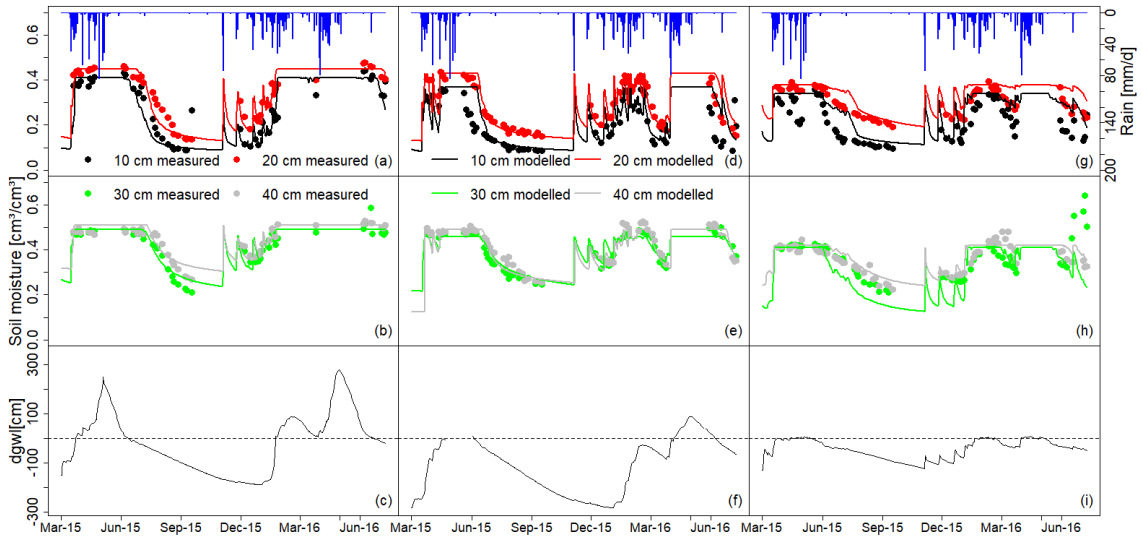

Fig. 8.5. Comparison of measured (averaged from all plots) and modelled soil moisture from the averaged calibrated hydraulic parameters at each hydrological zone. (a), (b) and (c); riparian zone, (d), (e), and (f); middle zone, (g), (h), and (i); fringe zone; dgwl: measured depth to groundwater level.

Overall, modelled soil moisture time series showed good agreement with the averaged measured soil moisture content. There were some discrepancies between the modelled and measured soil moisture content values. This could be explained by the low variations in the hydraulic parameters observed at each individual plot of the respective hydrological zones. Generally, the model performance was good at the different hydrological zones. For example, R^2 varied from 0.78 to 0.90, NSE = 0.74 - 0.87, and RMSE ranged from 0.03 to 0.06 at the riparian zone, at the middle zone, R^2= 0.62 - 0.90, NSE= 0.54 - 0.86, and RMSE= 0.03 - 0.06, and for the fringe zone, R^2= 0.75 - 0.82, RMSE= 0.03 - 0.07, NSE ranged from 0.37 to 0.75 (Table 8.9).

Table 8.9 Hydrus-1D performance for soil moisture simulation after using averaged hydraulic parameters calculated from all the calibrated plots for each hydrological zone.

Soil depth	Riparian zone			Middle zone			Fringe zone		
	R^2	NSE	RMSE	R^2	NSE	RMSE	R^2	NSE	RMSE
10	0.78	0.74	0.06	0.62	0.54	0.06	0.75	0.37	0.07
20	0.90	0.87	0.04	0.89	0.86	0.03	0.75	0.42	0.05
30	0.90	0.87	0.03	0.90	0.86	0.03	0.82	0.37	0.05
40	0.82	0.79	0.03	0.90	0.86	0.03	0.80	0.75	0.03

Validation results and prediction of spatial soil moisture content

We randomly validated the calibrated plots against the neighboring plots with measured soil moisture content data at 10 and 30 cm soil depths for each hydrological zone. In doing so, we were able to test the transferability of model parameters calibrated at one plot to predict spatial soil moisture dynamics of another plot located in the same hydrological zone. As expected, model accuracy was higher for calibration than validation. Nevertheless, the modelled results are reasonable with low variability against the measured soil moisture content at each plot along the different soil depths by visual comparison (Fig. 8.6). Validation resulted in R^2= 0.64 - 0.89 and RMSE = 0.06 - 0.07 for riparian zone; R^2= 0.36 – 0.82 and RMSE = 0.07 - 0.13 for the middle zone; and R^2= 0.52 – 0.91, and RMSE = 0.04 - 0.10 for the fringe zone (Table 8.10). The goodness-of-fit values indicated satisfactory agreement between modelled values and field measurements for both rain and dry seasons and demonstrated the acceptable accuracy of model simulations. Thus, supporting the hypothesis on the model's feasibility to simulate spatial soil water dynamics within sites of similar topography, and other biophysical properties once it is well calibrated.

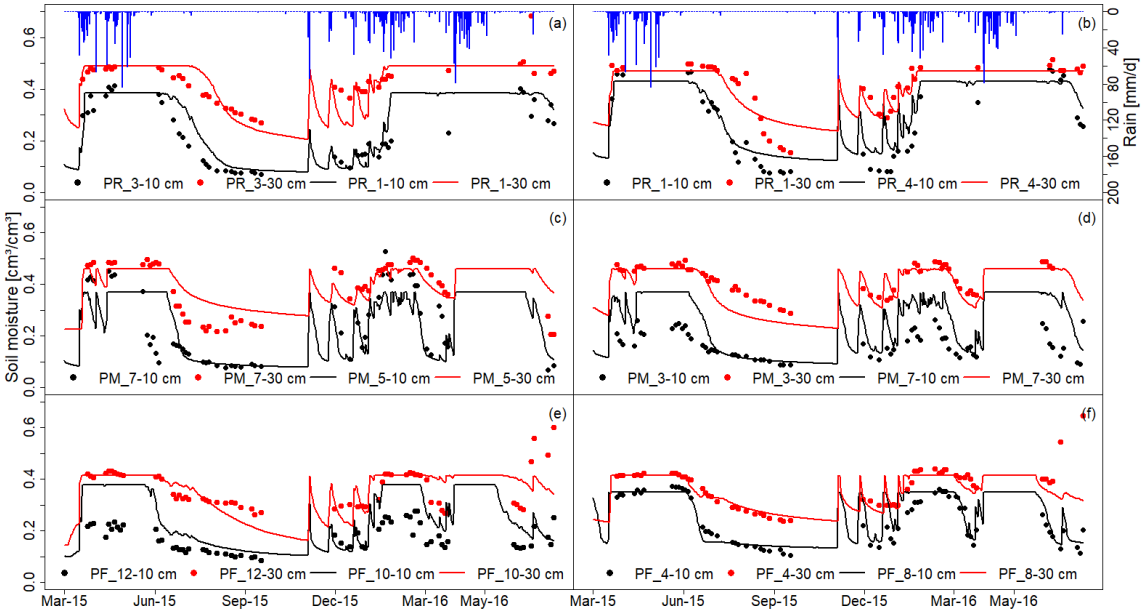

Fig. 8.6 Modelled and measured soil moisture content from selected plots at 10 and 30 cm depth in each hydrological zone. PR, PM, PF represent riparian, middle and fringe zone, respectively. a and b, riparian, c and d, middle, e and f, fringe. 1, 3, 4, 5, 7, 8, 10, and 12, denote plot numbers at the different hydrological zones.

Table 8.10 Hydrus-1D performance for soil moisture simulation after validation.

Hydrological zone	Statistic measure	Soil depth			
		10 cm	20 cm	30 cm	40 cm
Riparian	Plot PR_4 vs PR_1				
	R^2	0.89	0.79	0.77	0.80
	NSE	0.80	0.69	0.74	0.49
	RMSE (cm^3cm^3)	0.06	0.07	0.05	0.07
	Plot PR_1 vs PR_ 3				
	R^2	0.79	0.75	0.64	0.65
	NSE	0.68	0.42	0.14	0.07
	RMSE (cm^3cm^3)	0.07	0.07	0.09	0.06
Middle	Plot PM_5 vs PM_7				
	R^2	0.36	0.84	0.69	0.61
	NSE	0.31	0.84	0.59	0.40
	RMSE (cm^3cm^3)	0.13	0.05	0.07	0.09
		Plot PM_7 vs PM_3			
	R^2	0.63	0.76	0.82	0.87
	NSE	<<0	0.28	0.15	0.74
	RMSE (cm^3cm^3)	0.11	0.07	0.13	0.03
Fringe	Plot PF_8 vs PF_4				
	R^2	0.84	0.83	0.91	0.85
	NSE	0.81	0.53	0.46	0.84
	RMSE (cm^3cm^3)	0.04	0.06	0.06	0.03
	Plot PF_10 vs PF_12				
	R^2	0.81	0.63	0.52	0.61
	NSE	<<0	<<0	0.28	<<0
	RMSE (cm^3cm^3)	0.10	0.06	0.05	0.07

8.3.2. Soil water availability at the different hydrological zones

To assess soil water availability, annual soil water balance was established at each hydrological zone for a period of one year (July 2015 to June 2016). Modelled water fluxes showed high temporal variability (Fig. 8.7) and distinct differences in annual values (Table 8.11) among the three hydrological zones. Results showed positive and negative cumulative bottom flux among the three hydrological zones for the simulation period. Negative bottom flux indicated drainage from the profile and groundwater recharge, moreover positive bottom fluxes were associated with capillary rise and groundwater discharge. The highest positive cumulative bottom flux was observed at the riparian zone (296.2 mm), and the least value observed at middle zone (116.2 mm) of the floodplain during simulation period (Fig. 8.7).

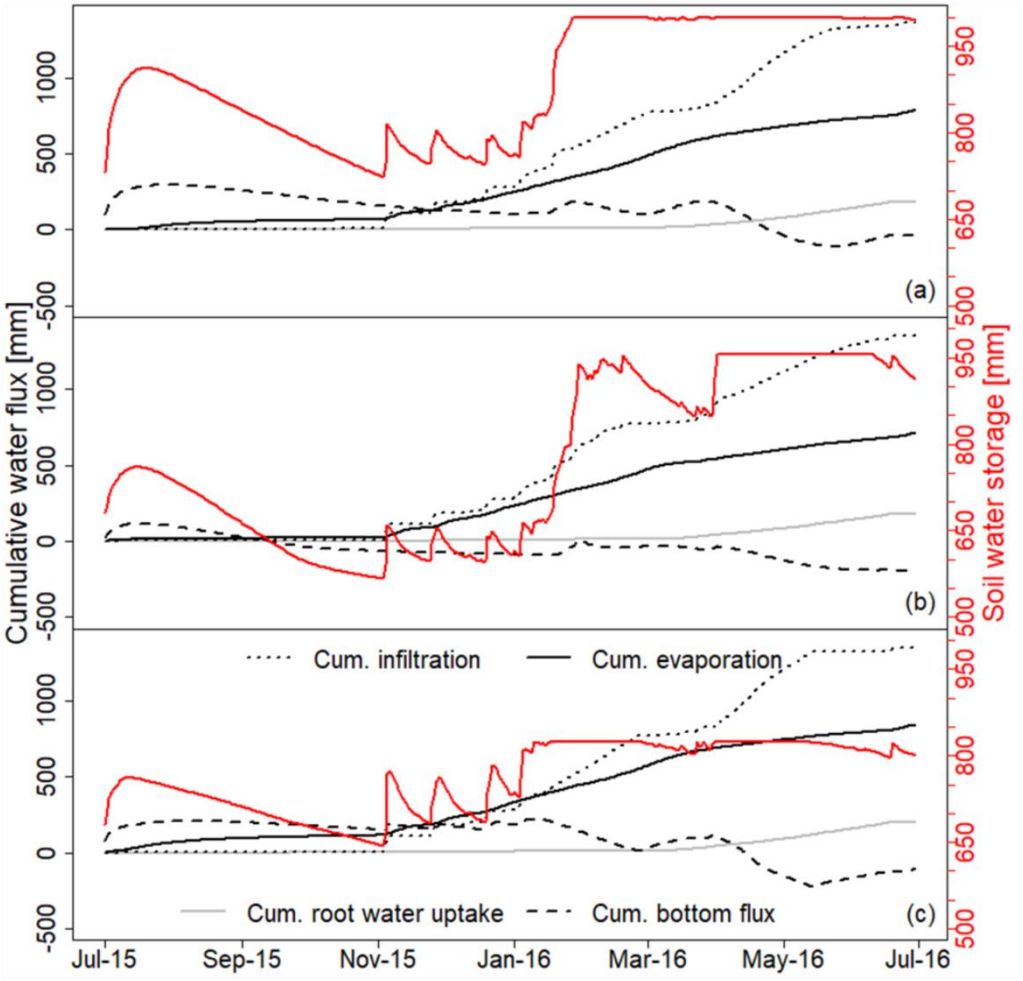

Fig. 8.7. Cumulative water fluxes for one year. (a); riparian zone, (b); middle zone, and (c); fringe zone.

Table 8.11 Annual water balance from Hydrus-1D for each hydrological zone.

Hydrological zone	P	PET	ET_a	G_o	G_i	ΔS
			mm			
Riparian zone	1364.7	1561.0	969.4	108.9	296.2	262.8
Middle	1364.7	1561.0	896.1	196.4	116.2	232.9
Fringe	1364.7	1561.0	1043.9	219.8	222.2	120.1

P, Precipitation; PET, Potential evapotranspiration; ET_a, Actual evapotranspiration; G_o, groundwater recharge; G_i, capillary rise/ groundwater discharge; ΔS, change in soil water storage.

The largest annual change in soil water storage was observed at the riparian zone. An increase of about 262.8 mm was calculated at the riparian zone, followed by the middle zone (232.9 mm), and fringe zone (120.1 mm) (Table 8.11). During the short (October to December 2015) and long (March to June 2016) rainy seasons, and months of January and February 2016, soil water storage increased due to the filling up of the soil profile by infiltration process. While in the dry season (July to September 2015), soil water storage gradually decreased at all the hydrological zones. Noteworthy, at the middle zone, the decrease reached values below zero (Fig. 8.7).

Cumulative root water uptake was highest at the fringe zone, followed by middle and riparian zones (Fig. 8.7). Annual cumulative root water uptake reached 201.0 mm at the fringe, 183.3 mm at the middle, and 183.5 mm at the riparian zone. Annual cumulative evaporation was substantially higher at the fringe (842.9 mm), than the riparian (785.9 mm) and middle (712.8 mm) zone during the simulation period. Therefore, actual evapotranspiration was highest at the fringe (1043.9 mm), contributing to 76.5% of the water loss from precipitation, followed by the riparian zone (969.4 mm, 71% water loss), and the middle zone (896.1 mm, 65.7% water loss) at each hydrological zone (Table 8.11).

8.3.3. Sensitivity analysis

Sensitivity analysis was performed to analyse the impact of changes in the depth to groundwater level on root water uptake, evaporation and change in soil water storage. Fig. 8.8 and Table 8.12 show the results of the sensitivity analysis. The sensitivity analysis revealed that among the water flux components, evaporation was the most sensitive parameter to changes in dgwl followed by change in soil water storage at all the hydrological zones. Root water uptake was sensitive at the middle zone while insensitive to changes in dgwl at the fringe and riparian zones. Change in soil water storage and evaporation were highly sensitive at the fringe followed by the middle zone. The most sensitive parameter at the fringe and middle zone was change in soil water storage while evaporation was highly sensitive at the fringe zone for all the changes in dgwl. Sensitivity indices increased with increase in changes to dgwl for all the water flux components at the three hydrological zones.

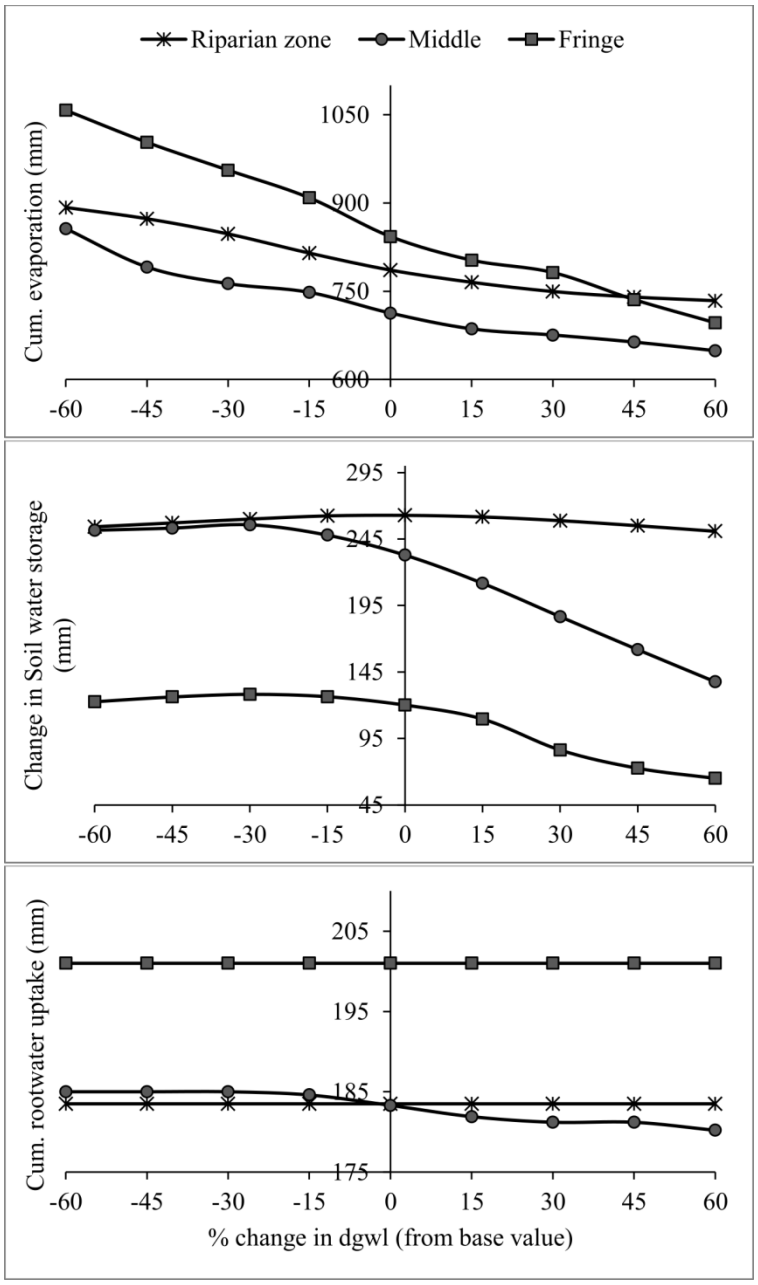

Fig. 8.8. Sensitivity analysis for different water fluxes on changes in depth to groundwater level, dgwl, depth to groundwater level.

Table 8.12 Sensitivity indices SI for different water fluxes calculated after changes in dgwl.

Water flux component	SI-15% dgwl	SI-30% dgwl	SI-45% dgwl	SI-60% dgwl
Riparian zone				
Cum. evaporation	0.063	0.125	0.169	**0.202**
Change in soil water storage	0.003	0.005	0.008	0.013
Cum. root water uptake	0.000	0.000	0.000	0.000
Middle zone				
Cum. evaporation	0.087	0.122	0.139	0.291
Change in soil water storage	0.156	0.297	0.392	**0.489**
Cum. root water uptake	0.015	0.021	0.021	0.026
Fringe zone				
Cum. evaporation	0.126	0.206	0.317	0.429
Change in soil water storage	0.140	0.349	0.446	**0.480**
Cum. root water uptake	0.000	0.000	0.000	0.000

Numbers in bold are the most sensitive parameters at each hydrological zone

At the fringe zone, cumulative evaporation and change in soil water storage had the maximum annual values of 1057.7 mm and 128.2 mm, higher than their respective references when dgwl decreased by 60% and 30%, respectively. The minimum values of 696.4 mm and 65.0 mm for cumulative evaporation and change in soil water storage, respectively were observed when dgwl increased by 60% from the reference (Fig. 8.8). In summary, the sensitivity analysis results indicate that very shallow or very deep groundwater levels will have great impacts on evaporation and change in soil water storage.

8.4. Discussion

The variations between calibrated and measured saturated hydraulic conductivity can be partly explained by the existence of macro pores (Guber et al., 2010; Bodner et al., 2013) due to soil cracking, and also from the sampling and measurement errors (Ritter et al., 2003). The discrepancies between measured and modelled soil moisture content are probably indicative of soil heterogeneity, model uncertainty, and measurement errors, which are inevitable in field conditions and model setup (Gribb et al., 2009; Jing et al., 2014). Overall, the calibrated soil water model Hydrus-1D simulated the spatial soil moisture dynamics at the different hydrological zones in a reasonable manner. Therefore, the model can be used to predict spatial soil moisture dynamics as well as close soil moisture data gaps within sites of similar biophysical properties, and rainfall in

the floodplain. The results also demonstrate that Hydrus-1D is an effective tool for evaluating soil water dynamics and hence would be acceptable for performing scenario simulations. The findings of the current study corroborate with those of (Chen et al., 2014) who successfully applied a calibrated Hydrus-1D model with soil moisture measurements from one site to predict soil moisture conditions at another site, given that biophysical properties and rainfall were similar. The results of (Joris et al., 2003) further confirm the ability of Hydrus model in reproducing spatial soil moisture content dynamics in floodplains although the study applied the Hydrus-2D version.

Our observations and modeling results showed distinct spatial pattern of soil moisture time series along the defined hydrological zones. Soil moisture content increased from the surface layer (10 cm depth) to the bottom layer (40 cm depth). Furthermore, soil moisture content and change in soil water storage increased towards the riparian zone. Since all the hydrological zones have similar rainfall, land use and are situated a few kilometers apart from each other, the dynamics in soil moisture content and change in soil water storage can be explained by depth to groundwater level according to distance from the river, overbank flow, atmospheric influence and soil properties.

Factors such as flooding from river overbank flow, rainfall, and seasonally shallow depth to groundwater level replenish soil water storage and soil moisture content at the riparian and middle zones during the long rainy season. Conversely, the fringe zone doesn't experience flooding from river overbank flow due to the distance from the river. Rainfall and lateral flow from the mountains are the main sources of water causing flooding (Burghof et al., 2017) and replenishment of the soil water storage at the fringe zone. During the dry and short rainy seasons, soil moisture dynamics at the riparian and middle zones is mainly controlled by atmospheric influence, rainfall, soil properties and the influence of river water level on the depth to groundwater. Furthermore, the riparian and middle zones are directly connected to the river (Burghof et al., 2017). Therefore, a decrease or increase in river water level directly impacts on the depth to groundwater level in these zones. Similar results on the direct impact of river water level on the depth of groundwater level in floodplains have been observed by (Sophocleous, 2002; Karim et al., 2013). Soil moisture dynamics in the dry and short rainy seasons is independent of the influence from depth to groundwater level at the riparian and middle zone of the floodplain as indicated by both the modelled and measured time series. Similar results from (Leemhuis et al., 2017) indicated that decreasing low flows were directly linked to the surface water-groundwater interaction in the floodplain during the dry season, altering the depth to groundwater level dynamics and hence the soil water availability in the floodplain of Kilombero valley. The soil water storage after flood

recession at the riparian and middle zones provide conditions for cultivation of short-cycled upland crops like vegetables following the lowland rice, however, at the fringe zone, the soil water storage and the low depth to groundwater level throughout the year provides an opportunity for the cultivation of deep rooted upland crops.

Furthermore, the increasing clay and soil organic carbon content towards the riparian zone could partly explain the high soil water storage observed at this zone. Our results show high soil moisture content with increasing clay content in soils, which is in line with studies by (Markewitz et al., 2001) and (Chen et al., 2014). From the theoretical point of view, the observed increasing soil organic carbon and clay content towards the riparian zone would imply high residual and saturated water content (Amundson, 2001; Rawls et al., 2003). Subsequently, the riparian zone of the floodplain has a high agricultural production potential.

Atmospheric influence especially of the potential evapotranspiration on soil moisture dynamics is more pronounced at the fringe. The highest actual evapotranspiration at the fringe zone could partly explain the lowest soil moisture content observed at this zone. Actual evapotranspiration is always lower than the potential evapotranspiration at all the hydrological zones, thus indicating limited water availability (Verstraeten et al., 2008; Lu et al., 2017). The high sensitivity of actual evaporation and soil water storage to changes in depth to groundwater level was indicative of the influence of groundwater table. Comparing the different hydrological zones, the highest sensitivity of actual evaporation at the fringe zone could be partly explained by the relatively low depth to groundwater level observed during the study throughout the year, as a result of direct recharge and lateral flow from the surrounding mountains (Burghof et al., 2017). For this reason, to reduce on the loss of soil water through evaporation soil and water management strategies like mulching can be used for sustainable agricultural production at the local scale.

The temporal soil moisture variability at the fringe zone is mainly determined by the depth to the groundwater (more so during the dry and short rainy season, soil moisture was directly responsive to changes in depth to groundwater), soil properties, precipitation and atmospheric influence. Similar findings were observed by (Pirastru et al., 2013) who conducted a study in the alluvial floodplain of the Baratz Lake watershed, in the northwest of Sardinia, Italy. Their study showed that groundwater dynamics in the flood plain are an important source of temporal variability in soil moisture and vertical recharge processes in the alluvial floodplain. On the contrary, at the riparian and middle zone, soil moisture content is less responsive to depth to groundwater level, which continuously declines as soil moisture directly responds to rain event during the short rain season.

This finding is supported by the sensitivity analysis results which showed that variations in depth to groundwater level have a greater impact on soil water storage at the fringe than at middle and riparian zones of the floodplain. Therefore, agricultural practices that might cause the depth to groundwater level to decline further, have to be implemented with caution especially at the fringe zones, whose soil moisture dynamics, soil water storage and evapotranspiration are strongly controlled by groundwater level. Our sensitivity analysis results indicate that increase in depth to groundwater level below surface will decrease soil water storage and actual evapotranspiration at all the hydrological zones.

The observed high positive cumulative bottom flux at riparian and fringe zones compared to the middle zone, could be due to the contribution of groundwater flow from overbank flow towards the riparian zones and lateral flow from the mountains to the fringes. For detailed understanding of the interacting hydrological processes among the river, floodplain and its headwaters, the current Hydrus- 1D model has to be extended to a 2D model. This will explicitly account for the lateral flows and subsurface runoff, which are not accounted by the current model used in this study. Nonetheless, the model is adequate as the first attempt in the floodplain of Kilombero floodplain to achieve the study objectives.

8.5. Conclusion

Hydrus-1D model was calibrated and validated using daily field measurements of soil moisture content, over a period of one year in the floodplain of the Kilombero catchment, southern Tanzania. Simulated soil moisture content from the model fit quite well with the measured values at all the four soil depths for all the hydrological zones. Calibrated soil water model at one site can be used to predict spatial soil moisture content, and also close data gaps at other sites within the hydrological zone, with similar biophysical properties and rainfall.

Soil water storage increases towards the riparian zone. The highest evapotranspiration is observed at the fringe followed by riparian and middle zone. Riparian zone has the highest capillary rise and groundwater discharge followed by fringe and middle zone. Fringe zone maintains relatively low depth to groundwater level throughout the year due to the lateral flow contribution from mountains. Flooding from river overbank flow, local rainfall, and groundwater contribution replenish soil water storage during long rainy season at the riparian and middle zone. A combination of local rainfall and lateral flow from mountains are the main sources of water supply at the fringe, replenishing soil water storage during long rainy season. During the dry season, soil properties and

atmospheric influence control change in soil water storage and soil moisture dynamics at the riparian and middle zone whereas, in addition to these factors, depth to groundwater and lateral flow from mountains play an important role in controlling soil moisture dynamics at the fringe. In the short rainy seasons, local rainfall and soil properties control soil moisture dynamics at the riparian and middle zone. Local rainfall, soil properties, lateral flow from mountains and depth to groundwater level control soil moisture dynamics at the fringe.

Actual evaporation and change in soil water storage are highly sensitive to changes in depth to groundwater level at all the hydrological zones. Noteworthy, the sensitivity of actual evaporation and change in soil water storage is highest at the fringe zone.

The results are helpful for a better understanding of the groundwater - soil water interactions, and may provide references for wetland conservation and sustainable agricultural water management. The calibrated and validated model can be used for climate and land use scenario studies. This study has shown that local scale water fluxes and soil moisture availability is driven by catchment scale processes. Flooding of the riparian zone depends on catchment scale processes which are sensitive to land use and climate change (Leemhuis et al., 2017). Lateral fluxes and groundwater availability at the fringe will be influenced by land use and climate change. However, the one of the limitations of the study was to describe the lateral flow, henceforth, analyzing future water availability, the 1D modeling approach used in this study has to be linked to a 3D catchment scale model which is able to provide the lower boundary conditions required to run Hydrus-1D and also account for the lateral flows within the floodplain.

9. General conclusions and perspectives

Considering the current rate of wetland conversion and the diverse ecosystem services that wetlands fulfill in East Africa, there is a strong need to provide scientific guidelines for future food production and water resources management. Such planning and management of the wetland water resources requires detailed spatial and quantitative information on their hydrological processes under the ongoing land use/land cover (LULC) and climate change. Therefore, in this study a selected agriculturally used tropical inland valley in Uganda (Fig. 2.2) and a tropical floodplain in Tanzania (Fig. 2.5) were studied to assess the spatial and temporal dynamics of soil water availability and the impact of changing LULC and climate on the water resources. The general approach of this study combines field investigation and multi-scale hydrological modeling at the point and the wetland-catchment scale and the application of LULC and climate scenarios.

The methodological approach applied involved: (1) subdividing the toposequence of both wetland systems into three main hydrological positions: fringe, middle and the riparian positions. (2) These hydrological positions were equipped for field data collection. In addition, data mining from the different sources was inevitable**.** (3) The hydrological regimes in the inland valley were determined using measured soil moisture, groundwater and digital elevation data at a wetland scale. (4) While at a wetland –catchment scale, the impact of the different LULC on the inland valley water resources were evaluated using a hydrological response unit (HRU)-based (ArcSWAT2012) and a grid-based setup (SWATgrid) of the Soil Water Assessment Tool (SWAT model). The SWATgrid setup was applied to explicitly evaluate the spatial patterns of the hydrological processes with respect to the differing spatial discretization scheme from the ArcSWAT2012. (5) The hydrological response of the inland valley (at a wetland-catchment scale) to changing climate and LULC during the projected period by the year 2050 was examined. (6) The spatial soil water dynamics along a valley transect of the Kilombero floodplain wetland was investigated using a one-dimensional soil water dynamic model, Hydrus-1D at a point scale.

In addition to determining the hydrological regimes along the transects of the inland valley wetland from the collected field based data, the accuracy and reliability of the digital elevation data with different resolutions from (1) freely available digital elevation model (DEM) products (Shuttle Radar Topography Mission (SRTM) with 30 m resolution and the TanDEM-X mission with 12 m resolution), and (2) a field derived 5m DEM were assessed in determining the different soil

hydrological regimes. Furthermore, in the floodplain, the hydrological regimes were spatially delineated using TanDEM-X-12 m data together with the Landsat 7 Enhanced Thematic Mapper Plus (ETM+) and 8 Operational Land Imager (OLI) surface reflectance images.

For the hydrological modeling at the wetland-catchment scale using SWAT in the inland valley, spatial details on soil and land use relevant for the simulations in addition to climate data were required, yet not available at such a small scale. Therefore, the soil physical properties were determined and a soil map describing the predominant soil types was developed based on the FAO guidelines (FAO, 2006). A land use map was created from Sentinel-2 images of 2016 with a 10 m spatial resolution (Drusch et al., 2012). Based on the congregated data, the SWAT model was calibrated and validated for the inland valley. Four land use management options were developed with different conservation levels (*Conservation, Slope conservation, Protection of the headwater catchment, and Exploitation*) in addition to the current land use system to quantify the impact of land use on water resources in the inland valley. Furthermore, an ensemble of future climate projection was applied as climate change scenarios to assess their impacts on the water resources of the inland valley.

For the point scale, depth to shallow groundwater, soil moisture content, climate, and soil physical data measured along the hydrological zones facilitated the calibration and validation of Hydrus-1D model in the floodplain.

The attained results guided in answering the different research questions stated in the general introduction as follows:

(i) What are the different hydrological regimes and the spatial and temporal dynamics of soil water availability in the inland valley wetland and how accurate and reliable are the freely available digital elevation models with different resolutions in determining these hydrological regimes?

The spatial and temporal variability of soil moisture, hydrological regimes and the digital elevation models were analysed. Soil moisture content significantly increased towards the riparian zone although there was no difference in soil moisture between the riparian zone and the valley bottom. Contrasting hydrological regimes, saturated, near-, and non-saturated, exist across the hydrological positions due to temporal and spatial variability in soil moisture content and depth to groundwater. Therefore, the hypothesis that soil hydrological regimes correlate with three positions (fringe, middle and riparian zone) could not be supported for inland valley. Precipitation and soil depth strongly

control the temporal variability while mosaic-like topographic variability, soil properties, distance from the stream, anthropogenic activities and land use practices control the spatial variability in soil moisture content and depth to groundwater.

DEM resolution has a significant impact on mapping ground surface elevation and microscale topography thus the depth to groundwater which determines the different soil hydrological regimes in the inland valleys. Compared to SRTM-30 m, TanDEM-X-12 m provides a better estimate of ground surface elevation and microscale topography, which influence depth to groundwater and thus soil hydrological regimes in the valley. Therefore, since developing a local scale high-resolution DEM is rather time-consuming and expensive, the application of TanDEM-X-12 m data can be used as an option to predict soil hydrological regimes especially in data scarce regions like Sub-Saharan Africa. However, knowledge of land use data prior to the DEM analysis improves the accuracy of the output of TanDEM-X-12 m.

(ii) What is the impact of different land use management options on the water resources of an inland valley?

The impact of on-going land use and land use management practices on the water resources of an inland valley was successfully evaluated. An HRU-based interface (ArcSWAT2012) and a grid-based interface (SWATgrid) of the Soil and Water Assessment Tool (SWAT) model gave a realistic water balance after calibration and validation using daily discharge data at the outlet. SWATgrid simulated more surface runoff than the ArcSWAT2012. This is an important finding as both models have advantages and disadvantages. The HRU concept of ArcSWAT is computationally efficient but has no lateral exchange between the simulation units. Therefore, the spatial arrangement of the most important attributes soil, land use, topography is of minor importance which is acceptable for larger catchments but not at smaller scales. SWATgrid requires significant larger computing time but considers the spatial pattern in a landscape. In studies where this is of importance like in the catchment - wetland interaction study, this provides the possibility to evaluate management options which ArcSWAT does not offer. Both model setups indicated similar trends albeit differences in magnitude in the total discharge following the application of land use scenarios. A decrease in total discharge and annual water yield follows land use management options

in the order *Conservation* < *Slope conservation* < *Protection of headwater catchment* < *Exploitation*, moreover, an increase in the total discharge and annual water yield for exploitation land use option was observed.

(iii) **How does possible future climate change impact the water resources of the inland valley**?

The historical simulation of precipitation and temperature of an ensemble of six RCM-GCM data was compared to the ground observation for a period of 1976-2005. A bias correction of the rainfall and temperature was conducted due to a misrepresentation of the patterns by the climate models. Bias correction of the climate models improved the estimates of local precipitation and temperature in relation to the ground observations. The applied bias correction method did not alter the precipitation change signal except the magnitude compared to the historical data.

In future (2021-2050), a general increase in annual temperature change of 1.4°C and 1.6°C under RCP4.5 and 8.5 respectively is expected. Individual climate model simulations disagree on the likely direction and magnitude of the annual and monthly precipitation change, although on average, an increase in annual precipitation of +7.4% and 21.8% under RCP4.5 and 8.5 respectively is projected.

The bias corrected precipitation and temperature were used as SWAT model inputs to simulate the future water balance and total discharge of the inland valley. The climate model projections provide contrasting evidence with regard to future impacts on the total discharge and water balance by 2050. Since discharge and water balance in the inland valley is strongly controlled by precipitation, no clear trend in the future development of water resources can be concluded. However, more discharge is projected in the rainy season (MAM and SON) than in the dry season (JJA and DJF). This variability in the future discharge and water balance has to be taken into account when planning for climate change adaptation strategies for the inland valleys in the region.

A combined effect of climate and land use management change scenarios showed that climate change will have a dominant effect on the hydrological processes in the inland valley. However, adoption of functional landscape approach (FLA) described by Dixon et al. (2012) such as: C*onservation, Slope conservation and protection of the headwater*

catchment land use management approaches, will reduce the impacts of climate change on the water balance components (e.g. total water yield and surface runoff.) and increase evapotranspiration and lateral flow in the inland valley. Therefore, increasing water availability and improving other ecosystem functions in these inland valleys are undergoing changes from their pristine state in the East African region.

(iv) What are the spatial variabilities in soil water availability in a tropical floodplain and what factors influence them?

Hydrus-1D model was successfully calibrated and validated using daily field measurements of soil moisture content along the hydrological zones. It was shown that the calibrated soil water model at one site can be used to predict spatial soil moisture content, and also close data gaps at other sites within the hydrological zones with similar biophysical properties and rainfall. Soil water storage increased towards the riparian zone. The highest evapotranspiration is observed at the fringe followed by riparian and middle zone. Riparian zone has the highest capillary rise and groundwater discharge followed by fringe and middle zone. Fringe zone maintains relatively low depth to groundwater level throughout the year due to the lateral flow contribution from mountains. Soil water storage at the riparian and middle zone is controlled by flooding from river overbank flow, local rainfall, and groundwater contribution during long rainy season. While in the same season, a combination of local rainfall and lateral flow from mountains control soil water storage at the fringe zone. During the dry season, soil properties and atmospheric influence control the change in soil water storage dynamics at the riparian and middle zone whereas, in addition to these factors, depth to groundwater and lateral flow from mountains play influence soil water storage dynamics at the fringe. In the short rainy seasons, local rainfall and soil properties control soil moisture dynamics at the riparian and middle zone. Local rainfall, soil properties, lateral flow from mountains and depth to groundwater level control soil moisture dynamics at the fringe.

Hydrological comparison of the two wetland systems

This study has shown that for both wetland systems, the local water fluxes and soil moisture availability are driven to some extent by catchment processes. Soil water availability increases towards the riparian zone for both wetland systems.

The Namulonge inland valley has a mosaic of land use practices prevailing at small scale. Crop cultivation is continuous throughout the year which involves uncontrolled drainage, diversion of the stream water for irrigation and cultivation on raised ridges mostly upland crops. These practices alter the hydrological behaviour of the system, specifically soil moisture content and groundwater which influence the hydrological regimes along the hydrological positions. In contrast, the Kilombero floodplain has a clear pattern of land use and management. Therefore, defining catena-like transects across the inland valley may not be representative to describe the different soil hydrological regimes existing in the inland valley due to a bunch of factors together with the micro-topographic variability, unlike in the Kilombero floodplain where the hydrological regimes are clearly delineated based on the soil water availability influenced by flooding extent, duration, groundwater and topography.

On a spatial scale, the transferability of the calibrated Hydrus-1D model to predict soil moisture within the same hydrological position may not be possible in the inland valley due to the intra-variability of soil moisture, groundwater, microscale topography and soil properties within the hydrological position. However, for the floodplain, it was confirmed from the modeling exercise that it is possible to predict soil moisture of another site in the same hydrological zone with similar rainfall using the calibrated soil water model. The application of a grid-based version of SWAT (SWATgrid) in the floodplain wetland and its surrounding catchment may not be feasible due to its large size (40,000 km^2) and a relatively uniform land scape pattern. Also, the significant larger computing time may not allow calibration of this large catchment.

In conclusion, this work is of a significant contribution for supporting sustainable wetland – catchment agriculture and water resource management strategies to improve food security and at the same time environmental protection of fragile ecosystems of the region. It also reveals the relevance and the efficiency of multi-scale modeling strategy used for understanding the hydrological processes at wetland-catchment scale, plot scale and also bridging the data gaps. The study is also of substantial contribution to water management researchers and decision makers for predicting the future impacts of land use management options and climate change on the inland valleys water availability in the region. Furthermore, the work provides an insight on the sensitivity of the different water balance components on the changes in depth to groundwater in the Kilombero floodplain. This will improve water management planning more so with the expected agricultural

development from SAGCOT plan which will probably involve large scale irrigation scheme, thus, affecting depth to groundwater in the floodplain.

In order to regionalize the results of this study in East Africa, especially in the perspective of hydrological processes, one has to test and check if the features and processes in the two wetland systems are representative for the other floodplain and inland valley wetlands in the East African region. Otherwise, the respective results of the two study sites are only valid for the wetland systems in the region with similar characteristics. Thus, these results call for more experiments at the wetland-catchment scales with long time hydrological monitoring under the different environment to better understand their hydrological behaviours. The methodology applied in this study, combining field investigation, hydrological modelling and application of climate and land use change scenarios can be transferred to other wetland systems and their surrounding catchments in East Africa or other regions. Future efforts should focus on understanding the combined impact of climate and land use change on the water quality (sediments and nutrient fluxes; nitrogen and phosphorus) and the degradation rate of these agriculturally used inland valleys in the region. Also, to conduct an effective quantitative evaluation of spatially distributed hydrological processes in the inland valleys, more spatial input data would be an option to spatially calibrate the grid-based version of SWAT (SWATgrid). Regarding the assessment of soil water dynamics in in the Kilombero floodplain, the 1D modeling approach used in this study has to be linked to a 3D catchment scale model which is able to provide the lower boundary conditions required to run Hydrus-1D and also to account for the lateral flows within the floodplain. Last but not least, field suitability assessment study for the major crops cultivated in these wetland systems should be explored for sustainable food production.

References

Abbaspour, K. (2015). SWAT-CUP: SWAT Calibration and Uncertainty Programs - A User Manual. NeprashtechnologyCa. doi: 10.1007/s00402-009-1032-4.

Abbaspour, K.C., Rouholahnejad, E., Vaghefi, S., Srinivasan, R., Yang, H., and Kløve, B. (2015). A continental-scale hydrology and water quality model for Europe: Calibration and uncertainty of a high-resolution large-scale SWAT model. *J Hydrol.* 524 -733–752 . doi: 10.1016/j.jhydrol.2015.03.027.

Acreman, M. C., and Miller, F. (2007). Hydrological impact assessment of wetlands. *Int. Symp. Groundw. Sustain.* 225–255.

Adhikari, U., Nejadhashemi, A. P., and Woznicki, S. A. (2015). Climate change and eastern Africa: a review of the impact on major crops. *Food and Energy Security, 4,* 110–132.

Agarwal, C., Green, G.L., Grove, M., Evans, T.P., and Schweik, C.M. (2002). A Review and Assessment of Land-Use Change Models : Dynamics of Space , Time , and Human Choice Chetan Agarwal. *Apollo Int Mag Art Antiq. 1*, 812–855. doi: 10.1289/ehp.6514.

Akurut, M., Willems, P., and Niwagaba, C. (2014). Potential Impacts of Climate Change on Precipitation over Lake Victoria, East Africa, in the 21st Century. *Water*, *6*(9), 2634–2659. https://doi.org/10.3390/w6092634

Allen, R. G., Pereira, L. S., Raes, D., Smith, M., and Ab, W. (1998). Crop evapotranspiration - Guidelines for computing crop water requirements - FAO Irrigation and drainage paper 56, 1–15.

Amundson, R. (2001). The carbon budget in soils. *Annu. Rev. Earth Planet. Sci. 29*, 535–562.

Anaba, L.A., Banadda, N., Kiggundu, N., Wanyama, J., Engel, B., and Moriasi, D. (2017). Application of SWAT to Assess the Effects of Land Use Change in the Murchison Bay Catchment in Uganda. *Comput Water, Energy, Environ Eng.* 6, 24–40.doi: 10.4236/cweee.2017.61003.

Andriesse, W, and Fresco, L.O. (1991). A characterization of rice-growing environments in West Africa. *Agric Ecosyst Environ. 33*,377–395 . doi: 10.1016/0167-8809(91)90059-7.

Arnold, J.G., Allen, P.M., Volk, M., Williams, J.R., and Bosch, D.D. (2010). Assessment of different representations of spatial variability on SWAT model performance. *Trans ASABE 53*,1433–1443 . doi: doi: 10.13031/2013.34913.

Arnold, J.G., Kiniry, J.R., Srinivasan, R., Williams, J.R, Haney, E.B., and Neitsch, S.L. (2013). Soil and Water Assessment Tool: Input/output documentation. version 2012. Texas Water Resour Institute, TR-439 650.

Arnold, J.G., Moriasi, D.N., Gassman, P.W., Abbaspour, K.C., White, M.J., Srinivasan, R., Santhi, C., Harmel, R.D, van Griensven, A., Van Liew, M.W., Kannan, N., and Jha, M.K. (2012). Swat: Model Use, Calibration, and Validation. *Asabe 55*,1491–1508.

Arnold, J.G., Srinivasan, R., Muttiah, R.S., and Williams, J.R. (1998). Large area hydrologic modeling and assesment Part I: Model development. *J Am Water Resour Assoc 34*, 73–89. doi: 10.1111/j.1752-1688.1998.tb05961.x.

Beck, A. D. (1964). The Kilombero valley of south-central Tanganyika. *East Afr. Geogr. Rev. 1964*, 37–43.

Beldring, S., Gottschalk, L., Seibert, J., and Tallaksen, L. M. (1999). Distribution of soil moisture and groundwater levels at patch and catchment scales. Agricultural and Forest Meteorology, 99, 305-324.

Beuel, S., Alvarez, M., Amler, E., Behn, K., Kreye, C., Kotze, D., Leemhuis, C., Wagner, K., Willy, D.K., Ziegler, S., and Becker, M. (2016). A rapid assessment of anthropogenic disturbances in East African wetlands. *Ecological Indicators* 67, 684-692.

Beven, K.J. (2012). Rainfall-runoff modelling: The primer, Second Ed. John and Wiley sons, Keith Beven Lancaster University, UK.

Bidlake, W.R. (2000). Evapotranspiration from a bulrush dominated wetland in the Klamath Basin, Oregon: *Journal of the American Water Resources Association, 36,* 1309–1320.

Black, E., Slingo, J. M., and Sperber, K. R.(2003). An observational study of the relationship between excessively strong short rains in coastal East Africa and Indian Ocean SST. *Mon. Weather Rev.*74–94, doi:10.1175/1520-0493(2003)131<0074:AOSOTR>2.0.CO;2.

Blume, T., Zehe, E., and Bronstert, A. (2009). Use of soil moisture dynamics and patterns at different spatio-temporal scales for the investigation of subsurface flow processes. *Hydrol. Earth Syst. Sci.13,* 1215–1233, doi:10.5194/hess-13-1215-2009.

Bodner, G., Scholl, P., Loiskandl, W., and Kaul, H. (2013). Geoderma Environmental and management influences on temporal variability of near saturated soil hydraulic properties. *Geoderma, 204–205,* 120–129, doi:10.1016/j.geoderma.2013.04.015.

Böhme, B., Becker, M., and Diekkrüger, B. (2013). Calibrating FDR sensor for soil moisture monitoring in a wetland in Central Kenya. *Physics and Chemistry of the Earth, 66,* 101–111.

Böhme, B., Becker, M., Diekkrüger, B., and Förch, G. (2016). How is water availability related to the land use and morphology of an inland valley wetland in Kenya? *Physics and Chemistry of the Earth, 93,* 84–95.

Bonarius, H. (1975). *Physical properties of soils in the Kilombero valley (Tanzania);*German Agency for Technical Cooperation, Ltd. (GTZ):D-6236 Eschborn 1, Stuttgarter Str.10,W. Germany,https://library.wur.nl/isric/fulltext/isricu_i2757_001.pdf.

Bruyère, C. L., Done, J. M., Holland, G. J., and Fredrick, S. (2013). Bias corrections of global models for regional climate simulations of high-impact weather. *Climate Dynamics*, *43*(7–8), 1847–1856. https://doi.org/10.1007/s00382-013-2011-6

Burghof, S. (2017). Hydrogeology and water quality of wetlands in East Africa: case studies of a floodplain and a valley bottom wetland. PhD thesis. University of Bonn.

Burghof, S., Gabiri, G., Stumpp, C., Chesnaux, R., and Reichert, B. (2017). Development of a hydrogeological conceptual wetland model in the data-scarce north-eastern region of Kilombero. doi:10.1007/s10040-017-1649-2.

Burt, T.P., Slattery, M.C., Burt, T.P., and Slattery, M.C. (2005). Land Use and Land Cover Effects on Runoff Processes: Agricultural Effects. *Encycl Hydrol Sci,* 1–8. doi: 10.1002/0470848944.hsa123.

Carvalho-Santos, C., Monteiro, A. T., Azevedo, J. C., Honrado, J. P., and Nunes, J. P. (2017). Climate Change Impacts on Water Resources and Reservoir Management: Uncertainty and Adaptation for a Mountain Catchment in Northeast Portugal. *Water Resources Management*, *31*(11), 3355–3370. https://doi.org/10.1007/s11269-017-1672-z

Camberlin, P., and Philippon, N. (2002). The East African March–May Rainy Season: Associated Atmospheric Dynamics and Predictability over the 1968–97 Period. *J. Clim. 15,* 1002–1019.

Chang, H. C., Ge, L. and Rizos, C. (2004). Assessment of digital elevation models using RTK GPS. *Journal of Geospatial Engineering, 6,* 13.

Chen, M.,Willgoose, G. R., and Saco, P. M. (2014). Spatial prediction of temporal soil moisture dynamics using HYDRUS-1D. *Hydrol. Process.28,* 171–185, doi:10.1002/hyp.9518.

Chuma, E., Masiyandima, M., and Finlayson, M. (2012). Guideline for sustainable wetland management and utilization: key cornerstones, 1–55.

https://doi.org/https://cgspace.cgiar.org/bitstream/handle/10568/21605/21605.pdf?sequence=1

Collins, M., Knutti, R., Arblaster, J., Dufresne, J. L., Fichefet, T., Friedlingstein, P., and Wehner, M. (2013). Long-term Climate Change: Projections, Commitments and Irreversibility. Climate Change 2013: The Physical Science Basis. Contribution of Working Group I to the Fifth Assessment Report of the Intergovernmental Panel on Climate Change, 1029–1136. https://doi.org/10.1017/CBO9781107415324.024.

Danner, M., Locherer, M., Hank, T., and Richter, K. (2015). Measuring Leaf Area Index (LAI) with the LI-Cor LAI 2200C or LAI-2200 (+2200Clear Kit) – Theory, Measurement, Problems, Interpretation. EnMAP Field Guide Technical Report, GFZ Data Services, http://doi.org/10.2312/enmap.2015.009.

Daniel, S., Gabiri, G., Kirimi, F., Glasner, B., Näschen, K., Leemhuis, C., Steinbach, S., and Mtei, K. (2017). Spatial distribution of soil hydrological properties in the Kilombero floodplain, Tanzania. *Hydrology 4*, 57, doi:10.3390/hydrology4040057.

Danvi, A., Giertz, S., Zwart, S.J., and Diekkrüger, B. (2018). Rice Intensification in a Changing Environment : Impact on Water Availability in Inland Valley Landscapes in Benin. Water 10,74. doi: 10.3390/w10010074.

Danvi, A., Giertz, S., Zwart, S.J., and Diekkrüger, B. (2017). Comparing water quantity and quality in three inland valley watersheds with different levels of agricultural development in central Benin. *Agric Water Manag 192*, 257–270 . doi: 10.1016/j.agwat.2017.07.017.

Decagon Devices Inc. (2016). 5TE Manuals, http://manuals.decagon.com/Manuals/13509_5TE_Web.pdf (accessed 15.04.2016).

Decagon Devices Inc. (2016). Em50 series data collection system operator's manual, http://manuals.decagon.com/Manuals/13453_Em50_Web.pdf (accessed 15.04.2016).

Deckers, J., Spaargaren, O., and Dondeyne, S. (2002). Soil survey as a basis for land evaluation. Encycl Life Support Syst II.

Delta-T Devices Ltd. *User Manual for the Profile Probe type PR2*; 2006; Vol. 104; https://www.delta-t.co.uk/product/pr2/.

Delta-T Devices Ltd. (2005). Profile Probe augering manual for PR2, https://www.delta-t.co.uk/wp-content/uploads/2016/09/AUG-Augering-User-Manual-v2.0.pdf (accessed 03.03.2014).

Delta-T Devices Ltd.(2013).User manual for the moisture meter type HH2.124, doi:10.1016/B978-0-08-051644-8.50054-X.

Dixon, A., Thawe, T., and Sampa, J. (2012). Striking a balance. Maintaining seasonal wetlands & their livelihood contributions in central Southern Africa Wetland. http://www.wetlandaction.org/wp-content/uploads/Wood-2009-Striking-a-Balance-Final-Report.pdf (accessed 13.01.2018).

Dixon, A. B. (2002). The hydrological impacts and sustainability of wetland drainage cultivation in Illubabor, Ethiopia. *Land Degradation and Development*, *13*, 17–31.

Dixon, A.B., and Wood, A. P. (2003). Wetland cultivation and hydrological management in eastern Africa: Matching community and hydrological needs through sustainable wetland use. *Natural Resources Forum, 27*, 117–129. https://doi.org/10.1111/1477-8947.00047

Dossou-Yovo, E.R., Baggie, I., Djagba, J.F., and Zwart, S.J. (2017). Diversity of inland valleys and opportunities for agricultural development in Sierra Leone. *PLoS One 12*, 1–19 . doi: 10.1371/journal.pone.0180059.

Drusch, M., Del Bello, U., Carlier, S., Colin, O., Fernandez, V., Gascon, F., Hoersch, B., Isola, C., Laberinti, P., Martimort, P., Meygret, A., Spoto, F., Sy, O., Marchese, F.,and Bargellini, P.

(2012). Sentinel-2: ESA's Optical High-Resolution Mission for GMES Operational Services. *Remote Sens Environ. 120*-25–36 . doi: 10.1016/j.rse.2011.11.026.

Duku, C., Rathjens, H., Zwart, S.J., and Hein, L. (2015). Towards ecosystem accounting: A comprehensive approach to modelling multiple hydrological ecosystem services. *Hydrol Earth Syst Sci.19* - 4377–4396 . doi: 10.5194/hess-19-4377-2015.

Eijkelkamp Laboratory permeameters.(2013).User manual, soil and water, 1–14. https://en.eijkelkamp.com/products/laboratory-equipment/soil-water-permeameters.html

Erasmi, S., Rosenbauer, R., Buchbach, R., Busche, T., and Rutishauser, S. (2014). Evaluating the Quality and Accuracy of TanDEM-X Digital Elevation Models at Archaeological Sites in the Cilician Plain, Turkey. *Remote Sensing, 6,* 9475–9493.

Farr, T. G., Rosen, P. A., Caro, E., Crippen, R., Duren, R., Hensley, S., and Alsdorf, D. (2007). The Shuttle Radar Topography Mission. *Review of Geophysics,* 45, RG2004.

FAO (Food and Agriculture Organization of the United Nations). (2006). Guidelines for Soil Description. FAO, Rome, Italy. http://www.fao.org/docrep/019/a0541e/a0541e.pdf (accessed 20.02.2016).

FAO (Food and Agriculture Organization of the United Nations).(1960).The Rufiji Basin Tanganyika. FAO Report to the Government of Tanganyika on the preliminary reconnaissance survey of the Rufiji Basin, Volume 2 Hydrology and Water Resources, Part 1 Computation and Analyses, Rome, 1960, 405 p.

Feddes, R. A., Kowalik, P. J., and Zaradny, H. (1978). Simulation of Field Water Use and Crop Yield, John Wiley and Sons, New York, NY.

Fenton, J.D., and Keller, R.J. (2001). The Calculation of Streamflow from Measurements of Stage. Cooperative research centre for catchment hydrology. http://johndfenton.com/Papers/Calculation-of-streamflow-from-measurements-of-stage.pdf (accessed 20.02.2018).

Futoshi, K. (2007). Development of a major rice cultivation area in the Kilombero valley, Tanzania. *African Study Monogr. Suppl.36,* 3–18.

Gabiri,G., Leemhuis,C., Diekkrüger,B., Näschen,K., Steinbach,S., and Thonfeld, F. (2019). Modeling the impact of land use management on water resources in a tropical inland valley catchment of central Uganda, East Africa. *Science of the Total Environment 653,* 1052-1066; https://doi.org/10.1016/j.scitotenv.2018.10.430.

Gabiri, G., Diekkrüger, B., Leemhuis, C., Burghof, S., Näschen, K., Asiimwe, I.,and Bamutaze, Y. (2018). Determining hydrological regimes in an agriculturally used tropical inland valley wetland in central Uganda using soil moisture, groundwater, and digital elevation data. *Hydrol. Process 32,* 349–362 . doi: 10.1002/hyp.11417.

Gabiri, G., Burghof, S., Diekkrüger, B., Leemhuis, C., Steinbach, S., and Näschen, K. (2018). Modeling spatial soil water dynamics in a tropical floodplain, East Africa, *Water 10,*191; doi:10.3390/w10020191.

Garbrecht, J., Martz, L., and Bingner, R. (2000). Topaz User Manual: Version 3.1, Technical ReportGrazinglands Research Laboratory, USDA. Agricultural Research Service, ElReno, Oklahoma.

Giertz, S., Diekkrüger, B., and Steup, G.(2006). Physically-based modelling of hydrological processes in a tropical headwater catchment (West Africa) – process representation and multi-criteria validation. *Hydrol. Earth Syst. Sci. 10,* 829–847.

Giertz, S., Steup, G., and Schönbrodt, S. (2012). Use and constraints on the use of inland valley ecosystems in central Benin: results from an inland valley survey. *Erdkunde 66,* 239-253.

Githui, F., Mutua, F., and Bauwens, W. (2009). Estimating the impacts of land-cover change on

runoff using the soil and water assessment tool (SWAT): Case study of Nzoia catchment, Kenya. *Hydrol Sci J 54*, 899–908 . doi: 10.1623/hysj.54.5.899.

Githui, F., Gitau, W., Mutua, F., and Bauwensa, W. (2009). Climate change impact on SWAT simulated stream flow in western Kenya. Int. J. Climatol. 29, 1823–1834, DOI: 10.1002/joc.1828

Gobin, A., Campling, P., Deckers, J., and Feyen, J. (2000). Integrated toposequence analysis to combine local and scientific knowledge systems. *Geoderma 97*,103–123.

Goddard, L., and Graham, N. E.(1999). Importance of the Indian Ocean for simulating rainfall anomalies over eastern and southern Africa. *J. Geophys. Res.104*, 19099, doi:10.1029/1999JD900326.

Gómez-Plaza, A., Alvarez-Rogel, J., Albaladejo, J., and Castillo, V. M. (2000). Spatial patterns and temporal stability of soil moisture across a range of scales in a semi-arid environment. *Hydrological Processes, 14*, 1261–1277.

Gomi, T., Sidle, R.C., Miyata, S., Kosugi, K., and Onda, Y. (2008). Dynamic runoff connectivity of overland flow on steep forested hillslopes: Scale effects and runoff transfer. *Water Resour Res 44*,1–16 . doi: 10.1029/2007WR005894.

Gowing, J. W. (2003). Food security for sub-Saharan Africa: does water scarcity limit the options? *Land Use and Water Resources Research, 3*(2003), 2.1-2.7.

Graham, D.N., and Butts, M. B. (2005). Flexible, integrated watershed modelling with MIKE SHE. In Watershed Models, Eds. V.P. Singh and D.K. Frevert Pages 245-272, CRC Press. ISBN: 0849336090.

Gribb, M. M., Forkutsa, I., Hansen, A., David, G., and Chandler, J. P. M. (2009). The Effect of Various Soil Hydraulic Property Estimates on Soil Moisture Simulations. *Vadose Zo. J. 8*, 321–331, doi:10.2136/vzj2008.0088.

GTK Consortium. (2012). Geological Map of Uganda 1:100,000, Sheet 61, Bombo.

Guber, A., Tuller, M., San, F., Martinez, J., Iassonov, P., and Martin, M. A.(2010). The Through Porosity of Soils as the Control of Hydraulic Conductivity. In *19th World Congress of Soil Science, Soil Solutions for a Changing World*; Brisbane, Australia, pp. 80–83.

Gudmundsson, L., Bremnes, J. B., Haugen, J. E., and Engen-Skaugen, T. (2012). Technical Note: Downscaling RCM precipitation to the station scale using statistical transformations and ndash; A comparison of methods. *Hydrology and Earth System Sciences*, *16*(9), 3383–3390. https://doi.org/10.5194/hess-16-3383-2012

Gupta, H.V., Kling, H., Yilmaz, K.K., and Martinez, G.F. (2009). Decomposition of the mean squared error and NSE performance criteria: Implications for improving hydrological modelling. *J. Hydrol. 377*, 80–91. https://doi.org/10.1016/j.jhydrol.2009.08.003.

Gupta, H.V., Sorooshian, S., and Yapo, P.O. (1999). Status of automatic calibration for hydrologic models: Comparison with multilevel expert calibration. *J. Hydrol. Eng. 4*, 135–143. https://doi.org/10.1061/(ASCE)1084-0699(1999)4.

Gutowski, J.W., Giorgi, F., Timbal, B., Frigon, A., Jacob, D., Kang, H., Raghavan, K., Lee, B., Lennard, C., Nikulin, G., O'Rourk, E., Rixen, M., Solman, S., Stephenson, T., and Tangang, F. (2016). WCRP COordinated Regional Downscaling EXperiment (CORDEX): A diagnostic MIP for CMIP6. *Geosci Model Dev. 9*,4087–4095 . doi: 10.5194/gmd-9-4087-2016.

Guzha, A.C., Rufino, M.C., Okoth, S., Jacobs, S., and Nóbrega, R.L.B .(2018). Impacts of land use and land cover change on surface runoff, discharge and low flows: Evidence from East Africa. *J Hydrol Reg Stud 15*, 49–67 . doi: 10.1016/j.ejrh.2017.11.005.

Harper, D.M., Mavuti, K.M. (1996). Freshwater wetlands and marshes. In: McClanahan T, Young T (eds) East African ecosystems and their conservation. Oxford University Press, New York

Hartmann, D.L., A. M.G., Klein Tank, M., Rusticucci, L.V., Alexander, S., Bronnimann, Y., and Charabi, et al. (2013).Observations: atmosphere and surface. Pp. 159–254 in Stocker, T. F., Qin, D., Plattner, G.K., Tignor, M., Allen, S. K., Boschung et al., eds. Climate change 2013: the physical science basis. Contribution of Working Group I to the fifth assessment report of the Intergovernmental Panel on Climate Change. Cambridge Univ. Press, Cambridge, United Kingdom and New York, NY, USA.

Hastenrath, S., Nicklis, A., and Greischar, L.(1993). Atmospheric-hydrospheric mechanisms of climate anomalies in the western equatorial Indian Ocean. *J. Geophys. Res.98*, 20219, doi:10.1029/93JC02330.

Hawinkel, P., Thiery, W., Lhermitte, S., Swinnen, E., Verbist, B.,Van Orshoven, J., and Muys, B.(2016).Vegetation response to precipitation variability in East Africa controlled by biogeographical factors. J. Geophys. Res. 121, 2422–44.

Hazelton, P., and Murphy, B. (2007). Interpreting soil test results: What do all the numbers mean? (2nd ed), CSIRO publishing, 150 Oxford street, Australia.

Hepworth, N., and Goulden, M. (2008). Climate Change in Uganda: Understanding the implications and appraising the response. *LTS International, Edinburgh*. https://doi.org/10.1680/ener.2008.161.2.87

Horiba Scientific. (2010). *a Guidebook To Particle Size Analysis*; Horiba instruments, INC.9755 Research Drive Irvine: Irvine, CA 92618 USA, www.horiba.com/us/particle.

Horwitz, P., and Finlayson, C. M. (2011). Wetlands as Settings for Human Health: Incorporating Ecosystem Services and Health Impact Assessment into Water Resource Management. *BioScience, 61*, 678–688.

Hughes, S. J., Cabecinha, E., Andrade dos Santos, J. C., Mendes Andrade, C. M., Mendes Lopes, D. M., da Fonseca Trindade, H. M., and Vitor Cortes, R. M. (2012). A predictive modelling tool for assessing climate, land use and hydrological change on reservoir physicochemical and biological properties. *Area*, *44*(4), 432–442. https://doi.org/10.1111/j.1475-4762.2012.01114.x

IPCC. (2014). Climate Change 2014: Synthesis Report. Contribution of Working Groups I, II and III to the Fifth Assessment Report of the Intergovernmental Panel on Climate Change. [Core Writing Team, R.K. Pachauri and L.A. Meyer (eds)]. IPCC, Geneva, Switzerland. https://doi.org/10.1017/CBO9781107415324.004

Jätzold, R. and Baum, E. (1968): The Kilombero Valley. Weltforum-Verlag GmbH, München, 147 p.

Jing, L., Zhang, Z., and Ni, L. (2014). Evaluation of water movement and water losses in a direct-seeded-rice field experiment using Hydrus-1D. *Agric. Water Manag.142*, 38–46, doi:10.1016/j.agwat.2014.04.021.

Jones, A., Breuning-Madsen, H., Brossard, M., Dampha, A., Deckers, J., Dewitte, O., Gallali, T., Hallet, S., Jones, R., Kilasara, M., Le Roux, P., Micheli, E., Montanarealla, L., Spaargaren, O., Thiombiano, L., Van Ranst, E., Yemefack, M. and Zougmore, R. (eds.) (2013): Soil Atlas of Africa. European Comission, Publications Office of the European Union, Luxembourg, 176 p.

Joris, I., and Feyen, J.(2003). Modelling water flow and seasonal soil moisture dynamics in analluvial groundwater-fed wetland. *Hydrol.Earth Syst. Sci. 7*, 57–66, doi:10.5194/hess-7-57-2003.

Junk, W. J., and An, S. (2013). Current state of knowledge regarding the world's wetlands and their future under global climate change : a synthesis. *Aquat Science, 61,* 151–167.

Kaggwa, R., Hogan, R.,and Hall, B. (2009). Enhancing Wetlands 'contribution to growth, employment and prosperity, pp.1–73, Kampala: UNDP/NEMA/UNEP Poverty Environment Initiative, Uganda. https://www.unpei.org/sites/default/files/e_library_documents/uganda-enhancing-wetlands-contribution-prosperity-final.pdf (accessed 21.05.2015)

Kakuru, W., Turyahabwe, N., and Mugisha, J. (2013). Total economic value of wetlands products and services in Uganda. *Science World Journal*. doi:10.1155/2013/192656.

Kamiri, H. W., Handa, C., Mwita, E., Sakané, N., Becker, M., Oyieke, O., and Misana, S. (2014). Agriculturally used Wetlands in Kenya and Tanzania: Characterisation based on Soil and Water Resources Availability. Global journal of Science Frontier Journal (H), 14, 61.

Kamiri, H., Kreye, C., and Becker, M. (2013). Dynamics of agricultural use differentially affect soil properties and crop response in East African wetlands. *Wetlands Ecology & Management, 21*, 417–431.

Kandelous, M.M., Kamai, T., Vrugt, J.A., Šimunek, J., Hansona, B., and Hopmans, J.W. (2012). Evaluation of subsurface drip irrigation design and management parameters for alfalfa. *Agric. Water Manag.109*, 81–93. doi:10.1016/j.agwat.2012.02.009.

Kangalawe, R.Y. M., and Liwenga, E.T. (2005). Livelihoods in the wetlands of Kilombero valley in Tanzania: Opportunities and challenges to integrated water resource management. *Physics and Chemistry of the Earth, 30,* 968–975.

Karim, F., Kinsey-Henderson, A., Wallace, J., Godfrey, P., Arthington, A. H., and Pearson, R.G. (2013). Modelling hydrological connectivity of tropical floodplain wetlands via a combined natural and artificial stream network. *Hydrol. Process.* DOI: 10.1002/hyp.10065

Kashaigili, J. J., Mccartney, M., and Mahoo, H. F. (2007). Estimation of environmental flows in the Great Ruaha River Catchment, Tanzania. *Physics and Chemistry of the Earth*, *32*(15–18), 1007–1014. https://doi.org/10.1016/j.pce.2007.07.005

Kigobe, M., and Griensven, A. van. (2010). Assessing hydrological response to change in climate : Statistical downscaling and hydrological modelling within the upper Nile. *IEMSs 2010 International Congress on Environmental Modelling and Software. Modelling for Environment's Sake*, (Figure 1), 2096–2105.

Kim, J., Waliser, D. E., Mattmann, C. A., Goodale, C. E., Hart, A. F., Zimdars, P. A., and Favre, A. (2014). Evaluation of the CORDEX-Africa multi-RCM hindcast: Systematic model errors. *Climate Dynamics*, *42*(5–6), 1189–1202. https://doi.org/10.1007/s00382-013-1751-7

Kimwaga, R.J., Bukirwa, F., Banadda, N., Wali, U.G., Nhapi, I., and Mashauri, A. (2012). Modelling the Impact of Land Use Changes on Sediment Loading Into Lake Victoria Using SWAT Model: A Case of Simiyu Catchment Tanzania. *Open Environ Eng Journal 5*, 66–76.

Kling, H., Fuchs, M., and Paulin, M. (2012). Runoff conditions in the upper Danube basin under an ensemble of climate change scenarios. *J Hydrol 424–425*, 264–277 . doi: 10.1016/j.jhydrol.2012.01.011.

Koutsouris, A. J., Chen, D., and Lyon, S. W. (2016). Comparing global precipitation data sets in eastern Africa: A case study of Kilombero Valley, Tanzania. *Int. J. Climatol.36*, 2000–2014, doi:10.1002/joc.4476.

Kyarisiima, C. C., Nalukenge, I., Kariuki, W., and Mesaki, S. (2008). Factors affecting sustainability of wetland agriculture within. *Journal of Agriculture and Social Research, 8,* 78–88.

Lacombe, G., Pavelic, P., Mccartney, M., Phommavong, K., and Viossanges, M. (2017). Climate Change Adaptation in Wetlands Areas (CAWA) Hydrological assessment of the Xe

Champone and Beung Kiat Ngong wetlands Final Report. FAO and IWMI report, (September).

Lambin, E.F., Rounsevell, M.D.A., and Geist, H.J. (2000). Are agricultural land-use models able to predict changes in land-use intensity? *Agric Ecosyst Environ 82*, 321–331 . doi: 10.1016/S0167-8809(00)00235-8.

Leemhuis, C.,Thonfeld, F., Näschen, K., Steinbach, S., Muro, J., Strauch, A., Ander, L., Daconto, G., and Games, I. (2017). Sustainability in the Food-Water-Ecosystem Nexus : The Role of Land Use and Land Cover Change for Water Resources and Ecosystems in the Kilombero Wetland , Tanzania. *Sustainability 9*, 1513, doi:10.3390/su9091513.

Leemhuis, C., Amler, E., Diekkrüger, B., Gabiri, G., and Näschen, K. (2016). East African wetland-catchment data base for sustainable wetland management. *Proceedings of the International Association of Hydrological Sciences*, *374*, 123–128.

Leemhuis, C., Erasmi, S., Twele, A., Kreilein, H., Oltchev, A., and Gerold. G. (2007). Rainforest conversion in central Sulawesi, Indonesia: Recent development and consequences for river discharge and water resources. *Erdkd Band 61*, 284–293.

Li, H., Yi, J., Zhang, J., Zhao,Y., Si, B., Hill, R. L., Cui, L., and Liu, X. (2015). Modeling of soil water and salt dynamics and its effects on root water uptake in Heihe arid wetland, gansu, China. *Water (Switzerland) 7*, 2382–2401, doi:10.3390/w7052382.

Li, Z., Deng, X., Wu, F., and Hasan, S.S. (2015). Scenario analysis for water resources in response to land use change in the middle and upper reaches of the heihe river Basin. *Sustain. 7*,3086–3108. doi: 10.3390/su7033086.

Li, Z., and Jin, J. (2017). Evaluating climate change impacts on streamflow variability based on a multisite multivariate GCM downscaling method in the Jing River of China. *Hydrology and Earth System Sciences*, *21*(11), 5531–5546. https://doi.org/10.5194/hess-21-5531-2017

Liu, J., Zhang, C., Kou, L., and Zhou, Q. (2017). Effects of Climate and Land Use Changes on Water Resources in the Taoer River. *J Environ Manage 2017*,1–14 . doi: 10.1016/j.jenvman.2005.08.008.

Loch, R.J. (2000). Effects of vegetation cover on runoff and erosion under simulated rain and overland flow on a rehabilitated site on the Meandu Mine, Tarong, Queensland. *Aust J Soil Res 38*, 299–312 . doi: 10.1071/SR99030.

Lu, N., Chen, S.,Wilske, B., Sun, G., and Chen, J. (2017). Evapotranspiration and soil water relationships in a range of disturbed and undisturbed ecosystems in thethe semi-arid Inner Mongolia, China. *J. Plant Ecol. 4*, 49–60, doi:10.1093/jpe/rtq035.

Maitima, J.M., Mugatha, S.M., Reid, R.S., Gachimbi, L.N., Majule, A., Lyaruu, H., and Mugisha, S. (2009). The linkages between land use change, land degradation and biodiversity across East Africa. *African Journal of Environmental Science and Technology*, *3*, 310–325.

Mango, L.M., Melesse, A.M., McClain, M.E., Gann, D., and Setegn, S.G. (2011). Land use and climate change impacts on the hydrology of the upper Mara River Basin, Kenya: Results of a modeling study to support better resource management. *Hydrol Earth Syst Sci 15*, 2245–2258 . doi: 10.5194/hess-15-2245-2011.

Maraun, D. (2016). Bias Correcting Climate Change Simulations - a Critical Review. *Current Climate Change Reports*, *2*(4), 211–220. https://doi.org/10.1007/s40641-016-0050-x

Markewitz, D., Devine, S., Davidson, E. A., Brando, P., and Nepstad, D.C. (2010). Soil moisture depletion under simulated drought in the Amazon : impacts on deep root uptake. *New Phytol.187*, 592–607.

McCartney, M., Rebelo, L.M., Senaratna Sellamuttu, S., and De Silva, S. (2010). *Wetlands, agriculture and poverty reduction*; IWMI Research Report,Vol. 137; ISBN 9290907347.

McCartney, M., Morardet, S., Rebelo, L.-M., Finlayson, C. M., and Masiyandima, M. (2011). A study of wetland hydrology and ecosystem service provision: GaMampa wetland, South Africa. *Hydrological Sciences Journal*, *56*(8), 1452–1466. https://doi.org/10.1080/02626667.2011.630319

Memarian, H., Balasundram, S.K., and Abbaspour, K.C., et al .(2014). SWAT-based hydrological modelling of tropical land-use scenarios. *Hydrol Sci J 59*,1808–1829 . doi: 10.1080/02626667.2014.892598.

Mileham, L., Taylor, R. G., Todd, M., Tindimugaya, C., and Thompson, J. (2009). The impact of climate change on groundwater recharge and runoff in a humid, equatorial catchment: Sensitivity of projections to rainfall intensity. *Hydrological Sciences Journal*, *54*(4), 727–738. https://doi.org/10.1623/hysj.54.4.727

Millennium Ecosystem Assessment (MEA). (2005). Ecosystems and human well-being: wetlands and water Synthesis. https://www.millenniumassessment.org/documents/document.358.aspx.pdf (accessed 10.05.2015).

Ministry of Water and Environment, Uganda. (2010). Operationalisation of Catchment-based Water Resources Management. Draft final report, https://www.google.com/url?sa=t&rct=j&q=&esrc=s&source=web&cd=1&ved=0ahUKEwiZ4KKtxcXNAhUEuRQKHbocBv4QFggeMAA&url=http://www.mwe.go.ug/index.php?option=com_docman&task=doc_download&gid=162&Itemid=41&usg=AFQjCNFrOK_cbw2gWLNZcFTcGm7OO (accessed 02.10.2015).

Ministry of Water URT. (2012). Rufiji IWRMD Plan Interim Report, Volume III, Current Water Use and Infrastructure Assessment. WREM International Inc., Atlanta, Georgia, USA, 227 p.

Mitsch,W., and Gosselink, J. G. (2015). *Wetlands of the World*; ISBN 978-1-119-01979-4.

Mohanty, B. P., Cosh, M. H., Lakshmi,V., Montzka, C. (2017).Soil Moisture Remote Sensing: State-of-the-Science. *Vadose Zo. J. 16*, 0, doi:10.2136/vzj2016.10.0105.

Mombo, F., Speelman, S., Huylenbroeck, G., Van Hella, J., and Moe, S.(2011). Ratification of the Ramsar convention and sustainable wetlands management : Situation analysis of the Kilombero Valley wetlands in Tanzania, *3*, 153–164.

Moriasi, D.N., Arnold, J.G., Van Liew, M.W., Bingner, R.L., Harmel, R.D., and Veith, T.L. (2007). Model evaluation guidelines for systematic quantification of accuracy in watershed simulations. *Trans ASABE 50*, 885–900 . doi: 10.13031/2013.23153.

Moss, R. H., Edmonds, J. A., Hibbard, K. A., Manning, M. R., Rose, S. K., Van Vuuren, D. P., and Wilbanks, T. J. (2010). The next generation of scenarios for climate change research and assessment. *Nature*, *463*(7282), 747–756. https://doi.org/10.1038/nature08823

Motsumi, S., Magole, L., and Kgathi, D. (2012). Indigenous knowledge and land use policy: Implications for livelihoods of flood recession farming communities in the Okavango Delta, Botswana. *Phys Chem Earth 50–52*,185–195 . doi: 10.1016/j.pce.2012.09.013.

Mulebeke, R., Kironchi, G., and Tenywa, M. M. (2013). Soil moisture dynamics under different tillage practices in cassava–sorghum based cropping systems in eastern Uganda. *Ecohydrol. Hydrobiol.13*, 22–30.

Mwalyosi, R. B. B.(2000). Resource Potentials of Tanzania Basin , the Rufiji River. *Ambio 19*.

Mwita, E. (2012). Detection of Small Wetlands with Multi - sensor data in East Africa. *Advances in Remote Sensing*, *1*, 64–73.

Mwita, E., Menz, G., Misana, S., Becker, M., Kisanga, D., and Boehme, B. (2013). Mapping small wetlands of Kenya and Tanzania using remote sensing techniques. *International Journal of Applied Earth Observation and Geoinformation*, *21*, 173–183.

Myamoto, K., Maruyama, A., Haneishi, Y., Matsumoto, S., Tsuboi, T., Asea, G., Okello, S., Takagaki, M., and Kikuchi, M. (2012). NERICA Cultivation and its Yield Determinants: The Case of Upland Rice Farmers in Namulonge, Central Uganda. *Journal of Agricultural Science 4*, 120-135.

NASA. (2014). Shuttle Radar Topographic Mission, downloaded from USGS EROS Data Center, http://www2.jpl.nasa.gov/srtm/cbanddataproducts.html (accessed 18 September 2015).

Nash, J.E., and Sutcliffe, J.V. (1970). River flow forecasting through conceptual models part I - A discussion of principles. *J. Hydrol.*10, 282–290. https://doi.org/10.1016/0022-1694(70)90255-6

Näschen, K., Diekkrüger, B., Leemhuis, C., Steinbach,S., Seregina, L.S.,Thonfeld, F., and van der Linden, R. (2018). Hydrological Modeling in Data-Scarce Catchments: The Kilombero Floodplain in Tanzania, *Water, 10*, 599

National Bureau of Statistics. (2018). National Population Projections. The United Republic of Tanzania, 53–54. Retrieved from http://www.nbs.go.tz

National Environment Management Authority (NEMA). (2008). State of the Environment Report for Uganda, http://www.nemaug.org/reports/n_s_o_e_r_2008.pdf (accessed 30.06.2014).

Neitsch, S. L., Arnold, J. G., Kiniry, J. R., and Williams, J. R., 2009. Soil and Water Assessment Tool, Theoretical Documentation, Grassland, Soil and Water Resources Laboratory, Temple, TX, USA. http://swat.tamu.edu/media/99192/swat2009-theory.pdf (accessed: 20.05.2015).

NEMC/WWF/IUCN. (1990). Development of a Wetland Conservation and Management Programme for Tanzania. JUCN, Gland, Switzerland. 113 pp

Niang, I., Ruppel, O.C., Abdrabo, M.A., Essel, A., Lennard, C., Padgham, J., and Urquhart, P. (2014). Africa. In Climate Change 2014: Impacts, Adaptation,and Vulnerability. Part B: Regional Aspects. Contribution of Working Group II to the Fifth Assessment Report of the Intergovernmental Panel on Climate Change, Barros, V.R., Field, C.B., Dokken, D.J.,Mastrandrea, M.D., Mach, K.J., Bilir, T.E., Chatterjee, M., Ebi, K.L., Estrada, Y.O., Genova, R.C., Girma, B., Kissel, E.S., Levy, A.N., MacCracken, S., Mastrandrea, P.R., and White, L.L (eds). Cambridge University Press: Cambridge,UK and New York, NY, 1199–1265.

Nikulin, G., Jones, C., Giorgi, F., Asrar, G., Büchner, M., Cerezo-Mota, R., and Sushama, L. (2012). Precipitation climatology in an ensemble of CORDEX-Africa regional climate simulations. *Journal of Climate*, *25*(18), 6057–6078. https://doi.org/10.1175/JCLI-D-11-00375.1

Nindi, S. J., Maliti, H., Kija, H., and Machoke, M. (2014). Conflicts over land and water resources in the kilombero valley floodplain, Tanzania. *African Study Monogr. Suppl 50*, 173–190.

Northrop, P. J., and Chandler, R. E. (2014). Quantifying sources of uncertainty in projections of future climate. *Journal of Climate*, *27*(23), 8793–8808. https://doi.org/10.1175/JCLI-D-14-00265.1

Nsubuga, F. N.W. (2000). Climatic Trends at Namulonge in Uganda : 1947-2009. *Geography and Geology*, *3*, 119–131.

Nsubuga, F.N.W., Namutebi, E.N. and Nsubuga-Ssenfuma, M. (2014): Water resources of Uganda: an assessment and review. *Journal of Water Resource and Protection, 6*: 1297-1315.

Nugroho, P., Marsono, D., Sudira, P.,and Suryatmojo, H. (2013). Impact of Land-use Changes on Water Balance. *Procedia Environ Sci 17*, 256–262 . doi: 10.1016/j.proenv.2013.02.036.

Ongoma, V., Chen, H., and Gao, C. (2017). Projected changes in mean rainfall and temperature over East Africa based on CMIP5 models. *International Journal of Climatology*, (October). https://doi.org/10.1002/joc.5252

Okalebo, J. R., Gathua, K.W., and Woomer, P. L. (2002). Laboratory Methods of Soil and Plant Analysis: A Working Manual (2nd ed.), Sacred African Publishers, Nairobi, Kenya, http://www.kalro.org:8080/repository/bitstream/0/8547/1/lab methods of soil and plant analysis.pdf (05.05.2015).

Okeyo-Owuor, J.B., and Raburu, P.O. (2016). Wetlands of Lake Victoria Basin, Kenya: distribution, current status and conservation challenges. Community Based Approach to Manag Nyando Wetl Lake Victoria Basin, Kenya 2–3. https://www.oceandocs.org/bitstream/handle/1834/7721/ktf0424.pdf?sequence=1 (accessed 18.02.2018).

Paul, H., and Steinbrecher, R.(2013). *New Alliance for Food Security and Nutrition.Who benefits,who loses ? Technical Report*; Oxford, UK, 2013; http://www.econexus.info/sites/econexus/files/African_Agricultural_Growth_Corridors_&_New_Alliance_-_EcoNexus_June_2013.pdf.

Pianosi, F., Beven, K., Freer, J., Hall, J.W., Rougier, J., Stephenson, D.B., and Wagener,T. (2016). Sensitivity analysis of environmental models: A systematic review with practical workflow. *Environmental Modelling and Software 79*, 214 – 232.http://dx.doi.org/10.1016/j.envsoft.2016.02.008.

Pignotti, G., Rathjens,, H., Cibin, R., Chaubey, I., and Crawford, M. (2017). Comparative Analysis of HRU and Grid-Based SWAT Models. *Water (Switzerland) 9*,272 . doi: 10.3390/w9040272.

Pirastru, M., and Niedda, M. (2013). Evaluation of the soil water balance in an alluvial flood plain with a shallow groundwater table. *Hydrological Sciences Journal 58*, 898–911.

Poff, N. L., Allan, J. D., Bain, M. D., Karr, R., Prestegaard, K. L., Richter, B. D., Sparks, R. E., and Stromberg, J. C. (1997). The natural flow regime: a paradigm for river conservation and restoration. *BioScience, 47*,769-84.

Post, D. A., and Jones, J. A. (2001). Hydrologic regimes of forested, mountainous, headwater basins in New Hamphsire, North Carolina, Oregon, and Puerto Rico. *Advances in Water Resources, 24*, 1195 - 1210.

Praskievicz, S., and Chang, H. (2009). A review of hydrological modelling of basin-scale climate change and urban development impacts. *Progress in Physical Geography*, *33*(5), 650–671. https://doi.org/10.1177/0309133309348098

Price, K. (2011). Effects of watershed topography, soils, land use, and climate on baseflow hydrology in humid regions: a review. Prog. Phys. Geogr. 35, 465–492, http://dx.doi.org/10.1177/0309133311402714.

Purinton, B., and Bookhagen, B. (2017).Validation of digital elevation models (DEMs) and comparison of geomorphic metrics on the southern Central Andean Plateau. *Earth Surface. Dynamics, 5*, 211-237.

Qiu, Y., Fu, B., Wang, J., and Chen, L. (2001). Soil moisture variation in relation to topography and land use in a hillslope catchment of the Loess Plateau , China. *240*, 243–263.

Radcliffe, D., and Šimůnek, J. (2010). *Soil Physics with HYDRUS: Modeling and Applications*; CRC Press, Taylor & Francis Group, 2010; ISBN ISBN-10: 142007380X, ISBN-13: 9781420073805.

Ramsar Convention. (1999). River basin management: Integrating Wetland Conservation and wise use into River Basin Management. “People and Wetlands: The Vital Link” ,7th Meeting of the Conference of the Contracting Parties to the Convention on Wetlands (Ramsar, Iran, 1971). San José,Costa Rica.

Ramsar Convention Secretariat. (2010). Wise use of wetlands: Concepts and approaches for the wise use of wetlands. Ramsar handbooks for the wise use of wetlands, 4th edn. Ramsar

Convention Secretariat, Gland, Switzerland.
Rathjens, H., and Oppelt, N. (2012a). SWAT model calibration of a grid-based setup. *Adv Geosci. 32*,55–61 . doi: 10.5194/adgeo-32-55-2012.
Rathjens, H., and Oppelt, N. (2012b). SWATgrid : An interface for setting up SWAT in a grid-based discretization scheme. *Comput Geosci. 45*, 161–167 . doi: 10.1016/j.cageo.2011.11.004.
Rathjens, H., Oppelt, N., Bosch, D.D., Arnold, J.G., and Volk, M. (2014). Development of a grid-based version of the SWAT landscape model. *Hydrol Process 29*, 900–914 . doi: 10.1002/hyp.10197.
Rawls, W. J., and Brakensiek, D. L. (1985). Prediction of soil water properties for hydrologic modeling, In: Jones, E.,Ward,T.J.(eds.),Watershed Management in the Eighties. Proceedings of a symposium ASCE. 30 Apr. - 1 May. 293-299.
Rawls, W. J., Pachepsky, Y. A., and Ritchie, J. C. (2003). Effect of soil organic carbon on soil water retention. *Geoderma 116*, 61–76, doi:10.1016/S0016-7061(03)00094-6.
Rebelo, L. M., McCartney, M. P., and Finlayson, C. M. (2010). Wetlands of Sub-Saharan Africa: Distribution and contribution of agriculture to livelihoods. *Wetlands Ecology & Management, 18*, 557–572.
Reddy, K. R., DeLaune, R., and Craft, C. B. (2010). Nutrients in wetlands: Implications to water quality under changing climatic conditions, http://www.ces.fau.edu/climate_change/everglades-recommendations-2014/pdfs/session-e-resource-3.pdf (accessed 25.08.2015).
Riahi, K., Rao, S., Krey, V., Cho, C., Chirkov, V., Fischer, G., … Rafaj, P. (2011). RCP 8.5-A scenario of comparatively high greenhouse gas emissions. *Climatic Change*, *109*(1), 33–57. https://doi.org/10.1007/s10584-011-0149-y
Ritter, A., and Muñoz-Carpena, R. (2013). Performance evaluation of hydrological models: Statistical significance for reducing subjectivity in goodness-of-fit assessments. *Journal of Hydrology*, 480, 33–45.
Ritter, A., Hupet, F., Muñoz-Carpena, R., Lambot, S., and Vanclooster, M. (2003). Using inverse methods for estimating soil hydraulic properties from field data as an alternative to direct methods. *Agric. Water Manag. 59*,77–96, doi:10.1016/S0378-3774(02)00160-9.
Robinson, D. A., Campbell, C. S., Hopmans, J. W., Hornbuckle, B. K., Jones, S. B., Knight, R., and Wendroth, O. (2008). Soil Moisture Measurement for Ecological and Hydrological Watershed-Scale Observatories: A Review. *Vadose Zone Journal*, *7*, 358.
Rodenburg, J., Zwart, S. J., Kiepe, P., Narteh, L.T., Dogbe,W., and Wopereis, M.C.S. (2014). Sustainable rice production in African inland valleys: Seizing regional potentials through local approaches. *Agricultural Systems, 123*, 1–11.
Roggeri, H. (1995). Tropical freshwater wetlands: a guide to current knowledge and sustainable management, Kluwer Academic Publishers, Dordrecht, The Netherlands and Bosten, USA and London, UK.
Rosenbaum, U., Bogena, H. R., Herbst, M., Huisman, J. A., Peterson, T. J., Weuthen, A., Western, A. W., and Vereecken, H. (2012). Seasonal and event dynamics of spatial soil moisture patterns at the small catchment scale. *Water Resour. Res. 48*, 1–22, doi:10.1029/2011WR011518.
RoTimi Ojo, E., Bullock, P. R., and Fitzmaurice, J.(2015). Field Performance of Five Soil Moisture Instruments in Heavy Clay Soils. *Soil Sci. Soc. Am. J. 79*, 20–29, doi:10.2136/sssaj2014.06.0250.
Sakané, N., Alvarez, M., Becker, M., Böhme, B., Handa, C., Kamiri, H.W., and van Wijk, M.T.

(2011). Classification, characterisation, and use of small wetlands in East Africa. *Wetlands, 31*, 1103–1116.

Sánchez, N., Martínez-fernández, J., González-piqueras, J., and González-dugo, M. P. (2012). Agricultural and Forest Meteorology Water balance at plot scale for soil moisture estimation using vegetation parameters. *Agric. For. Meteorol. 166–167*, 1–9, doi:10.1016/j.agrformet.2012.07.005.

Schaap, M. G., Leij, F. J., and Van Genuchten, M. T.(2001). Rosetta : a computer program for estimating soil hydraulic parameters with hierarchical pedotransfer functions. *J. Hydrol. 251*, 163–176.

Schenk, H. J., and Jackson, R. B.(2002). Rooting depths , lateral root spreads and below-ground / above-ground allometries of plants in water-limited. *J. Ecol. 90*, 480–494.

Schreyer, J., and Lakes, T. (2016). Deriving and Evaluating City-Wide Vegetation Heights from a TanDEM-X DEM. *Remote Sensing, 8*, 940.

Schuyt, K. D. (2005). Economic consequences of wetland degradation for local populations in Africa. *Ecological Economics, 53*, 177–190.

Shongwe, M. E., van Oldenborgh, G. J., van den Hurk, B., and van Aalst, M. (2011). Projected changes in mean and extreme precipitation in Africa under global warming. Part II: East Africa. *Journal of Climate, 24*(14), 3718–3733. https://doi.org/10.1175/2010JCLI2883.1

Shrestha, M.S., Artan, G.A., Bajracharya, S.R., and Sharma, R.R. (2008). Using satellite-based rainfall estimates for streamflow modeling: Bagmati Basin. J Flood Risk Management 1: 89-99.

Singh, R., and Singh, J.(1996). Irrigation planning in cotton through simulation modeling. *Irrig. Sci. 17*, 31–36.

Singh, R., Van Dam, J. C., and Feddes, R. A. (2006). Water productivity analysis of irrigated crops in Sirsa district, India. *Agric. Water Manag. 82*, 253–278, doi:10.1016/j.agwat.2005.07.027.

Šimůnek, J., Šejna, M., Saito, H., Sakai, M., and van Genuchten, M. T.(2013). The Hydrus- 1D Software Package for Simulating the One-Dimensional Movement of Water, Heat, and Multiple Solutes in Variably-Saturated Media:Manual version 4.17; Riverside, California, USA; https://www.pc-progress.com/en/Default.aspx?hydrus-1d.

Šimůnek, J., Šejna, M., Saito, H., Sakai, M., and van Genuchten, M. T. (2009). The Hydrus- 1D Software Package for Simulating the One-Dimensional Movement of Water, Heat, and Multiple Solutes in Variably-Saturated Media:Manual version 4.17; Riverside, California, USA.

Šimůnek, J., van Genuchten, M.Th., and Šejna, M. (2012). Hydrus: model use, calibration, and validation. *Transactions of the ASABE 55*, 1261-1274, American Society of Agricultural and Biological Engineers ISSN 2151-0032.

Siyal, A.A., Bristow, K.L., and Šimůnek, J. (2012). Minimizing nitrogen leaching from furrow irrigation through novel fertilizer placement and soil surface management strategies. *Agric. Water Manag. 115*, 242–251.

Slaton, N. A., Beyrouty, C. A.,Wells, B. R. I., Norman, R. J., and Gbur, E. E. (1990). Root growth and distribution of two short-season rice genotypes. *Plant Soil 121*, 269–278.

Sławiński, C., Cymerman, J., Witkowska-Walczak, B., and Lamorski, K. (2012). Impact of diverse tillage on soil moisture dynamics. *International Agrophysics, 26*, 301–309.

Smith, B., and Sandwell, D. (2003). Accuracy and resolution of shuttle radar topography mission data. *Geophysical Research Letters, 30*, 3–6.

Snyder, G. H. (2005). Everglades agricultural area soil subsidence and land use projections. *Soil and Crop Science Society of Florida Proceedings, 64*, 44–51.

Soil Conservation Service (SCS) (Ed.) (1972). Hydrology. In National Engineering Handbook; Soil Conservation Service: Washington, DC, USA.

Sophocleous, M. (2002). Interactions between groundwater and surface water: the state of the science. *Hydrogeology Journal 10*, 52–67, DOI 10.1007/s10040-001-0170-8

Souverijns, N., Thiery, W., Demuzere, M., and Lipzig, N. P. M. Van. (2016). Drivers of future changes in East African precipitation Drivers of future changes in East African precipitation. *Environmental Research Letters*, *11*, 114011.

Soylu, M. E., Istanbulluoglu, E., Lenters, J. D., and Wang, T. (2011). Quantifying the impact of groundwater depth on evapotranspiration in a semi-arid grassland region. *Hydrol. Earth Syst. Sci. 15*, 787–806, doi:10.5194/hess-15-787-2011.

Stevens Water Monitoring Systems Inc. (2007). The Hydra Probe ® Soil Sensor User's Manual, (July), https://www.fondriest.com/pdf/stevens_hydra_manual.pdf (accessed 06.03.2014).

Stevensons, S., and Frazier, S. (1999). Review on wetland inventory information in Africa, in: Global review on wetland resources and priorities for wetland inventory. Supervising Scientist Report 144, Wetlands International Publication 53, edited by: Finlayson, C. M. and Spiers, A. G., Supervising Scientist, Canberra.

Sweeney, B.W., Bott, T. L., Jackson, J. K., Kaplan, L. A, Newbold, J. D., Standley, L. J., and Horwitz, R. J. (2004). Riparian deforestation, stream narrowing, and loss of stream ecosystem services. Proceedings of the National Academy of Sciences of the United States of America, 101, 14132–14137. https://doi.org/10.1073/pnas.0405895101.

Thompson, J. R., and Polet, G. (2000). Hydrology and land use in a sahelian floodplain wetland 1. *Wetlands 20*, 639–659.

Thomsen, I. K., Schjønning, P., Jensen, B., Kristensen, K., and Christensen, B.T. (1999).Turnover of organic matter in differently textured soils. II. Microbial activity as influenced by soil water regimes. *Geoderma*, *89*, 199–218.

Thomson, A. M., Calvin, K. V., Smith, S. J., Kyle, G. P., Volke, A., Patel, P., and Edmonds, J. A. (2011). RCP4.5: A pathway for stabilization of radiative forcing by 2100. *Climatic Change*, *109*(1), 77–94. https://doi.org/10.1007/s10584-011-0151-4

Thornton, P. K., Ericksen, P. J., Herrero, M., and Challinor, A. J. (2014). A review. Climate variability and vulnerability to climate change: a review Global Change Biology 20, 3313–3328, doi: 10.1111/gcb.1258

Thornton, P.K., Jones, P.G., Alagarswamy, G., Andresen, J., and Herrero, M. (2010). Adapting to climate change: Agricultural system and household impacts in East Africa. *Agric Syst 103*, 73–82 . doi: 10.1016/j.agsy.2009.09.003.

Troy, B., Sarron, C., Fritsch, J.M., and Rollin, D. (2007). Assessment of the impacts of land use changes on the hydrological regime of a small rural catchment in South Africa. *Phys. and Chem. of Earth 32*, 984–994 . doi: 10.1016/j.pce.2007.07.049.

Turner, R. K., Bergh, J. C., van den, J. M., and So, T. (2000).The values of wetlands: landscape and institutional ecological-economic analysis of wetlands: scientific integration for management and policy. *Ecological Economics, 35*, 7–23.

Uganda Bureau of Statistics (UBOS). (2017). 2017 Statistical Abstract. *Uganda Bureau of Statistics 2017 Statistical Abstract*, *1*, 64. Retrieved from http://www.ubos.org/onlinefiles/uploads/ubos/pdf documents/abstracts/Statistical Abstract 2013.pdf

Uganda wetland atlas. (2016). Uganda Wetlands atlas Volume II. http://www.mwe.go.ug/sites/default/files/Uganda%20Wetlands%20Atlas%20Volume%20II_Popular%20Version.pdf (accessed 20.11.2017).

United States Department of Agriculture. (2014). Soil Texture Calculator, https://www.nrcs.usda.gov/wps/portal/nrcs/detail/soils/survey/?cid=nrcs142p2_054167 (06.08.2015).

van Dam, A. A., Dardona, A., Kelderman, P., and Kansiime, F. (2007). A simulation model for nitrogen retention in a papyrus wetland near Lake Victoria, Uganda (East Africa). *Wetlands Ecology and Management, 15*, 469–480.

Vanderkelen, I., Lipzig, N. P. M. Van, and Thiery, W. (2018). Modelling the water balance of Lake Victoria (East Africa), part 2 : future projections. *Manuscript under Review for Journal Hydrol. Earth Syst. Sci.*, (April).

Van Genuchten, M. T.(1980). Aclosed-form Equation for predicting Hydraulic Conductivity of Unsaturated soils. *Soil Sci. Soc. Am. J. 44*.

Varut, G., Wei, X., Huang, D., Shinde,D., and Price, R.(2011). Application of MODHMS to Simulate Integrated Water Flow and Phosphorous Transport in a Highly Interactive Surface Water Groundwater System along the Eastern Boundary of the Everglades National Park, Florida; MODFLOW and More 2011: Integrated Hydrologic Modeling; The Colorado School of Mines, Golden, Colorado. June 5-8

Venkatesh, B., Lakshman, N., Purandara, B. K., and Reddy, V. B. (2011). Analysis of observed soil moisture patterns under different land covers in Western Ghats, India. *J. Hydrol. 397*, 281–294, doi:10.1016/j.jhydrol.2010.12.006.

Vereecken, H., Huisman, J. A., Bogena, H., Vanderborght, J., Vrugt, J. A., and Hopmans, J. W. (2008). On the value of soil moisture measurements in vadose zone hydrology : A review. *Water Resour. Res.44*, 1–21, doi:10.1029/2008WR006829.

Verstraeten, W. W.,Veroustraete, F., and Feyen, J. (2008). Assessment of Evapotranspiration and Soil Moisture Content Across Different Scales of Observation. *Sensors 8*, 70–117.

von der Heyden, C. J., and New, M. G. (2003). The role of a dambo in the hydrology of a catchment and the river network downstream. *Hydrology and Earth System Sciences, 7*, 339–357.

von der Heyden, C. J. (2004). The hydrology and hydrogeology of dambos: a review. *Progress in Physical Geography*, *28*(4), 544–564. https://doi.org/10.1191/0309133304pp424oa

Waithaka, M., Nelson,G. C., Thomas, T. S., and M. K. (2013). East African Agriculture and Climate change. *A Comprehensive Analysis*, *IFPRI issu*(76), 1–4. https://doi.org/10.2499/9780896292055

Wantzen, K. M., Yule, C. M., Tockner, K., and Junk, W. J. (2008). Riparian wetlands of tropical streams. *Tropical Stream Ecology*, 199 – 217.

Westerhof, A.B., Härmä, P., Isabirye, E., Katto, E., Koistinen, T., Kuosmanen, E., Lehto, T., Lehtonen, M.I., Mäkitie, H., Manninen, T., Mänttäri, I., Pekkala, Y., Pokki, J., Saalmann, K. and Virransalo, P. (2014): Geology and Geodynamic Development of Uganda with Explanation of the 1:1,000,000-Scale Geological Map. Geological Survey of Finland, Special Paper 55, 387 p.

Wessel, B., Bertram, A., Gruber, and Bemm, S. (2016). A new high - resolution digital elevation model of Greenland derived from TanDEM-X. ISPRS Annals of the Photogrammetry, Remote Sensing and Spatial Information Sciences, XXIII ISPRS Congress Prague, 1 -8.

Wessel, B. (2013).TanDEM-X Ground Segment- DEM Products Specification Document.Project Report. EOC, DLR, Oberpfaffenhofen, Germany, Public Document TD-GS-PS-0021, Issue 3.0, http://elib.dlr.de/108014/1/TD-GS-PS-0021_DEM-Product-Specification_v3.1.pdf (accessed 20.04.2017).

Windmeijer, P. N., and Andriesse, W. (1993). Inland Valleys in West Africa: An Agro-Ecological Characterization of Rice-Growing Environments, 160. http://edepot.wur.nl/73431.

WMO (World Meteorology Organization). (2008). Guide to Hydrological Practices Volume I : Hydrology – From Measurement to Hydrological Information. WMO-No. 168.

Wood, A., and Dixon, A. (2008). Wetland Use as an Adaptive Response to Climate Change in East and South Africa : Sustainable Wetland Management. http://www.wetlandaction.org/wp-content/uploads/SAB-Policy-Briefing-5-Adaptive-Responses-to-Climate-Change.pdf (accessed 13.01.2018).

Wood, A., Dixon, A., and McCartney, M. (2013). Wetland Management and Sustainable Livelihoods in Africa. Routledge publisher, 2 Park Sqaure, Milton Park, Abingdon, Oxon, Ox14 4RN, UK, ISBN13:978-1-84971-411-2.

Wood, A., and van Halsema, G. E.(2008). *Scoping agriculture – wetland interactions*; ISBN 9789251060599.

Worou, O. N., Gaiser, T., Saito, K., Goldbach, H., & Ewert, F. (2012). Simulation of soil water dynamics and rice crop growth as affected by bunding and fertilizer application in inland valley systems of West Africa. *Agriculture, Ecosystems and Environment*, *162*, 24–35. https://doi.org/10.1016/j.agee.2012.07.018

WRB (World Reference Base for Soil Resources). (2014). International soil classification system for naming soils and creating legends for soil maps. Food and Agriculture Organization. http://www.fao.org/3/i3794en/I3794en.pdf (accessed 02.02.2016).

WWDR. (2018). Nature-Based Solutions for Water. *The United Nations World Water Development Report 2018*. Retrieved from http://unesdoc.unesco.org/images/0026/002614/261424e.pdf

Wu, D. D., Anagnostou, E.N., Wang, G., Moges, S., and Zampieri, M. (2014). Improving the surface-ground water interactions in the Community Land Model: Case study in the Blue Nile Basin. *Water Resour. Res.50*, 8015–8033, doi:10.1002/2013WR014501.

WWF. (2006). Climate Change Impacts on East Africa. A Review of the Scientific Literature. *WWF-World Wide Fund For Nature,Gland, Switzerland*, 12. https://doi.org/10.1007/978-3-642-14776-0_36

Xu, X., Zhang, Q., Li, Y., and Li, X. (2016). Evaluating the influence of water table depth on transpiration of two vegetation communities in a lake floodplain wetland. *Hydrology Research 47*, 293-312, doi:10.2166/nh.2016.011.

Yira, Y., Diekkrüger, B., Steup, G., and Bossa, A.Y. (2016). Modeling land use change impacts on water resources in a tropical West African catchment (Dano, Burkina Faso). *J Hydrol 537*,187–199 . doi: 10.1016/j.jhydrol.2016.03.052.

Yost, D. and Eswaran, H. (1990): Major land resource areas of Uganda. World Soil Resources, Soil Conservation Service, USDA, Washington DC, 218 p.

YSI Incoporated. (2010). 6 – Series multiparameter water quality sondes user manual. https://www.ysi.com/File%20Library/Documents/Manuals/069300-YSI-6-Series-Manual-RevJ.pdf (accessed 02.02.2016).

Zalewski, M. (2002). Ecohydrology - the use of ecological and hydrological processes for sustainable management of water resources. *Hydrol Sci J 47*, 823–832 . doi: 10.1080/02626660209492986.

Zehe, E., Graeff, T., Morgner, M., Bauer, A., and Bronstert, A. (2010). Plot and field scale soil moisture dynamics and subsurface wetness control on runoff generation in a headwater in the Ore Mountains. *Hydrol. Earth Syst. Sci.14*, 873–889, doi:10.5194/hess-14-873-2010.

Zinyengere,N., Araujo,J., Marsham,J., and Rowell, D.(2016). Current and projected future climate; Future Climate for Africa | Africa's climate: Helping decision-makers make sense of climate information, www.futureclimate.org